Evolution of the ZRS and the Regulation of SHH Expression in the Forelimbs of Bats

Denise Ribeiro Arthur Brito

Department of Molecular and Cell Biology
University of Cape Town
November 2011

Supervisors:
Prof. Nicola Illing
Assoc. Prof. David S. Jacobs

Dissertation presented for a Master in Science in Department of Molecular and Cell Biology, at the University of Cape Town.

Declaration

I, Denise Ribeiro Arthur Brito, declare that this is my own unaided work, apart from those sections that have been acknowledged. This thesis or any part of it has not been, nor will be submitted for any degree at this or any other university.

Signature:_____ Date: _____

Acknowledgements

I would like to thank my supervisors, Prof. Nicola Illing and Prof. David Jacobs, who have played an essential role in the concept, financing, support and completion of this study. I would also like to acknowledge the financial assistance of the National Research Foundation (NRF) towards this research project. Funding awards obtained were the International Students Scholarships, provided by the UCT Postgraduate Funding Office; and the Equity Development Programme Scholarship, imparted by the Department of Molecular and Cell Biology. I must also thank Dr. Laura Lettice and Paul Devenney for their collaboration. My thanks go to Dorit Hockman and Mandy K. Mason for their intellectual advice and moral support throughout the project. I would like to thank Kayshinee Rye Ramchurn for helping with language of the final version this thesis. Thanks to the Evo-Devo Lab (425) and the Bat Lab for their support. Faezah Davids is also greatly thanked for her technical support in the lab. I would also like to thank my family for their moral support and encouragement.

Abstract

The characterisation of *sonic hedgehog* (*Shh*) in the developing limbs of the two bat species *Miniopterus natalensis* and *Carollia perspicillata* showed that *Shh* expression pattern was different from that observed in mouse limbs. An interesting discovery was that bat embryos display a second round of expression at stage CS16/E12.5. The aim of this thesis is to investigate the cause of the *Shh* expression pattern in developing limbs of the bat. *Sonic hedgehog* expression in the limb is regulated by a long-distance *cis*-regulatory sequence called the ZPA-regulatory sequence (ZRS). Mutations in the ZRS are known to result in limb deformities in humans, mice and cats. I investigated whether conserved mutations occurring in the bat ZRS are the cause of the change in *Shh* expression in bat limbs during embryonic development. Comparison of the ZRS of eighteen bat species to the ZRS of twenty other vertebrates revealed five conserved mutations that are unique to the bat ZRS. To test if the bat ZRS has the ability to change the expression pattern of *Shh,* the ZRS from *M. natalensis* and *Rhinolophus clivosus* (which have different wing shapes) was linked to a β-globin-*LacZ* reporter construct and used in transgenic mice experiments. A mouse ZRS with bat mutations as well as a wild type mouse ZRS (the control) were also tested. Transgenic results suggest that the bat ZRS has the elements necessary to alter the spatial expression pattern of *Shh*, but that may not be able to induce a second round of expression. The two bat ZRS reporter construct species produce different β-galactosidase expression patterns - a result of having very different ZRS sequences - thus implying that there is interspecies variation of the *Shh* expression pattern. Phylogenetic analysis of bat ZRS grouped the bat species in three well supported clades, which may not only reflect differences in S*hh* expression but also differences in wing shape. To test this hypothesis, it was first necessary to identify which skeletal elements within the handwing vary the most across the bat species, and consequently account for the variation in wing shape. Analysis of wing morphology revealed that phalange I of digits 3 and 4, and phalange II of digits 3, 4 and 5 showed significant variation across 53 bat species, along with Aspect ratio, which is an indicator of wing shape. Comparisons of Aspect ratio between bat species in the ZRS clades imply a relationship between differences in the ZRS sequences of bats and wings. Analysis of the variation of lengths of five skeletal elements mentioned above between the ZRS clades suggest that the wing shape is determined by different combinations of the length of 3PII, 3PI, 4PI, 4PII, and 5PII. This suggests that the variation of the skeletal elements may be a result of post-natal development as juvenile bats learn to fly, or that there is another mechanism determining wing shape.

Table of Contents

List of Figures

List of Tables

Chapter 1: Development of the Bat Wing

Bats are the only mammals that combine powered flight with the ability to echolocate (Simmons 2005; Simmons et al. 2008; Speakman 2001; Speakman 2008). The bat wing has two unique features (Figure 1.1) that allow these unique mammals to fly: the elongation of digits II-V (with the absence of claws in most species) in the forelimb, and the expansive patagia (wing membranes) that are found between these elongated digits (Sears 2008; Weatherbee et al. 2006; Thewissen & Babcock 1992). By contrast, the hindlimb of bats are not elongated, and all the digits are the same length (Figure 1.1) (Swartz 1997; Sears et al. 2006). Prior to the advent of modern molecular techniques, many scientists investigated the evolution of flight in bats using phylogenies based on morphological differences (Thewissen & Babcock 1992; Simmons et al. 2008; Speakman 2001). This proved difficult since no intermediate fossil has yet been found (Stockwell 2001; Thewissen & Babcock 1992; Simmons et al. 2008). The developments of molecular techniques in phylogenetics and developmental biology have made major contributions to our understanding of the evolution of flight in bats.

Morphological Adaptations to Flight

To be able to fly, bats have evolved certain morphological characteristics, the most obvious of which are the reduction of the hindlimb and its muscles, and the elongation of the forelimb digits to form an aerofoil i.e. the bat wing described above (Figure 1.1) (Simmons 2005; Thewissen & Babcock 1992; Swartz 1997). In fact, Swartz and Middleton (2008) showed that bats have significantly longer forelimbs relative to their body size than other mammals. Although these morphological characteristics are important, they are not the only essential adaptations for flight. Bats also have relative large pectoral muscles and a propatagial muscle complex (that starts at the end of the neck and runs along the anterior edge of the wing) to provide power for flight and a cephalic vein that supplies most of the blood to the wing (Thewissen & Babcock 1992). In contrast to the forelimb, the bat hindlimb is significantly smaller relative to body size than in other mammals, and the hip bone has been modified so that the knee stands out in a perpendicular position to the body (Thewissen & Babcock 1992; Swartz & Middleton 2008). These changes allow for both an increase in wing area and a decrease in total weight (Thewissen & Babcock 1992; Swartz 1997; Swartz & Middleton 2008).

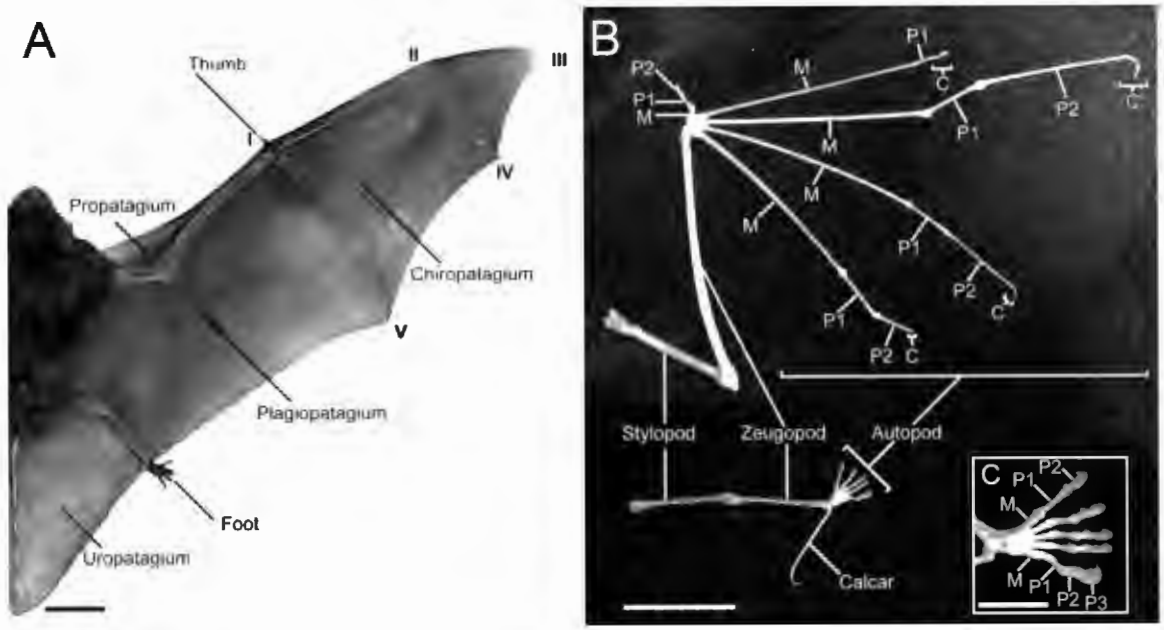

Figure 1.1: The anatomy of the forelimb (wing) and hindlimb of bats. A: digits II-V are quite elongated and there is webbing between them that acts as an aerofoil that allows flight. B: The skeletal structure of the bat forelimb clearly shows that digits II-V are elongate (M- metacarpals, P1- phalange 1, P2-phalange 2, P3- phalange 3 C- claw), while the hindlimb has a calcar and no elongation of the digits. C: The skeletal structure of the bat hindlimb shows that digits I-V are all the same length. (Hockman et al. 2009)

Wing Morphology and Ecology

Survival of a bat is dependent on the ability to fly efficiently within its habitat, and since bats inhabit a diverse range of environments, it is not surprising that there is a large variation in wing shapes and sizes, thereby enabling bats to forage in different environments (Norberg & Rayner 1987; Adams 2008). Consequently, there is a strong correlation between the bat wing shape and the environment they occupy (Norberg & Rayner 1987). Bats with broad, short wings are slow but manoeuvrable and are thus adapted for foraging within vegetation, while bats with narrow, long wings are fast but are not as manoeuvrable and are therefore better adapted to foraging above vegetation in open areas (Norberg & Rayner 1987). While this correlation has been studied extensively, the exact elements in the wing that allow for such a variation in wing shape have yet to be investigated.

A starting point for understanding such variation would be to understand the genetic basis of wing shape in bats. Extensive research in model organisms (chicken, mice and humans) has resulted in a comprehensive model of the genetic mechanism involved in the patterning of the limbs during development (Tanaka et al. 2002; Sagai et al. 2004; Zeller et al. 2009; Zeller 2010; Bangs et al. 2010). Recent work has focused on how variation in these genetic mechanisms gave rise to the

diversity of vertebrate limbs, including the bat wing (Shapiro et al. 2003; Sears et al. 2006; Weatherbee et al. 2006; Cretekos et al. 2007; Hockman et al. 2008).

General Limb Development Model

The development of the vertebrate limb bud in developing embryos is the result of complex molecular interactions and feedback loops between genes, such as *Fibroblast growth factors (Fgf)*, *Bone morphogenetic proteins (Bmp)*, *Sonic hedgehog (Shh)*, *Gli proteins (Gli)*, *heart and neural crest derivatives (dHand/Hand2)*, *Gremlin (Grem1)* and 5'-*Hoxd* gene *(i.e.Hoxd10-13)* (Duboc & Logan 2009; Fernandez-Teran et al. 2000; Niswander 2003; McGlinn & Tabin 2006; Tickle 2006; Zeller et al. 2009). The developing limb grows along three axes (Figure 1.2): the anterior-posterior axis (A-P, from digit 1 to digit 5) the proximal-distal axis (Pr-D, from the shoulder to the tips of the digits) and the dorsal-ventral axis (Do-V, from the palm to the back of the hand) (Duboc & Logan 2009; Niswander 2003; Tickle 2006). Patterning of the limb along these axes is coordinated by two "control centres" (Figure 1.3A), the zone of polarizing activity (ZPA) in the posterior tip of the limb bud and the apical ectodermal ridge (AER) in the distal tip (Duboc & Logan 2009; Schwabe et al. 1998; Tickle 2006; Zeller et al. 2009).

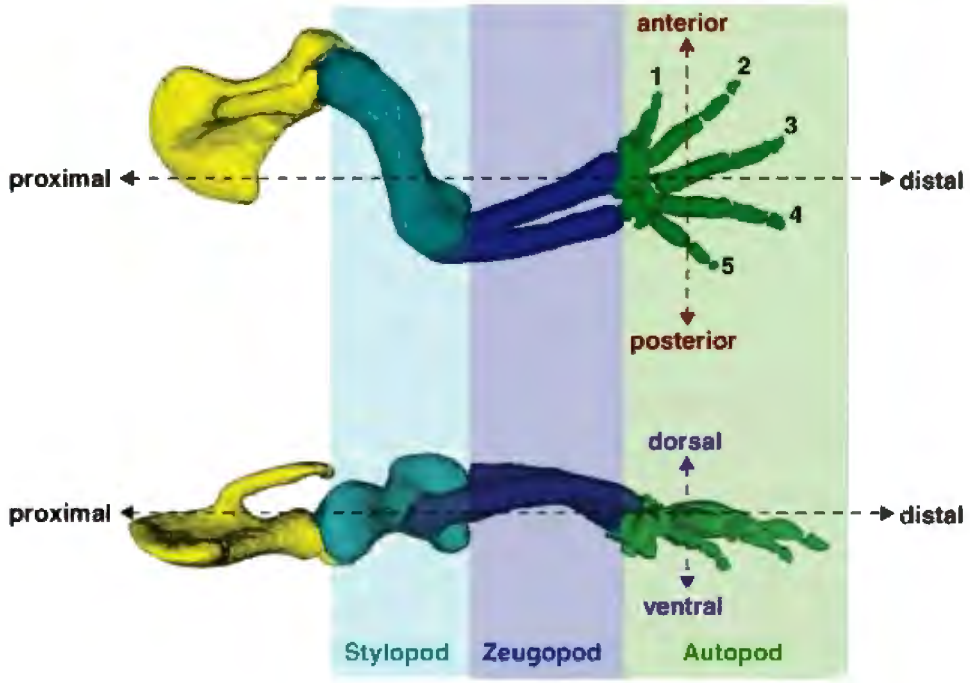

Figure 1.2: The universal anatomy of all vertebrate limbs. There are three limb elements, namely the stylopod, zeugopod and autopod, and the three axes through which limb patterning occurs. The anterior-posterior axis (A-P) is from digit 1 to digit 5, the proximal-distal axis (Pr-D) is from the stylopod to the tips of the digits and the dorsal-ventral axis (Do-V) is from the palm to the back of the hand (Duboc & Logan 2009).

The interaction between the ZPA and AER allows for the proper development of the vertebrate limb. Growth and patterning of the limb can be sub-divided into three stages (Figure 1.3 B and C): initiation, propagation and termination (Duboc & Logan 2009; McGlinn & Tabin 2006; Niswander 2003; Bouldin et al. 2010; Zeller et al. 2009; Zeller 2010). During the initiation stage the two "control centres" are established: the AER is crucial for Pr-D patterning and the ZPA is important for A-P patterning (McGlinn & Tabin 2006; Niswander 2003; Zeller 2010). The initiation stage is defined by expression of *dHand* and *5'Hoxd* genes, which are restricted to the posterior end of the limb bud by Gli3, and up-regulation of *Shh* in the ZPA (Figure 1.3 B) (Duboc & Logan 2009; McGlinn & Tabin 2006; Niswander 2003; Schwabe et al. 1998; Zeller et al. 2009; Fernandez-Teran et al. 2000; Galli et al. 2010). In parallel, BMP4 is expressed at high concentration therefore defining the AER by isolating FGF expression in the distal end of the limb bud (Figure 1.3 C) (Duboc & Logan 2009; Zeller et al. 2009; Zeller 2010). In the propagation stage, SHH up regulates the expression of *Grem1* that inhibits BMP4, allowing expression of *Fgf4* and *Fgf8* in the AER (Duboc & Logan 2009; Zeller et al. 2009; Zeller 2010; Zeller & Zuniga 2007). Fibroblast growth factor 4 and FGF8 reinforces SHH expression and inhibits *Grem1* expression, creating the SHH-BMP-FGF feedback loop (Duboc & Logan 2009; McGlinn & Tabin 2006; Niswander 2003; Zeller 2010; Tickle 2006). This SHH-BMP-FGF feedback loop (Figure 1.3 D) allows cells to continue proliferating until a certain limb bud size has been reached (Niswander 2003; Zeller et al. 2009). The termination stage of the feedback loop is characterized by high concentrations of FGF4 and FGF8 from the AER and low concentrations of SHH in the area of GREM1 expression, resulting in a decrease in Grem1 and an increase in BMP4 (Zeller 2010; Zeller et al. 2009). This SHH-BMP-FGF feedback loop has been shown to be essential for the patterning and development of the limb bud across the vertebrate phylogeny (Zeller 2010; Zeller et al. 2009; Tickle 2006; Niswander 2003; McGlinn & Tabin 2006; Galli et al. 2010; Fernandez-Teran et al. 2000; Schwabe et al. 1998; Duboc & Logan 2009; Bouldin et al. 2010). Disruption of this feedback loop results in malformation of the adult limb (Zeller 2010; Zeller et al. 2009; Tickle 2006; Niswander 2003; McGlinn & Tabin 2006; Galli et al. 2010; Fernandez-Teran et al. 2000; Schwabe et al. 1998; Duboc & Logan 2009; Bouldin et al. 2010). It has been suggested that small changes in the temporal and spatial patterns of genes in these feedback loops may result in the evolution of new limb morphologies (Duboc & Logan 2009; Shapiro et al. 2003).

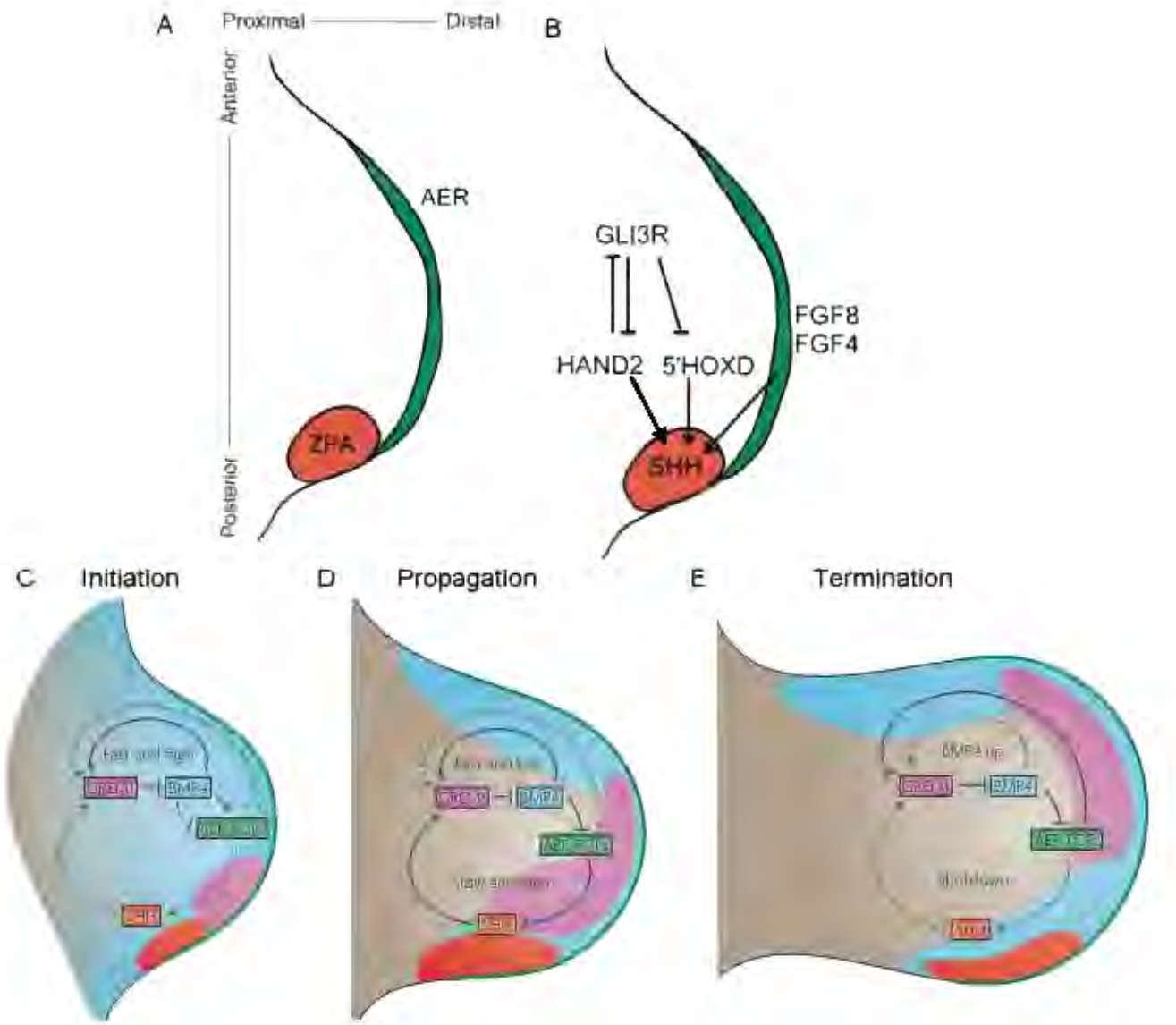

Figure 1.3: The two control centres and genes involved in early limb development. A: The ZPA (orange) is located at the posterior end of the limb while the AER (green) is situated at the most distal end of limb bud. B: During limb development SHH (orange) is activated in the ZPA by HAND2 and 5'HOXD genes and at the same time FGF4 and FGF8 (green) are upregulated in the AER. C: Initiation stage – BMP4 (blue) upregulates GREM1 while SHH expression initiates independent of GREM1 (pink) and FGFs expression. D: Propagation stage - SHH promotes GREM1 expression, which in turn up regulates FGFs expression in the AER by inhibiting BMP4. The FGFs then strengthen SHH expression in the ZPA, establishing the SHH-BMP-FGF feedback loop. E: Termination stage – As the limb bud grows SHH concentration is no longer high in the GREM1 domain; thus BMP4 expression increases and FGFs expression is repressed, bringing an end to the SHH-BMP-FGF feedback loop. (Adapted from Duboc & Logan 2009; Zeller et al. 2009).

The Molecular Mechanism of the Limb Development in Bats

Changes in the expression of several key genes involved in vertebrate limb development have been implicated in the evolution of the bat wing. These include genes that have been associated with the elongation of the forelimb (for e.g. *Hoxd13, prx1, Shh, Fgf8*) and retention of the interdigital webbing (*Bmps*).

Homeobox protein Hox-D13

Hoxa and Hoxd complexes have been classified as major players in anterior-posterior patterning of the limb bud in bats (Schwabe et al. 1998). Hoxd13, in particular, is involved in the development of the autopod growth and skeletal patterning. Consequently, a change in *Hoxd13* expression will mostly likely change skeletal patterns and morphology in the limb (Chen et al. 2005). Chen et al. (2005) investigated the expression of *Hoxd13* in the development of the bat wing, *Carollia perspicillata,* and relative to the mouse limb. The expression of *Hoxd13* in the bat limb bud is very similar to that in mouse limb buds except that in bats *Hoxd13* expression (in embryo stages - Carollia stage (CS) 14-15) is biased towards the distal end of the limb bud. The authors proposed that this change in expression may result in a reduced ulna that is fused to the radius in bats. The study also noted that Hoxd13 expression in the hindlimb begins at a later stage than in mice, and is present at a uniform concentration across the limb bud, suggesting that this gene may be responsible for the digits in the hindlimb being the same length. The authors speculated that there may be a shift in the interaction between *Shh, Fgf4, Bmp* and *Gli3* that results in a change in expression of *Hoxd13* (Chen et al. 2005).

Ray and Capecchi (2008) took the next step and compared the amino acid sequence and Global Control Region (GCR) of *Hoxd13* from bats with other vertebrates. The *Hoxd13* cDNA sequence from *Myotis lucifugus* was shown to be highly conserved when compared to *C. perspicillata* (sequence from Chen et al. 2005), and other vertebrates. The only conserved mutational change between the coding regions of the two bat species, M*. lucifugus* and *C. perspicillata,* was a single serine to alanine mutation. Instead, the key to this novel expression domain most likely lies in the Global Control Region (GCR) of *Hoxd13*. To determine whether this is so, the *Hoxd13* GCR of *M. lucifugus* and *Rhinolophus ferrumequinum* (i.e. one species from each of the two sub-orders of bats, see Figure 2.1) was compared to the Hoxd GCR from other vertebrates (Ray & Capecchi 2008). Twenty six unique insertions (ranging from 10bp to 300bp) were identified which were conserved in the bat GCR; however, these insertions were outside the ultraconserved CsA and CsB regions (Figure 1.4). Six conserved mammalian sequences were absent from the two bat GCR sequences (Ray & Capecchi 2008). These authors also found seven mutations, consisting of changes of 1bp to 3bp, in the ultraconserved regions of the vertebrate GCR that were specific to the bat GCR (Ray & Capecchi 2008). To demonstrate that the difference in expression of HoxD13 in the developing bat was in fact due to changes in the GCR, Ray and Capecchi (2008) linked the bat GCR to a *LacZ* reporter gene to assess enhancer activity of the bat GCR. Ancestral activity domains

were present when using the bat GCR, e.g. *LacZ* activity is seen in the autopod of the developing limb, but there were novel activity domains (Ray & Capecchi 2008). There were also novel regions of activity in the zeugopod and stylopod initiating from stage E11.5 to E16.5, and in the outer ear from stage E13.5 to E16.5. They concluded that in the case of the HoxD cluster, the mutations in the GCR leads to changes in the expression of Hoxd13 in the developing bat limb (Ray & Capecchi 2008).

Figure 1.4: Global Control Region (GCR) of Hoxd13 (black) indicating the location of CsA and CsB regions (purple) and the location of the two bat mutations (red). (Adapted from Ray and Capecchi 2008)

Paired-related homeobox gene effect on limb development

The paired-related homeobox gene (*Prx1 or Prrx1)* contributes greatly towards promoting elongation of the limb skeletal elements in mice (Berge et al. 1998). Based on this, Cretekos et al. (2008) hypothesized that the over-expression of *Prx1* during development may play an important role in the extended growth of the bat wing along the proximal-distal axis. Cretekos et al. (2008) found that early in development (from E9.5 and CS12 up to stage E11.5 and CS15), *Prx1* expression in both bat (*C. perspicillata*) and mouse limb buds is similar. However, during stages E12.0-12.5 and CS16-16L, *Prx1* is up-regulated in bats. Cretekos et al. (2008) investigated whether the up-regulation of the *Prx1* transcripts participated in the extended growth of the bat wing. Replacement of the mouse Prx1 enhancer with the bat *Prx1* enhancer, Cretekos et al. (2008), led to an increase in chondrocyte proliferation in limbs and a 6% increase in the forelimb length in $Prx1^{BatE/BatE}$ transgenic mice. Thus, changes in the *Prx1* enhancer appear to play a small but essential role in the evolution of bat wing together with changes of expression of the other developmental genes (Cretekos et al. 2008), some of which are discussed here.

Bone Morphogenic Proteins and Fibroblast Growth Factor 8

Bone morphogenic proteins (BMPs) also play a vital role in the molecular mechanism of limb development (Tickle 2006) and are known to participate in regulating chondrocyte proliferation. Sears et al. (2006) looked at the contribution of BMPs in the development of the bat wing digits to determine if any evolutionary change may have occurred. They compared the development of the digits in bat forelimbs and mice, looking for physical and molecular differences (Sears et al. 2006). The major difference in morphology was an expansion of the hypertrophic zone of differentiated

chondrocytes in the metacarpals and phalanges of the 3rd, 4th and 5th digits, and an increase in the rate of chondrocyte proliferation in *C. perspicillata* relative to the mouse. (Sears et al. 2006). The expression levels of *Bmp2* transcripts in the developing bat forelimbs (which affect chondrocyte proliferation and differentiation) were increased when compared to mice and rats (Sears et al. 2006). Bat digits increased in length when embryonic bat handplates were cultured in the presence of Bmp2, and adding Noggin (a BMP suppressor) resulted in stunted digits in bats. Thus, the up-regulation of *Bmp2* in the embryonic bat forelimb at CS20 appears to be fundamental for the elongation of the bat digits (Sears et al. 2006)

In the mouse forelimb and the bat hindlimb, the interdigital webbing regresses due to apoptotic events. However, this webbing persists in the bat forelimb and expands to form the chiropatagia. Interdigital webbing also persists in the feet of ducks (Merino et al. 1999). In duck hindlimbs, *Bmps* and the expression of their downstream target *Msx1* is inhibited by the expression of Gremlin in the interdigital tissue, which prevents apoptosis and results in the webbing in duck feet being retained (Merino et al. 1999). Therefore, Weatherbee et al. (2006) proposed that the retention of the interdigital tissue in bat wings might be due to the same or a similar mechanism, i.e. a shift in the expression of *Bmps, Fgfs* and *Gremlin* might explain the retention of the interdigital tissue in bat forelimbs. They examined the expression patterns of *Bmp2, Bmp4, Bmp7, Gremlin, Msx* and *Fgf8* at CS16 and CS17 and found that this was not the case (Weatherbee et al. 2006). Although Gremlin is expressed in the bat forelimb interdigital tissue, unlike in the duck, the expression of downstream targets of BMP signalling, *Msx1* and *Msx2,* was not inhibited in the forelimb interdigital webbing. Their result revealed expression of *Bmp*s in the bat forelimb and a slight down regulation in the interdigital member during CS16 and CS17 through *Gremlin*, which is expressed in the interdigital webbing (Weatherbee et al. 2006).

Fibroblast growth factors (FGF) are another important family of proteins implicated in limb development and, more specifically, *Fgf8* and *Fgf4* are involved in signalling from the AER to stimulate outgrowth of the limb (Niswander 2003; Tickle 2006; Bouldin et al. 2010). Weatherbee et al. (2006) and Cretekos et al. (2007) looked at *Fgf8* expression in the bat limb. Cretekos et al. (2007) looked at the bat *Fgf8* gene sequence and expression (CS11-CS15) in *C. perspicillata,* and compared it to that of the human and the mouse. The width of expression of*Fgf8* in the AER of the bat forelimb was wider than that in the mouse at stages CS12 and CS14 (Cretekos et al. 2007). Although the forelimb bud of both bats and mice stage CS12/E9.5 are initially similar in size, at a later stage (CS14/E10.5) in embryogenesis the bat forelimb bud becomes slightly larger than that

of the mouse (Cretekos et al. 2007). Weatherbee et al. (2006) discovered that unlike mouse autopods, there was expression of *Fgf8* in the interdigital region of the bat, predominately around the posterior digits, at stage CS16 and CS17. This suggests that expression of *Fgf8* in the forelimb may be responsible for the retention of the interdigital tissue in the bat (Weatherbee et al. 2006). Regression of the interdigital tissue could be induced in developing bat forelimbs by inhibiting *Fgf8* signalling and increasing BMP concentration (Weatherbee et al. 2006). Therefore, the combination of *Fgf8* expression and diminished expression of *Bmps* in interdigital tissue could be important for retention of interdigital tissue and the formation of the chiropatagium (Weatherbee et al. 2006).

The above results reveal a delicate interplay between BMP and FGF signalling pathways during limb development in bats at CS16 and CS17. The up-regulation of *Bmps* promotes elongation of the digits, which also promotes apoptosis in the interdigital tissue (Sears et al. 2006). To retain the interdigital membrane, *Fgf8* and *Gremlin* are expressed to inhibit apoptosis and *Bmp* expression (Weatherbee et al. 2006). This suggests that the change in *Fgf8* expression combined with the change in *Bmps* expression was another crucial step in the evolution of the bat wing, allowing the retention of the interdigital membrane and elongation of the digits (Sears et al. 2006; Weatherbee et al. 2006; Cooper & Tabin 2008; Hockman et al. 2008).

Sonic Hedgehog

S*onic hedgehog (Shh)*, a key regulator of anterior-posterior patterning of the autopod, is differentially expressed during limb development in bats (Hockman et al. 2008). Knowing the essential role SHH plays in limb development, Hockman et al. (2008) characterised *Shh* expression and its downstream target *Patched* during bat limb development (early CS14-CS17) in the bat species, *Miniopterus natalensis* and *C. perspicillata,* and compared it to expression in mice. In bats, there was an expansion of the *Shh* expression domain in the forelimb during CS14 (E11.5), similar to the expansion of *Fgf8* expression described by Cretekos et al. (2007). At developmental stage CS16 (E13.0) there is a 'second wave' of *Shh* expression and its downstream target *Patched* in the interdigital membrane in the bat embryos (Hockman et al. 2008). In the bat forelimb, *Fgf8* expression in the interdigital tissue precedes *Shh* expression, and is first detected at early CS15 (E12.0) (Hockman et al. 2008). The second wave of *Shh* expression begins at very early CS16, starting between digits 3 and 4; later, at early CS16 (E12.5), *Shh* expression is extend across from the limb bud with higher concentration at the posterior end (Hockman et al. 2008). In the bat hindlimb, *Fgf8* expression in the interdigital tissue begins at very early CS16, while reactivation of *Shh* expression begins at early CS16 and is uniformly expressed across the limb bud (Hockman et

al. 2008). By CS17 (E13.5) *Shh* expression is turned off in both the forelimb and hindlimb (Hockman et al. 2008). Hockman et al. (2008) postulated that the reactivation of the SHH-BMP-FGF signalling loop plays a major role in the evolution of the bat wing, and this 'second wave' of *Shh* expression in bat limbs is another crucial piece of the puzzle. Fossil evidence suggests that flight evolved once in the bat phylogeny (Simmons et al. 2008), thus hinting that the spatial and temporal change in *Shh* expression in the bat may have been an ancient one (Hockman et al. 2008).

The expression of the *Shh* gene during limb development is regulated by a highly conserved limb-specific long distance *cis*-regulatory sequence known as the ZPA regulatory sequence (ZRS) or mammals-fishes-conserved-sequence 1 (MFCS1) located in intron 5 of *Limb region 1 homolog (Lmbr1)* gene, which is 1Mb upstream of the *Shh* (Sagai et al. 2004; Sagai et al. 2005; Hill 2007; Lettice et al. 2003). The importance of this region in regulating Shh expression is supported by congenital disorders. For example, polydactyly in humans, mice, cats and dogs has been linked to point mutations in the ZRS. The lack of the ZRS has resulted in the loss of limbs in snakes and in limbless newts (Hill 2007; Lettice et al. 2003; Furniss et al. 2008; Lettice & Hill 2005; Lettice et al. 2008; Gurnett et al. 2007; Park et al. 2008; Sagai et al. 2004). It has been shown that expression of *Shh* involves looping of the chromatin so that the ZRS interacts directly with the *Shh* promoter, thereby allowing precise control over spatial-temporal expression of *Shh* (Amano et al. 2009). It has been speculated that mutations in the highly conserved ZRS might have lead to the reactivation of *Shh* expression in bat limb (Hockman et al. 2008).

Aims

In this thesis, I have first investigated the hypothesis that the reactivation of *Shh* expression during limb development in the bat is a result of mutations in the ZRS. Fossil evidence suggests that flight evolved once in the bat phylogeny, and one would therefore expect that these mutations should be conserved across the bat phylogeny (Hockman et al. 2008). I amplified and cloned the ZRS from several bat species representative of the bat phylogeny, and identified any nucleotide changes that were different from the highly conserved vertebrate ZRS, but conserved across the bat phylogeny. Secondly, I compared the ability of the bat ZRS and highly conserved mouse ZRS regions in driving expression of a *LacZ* reporter gene in transgenic mice. Finally, I investigated whether variations in the ZRS between bats correlated with a change in bat wing shape, and whether any particular skeletal element in the bat wing autopod could explain the variation seen in wing shape, i.e. from short, broad wings to long, narrow wings, across bat species.

Chapter 2: Characterisation of the Bat ZRS and the Expression of SHH in the Bat limb

Sonic hedgehog (Shh) has been shown to be a crucial gene in regulating the anterior-posterior patterning and the number of digits in the autopod during limb development as part of the SHH-BMP-FGF feedback loop (Niswander 2003; McGlinn & Tabin 2006; Zeller et al. 2009; Bouldin et al. 2010). The co-option of this signalling loop at a later stage in bat limb development points to a novel role for Shh in regulating the extended outgrowth of the bat metacarpals and phalanges, and the retention of the interdigital tissue during limb development (Hockman et al. 2008). In this chapter, I investigated whether mutations could be identified in the highly conserved vertebrate ZPA regulatory sequence (ZRS) that were retained across diverse bats, which might underpin the change in *Shh* gene expression in limbs during bat development, and the evolution of flight in mammals.

The ZRS and the regulation of SHH in Limbs

The ZRS region was originally identified through studies of preaxial polydactyly (PPD), a congenital physical disorder found in humans, mice, cats and dogs where the individual has extra fingers or toes. Research suggests that the cause of this disorder is a result of change in *Shh* expression (Heutink et al. 1994; Hing et al. 1995; Zguricas et al. 1999; Heus et al. 1999; Lettice et al. 2003; Lettice & Hill 2005; Hill 2007; Lettice et al. 2008; Park et al. 2008). Researchers mapped the mutations that cause these malformations to chromosome 7q36 in human and chromosome 5 in the mouse, where it is located 1 Mb upstream of *Shh,* in intron 5 of *Lmbr1* (Figure 2.1A) (Heutink et al. 1994; Hing et al. 1995; Zguricas et al. 1999; Heus et al. 1999; Lettice et al. 2002). Lettice et al. (2003) showed that within this intron, a region of about 400bp was found to be conserved in human, mouse, chicken and fugu (pufferfish) and a 1.3kb region is conserved in mammals. It was established that the ZRS (approximately 800bp) was responsible for both initiation of *Shh* expression and for defining its spatial expression (i.e. limiting it to the posterior end of the limb) (Lettice et al. 2003).

Lettice et al. (2003) used transgenic mouse experiments to show that the ZRS regulates *Shh*, using a *LacZ* reporter gene linked to a β-globin promoter (BGZ), a promoter also regulated by a long distance control region or enhancer (Q. Li et al. 1999). The 400bp (from fugu) and 1.7kb (i.e. intron 5 of *Lmbr1*) was cloned into the *LacZ* reporter construct just before the promoter, and these constructs were then microinjected into the pronucleus of fertilized mouse eggs (Gordon et al.

1980; Lettice et al. 2003). These eggs were implanted into pseudo-pregnant female mice and either harvested at the desired stage or grown to term to create stable lines (Gordon et al. 1980; Lettice et al. 2003). PCR was used to screen the harvested embryos to confirm positive integration of the construct into the genome of mouse, and β-galactosidase (β-gal) staining was then used to detect expression of the *LacZ* gene (Lettice et al. 2003). They performed *in situ* hybridization of *Shh* mRNA and β-gal staining on the transgenic mice and showed that the 1.7kb reporter construct does in fact mimic endogenous *Shh* expression at stages E10.5-E12.5. The Fugu construct they used also mimicked endogenous *Shh* expression, although it gave a slightly weaker signal (Lettice et al. 2003). A limitation of this method is that activation of the *LacZ* reporter by the ZRS leads to sustained expression of the β-galactosidase enzyme and the permanent marking of SHH-expressing cells. Thus, *LacZ* expression in mice is seen in the autopod beyond E12.5, where detection of *Shh* mRNA transcripts by *in situ* hybridization normally subsides. This suggests that while the ZRS contains the necessary information to initiate *Shh* expression there are other factors that influence precise spatial-temporal expression of *Shh,* such as chromosomal remodelling, which are required to turn it off distance (Lettice et al. 2003).

Sagai et al. (2004) used *in situ* hybridization on a mouse mutant, *Hemimelic-extratoes* (*Hx*), to show that mutations in the ZRS conserved region caused *Shh* to be expressed in both the anterior and posterior of the limb buds. The *Hx* mutant has *Shh* and *Patched* expression not only in the ZPA (i.e. posterior end of the limb bud) but also on the anterior end of the limb bud at E11.5. Based on this, they hypothesized that if *Shh* had such a crucial role in the development of autopods then this *cis*-regulatory sequence should be present in vertebrate lineages in which *Shh* is expressed in limbs or fins. This was confirmed with an alignment of the ZRS sequences amplified from various tetrapods and bony fish, and was further supported with Southern blots showing the absence of the ZRS in snakes and limbless newts. Furthermore, knocking out the ZRS results in loss of *Shh* expression and truncated limbs (Sagai et al. 2005), hence supporting the theory that the ZRS is a limb specific *cis*-regulator of *Shh.*

Maas and Fallon (2005) used the transgenic experiments (described above) to test whether in fact single base changes in the ZRS do result in anterior expression of *Shh*. Maas and Fallon (2005) had two variations of *heat shock protein 68 (Hsp68)* promoter/*LacZ* gene construct: one has the wild-type 1.7kb conserved fragment identified by Lettice et al. (2003), and the other has the same fragment with a single nucleotide mutation identified in *Hx* mutants. Analysis of the transgenic mice showed that the transgenic embryos with the *Hx* mutation reporter construct expressed β-

galactosidase in both the anterior and posterior ends of the limb buds, while the transgenic embryos containing the wild-type construct only showed expression in the posterior end of the limb buds (Maas & Fallon 2005).

Lettice et al. (2008) conducted a series of transgenic experiments showing that the severity of the PPD phenotype is linked to the degree of change in SHH expression, which directly linked to specific point mutations in ZRS. To do this, they compared two human PPD causing mutations: the Cuban mutation, which has a severe phenotype; and the Belgian 2 mutation, which has a milder phenotype. They introduced each mutation into the mouse ZRS-lacZ reporter and then used transgenic experiments to characterise the difference in expression. The Cuban mutation resulted in β-gal expression in the anterior and the posterior of limb buds, while the Belgian2 mutation caused only a weak expression of β-gal in the anterior of the limb buds. To confirm that the β-gal expression patterns caused by the mutations in mouse ZRS is the same as if the mutations were in human ZRS, they cloned the human ZRS with the Cuban mutation into the BGZ reporter construct. Transgenic results of the human and mouse ZRS were in fact similar, leading to the conclusion that the severity of the PPD phenotype is directly linked to changes in SHH expression (Lettice et al. 2008).

Since this discovery, many researchers have identified other single base pair mutations that cause a disruption or change in *Shh* expression (and that of downstream targets) resulting in polydactyly, triphaliangeal thumb-polysyndactyly syndrome (a congenital physical disorder characterised by webbing of the fingers and thumbs with three bones instead of two), and other limb malformations in humans and other mammals like mice, cats and dogs (Sagai et al. 2005; Maas & Fallon 2005; Gurnett et al. 2007; Hill 2007; Lettice et al. 2008; Park et al. 2008).

Lettice et al. (2008) identified three different point mutations that cause PPD in cats (see Figure A-1 for location of the mutations in ZRS). The first transgenic experiments involved five different variations of BGZ construct, one containing the cat wild type ZRS, one with the UK2 cat ZRS (A to T mutation), one with the Hemingway (Hw) cat ZRS (A to G mutation), one with the mouse ZRS containing the UK2 mutation and then one with the mouse ZRS containing the Hw mutation. The wild type cat type ZRS generated β-gal expression in the posterior end of the limb bud and extended along distal margin. The Hw mutant cat ZRS shows expression similar to the wild type, except that there was ectopic β-gal expression in the anterior end of the forelimbs, while the UK2 cat ZRS showed ectopic expression in the anterior end in the hindlimbs. The embryos injected with

the mouse ZRS containing either the Hw or the UK2 both had low β-gal expression in the anterior end of both the forelimb and hindlimb, along with normal expression in the posterior end of the limbs (Lettice et al. 2008).

Park et al. (2008) discovered two mutations (DC1 and DC2) causing hindlimb specific PPD in dogs and are located upstream of the ZRS, in what they classified as the pZRS element. They then linked wild type dog ZRS and the two mutated dog ZRS to BGZ and microinjected this into mouse embryos. Transgenic embryos with the mutated pZRS-ZRS construct showed similar expression to wild type at stage E11.5, β-gal expression in posterior end of the limb bud. At E13.5, β-gal expression was the same in the forelimb of both mutated and wild type transgenic embryos; the expression was in the posterior end of autopod covering digits 3 to 5. On the other hand, in hindlimb of the mutated transgenics, there was expression from digits 2 to 5, while the wild type expression was in digits 3 to 5. This suggests the pZRS element could be involved in another mechanism underlying the unique hindlimb-specific digit patterning in the dog PPD (Park et al. 2008).

Researchers have postulated that the ZRS uses a similar mechanism to the β-globin locus control region (LCR) to interact with *Shh* (Sagai et al. 2005; Zeller & Zuniga 2007), i.e. interaction between *Shh* promoter and the ZRS would involve looping of the DNA strands, as shown in the case of the LCR (Q. Li et al. 1999; Palstra et al. 2008). In 2009, Amano and colleagues showed that interaction between the ZRS and the *Shh* promoter proved to be similar to the LCR. For SHH expression to occur in the limb bud, chromosome 5 must change its conformation so that the ZRS comes into contact with the *Shh* transcriptional start site and the *Shh* coding region must loop out of its chromosome territory (CT) to start transcription of *Shh* (Figure 2.1 B-D) (Amano et al. 2009). This leads to the classification of three chromosome conformation states: the silent state (Figure 2.1B) – where the ZRS is far away from the *Shh* promoter, the poised state – where the ZRS interacts with the SHH promoter but remains in the CT (Figure 2.1C) and the active state – where ZRS interacts with the SHH promoter and the SHH coding region loops out of the CT (Figure 2.1D) (Amano et al. 2009). To determine the role that ZRS may play in the remodelling of the chromosome, the authors looked at the limb cells from ZRS knock-out transgenic mice. Their results showed that while there was still a direct interaction between the *Shh* promoter and intron 5 of the *Lmbr1* gene in the mutant mice, there was no relocation of this region to the outside of the CT (Figure 2.1 C), suggesting that the ZRS is vital for the 'looping out' of the CT (Figure 2.1 D). Another surprising finding was that, in wild type cells, only about 18% of the cells in the ZPA were

in the active state conformation during SHH expressions, which led the authors to speculate that the state of chromosome conformation of individual ZPA cells varies between the three states, hence allowing for finer regulation of the spatiotemporal patterns and concentration of SHH during limb development (Amano et al. 2009).

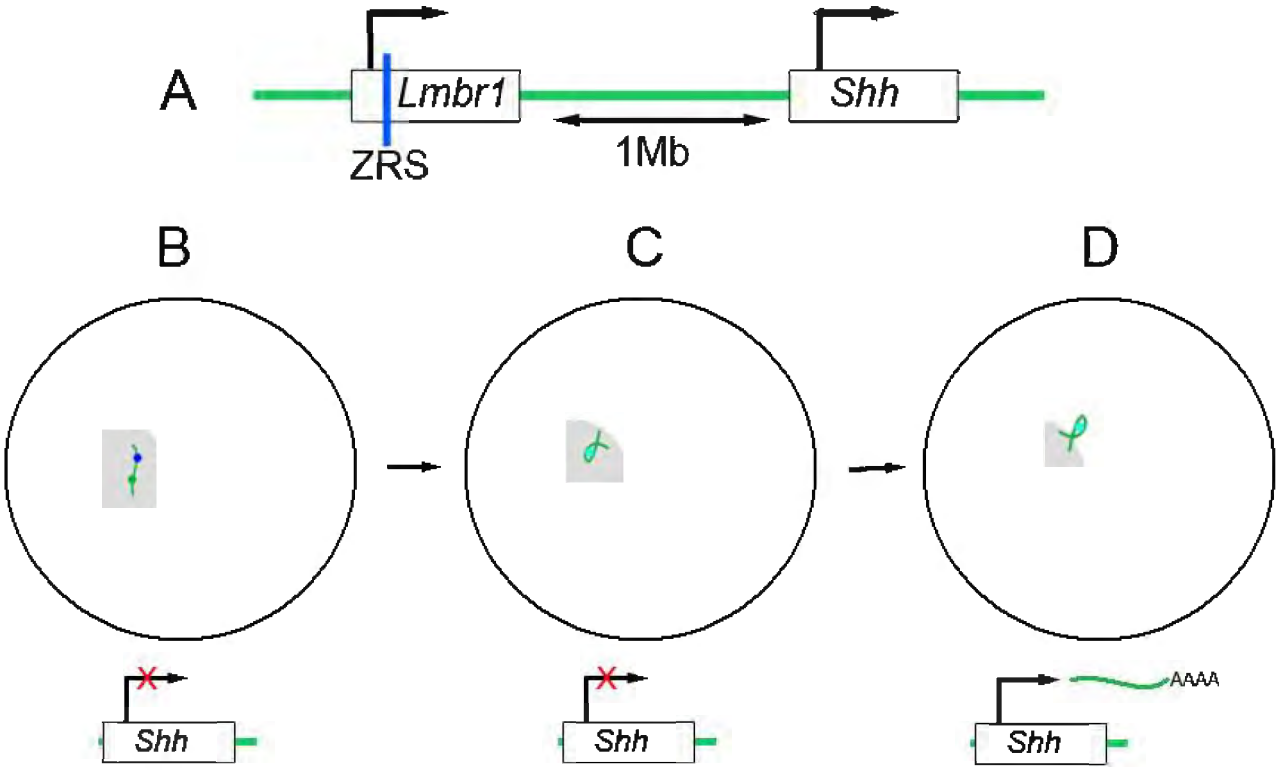

Figure 2.1: The mechanism by which the ZRS and *Shh* interact to initiate expression. A: A graphical representation of the locations of the ZRS in the *Lmbr 1*gene (represented in blue), upstream of the *Shh* gene. B: The circle represents the cell's nucleus and the grey area is the CT of chromosome 5. The green strand highlights the position of the ZRS (blue dot) and the UTR of *Shh* (green dot). In this case, there is no interaction between the ZRS and *Shh* and thus no transcription. C: The DNA loops on itself so that the ZRS and the *Shh* interact in *cis* (cyan dot), but because in remains in the CT there is still no transcription. D: Transcription of the *Shh* gene only occurs once the ZRS and *Shh* are interacting and 'loop' out of CT of chromosomes 5.

As mentioned in chapter one, the central hypothesis of this thesis is that the reactivation of *Shh* during limb development in bats is a result of changes in the ZRS, and that such changes in sequence should be conserved across bat phylogeny. The purpose of this chapter is therefore to identify any mutations in the bat ZRS that are conserved across the bat phylogeny, and to compare the ability of the bat ZRS and mouse ZRS in driving expression of a *LacZ* reporter gene in transgenic mice.

Material and Methods

Bat Tissue

Tissue samples used were either wing or liver biopsies taken from a variety of bat species, including *Anthops ornatus*, *Chaerophan jabensis*, *Cardioderma cor*, *Carollia perspicillata, Hipposderos commersoni*, *Macroderma gigas*, *Megaderma lyra*, *Miniopterus natalensis, Mystacinca tuberculata*, *Natalus major*, *Natalus micropus*, *Nocitilio albirentras*, *Pteronotus parentelli*, *Rhinolophus capensis, Rhinolophus clivosus, Rhinolophus darlingii*, *Rhinolophus swinnyi*, *Rhinopoma hardwickii* and *Rhinopoma microphyllum*, which were selected according to the family they belong to on the Bat phylogenic tree (see Figure 2.2) (Eick et al. 2005). Bat tissue samples, which were stored in 70% ethanol at -20°C, were provided by Assoc. Prof. David Jacobs (Zoology Department, UCT), with the exception of *Carollia perspicillata,* which was provided by Richard Behringer (Department of Molecular Genetics, The University of Texas, Houston, Texas, U.S.A).

Genomic DNA Extraction

The bat tissue was incubated in 400µl Lysis buffer (0.91mM Tris-HCl (pH8), 1.82mM EDTA, 4.55mM NaCl, and 4.5% SDS (v/v)), adding 100µl Proteinase K (10µg/µl) at 55°C overnight, or until the tissue was completely digested. The cellular debris was removed by precipitating using 250µl of 5M NaCl and then centrifuged. The supernatant was transferred to a new eppendorf and 600µl of chloroform:isoamyl alcohol (24:1 v/v) was added, then centrifuged. The aqueous layer was transferred to a new eppendorf and mixed with 1ml of isopropane, and left to precipitate overnight at -20°C. The solution was centrifuged and the DNA pellet was washed twice with 70% ethanol (v/v). All centrifugation was done at 13000xg for 10 min. The DNA pellet was then resuspended in 50µl DNase and RNase free water. DNA purity and concentration was measured by A_{230nm}, A_{260nm} and A_{280nm} absorbance readings on a © ND-1000 Spectrophotometer (Labtech International LTD, USA).

Tissue samples for some of the bat species were not available (*Artibeus jamaicensis*, *Miniopterus schreibersii*, *Molossops themincki*, *Rhinolophus capensis*, *Rhyneonycteis naso* and *Throyptera lavali*). The genomic DNA for these species were obtained from stored samples purified by Geeta Eick (Eick et al. 2005).

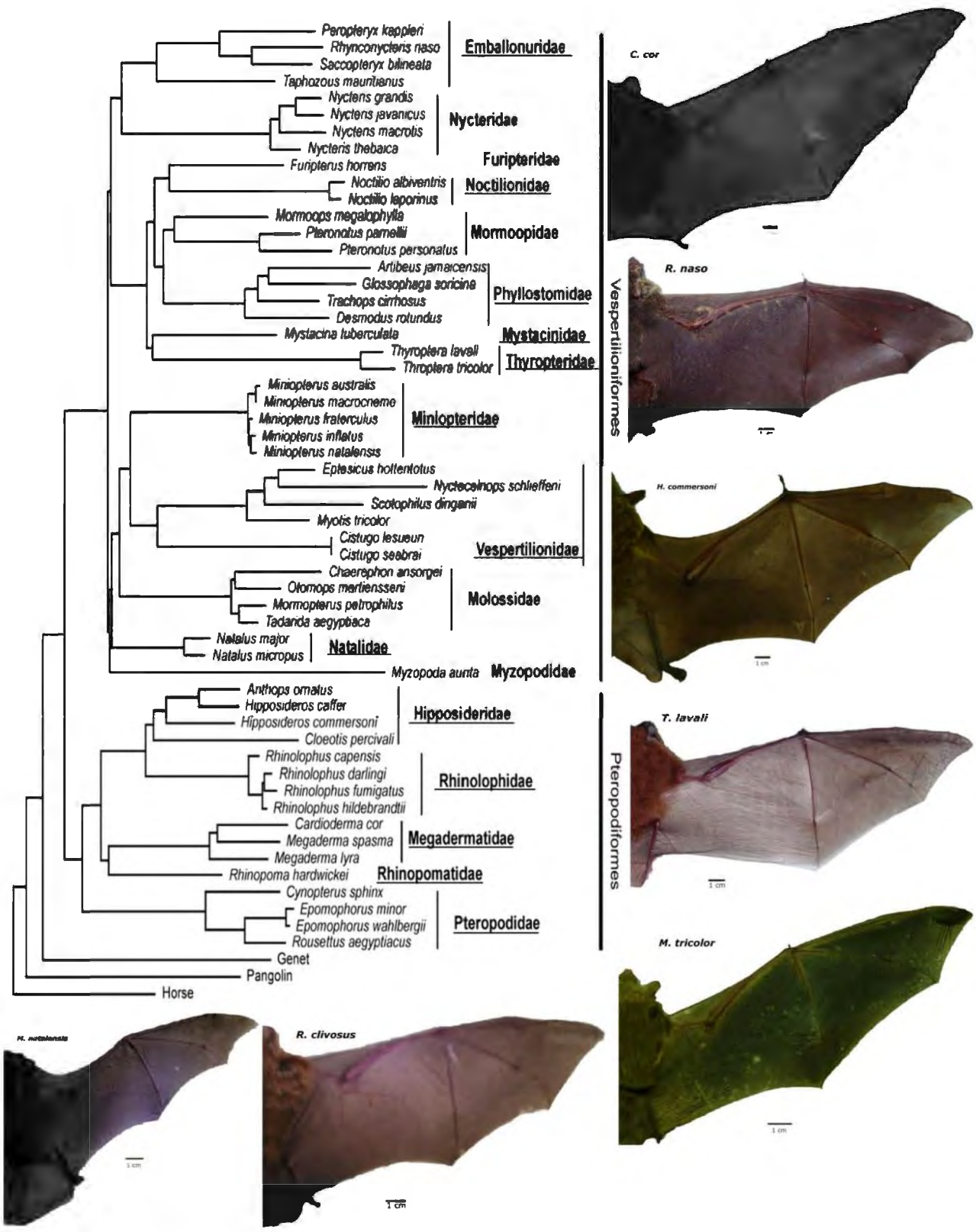

Figure 2.2: A maximum likelihood phylogenetic tree constructed using introns from four nuclear genes (PRKC1, SPTBN, STAT5A, and THY) adapted from Eick et al (2005). Photos were provided by Assoc. Prof. David S. Jacobs's laboratory. The phylogenetic tree shows the distribution of the bat phylogeny, and the families from which samples were taken from are underlined.

Amplification of the bat ZRS by PCR

SuperTherm *Taq* PCR Kit (Medox Biotech., India) was used for amplification of the full length ZRS from bat genomic DNA. The total volume of each PCR reaction was 25µl and the final concentrations of components in the PCR reaction were 0.1U/µl of SuperTherm *Taq* polymerase, 1x PCR buffer, 1.5mM magnesium chloride ($MgCl_2$), 0.2mM dNTPs, 1.0µM for each primer and 8ng/µl of genomic DNA template. The Gene AMP© PCR System 9700 (Applied Biosystems, Singapore) was used for all PCRs. See Table 2.1 for the primers used to amplify the bat *Shh* ZRS. Thermal cycling conditions for the ZRS PCR pair of primers were an initial denaturing step of 5 min at 95°C, followed by a total of 30 cycles of30 sec at 95°C, 30 sec at 60°C, 30 sec at 72°C, and a subsequent elongation step of 5 min at 72°C, followed by a 5 min cooling down step at 4°C.

Table 2.1: The following table shows the primers sets used for this research and their sequences. The nucleotides highlighted in green indicates where *HindIII* restriction enzyme sites were incorporated in the subcloning primers and the nucleotides in red show the position of mutations in the mutagenesis primers, where INT refers to a bat insertion, DEL refers to a deletions and BC refers to base pair changes (BC).

Method	Primer name	Primer sequence (5' to 3')
ZRS PCR	BAT ZRS 800 FRW	TCACCTTAATGCCGATCTTTGATTTGAAATCATAGC
	BAT ZRS 800 REV	AACACATAACAGTGGTCAGTGAGATATGACTCC
Subcloning primers	BAT ZRS 800 - Hind III FRW	TGTATAAGCTTCACCTTAATGCCGATCTTTGATTTGAAATCATAGC
	BAT ZRS 800 - Hind III REV	ATGACAAGCTTACACATAACAGTGGTCAGTGAGATATGACTCC
Mutagenesis primers	Mutation 1 - INT Sense	TCTTAAAGAGACGCAGAGAGTAGGAAGTCC
	Mutation 1 - INT 2 Sense	CTCAGGCCTCCATCTTAAAGAGACGCAGAGAGTAGGAA
	Mutation 1 - INT 2 AntiSense	TTCCTACTCTCTGCGTCTCTTTAAGATGGAGGCCTGAG
	Mutation 2 - DEL Sense	AAACTCAGTCGGTTCTGCTGGGTGAAAGG
	Mutations 3-5 - BC Sense	TGCAAGGAAATTCGACCAGGGCATGTTTTGATC
Sequencing primers	pBGZ40 -seq	GCTGCAGGAATTCGATATCAA

Gel Electrophoresis and Gel purification of PCR products

All agarose gels were made at a concentration of 1% (w/v) with 1x Tris-acetate buffer and 1µl of ethidium bromide was added to 50mls of agarose solution. Gels were electrophoresed at 110V for 30 to 45 min. The following three different markers were used to indicate PCR product sizes; MassRuler™ DNA ladder (M1), GeneRuler™1kb DNA ladder (M2) and FastRuler™ Low Range ladder (M3) (Fermentas, USA).

PCR products were cut out of the gel over a long wavelength UV. The Wizard PCR and Gel extraction kit (Promega, USA) were used according to the manufacturer's protocol except for the final step. The elution buffer, or DNase and RNase free water, was applied to the column and incubated for 10 to 15 minutes at room temperature to increase yields.

Cloning PCR Products: Ligations and Transformation

All PCR products were cloned into the pGEM-T Easy Vector System (Promega, USA), according to the manufacturer's suggested protocol. All ligations were incubated at 4°C overnight and inactivated at 70°C for 15 min before transformations into competent *E. coli XL-1 Blue* cells (kindly provided by Lab 425, Dept of Molecular and Cell Biology).

A standard heat shock transformation method was used. After inactivation, 2- 5µl of the ligation reaction were added to 100µl of competent cells and incubated on ice for 10 min. Cells were then heat shocked at 37°C for 5 min and snap cooled on ice for 2 min. Cells were incubated for 1 hour at 37°C after adding 900µl of Luria broth (LB) to each transformation reaction.

When spread plating, a 100µl of each culture was spread on Luria agar (LA) – Ampicillin – IPTG –X-Gal plates to use white/blue selection of recombinant plasmids. Cells were centrifuged at 8000xg and the pellet was resuspended in 100µl of LB, to concentrate cells, prior to plating. Plates were incubated overnight at 37°C. With each transformation reaction, there was a pSK (1ng/µl) transformation control, so as to calculate transformation efficiency, and a no plasmid control, to control for contamination.

Subcloning the bat ZRS inserts and the mouse ZRS into the pBGZ40 transgenic mouse expression vector

The ZRS from *Mus musculus* (provided by Dr. Laura Lettice, at the MRC Human Genetics Unit, Western General Hospital, Edinburgh, UK), *M. natalensis* and *R. clivosus,* were cloned into the pBGZ40 (#1230) plasmid that contains a β-globin minimal promoter that drives the expression of LacZ reporter gene (provided by Dr. Laura Lettice) for the transgenic experiments (see below) (Lettice et al. 2002). All restriction enzyme digests were done using the *HindIII* enzyme (Fermentas, USA).

The pBGZ40 plasmid was linearized by digestion with 10U of *HindIII* enzyme in a 20µl total volume with final concentration 250ng/µl of plasmid DNA, and 1x Red Buffer. The restriction enzyme reaction was incubated at 37°C for 2 hours. The enzyme was then heat inactivated at 80°C for 10 min before 5U of Thermosensitive Alkaline Phosphatase (TSAP, Promega, USA) was added to the

pBGZ40 reaction, so as to prevent self-ligation of the plasmid, and incubated at 37°C for 30 min. Once again, TSAP enzyme was heat inactivated at 80°C for 10 min. Reactions were run on a 1% agarose gel and purified using the above protocol.

For the cloning of the bat (*M. natalensis* and *R. clivosus*) ZRS sequences into the pBGZ40 expression vector, PCR was used to first add flanking *HindIII* sites on either side of the inserts using the primers shown in Table 2.1. For the PCR, the Advantage 2 PCR kit (Clonetech, USA) was used to minimize the error rate during cloning. The total volume of each PCR reaction was 50µl and the final concentrations were 0.022µg/µl Advantage 2 Polymerase mix, 1x PCR buffer, 0.2mM/µl (each) dNTP Mix, 0.2µM for each primer and 2ng/µl of plasmid DNA template. The thermal cycling conditions for this PCR were an initial denaturing step of 5 min at 95°C, followed by 30 cycles of: 30 sec at 95°C, 1 min at 68°C, 30 sec at 72°C, and then a 5 min elongation step at 72°C, and a final cooling down step for 5 min at 4°C. The PCR products were extracted from the agarose gel using the protocol described previously. The two bat ZRS PCR products with flanking *HindIII* sites were digested using the *HindIII* restriction enzyme in a reaction of 20µl containing a final concentration of 19ng/µl of PCR product, 10U of enzyme and 1x Red Buffer. Reactions were incubated at 37°C for 3 hours and were run on an agarose gel, then purified using the above protocol.

The *M. musculus* ZRS in pBGZ40 (pMmu -BGZ 1) was subcloned into unaltered pBGZ40 plasmid to insure that there were no mutations to the β-globin LacZ construct. The mouse ZRS was isolated by doing a RE digest, in a total 20µl with final concentration of the reagents were 250ng/µl of plasmid DNA, 1U/µl of *HindIII* and 1x Red Buffer. The RE reaction was incubated at 37°C for 2 hours. The enzyme was then heat inactivated at 80°C for 10 min. The reaction was then run on a 1% agarose gel and then purified using protocol described previously.

T4 DNA ligase (Fermentas, USA) was used to ligate the three ZRS PCR products into linearized pBGZ40 according to the manufacturer's protocol. Reactions were incubated at room temperature for an hour. Reactions were inactivated at 80°C for 15 min before transformation into competent E. coli XL1-Blue (protocol described above).

Colony PCR to confirm recombinant plasmids

PCR using T7 and SP6 primers, which flank the insert site on pGEM-T, was performed on white colonies to confirm the presence of inserts of the correct size. Final PCR reagent concentrations in 20µl were: 1U of SuperTherm (Medox Biotech India Pvt. Ltd., India) *Taq* polymerase, 0.2mM of dNTPs, 1.5mM $MgCl_2$, 0.5 µM of each primer, 1x PCR Buffer. One colony was picked with a sterile

toothpick, spotted on a master plate (which was incubated at 37°C overnight) and then the toothpick was plunged into the PCR mix. The following thermal cycling conditions were used in those colony PCR reactions: an initial denaturing step of 5 min at 95°C, followed by 30 cycles of 30 seconds at 95°C, 30 seconds at 52°C, 30 seconds at 72°C, and then an elongation step of 5 min at 72°C, and a cool down step of 5 min at 4°C.

Mutagenesis of the Mouse ZRS

The QuikChange II Multi Site-Directed Mutagenesis Kit (Stratagene, USA) and QuikChange II Site-Directed Mutagenesis Kit (Stratagene, USA) were used to insert the five conserved bat point mutations into the mouse ZRS cloned in the pBGZ40 vector. The mutagenesis PCR primers (see Table 2.1) were designed according to the manufacturer's instructions. These protocols had 3 steps: Step 1 - mutagenesis PCR, Step 2 - digestion of original vector and Step 3 - transformation of mutated vector (Figure 2.3).

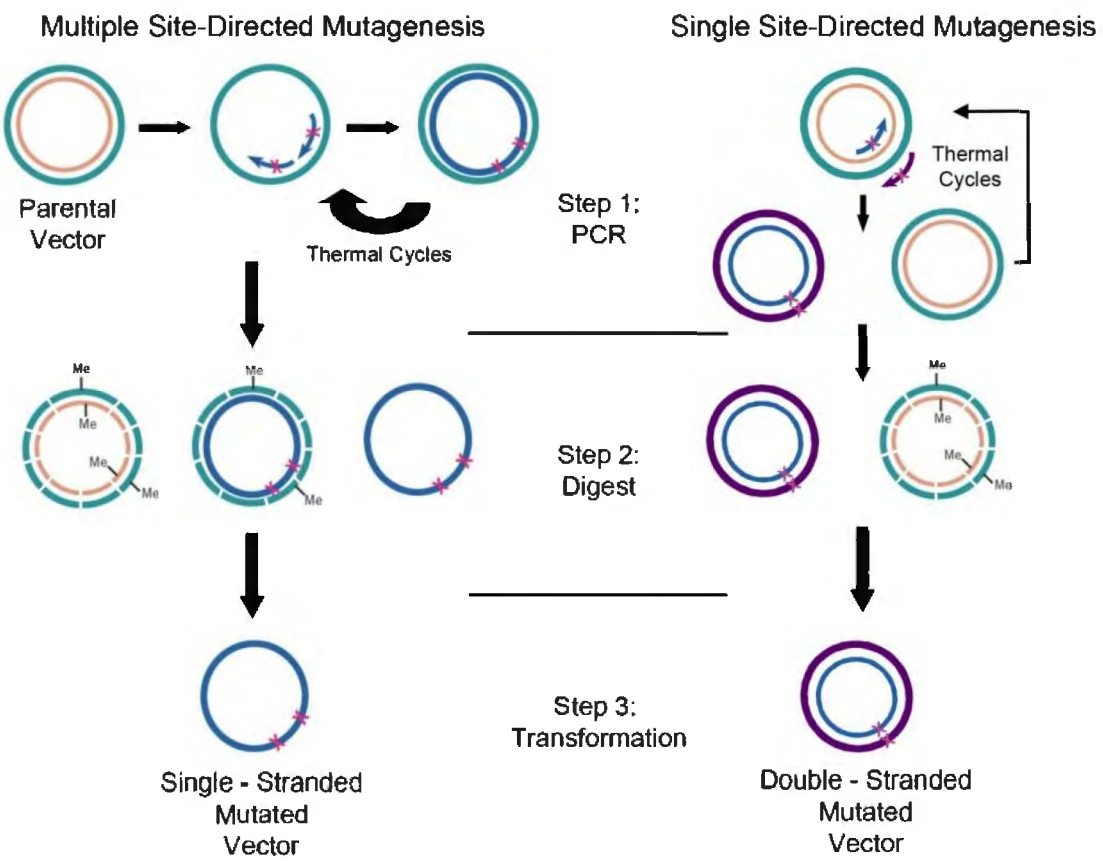

Figure 2.3: Overview of the Site-Directed Mutagenesis procedure. The blue (sense) and purple (anti-sense) arrows with pink 'X' represent the primers with the desired mutations. Step 1 is the inserting or deleting or mutating base pairs in the parental vector that are methylated (-Me) through PCR, so that the predominating vector contains the desired mutations. Step 2 is removal of the parental vector through restriction enzyme reaction using *Dpn I*, which only cuts methylated DNA. Step 3 is transforming the intact mutated vector into the competent cells. (Adapted from Manufacturer's manual)

Step 1: Mutagenesis PCR

To insert all 5 point mutations into the mouse ZRS, the QuikChange II Multi Site-Directed Mutagenesis Kit (Stratagene, USA) was used in combination with the following primers: Mutation 1-INT Sense, Mutation 2-DEL Sense and Mutation3-5-BC Sense. Final reagent concentrations for the PCR mutagenesis reaction in 25 µl were: 0.1U/µl of QuikChange Multi enzyme blend, 1 µl of dNTP mix, 1x of QuikChange Multi reaction buffer, 4ng/µl of pBGZ-MZ vector, 8ng/ µl of mutagenesis primer, and 0% or 3.2% of QuikSolution (v/v). Primers were omitted in a control reaction for the original vector not being fully digested in Step 2. Final reagent concentrations for the manufacturer's positive control reaction in 25 µl were: 0.1U/µl of QuikChange Multi enzyme blend, 1 µl of dNTP mix, 1x of QuikChange Multi reaction buffer, 2ng/µl of control template (a pBluescript II SK derived plasmid), and 4ng/µl of each control primer. Once again, the same reaction was repeated without primers as a control for Step 2.

Thermal cycling conditions were as follows: 1 min at 95°C, and 30 cycles of 1 min at 95°C, 1 min at 55°C, 18 min at 65°C. Reactions were then placed on ice for 2 min.

To insert mutation 1 (i.e. mutation CGC) into the mouse ZRS, the QuikChange II Site-Directed Mutagenesis Kit (Stratagene, USA) was used with primers Mutation 1-INT 2 Sense and Mutation 1-INT 2 Antisense. Final reagent concentrations for the experimental reaction in 50µl were: 0.05U/µl of *Pfu Ultra* High Fidelity DNA polymerase, 1µl of dNTP mix, 1x of QuikChange reaction buffer, 0.2 or 1ng/µl of pBGZ40-Mmu vector, and 2.5ng/ µl of each mutagenesis primer. The same reactions were repeated without primers as a control for Step 2. Final reagent concentrations for the manufacturer's control reaction in 50µl were: 0.05U/µl of *Pfu Ultra* High Fidelity DNA polymerase, 1µl of dNTP mix, 1x of QuikChange reaction buffer, 0.2ng/µl of pWhitescript (control plasmid), and 2.5ng/µl of each control primer. Once again, this reaction was repeated without primers as a control for Step 2.

Thermal cycling conditions were as follows: 1 min at 95°C, and 18 cycles of 1 min at 95°C, 1 min at 60°C, 8 min at 68°C, and a final elongation step of 7 min at 68°C. Reactions were then placed on ice for 2 min.

Step 2: Digestion of parental vector

To remove the parental vector, 1U of *DpnI* restriction enzyme was added to each reaction, after completing step 1, and incubated at 37°C for an hour. *DpnI* only digests methylated DNA;

therefore the enzyme would only digest the parental vector because it is extracted from *E.coli* XL-blue, a bacteria that methylates its DNA.

Step 3: Transformation of mutated vector

The reactions were then transformed into XL-1Blue *E. coli* competent cells using the protocol described above, except that 10µl of each reaction was used for transformation. The clones were then screened using blue-white selection and sent for sequencing to confirm that the mutagenesis had been successful.

Plasmid Purification

Colonies shown to have inserts were grown overnight in 5ml LB-AMP at 37 °C. The PureYield© Miniprep Kit (Promega, USA) was used to isolate plasmid from overnight cultures. The manufacturer's protocol was followed except for the final step, whereby the DNase and RNase free water was applied to the column and incubated for 10 to 15 min at room temperature to increase yields. For higher yields of the plasmids, the PureYield© Midiprep Kit (Promega, USA) was used with the Vacuum manifold (Promega, USA) and the manufacturer's protocol was followed without alterations.

Sequencing of Bat ZRS Clones

Purified recombinant plasmids with the ZRS from various bat species were sent to Macrogen (Korea) for sequencing using T7 and SP6 primers. The *Myotis lucifugus* ZRS, *Pterotrus vampyrus* and other vertebrate ZRS sequences were downloaded from the Ensembl database (Flicek et al. 2010).

The clones from the mutagenesis PCR experiments were sent to the University of Washington High-Throughput Genomics Unit (UWHTGU) in Seattle, Washington, USA for sequencing, using the T3 vector primer and a custom forward primer pBGZ40-seq (see Table 2.1).

Sequence Analysis

Bioedit software (Hall 1999) was used for visualization of nucleotide sequences and trimming of vector sequences from all the bat ZRS clones. The sequences were blasted against the NCBI database (using the blastn algorithm) to confirm their identity as ZRS homologues (Camacho et al. 2009). PRANKSTER (Löytynoja & Goldman 2005; Löytynoja & Goldman 2008) was used to align the bat ZRS sequences with various vertebrate ZRS sequences to identify conserved difference in the bat ZRS sequences.

For the mutated mouse ZRS sequences, SeqTrim (Falgueras et al. 2010) was used to remove all vector sequences. All sequences were subsequently aligned to the original mouse ZRS sequence using ClustalW in Bioedit (Hall 1999) to check whether mutagenesis was successful.

Table 2.2: List of bat species and vertebrates used for sequence analyses.

Bat Species	GenBank ID	Animal	Ensembl id
Anthops ornatus	JN800405	Anole lizard	ENSACAG00000011102
Hipposideros commersoni	JN800418	Cat	ENSFCAG00000008207
Artibeus jamaicensis	JN800415	Chicken	ENSGALG00000006400
Carollia perspicillata	JN800413	Chimpanzee	ENSPTRG00000019915
Mystacina tuberculata	JN800414	Cow	ENSBTAG00000030817
Natalus major	JN800410	Dog	ENSCAFG00000005134
Noctilio albiventris	JN800411	Dolphin	ENSTTRG00000009617
Rhinlophus capensis	JN800419	Elephant	ENSLAFG00000017746
Rhinlophus clivosus	JN800407	Frog (Xenopus)	ENSXETG00000013512
Rhinolophus darlingii	JN800409	Gorilla	ENSGGOG00000015072
Rhinopoma hardwickii	JN800417	Guine pig	ENSCPOG00000003305
Rhynconycteris naso	JN800416	Horse	ENSECAG00000024396
Thyroptera lavalii	JN800408	Human	ENSG00000105983
Carioderma cor	JN800406	Mouse	ENSMUSG00000010721
Miniopterus natalensis	JN800412	Mouse lemur	ENSMICG00000015471
Miniopterus schreibersi	JN800420	Opossum	ENSMODG00000005081
Myotis lucifugus	ENSMLUG00000015310	Orangutan	ENSPPYG00000018221
Pteropus vampyrus	ENSPVAG00000014758	Pig	ENSSSCG00000016412
		Rat	ENSRNOG00000005306
		Zebra finch	ENSTGUG00000000698

Expression Analysis of Bat ZRS in Transgenic Mice

Transgenic mouse experiments were used to test the functional importance of changes in the bat ZRS sequence compared to the mouse ZRS. The BGZ40 plasmids, pMna-BGZ, pRcl-BGZ and pMmu^{5m}-BGZ, were sent to Dr. Laura Lettice at the MRC Human Genetics Unit (Western General Hospital, Edinburgh, UK) for micro-injection into mouse embryos. These vectors were linearized and individually microinjected into CBA/C57B16 mouse embryos, and then placed in the uterus of pseudo-pregnant female mice. Whilst some batches of generation zero (G_0) embryos were harvested at E11.5 and E13.5 stages of pregnancy, other batches were allowed to go to term to generate stable lines. Embryos from stable lines, were collected and E10.5, E11.5, E12.5 and E13.5.

All embryos were stained for β-galactosidase activity as described by Lettice et al. (2003), which was done at t the MRC Human Genetics Unit (Western General Hospital, Edinburgh, UK).

Results

Extraction of Genomic DNA

Genomic DNA (gDNA) was extracted from wing biopsies of various bat species, which were selected based on their location on the Bat phylogenic tree published by Eick et al. (2005) and the family they belonged to (Figure 2.2). Good quality, intact gDNA was purified in an initial trial gDNA extraction using *M. natalensis* and *R. clivosus* wing membrane samples (Figure 2.4A, Table 2.2) This DNA was then used for a trial PCR, and a single PCR product of the expected size of approximately 800bp was amplified (Figure 2.4B).

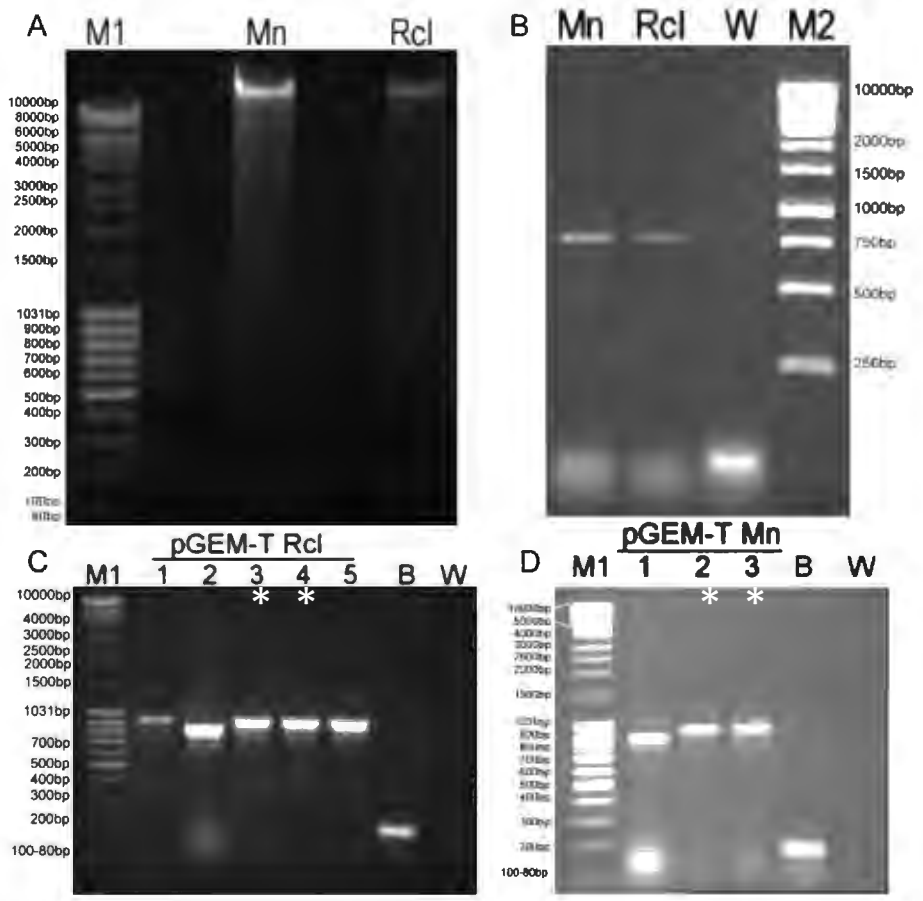

Figure 2.4: The successful results of the gDNA extraction and the PCRs done on *M. natalensis* (Mn) and *R. clivosus* (Rcl) tissue samples. A: Genomic DNA purifiedfrom *M. natalensis* and *R. clivosus* can be seen as an intact band migrated above 10 000bp. B: The ZRS from both *M. natalensis* and *R. clivosus* was amplified during the PCR and is shown by the single band migrating to just above 750bp. C: Colony PCR results for *R. clivosus* ZRS. D: Colony PCR results for *M. natalensis* ZRS. The water control (W) shows no foreign contamination and the negative control is a blue colony (B) i.e. pGEM-T easy with no inserts. The asterisks (*) show the clones sent off for sequencing.

Genomic DNA extractions for the other species gave varied results as shown by the gel photos (Figure A.1) and spectrophotometer results (Table A.1). Some gDNA samples showed signs of degradation (such as the RhH sample in Figure A.1) and some were contaminated with phenol, giving poor 260/280 ratios. These variable results could be due to the sampling and storage

conditions of the bat biopsies. Nevertheless, all the extracted gDNA samples were used for PCR because of the limited amount of tissue biopsies available. Although no gDNA was visible for *Cardioderma cor,* this was because the gDNA was at such a low concentration (Table A.1); therefore the sample was used. Some of the gDNA used was extracted by previous postgraduates because there was no available tissue for the following species: *Artibeus jamaicensis* (ArJ), *Carollia perspicillata* (CrP), *Miniopterus schreibersii* (MiS), *Molossops themincki* (MoT), *Rhinolophus capensis* (Rcp), *Rhyneonycteis naso*(RhN) and *Throyptera lavali* (ThL) (Eick et al. 2005; Hockman et al. 2008).

Amplification and Cloning of the Bat ZRS

The amplification of the ZRS from the other bat species proved to be more difficult, and multiple PCRs were performed using *R. clivosus* gDNA as a positive control. Bands of the right size, i.e. above the 750bp, were considered positive ZRS sequence (Figure 2.5). The ZRS was amplified from 16 bats species: *A. ornatus, A. jamaicensis, C. cor, C.perspicillata, H. commersoni, M. natalensis, M. schreibersii, M. tuberculata, N. major, N. albirentras, R. capensis, R. clivosus, R. darlingii, R. hardwickii, R. naso* and *T. lavali.*

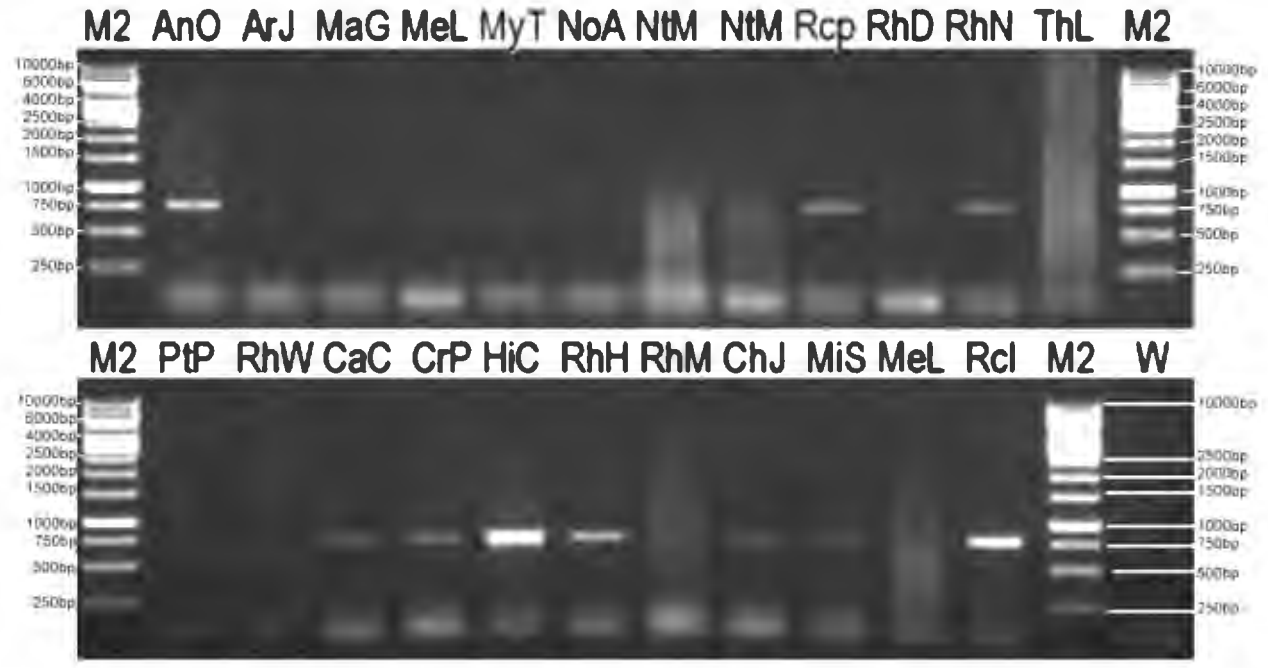

Figure 2.5: PCR results of A. ornatus, A. jamaicensis, C. cor, C. jabensis, C. perspicillata, H. commersoni, M. gigas, M. lyra, M. natalensis, M. schreibersii, M. tuberculata, M. themincki , N. major, N. micropus, N. albirentras, P. parentelli, R. capensis, R. clivosus, R. darlingii, R. swinnyi, R. hardwickii, R. microphyllum, R. naso and T. lavali

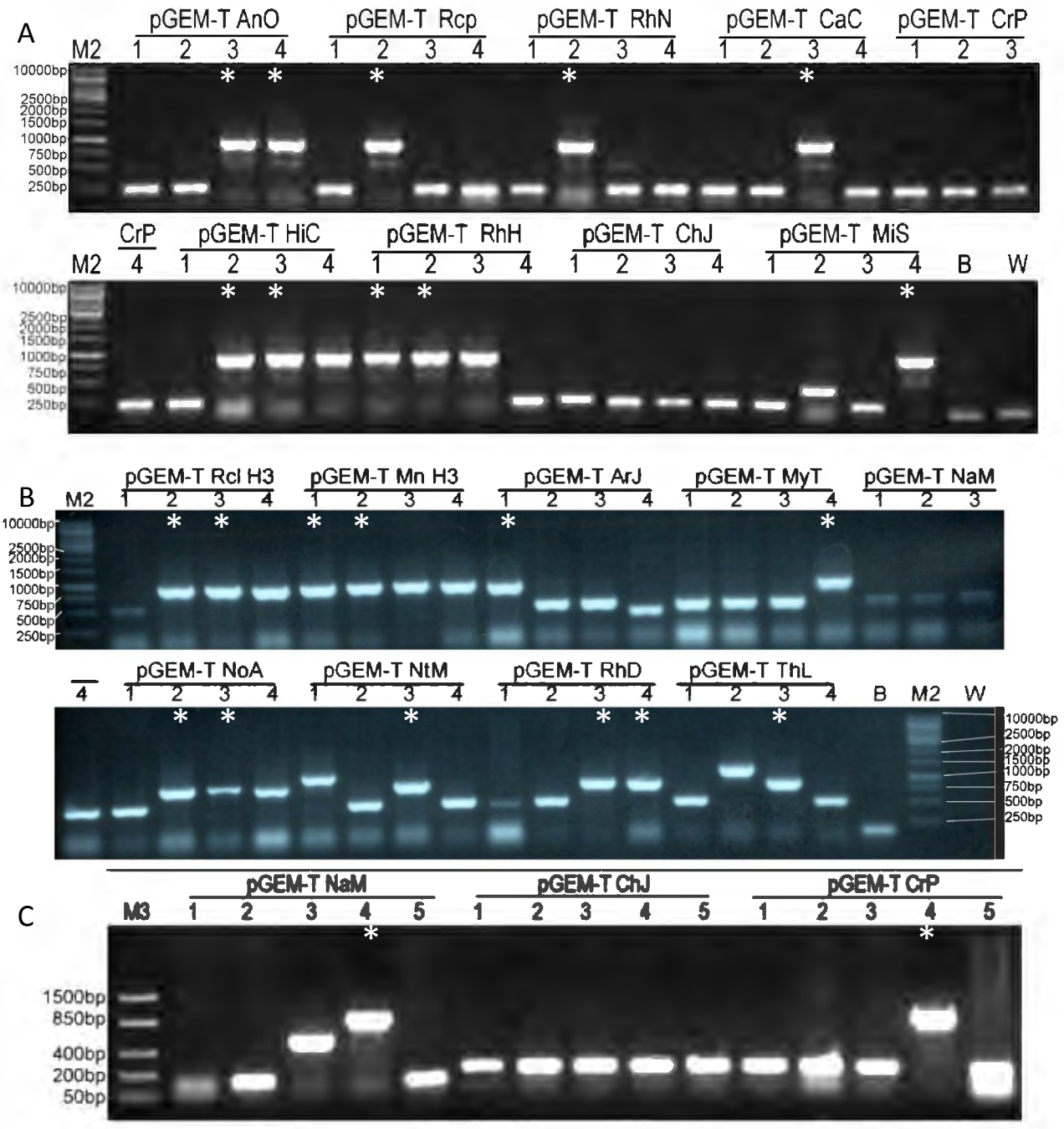

Figure 2.6: Colony PCR results (B – negative control (blue clones), W – water control). A: Colony PCR results *A. ornatus*, *C. cor*, *C. jabensis*, *C. perspicillata*, *H. commersoni*, *M. schreibersii*, *R. capensis*, *R. hardwickii,* and *R. naso*. B: Colony PCR results *A. ornatus*, *A. jamaicensis*, *M. tuberculata*, *N. major*, *N. micropus*, *N. albirentras*, *R. darlingii*, *T. lavali*, *R. clivosus* with flanking *HindIII* and *M.natalensis* with flanking *HindIII*. C: Colony PCR results *N. micropus* ZRS, *C. jabensis* ZRS and *C. perspicillata* ZRS. The numbers correspond to the clones on the master plate that were screened per species and the asterisks (*) show the clones were for sequenced.

Alignment of Vertebrate ZRS

The ZRS sequences from 18 bat species were aligned with 20 vertebrate ZRS sequences using PRANKSTER, a program that uses the PRANK algorithm designed for alignment of non-coding sequence (Löytynoja & Goldman 2005; Löytynoja & Goldman 2008) (see Appendix Figure A.2 for the full alignment). Five point mutations (B1-B5) were identified in the multiple sequence

alignment that was conserved in all 18 bat species, relative to the conserved vertebrate ZRS (Figure 2.7). These mutations are located towards the 3' end of the ZRS. The first bat conserved mutation (B1) is a transition where a guanine replaces a conserved adenine (G466A). Further downstream, there is a deletion of a thymine (B2, Δ625T). At nucleotide 694, all bats have a cytosine instead of a thymine (B3, C694T) and four nucleotides thereafter, a cytosine and adenine replace two thymine nucleotides (B4, C698T and B5, A699T). All nucleotide positions given are relative to the human sequence. Refer to Table 2.3 for the relative positions of these mutations in either the ZRS alignment or individual bat sequences. B1 was located next to two cat mutations (Fd2 and Fd3), B2 is 11bp downstream of a human mutation (Hs5) and B3-5 are 36bp upstream of another human mutation (Hs6) (Figure A.2). The alignment also revealed that there were other changes in the conserved areas ZRS; these polymorphisms were either species-specific or specific to sub-groups of bat species.

Table 2.3: The relative positions of the five point mutations conserved in all 18 bat species. The nucleotide position of each mutation in the 18 bat sequences are given under columns labelled BS (bat sequence), while the position relative to the human sequence are under columns HS. The position of each mutation within the alignment is under AN (alignment number).

Species	Mutation 1			Mutation 2			Mutation 3			Mutation 4			Mutation 5		
	B	HS	AN	BS	HS	AN	BS	HS	AN	BS	HS	AN	BS	HS	AN
A. ornatus	468	466	563	DEL	625	749	693	694	835	697	698	839	698	699	840
H. commersoni	468	466	563	DEL	625	749	692	694	835	696	698	839	697	699	840
A. jamaicensis	468	466	563	DEL	625	749	692	694	835	696	698	839	697	699	840
C. perspicillata	468	466	563	DEL	625	749	692	694	835	696	698	839	697	699	840
M. tuberculata	468	466	563	DEL	625	749	692	694	835	696	698	839	697	699	840
N. major	468	466	563	DEL	625	749	692	694	835	696	698	839	697	699	840
N. albiventris	468	466	563	DEL	625	749	692	694	835	696	698	839	697	699	840
R. capensis	467	466	563	DEL	625	749	692	694	835	696	698	839	697	699	840
R. clivosus	468	466	563	DEL	625	749	691	694	835	695	698	839	696	699	840
R. darlingii	467	466	563	DEL	625	749	691	694	835	695	698	839	696	699	840
R. hardwickii	468	466	563	DEL	625	749	692	694	835	696	698	839	697	699	840
R. naso	468	466	563	DEL	625	749	692	694	835	696	698	839	697	699	840
T. lavalii	468	466	563	DEL	625	749	692	694	835	696	698	839	697	699	840
C. cor	472	466	563	DEL	625	749	695	694	835	699	698	839	700	699	840
M. natalensis	464	466	563	DEL	625	749	691	694	835	695	698	839	696	699	840
M. schreibersi	464	466	563	DEL	625	749	691	694	835	695	698	839	696	699	840
M. lucifugus	454	466	563	DEL	625	749	682	694	835	686	698	839	687	699	840
P. vampyrus	472	466	563	DEL	625	749	699	694	835	703	698	839	704	699	840

Figure 2.7: Alignment of the ZRS of 18 bat species and 20 other vertebrates using PRANKSTER. The five point mutations that are conserved in all bats are shown by an arrow (↓) and numbers above are used as identification of mutations. Mutation 1(B1) is a transition from an adenine to a guanine at alignment position 563 (G466A). Mutation 2 (B2) is a deletion of a thymine at position749 (Δ625T). Mutation 3 and 4 (B3 and B4, respectively) are another transition from thymine to cytosine at positions 835 (C694T) and 839 (C698T) respectively. Mutation 5 (B5) is a transversion from a thymine to an adenine at position 840 (A699T).

Regulatory Activity of the Bat ZRS

This set of 5 mutations conserved across the spectrum of the Bat phylogeny might explain the differences in *Shh* expression observed during bat wing development (Hockman et al. 2008). In order to test this hypothesis, I first compared the expression patterns of a β-galactosidase reporter plasmid (pBGZ40), driven by the ZRS from *M. natalensis* (MnaZRS) or *R. clivosus* (RclZRS) in transgenic mice. These two species were selected because they are distantly related and have different wing shapes (Eick et al. 2005; Norberg & Rayner 1987). The *Shh in situ* expression patterns were originally described in *M. natalensis* (Hockman et al. 2008), a species characterized by narrow, long wings (Norberg & Rayner 1987). *R. clivosus,* which comes from a different family, and has broad, short wings (Norberg & Rayner 1987). I was interested in whether *M. natalensis ZRS* would drive a similar pattern of β-gal expression in transgenic mice as *R. clivosus ZRS*.

Cloning of the Bat ZRS into the BGZ40 plasmid

PCR was used to add *HindIII* sites on both ends of the ZRS from *M. natalensis* (from the Vespertilioiformes suborder) and *R. clivosus* (from the Pteropodiforme sub-order) to facilitate subcloning into pBGZ40 reporter plasmid from the pGEM-T clones (Figure 2.8 A). The PCR products were then purified and immediately digested with *HindIII* (Figure 2.8 B). The digested PCR product was then ligated into pBGZ40 and transformed into competent cells. Successful sub-cloning was identified by colony PCR using ZRS primers (Figure 2.8 C and D), and four clones from each species (indicated by the asterisks) were then sent for sequencing in both directions (using the primers pBGZ40-seq and T3, Table 2.1). Sequencing of clones showed no mutations in pBGZ40 clones (Figure A.3 and A.4) caused by the PCR or sub-cloning, and that pRcl-BGZ clone 4 and pMna-BGZ clone 10 plasmids had the inserts in the correct orientation.

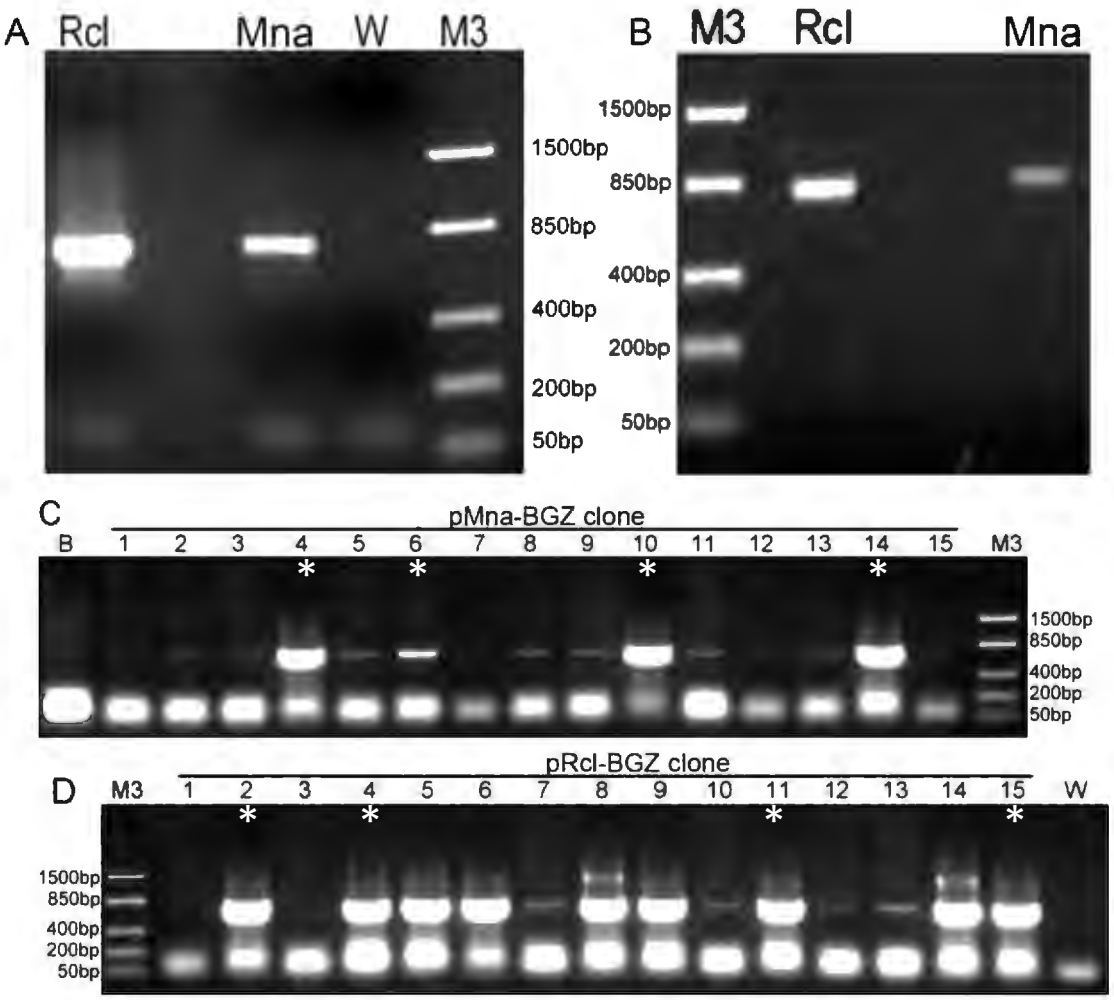

Figure 2.8: Sub-cloning of the ZRS of *M. natalensis* and *R. clivosus* from pGEM-T easy vector. A: Restriction enzyme digests of the ZRS of *M. natalensis* and *R. clivosus* with flank *HindIII* sites. B: PCR of *M. natalensis* and *R. clivosus* from pGEM-T easy clones, thus flanking the ZRS with *HindIII* sites. C: Positive clones for the *M. natalensis* ZRS in pBGZ40. D: Positive clones for the *R. clivosus* ZRS in pBGZ40. The numbers correspond to the clones on the master plate that were screened for each species and the asterisks (*) show the clones that were sequenced.

Transgenic Results of the M. natalensis ZRS and R. clivosus ZRS

To verify the effects of the *M. natalensis* ZRS and *R. clivosus* ZRS on the patterns of expression of *Shh* linearised Mna-BGZ, Rcl-BGZ and Mmu-BGZ plasmids (Figure 2.9) were microinjected into fertilized mouse oocytes. Table 2.4 summarises the total number of successful transgenic embryos generated per construct, and Table 2.5 summarises the total number of successful transgenic lines generated.

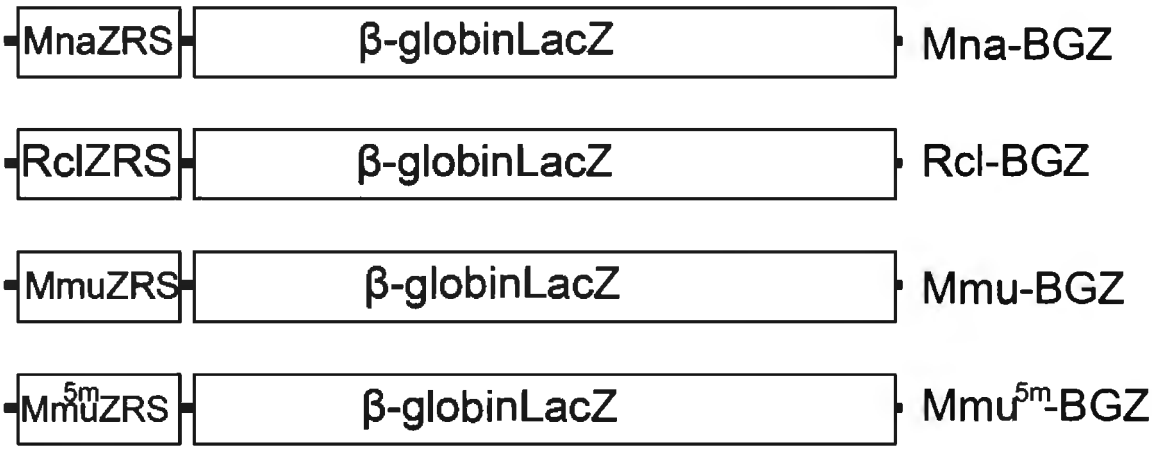

Figure 2.9: Linearized constructs of pBGZ40 clones used for transgenic expressions. Mna-BGZ is the *M. natalensis* ZRS linked to the β-Globin-LacZ construct (BGZ) and Rcl-BGZ is the *R. clivosus* ZRS linked to the BGZ. Mmu-BGZ is the mouse ZRS linked to the BGZ and Mmu^{5m}--BGZ is the mutated mouse ZRS (i.e. mouse ZRS containing the five conserved at mutations) linked to the BGZ.

Table 2.4: Summary of G_0 transgenic mouse experiments. Showing the number of G_0 transgenic embryos generated by pronuclear injection and the number of G_0 embryos that expressed *LacZ*.

Construct	Positive PCR		Expression	
	E11.5	E13.5	E11.5	E13.5
Mmu-BGZ	9	5	5	4
Mna-BGZ	11	7	5	7
Rcl-BGZ	9	15	7	7
Mmu^{5m}-BGZ	13	14	4	4

Table 2.5: Summary of transgenic lines generated. Table shows the total number of transgenic lines generated by pronuclear injection, and the number of lines in which embryos showed expression *LacZ* during development.

Construct	Positive PCR	Expression
Mmu-BGZ	7	2
Mna-BGZ	4	2
Rcl-BGZ	6	2
Mmu^{5m}-BGZ	N/A	N/A

The ZRS reporter construct from *M. natalensis* (Mna-BGZ) revealed a different β-gal expression pattern to that of the mouse ZRS (Mmu-BGZ) (Lettice et al. 2003) (Figure 2.10, 2.11, 2.12, and 2.13). At E11.5, the majority of Mna-BGZ G_0 embryos had β-gal expression in the posterior end of limb bud (ZPA area) as well as to varying degrees along the anterior margin of the distal limb bud (Figure 2.10 F-J). This anterior domain was not coincident with the AER (Figure 2.13 A and B). One embryo had low expression restricted to the ZPA (Figure 2.10 F) while another embryo had expression across the whole autopod (Figure 2.10 G). Even with a weak signal, a distinct area of expression was observed at both the posterior and at the anterior (thumb area) ends of the limb bud (indicated by a black arrow in Figure 2.10 J, 2.13 A). By contrast, B-gal expression in G_0 Mmu-BGZ embryos was restricted to only the ZPA at E11.5 in agreement with Lettice et al. (2003) (Figure 2.10 A-E, 2.13 E and F). At stage E13.5, expression of β-gal was restricted to the tips of the digits 2 to 5, and along the posterior length of the limb. This domain includes digits 4 and 5 in G_0 embryos with a strong signal, and only digit 5 in G_0 embryos with a weaker signal (Figure 2.11 E-K, 2.13 C

and D). Although β-gal expression was limited to a digits 4 and 5 in E13.5 G_0 Mmu-BGZ embryos, with the exception of one embryo (Figure 2.11 D), this expression did not extend to the distal zeugopod, nor was there any expression in the distal tips of the digits 2-5 (Figure 2.11 A-D) in agreement with Lettice et al. (2003). Two of the seven Mn-BGZ lines expressed *LacZ*, Line 1 (Figure 2.12 F-I) and Line 2 (Figure 2. 12 K-L); in a similar pattern to the G_0 embryos. At E10.5 there was β-gal expression in the distal posterior and along the edge of anterior forelimb (Figure 2.12 F). At stage E11.5, β-gal expression in Line 1 extended along the posterior margin along the length of limbs with limited expression at the distal anterior tip (Figure 2.12 G); Line 2 only showed expression in the posterior domain along the length of the limb (Figure 2.12 K). Expression of β-gal in the tips of digits 2 to 4 is first detectable at Stage E12.5 (Figure 2.12 H). At E13.5, β-gal expression in the lines is similar to the G_0 E13.5 embryos. β-galactosidase expression in line 1 is clearly detectable at the tips of digits 2 to 4 and in a more distal posterior domain that extends from the base of the autopod to the proximal zeugopod (Figure 2.12 I). While expression of β-gal in Line 2 was similar to Line 1 and the G_0 embryos (Figure 2.12 K). Expression of β-gal in two of the Mmu-BGZ lines agreed with the G_0 embryos, with β-gal expression at E13.5 limited to digits 4 and 5 only (Figure 2.12 A-E).

At E11.5, the G_0 Rcl-BGZ embryos displayed similar expression patterns to the G_0 Mmu-BGZ embryos albeit β-gal expression was less robust (Figure 2.10 K-Q and 2.11 L-R). β-galactosidase expression was limited to the ZPA in all E11.5 G_0 embryos (Figure 2.10 K-Q and 2.13 I-J), even in the embryo that showed low signals of expression (Figure 2.10 L-O, Q and 2.13 I). At E13.5 four out of seven embryos had expression limited to the posterior domain of the limb extending from digit 4 to 5 along the length of the posterior zeugopod (Figure 2.11 L,M, Q, R and 2.13 L). In the embryos with a weaker β-gal signal, expression was restricted to the cells between digits 4 and 5 (Figure 2.11 N, O, P and 2.13 K). Two Rcl-BGZ lines (Figure 2.12 M-S) gave weak expression of β-gal which was limited to digits 4 and 5, similar to the weaker G_0 embryos and the Mmu-BGZ embryos. At E10.5 and E11.5, β-gal expression was limited to the ZPA (Figure 2.12 M, N and Q). At Stages E12.5 and E13.5, β-gal expression is limited to digits 4 and 5 in the autopods of the limbs (Figure 2.12 O and R), with a very weak signal being detectable at E13.5 (Figure 2.12 P and S).

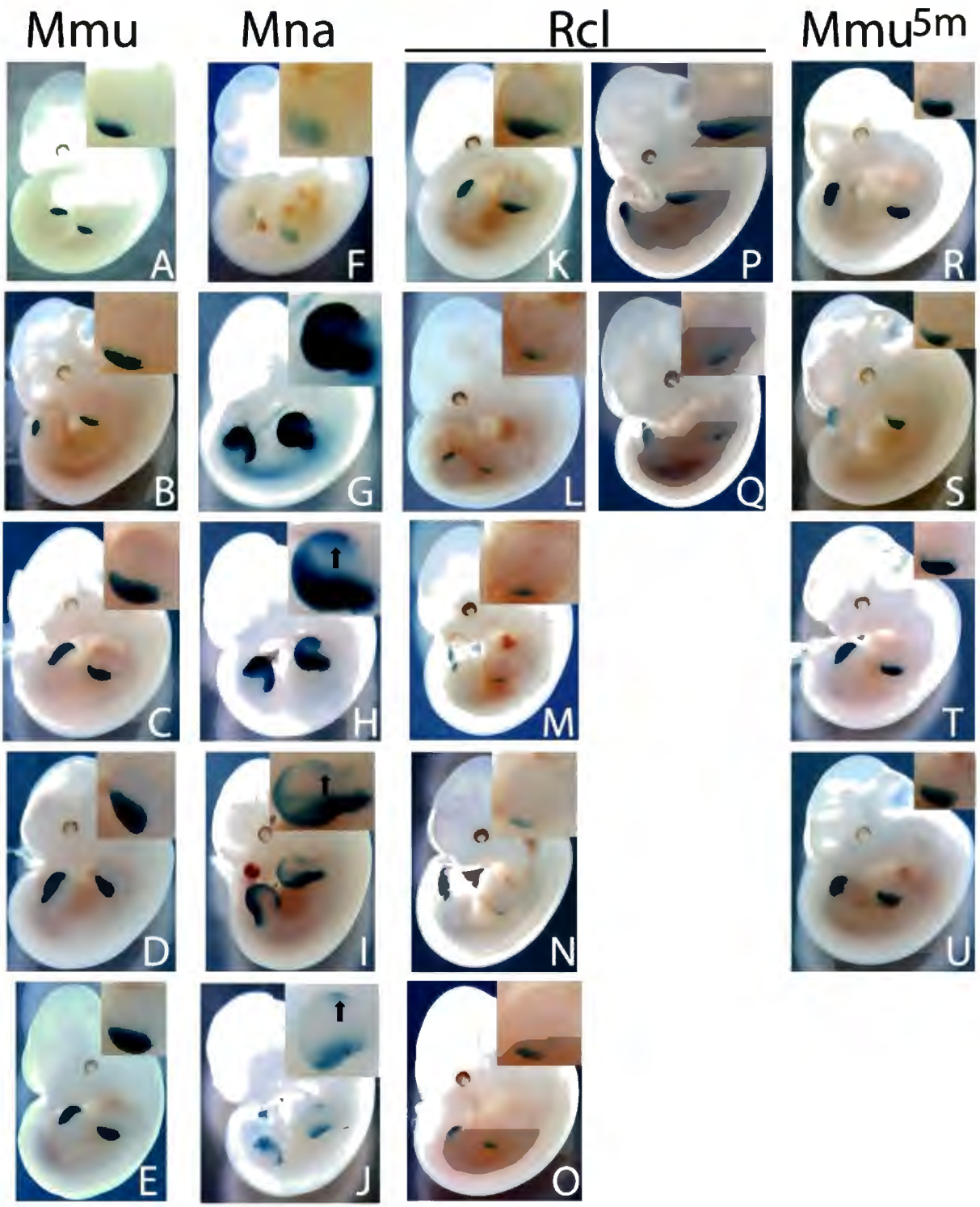

Figure 2.10: The β-gal expression in G_0 embryos at stage E11.5. A-E: Embryos injected with Mmu-BGZ construct. F-J: Embryos injected with Mna-BGZ. The black arrows show ectopic β-gal expression in the anterior end of the limb buds at E11.5. K-Q: Embryos injected with Rcl-BGZ. R-U: Embryos injected with Mmu^{5m}-BGZ. On the top right of each embryo is magnified picture of the forelimb of said embryo.

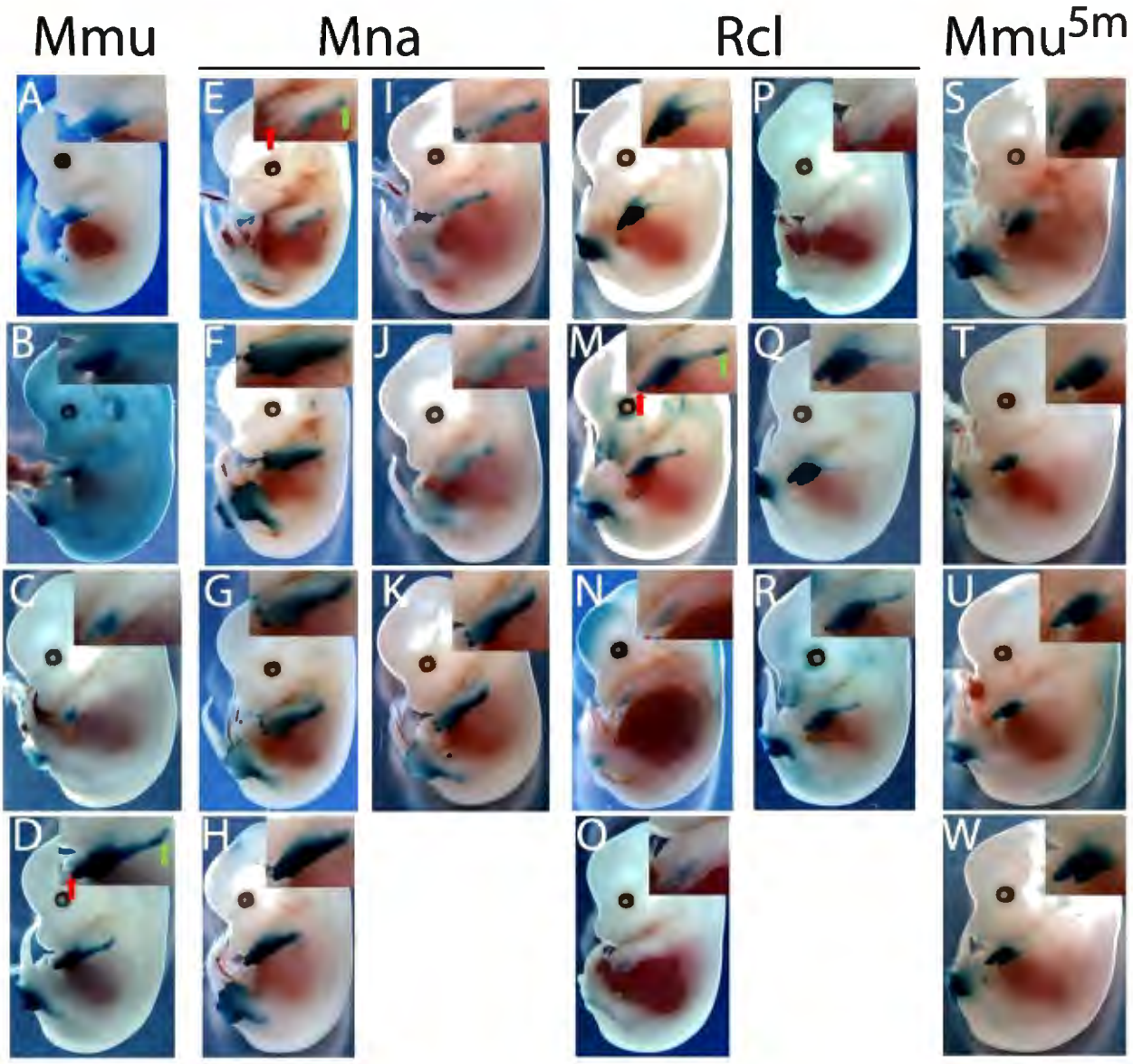

Figure 2.11: The β-gal expression in G_0 embryos at stage E13.5. A-D: Embryos injected with Mmu-BGZ construct. E-K: Embryos injected with Mna-BGZ. L-R: Embryos injected with Rcl-BGZ. S-W: Embryos injected with Mmu^{5m}-BGZ. The red arrow indicates expression at the tips of digit 3 (in the Mna-BGZ embryos) and digit 4 (in the Mmu-BGZ aand Rcl-BGZ embyros) at E13.5. The green arrow highlights the end of the β-gal expression along the posterior end of the forelimbs (the elbows) in the embryos at E13.5. On the top right of each embryo is magnified picture of the forelimb of said embryo.

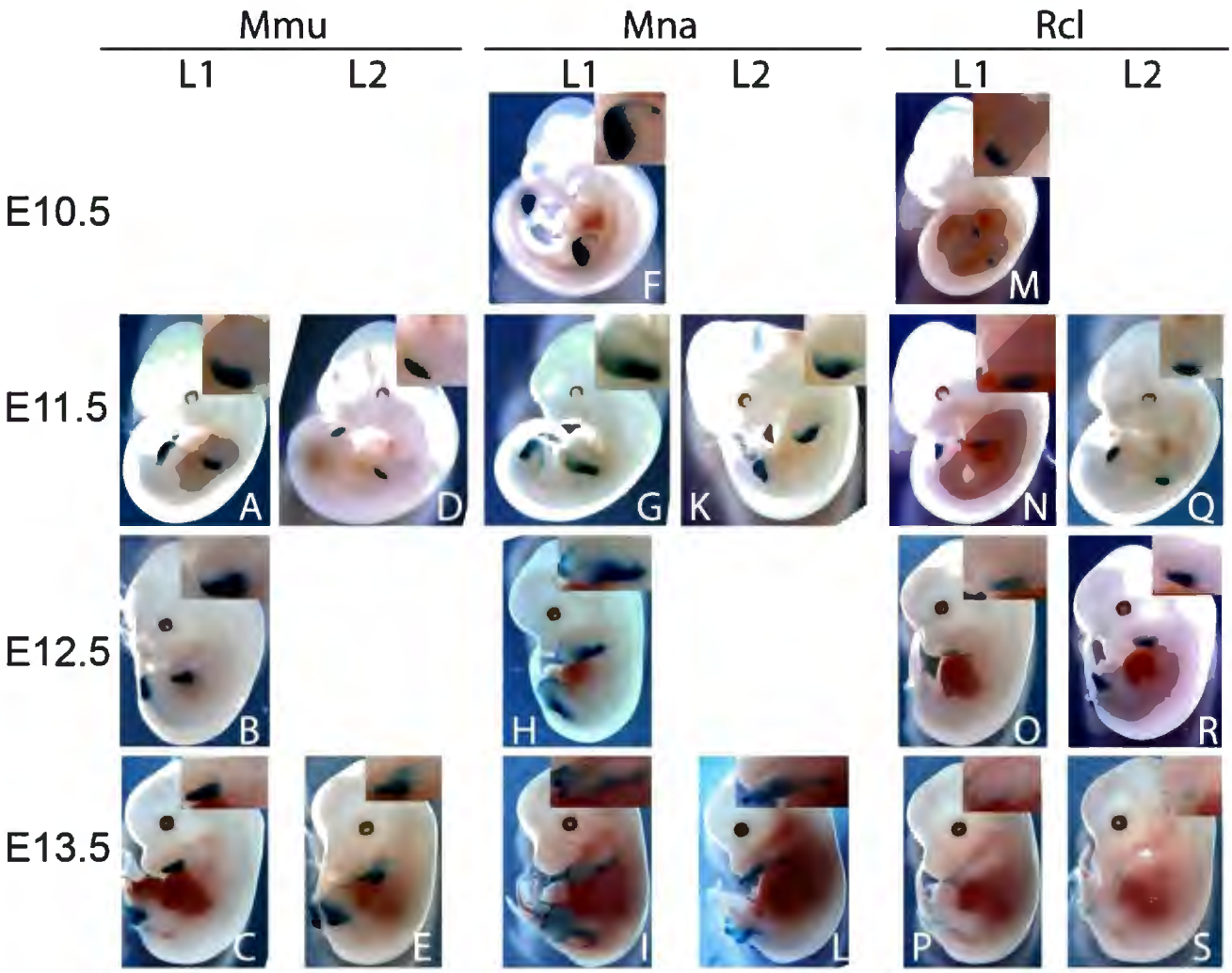

Figure 2.12: Transgenic lines containing the Mmu-BGZ, Mna-BGZ and Rcl-BGZ constructs. Transgenic embryos were collected at four stages: E10.5 (F and M), E11.5 (A, D, G, K, N and Q), E12.5 (B, H, O and R) and E13.5 (C, E, I, L, P and S). A -E: Embryos from lines injected with Mmu-BGZ construct. F-L: Embryos from lines injected with Mna-BGZ. M-S: Embryos from lines injected with Rcl-BGZ. Only two independent stable lines were successfully produced per constructs, indicated above as line 1 (L1) and line 2 (L2). On the top right of each embryo is magnified picture of the forelimb of said embryo.

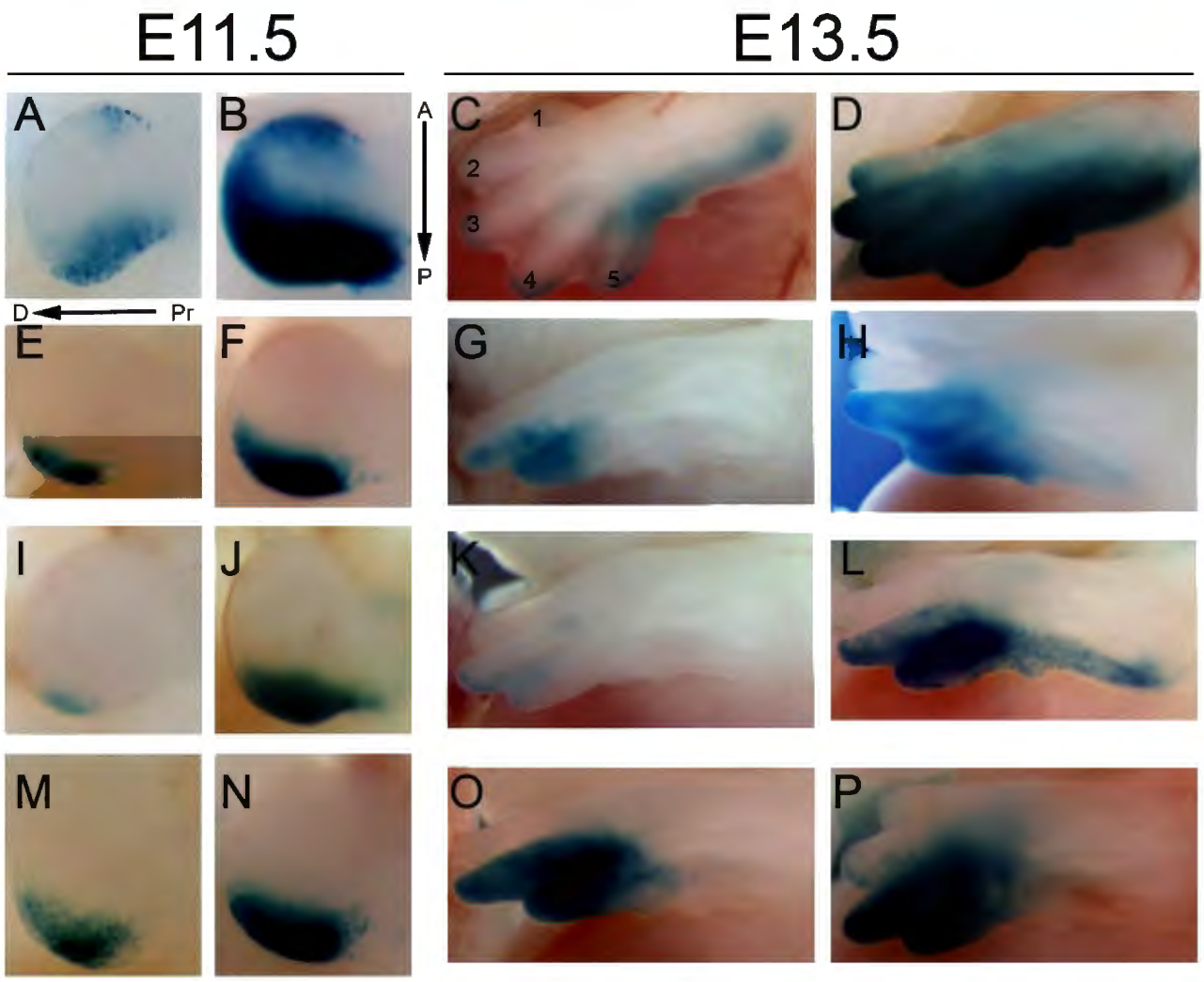

Figure 2.13: Summery of the forelimbs from the G_0 embryos, on left are embryos with weak signal and on the right embryos with strong signal. Mna-BGZ forelimbs (A-D), Mmu-BGZ forelimbs (E-H), Rcl-BGZ (I-L) and Mmu^{5m}-BGZ (M-P). A: This embryo seems to have two areas of low expression at the posterior and anterior ends of the limb bud. B: Expression is seen in the posterior half of the limb bud and there is ectopic expression at the anterior end of the limb buds. C: There is expression along the posterior edge of the limb, starting at the tip of digit 5 and ending at the 'elbow' of the limb. D: Expression is seen strongly along the posterior end of the limb and includes digits 3-5 with expression at the tips of digits 2-5. Again there seems to also be with distinct areas of expression at the tips of digits 2-4 on the hindlimb. E and F: β-gal expression restricted to the ZPA area. G: Expression seems to be limited to digit 5 and the posterior cells of digit 4. H: Expression is at the posterior area of the autopods, covering digits 4-5 and the proximal tissue. I: There is a faint and small area of expression at the posterior tip of the limb bud. J: There is strong β-gal expression in the most posterior end of the limb buds in the ZPA area. K: The embryos have very faint expression in the interdigital tissue between digits 4 and 5. L: β-gal expression is located along the posterior of the limb ending at the 'elbow' and includes digits 4-5. M and N: Expression is at the posterior end of the limb bud, i.e. in the ZPA area. O: Expression seems to be from digits 4 to 5. P: β-gal expression restricted to the posterior end of autopod, i.e. it starts at posterior edge of digit 3 and end at the proximal, posterior end of digit 5. A- Anterior end of the limb, P- posterior end of the limb, D-distal end of the limb, and Pr-proximal end of the limb. On the top right of each embryo is magnified picture of the forelimb of said embryo.

Mutagenesis of the Mouse ZRS

In order to test whether the five conserved bat mutations identified in this study (Figure 2.7) affect the activity of the ZRS, as measured by the ZRS-*LacZ* transgenic mouse assay, I replaced the five sites in the mouse ZRS with the bat mutations by site-directed mutagenesis.

The first step was to subclone the mouse ZRS into a fresh pBGZ40 vector to insure that identical vector backbone was being consistently used, in these experiments, to eliminate the possibility that any mutations would have accrued in the Mmu-BGZ construct used. The mouse ZRS was cut out of its vector, pMmu-BGZ1, using *HindIII* and was subcloned into a freshly linearized pBGZ40 plasmid (Figure 2.14 A). All positive clones (Figure 2.14 B) were sent for sequencing to confirm the identity and orientation of the sequence within the vector. Sequencing results showed that all clones were the mouse ZRS, and that clones 6 and 12 were in the correct orientation and had no mutation. Clone 12 was used for the mutagenesis experiments and will be referred to as pMmu-BGZ 2 (Figure A.5).

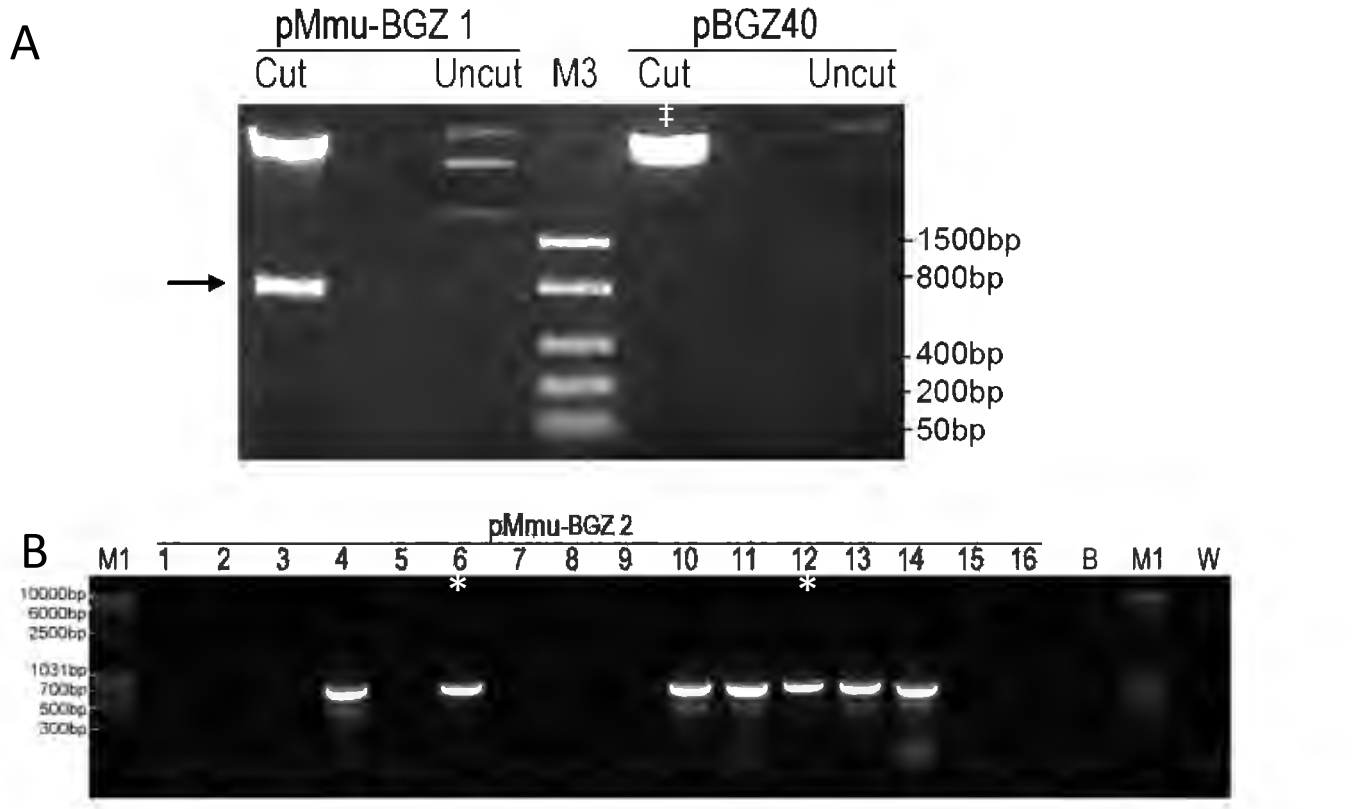

Figure 2.14: Subcloning of the mouse ZRS. A: Restriction enzyme digest results of the digestion of pMmu-BGZ1, to isolate the mouse ZRS, and of pBGZ40 for subcloning. The black arrow highlights the 800bp band that has been cut out of pMmu-BGZ1, which is the approximate size of the mouse ZRS. ‡ indicates the linearized pBGZ40 plasmid. B: Colony PCR showing plasmids containing the mouse ZRS, pMmu-BGZ2, were B is a clone with no insert and W is the no template control. The numbers correspond to the clones on the master plate that were screened and the asterisks (*) show the clones that were sequenced

The site-directed mutagenesis experiments using the QuikChange II Multi Site-Directed Mutagenesis Kit (Stratagene, USA) had mixed results with a mutagenesis efficiency of 56%. 37 plasmids from this mutagenesis experiment (Table 2.6) were sequenced, and no plasmid had all 5 mutations. However, two clones (plasmids 12 and 31) had four of the five bat mutations (mutations 2 to 5) replaced in the mouse ZRS sequences (Table 2.6). Bat mutation 1 was not introduced in any of the clones.

Table 2.6: Summary of mutagenesis results using QuikChangeII Multi Site-Directed Mutagenesis Kit (Stratagene, USA)

Introduced mutations	Number of clones	Plasmid Numbers
B1-5	0	-
B1	0	-
B2	6	4,13,15, 20,32,37
B3-5	1	2
B2-5	2	12, 31

The QuikChange II Site-Directed Mutagenesis Kit (Stratagene, USA) with primers Mutation 1-INT 2 Sense and Mutation 1-INT 2 Antisense mutation 1 was used to insert the bat mutation 1 into the mouse ZRS (2-5) clone 12. This mutagenesis experiment had a Mutagenesis Efficiency of 93% and the sequencing result showed 12 clones of 48 had all 5 mutations inserted. The p Mmu^{5M}-BGZ (i.e. mouse with bat mutations) clone 1 plasmid had no other unwanted mutations in the ZRS sequence (Figure 2.8) and was therefore used in transgenic mouse experiments.

Transgenic Results of Mmu^{5M}

The Mmu^{5M}-BGZ reporter construct showed expression pattern similar to that of the control, Mmu-BGZ (Figure 2.10 R-U, 2.11 S-W and 2.13 M-P). At E11.5, all embryos had a strong expression at the posterior end of limb bud (Figure 2.10 R-U and 2.13 M-N). Unlike the Mna-BGZ G_o embryos, no β-gal expression was detectable in the anterior edge of the autopod. At E13.5, expression was seen at the posterior end of the hand and extends toward digit 4 (Figure 2.11 S-W and 2.13 O-P). However, unlike the Mna-BGZ embryos, no β-gal expression was detectable in the distal tips of digits 2-5 at E13.5. There are faint areas of expression at the proximal end of digits at E13.5, but it just might be the result of the assay used to stain the embryos (Figure 2.11 S and W).

Discussion

Sonic hedgehog was shown to be differentially expressed during limb development in bat embryos of *M. natalensis*: at E11.5, there is an enlarged area of SHH expression at CS14/E11.5 and reactivation of SHH expression at CS16E-CS16/E12.5-E13.0 (Hockman et al. 2008). Since there is abundance of evidence indicating that the mutations in the ZRS cause an alteration of the SHH expression in the limb during development (Lettice et al. 2003; Lettice & Hill 2005; Gurnett et al. 2007; Furniss et al. 2008; Lettice et al. 2008), I investigated the hypothesis that the difference in the pattern of *Shh* expression in bats was a result of changes in the bat ZRS that were conserved across all bats.

An in-depth analysis of the bat ZRS cloned from 18 species identified five point mutations towards the 3' end of the ZRS sequence that were conserved in all bats (Figure 2.7 and A.2). These mutations were in highly conserved areas of the ZRS and close to previously mapped ZRS mutations that are known to cause disruptions in the *Shh* expression (see Figure A.2). These results suggested that the five bat ZRS mutations may have played a role in the change in *Shh* expression during limb development in bats. The ZRS from *M. natalensis* and *R. clivosus* were cloned into a *LacZ* reporter plasmid and injected into fertilized mice oocytes to compare the ability of the bat ZRS sequences relative to the mouse ZRS sequence, to activate expression of a *LacZ* reporter construct in limbs in mice embryos.

If the bat ZRS were responsible for SHH expression changes in bats, there would then be a change in β-gal expression in the developing mouse compared to the mouse ZRS. If flight evolved once, then the two different bat ZRS should give a similar expression profile. The *M. natalensis* ZRS (Mna-BGZ) showed the most difference in change of *LacZ* gene expression. While the *R. clivosus* ZRS (Rcl-BGZ) gave an expression pattern similar to that of the mouse ZRS (Mmu-BGZ).

The *M. natalensis* ZRS transgenic embryos showed novel areas of β-gal expression when compared to the control (MmuZRS): there are quite a number of novel areas of activity consistent in both the G_0 transgenic embryos and the transgenic lines. For the G_0 embryos there is a defined and reproducible expression pattern. At stage E11.5, MnaZRS not only displayed expression in the posterior end of the limb buds but also had two novel areas of expression, being: an area of expression at the anterior end of limb buds and another along the distal edge of the limb buds. None of the control embryos showed any of these patterns. At E13.5, MnaZRS transgenics showed ectopic expressions at the tips of digits 2-5 and expression along the posterior end of limb. The

MnaZRS transgenic lines produce same expression patterns as the MnaZRS G_0 experiments. At E10.5 there is ectopic expression along the distal edge of the limb bud and an area of expression in the anterior end of limb bud (see Lettice et al. (2003) for E10.5 mouse transgenic embryos). This same expression pattern is seen at stage E11.5. At E12.5 in the MnaZRS transgenic, there is expression along the posterior end of the limb and at the tips of digits 2-4, while the control transgenics only have expression from digit 4-5. This same pattern is seen at stage E13.5. This suggests that there are elements within MnaZRS that may alter *Shh* expression, although the pattern is quite different then of that seen in bats (Hockman et al. 2008). At E12.5, there is a second round of the expression of *Shh*: in the forelimb there is a posterior-anterior gradient of expression in the autopod and in the hindlimb autopod there is a uniform expression pattern. In the MnaZRS transgenic embryos, there is no evidence to suggest a second wave of expression. This, and because the BGZ construct does not stop expression once activated, make it hard to determine if there is a second activation at this stage. This suggests that the ZRS alone is not enough for precise spatiotemporal expression of *Shh*, as suggested by Lettice, et al (2003) and Amano et al. (2009). Similar results were seen when researchers investigated mutations in bat Global Control Region of *Hoxd13* and its ability to alter the HoxD13 expression patterns in transgenic mice embryos (Chen et al. 2005; Ray & Capecchi 2008). Ray and Cappechi (2008) transgenic reporter assays showed that bat GCR embryos produce novel expression domains and that differed slightly the expression domain of endogenous HoxD13 in bat embryos.

The *R. clivosus* ZRS, most of the transgenic embryos produced β-gal expression patterns similar to that of the control. In the G_0 embryos, the RclZRS show the same expression as the control at E11.5, although most embryos had a faint area of expression at the very end of the posterior edge of the limb buds, while the control had a larger and stronger area of expression. At E13.5, three out of the seven G_0 embryos show expression similar to the control - expression is restricted to the tissue between digit 4 and 5. The other four G_0 embryos had expression from digits 4 to 5 and along the posterior end of the limb. In the lines, embryos at E10.5 and E11.5 have the same expression pattern as the control. At E12.5, expression is only in the tissue between digits 4 and 5, while the control expression encompasses digits 4 and 5. At E13.5, there is very faint expression in the posterior autopod, in the tissue between digits 4 and 5, while in the control embryos expression is from the digit 3 and 4 to the posterior end of digit from similar to that seen in MnaZRS. This almost suggests that *R. clivosus* ZRS causes repression of the *LacZ* gene as opposed to creating novel areas of expression as seen with the *M. natalensis* ZRS, although this 'repression'

may be a consequence of where the construct was integrated in the genome. On the other hand, it seems that the RclZRS produces a β-gal expression pattern similar to that of control embryos and not to MnaZRS embryos. Due to these conflicting results, more experiments need to be conducted in order to conclusively characterise the effect of the RclZRS on *Shh* expression.

To determine whether the five conserved point mutations identified above play a role in the differential expression of *Shh* in bats, they were inserted in to the mouse ZRS through mutagenesis (Mmu^{5M}-ZRS). The Mmu^{5M}-ZRS G_0 embryos have the same expression pattern as that of the MmuZRS, G_0 embryos. At E11.5, β-gal expression occurs at the posterior end of limb buds. At E13.5 β-gal expression is in the posterior end autopod, including digits 4 and 5. These results indicate the five mutations do not cause changes in ZRS activity in transgenic mice. Therefore, it seems that the five conserved point mutations do not change SHH expression during limb development.

A limitation of the ZRS-*LacZ* transgenic reporter mouse assays, while commonly used as a way to test *cis*-regulatory sequences, resides in the fact that it does not always mimic the *in vivo* mechanism of the said regulator. In this case, ZRS-*Shh* interaction is a complex mechanism that involves chromosome remodelling for precise spatiotemporal *Shh* expression (Amano et al. 2009). In order for there to be *Shh* expression in the limb, not only must ZRS and the *Shh* promoter come into contact (controlled by *Shh* promoter), *Shh* also needs to 'loop' out of its CT (controlled by the ZRS) (Amano et al. 2009). The β-Globin/*LacZ* construct does not use the same mechanism since the ZRS is linked about 100bp upstream of the β-Globin promoter. This is supported by the fact that the mouse ZRS does not stop expressing β-gal once it is activated at E10.5 (Lettice et al. 2003). Hence, to properly characterise the effects of the bat ZRS and conserved five bat mutations on *Shh* expression, these sequences need to be knocked-in into mouse replacing the native mouse ZRS.

Another limitation of this assay is that it is a descriptive technique, and therefore it is hard to identify significant differences when there are only slight variations, such as in the case of the Mmu^{5M}-ZRS embryos. One way to counter this is to use imaging software such as SigmaScan Pro5 (Aspire Software International, USA) or Image-Pro Plus (Media Cybernetic, USA) to calculate the area of expression in the limb buds and then use statistical analyses to test for significant differences between the transgenic experiments.

The original hypothesis was that flight evolved once, and therefore the conserved mutations would be responsible for the reactivation of SHH in bats. However, results presented here suggest

that the mutations conserved across bats are not sufficient to drive a change in expression of a reporter Mmu^{5M}-ZRS (Figure 2.13), and are thus unlikely to be responsible for the evolution of flight. The MnaZRS and RclZRS reporter constructs had different patterns of expression in the limbs of transgenic mouse embryos (Figure 2.13), and it is possible that differences in the activity of these enhancer constructs might explain the differences seen in their wing shape. However, this needs to be tested further by characterizing Shh expression in developing *R. clivosus* embryos

The analysis of the various bat ZRS also showed that there were other changes in the conserved areas ZRS that were either species-specific or specific to sub-groups of bat species. This suggests that there may be variation in SHH expression between bat species during development. Lettice et al. (2008) reported differences in the severity of PPD in humans that correlate not only with the type of mutation but also with how drastic the change in *Shh* expression was during development; this may be the case with the bat ZRS. Bat wings have a large of range of sizes and shapes which allow individual species to achieve optimal flight within their respective environments (Norberg & Rayner 1987). The results discussed above do seem to support this possibility, since MnaZRS and RclZRS give very different β-gal expression profiles in the transgenic mouse embryos. The next step is therefore to look at the morphological variation in bat wings across species, and explore the possibility of a connection between ZRS and the morphology of the adult bat wing.

Chapter 3: Understanding the Variation of Bat Wing Shapes

The forelimbs of bats have undergone drastic changes to produce an aerofoil with the aerodynamic requirements for powered flight (Norberg & Rayner 1987; Thewissen & Babcock 1992; Norberg 1998; Swartz & Middleton 2008).

The Bat Wing

It is the structure of the bat wing - composed of flexible bones, membrane and independently controllable joints - that gives bats powered flight capabilities (Swartz et al. 2006). The handwing is made up of 6 carpals (wrist bones), 5 metacarpals (hand bones), and 5 sets of phalanges (finger bones) with elongated digits 2 to 5 that support the chiropatagium (wing tip membrane; Figure 3.1) (Neuweiler 2000). Digit 1 is not elongated and is not incorporated into the wing membrane protruding past the leading edge of the wing (Neuweiler 2000). It has a claw that usually functions as a grasping tool (Neuweiler 2000). The plagiopatagium is the largest membrane that joins the hindlimb to the forelimb and extends along the proximal edge of the fifth digit (Neuweiler 2000). The protopatagium is a small membrane, in front of the forearm, that extends from the shoulder, along the forearm of the bat to its wrist (Neuweiler 2000). The uropatagium is a membrane that stretches between the tail and hindlimbs (Neuweiler 2000). These membranes and wing bones have evolved to produce lift during flight (Figure 1.1) (Swartz et al. 2006).

Adaptations of the Bat Wing's Skeletal Structure

One of the more obvious changes in the skeletal structure of the bat forelimb to form the wing, is the elongation of the bones in the forearm and hand (Figure 3.1) (Norberg 1998; Swartz 1997; Swartz & Middleton 2008). Not only are the bones in the forelimb significantly longer (except for carpals), but their diameter is also significantly larger than in similar-sized non-flying mammals (Swartz & Middleton 2008). The ulna in the bat, unlike other mammals, is much smaller than the radius, and is partially fused with the distal end of the radius. Another adaption is the lack of mineralisation in the distal tips of the digits. No mineralisation occurs in the most distal phalanges of the bat wing (Swartz 1997). These adaptations not only decrease the weight of the wing while increasing the surface area, but also allow flexibility in the wing bones so that they do not snap under the physical stresses associated with flight (Swartz 1997).

Final development of the wing membrane and bones occurs during postnatal development whilst young bats are learning to fly (Adams 2008). During this stage, "compensation growth" of the bone elements occurs in some species (Adams 2008). Compensation growth involving rapid

increases in length is particularly emphasized in the phalanges and metacarpals of digits 3 and 5 (Adams 2008; Lin et al. 2011). Such growth is suggested to be critical in achieving optimal wing form for flight and survival (Adams 2008; Lin et al. 2011). Between birth (flop, flutter and flap stages) and first flight, there are stresses experienced by the wing while the bat attempts flight. These stresses complete the final stages of development of the handwing bones, started in the foetal stage, to a wing shape suited to the habitat of the species (Lin et al. 2011). Evidence also suggests that further fine adjustment of the form of the handwing occurs after first flight, adapting the wing for flight in the bat habitat (Adams 2008; Lin et al. 2011).

Wing Shape and Ecology

Bats are one of the largest and most diverse Orders of mammals, occupying a large range of different environments. It is not surprising, therefore, that there is large variation in bat wing shapes and sizes (Norberg 1998; Simmons et al. 2008). Bat wing shape is associated with different flight patterns allowing negotiation of space within different habitats (Norberg & Rayner 1987). Bats with broad, short wings are slow flyers that can manoeuvre easily and are thus adapted for foraging within cluttered vegetation (Norberg & Rayner 1987). Bats with narrow, long wings are fast flyers but are less manoeuvrable, and are better adapted to foraging in open areas above vegetation or in gaps within vegetation (Norberg & Rayner 1987).

There are three parameters used in describing wing shape in bats: Aspect Ratio, Wing Loading and Tip Shape Index. Each variable reflects different aspects of adaptation for flight. Aspect ratio is a measure of the shape of the wing. A high aspect ratio is indicative of a long, narrow wing and a low aspect ratio is indicative of a short broad wing. It gives insight into the aerodynamic efficiency of the wing at different flight speeds and the energy losses during flight. Wing loading is a measure of the load that the wing has to carry during flight. A high wing loading means that the bat has to have high minimum flight speeds to stay aloft. A low wing loading means that the bat can retain lift at low flight speeds. Tip Shape Index is a measure of the shape of the wing tip, independent of the size of the bat. A correlation between these three variables and the type of flight and the environment in which the bat exists has been shown (Norberg & Rayner 1987). These parameters provide a broad view of the variation in wing shape and loading between bat species, but do not give an indication of which skeletal elements within the bat wing are responsible for this variation.

The aim of this chapter is to look at wing shape in a more detailed manner, by identifying the skeletal elements within the handwing (i.e. metacarpals and phalanges) that are responsible for

the variation of wing shape across bat species. Once the key elements are identified, the next step is to look at ZRS as possible component of the underlying genetic mechanism that determines wing shape. I tested the hypothesis that variation in the ZRS sequence of different bat species correlated with changes in wing shape.

Material and Methods

Bat Wing Photographs

Digital photographs of bat wings were provided by Assoc. Prof. David Jacobs (Zoology Department, UCT). Bats were held facing downwards on graph paper with their right wing extended and photographed using a Fuji Finepix S1PRO.E digital camera (Fuji Photo Film Co. Ltd, Tokyo, Japan). Photographs were used so as to include diverse number of species from across the globe within the sample groups and to standardise the data. Only measurements from photographs were used. One good quality photograph was chosen for each of 53 bat species for an analysis of interspecies differences in the skeletal structure of the bats' wings, the reason being that only one photograph was available for some of the foreign bat species.

Morphological Data Collection

To get a higher resolution of the structural differences between wings of different species than the traditional indices of wing shape and function provide, the metacarpals (MC) and phalange 1 (PI) and phalange 2 (PII) from digits 3 to 5 were measured using SigmaScan Pro version 5 (Aspire Software International, USA). The forearm length (FA) was used as the measure of body size because the mass of each individual was not available, this being because measurements were taken from photographs of bat wings as well as live specimens.

In some photographs, some of the landmarks shown in Figure 1.1 were obscured and some of the measurements could not be taken accurately. GEPAS (www.gepas.org) was used to impute the missing data for these species using the k-nearest neighbour algorithm (Tárraga et al. 2008; Vaquerizas et al. 2005) so as to have a complete data set.

For an indication of wing type, the aspect ratio (A) was calculated for each species using the equation: $A= B^2/S$, and then classified as either high aspect ratio (H - values above 7.5), medium aspect ratio (M - values between 7.5 and 6.5) and low aspect ratio (L - values below 6.5)(Norberg & Rayner 1987).

For the ZRS bat species (i.e. species whose ZRS have been sequenced – see Chapter 2) that had no available photography, aspect ratio was taken from Assoc. Prof. David Jacobs's laboratory database, and in cases where the species was not in the database, aspect ratio was taken from the available literature.

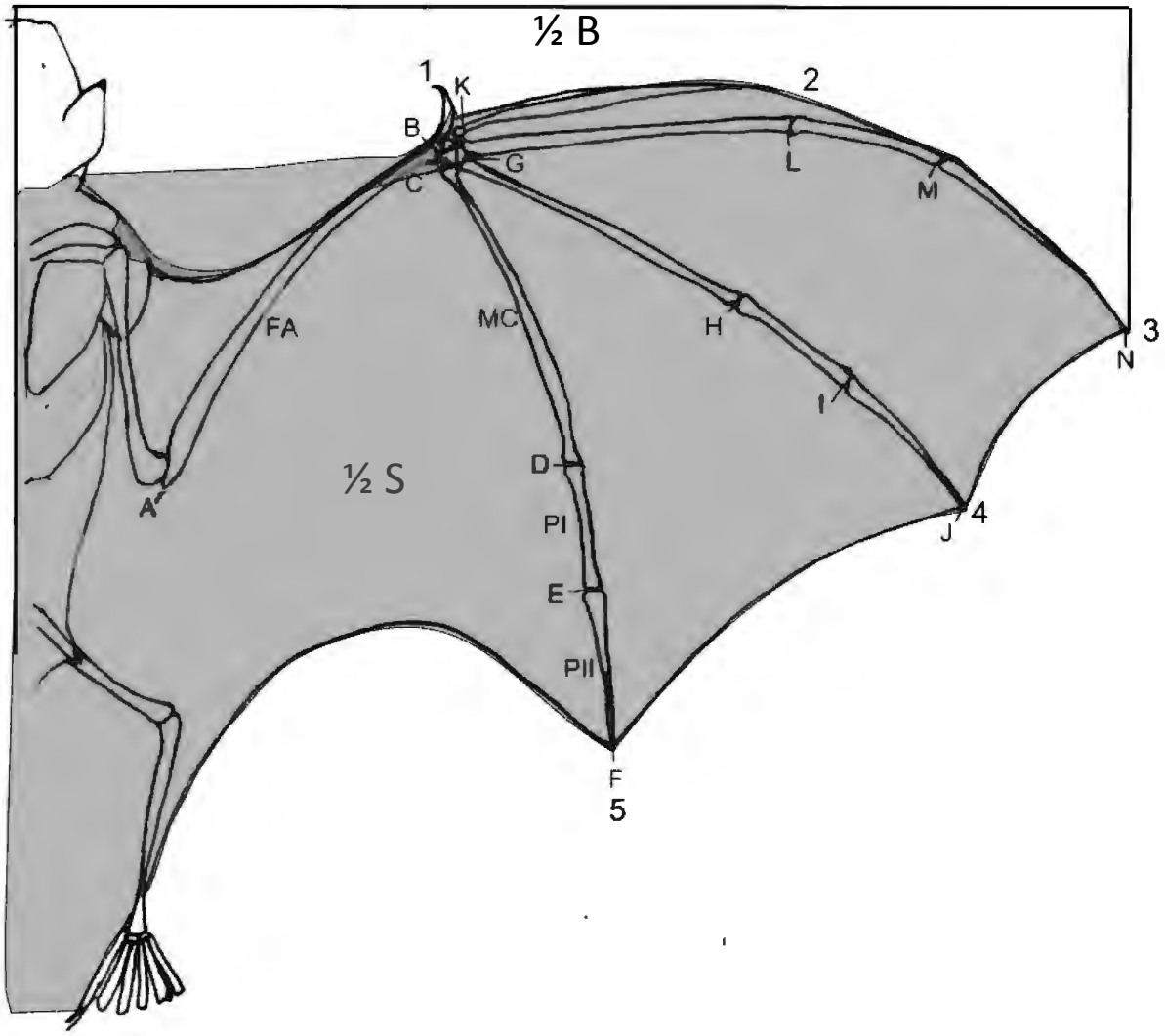

Figure 3.1: The basic morphological and skeletal structure of the bat wing and the morphological landmarks used in this study. Digit numbers are given at the end of each digit. Forearm length (FA) was measured from landmark A to B. For the 5th digit, the length of the metacarpal (5MC) was measured from landmark C to D, length of the 1st phalange (5PI) from D to E, and length of the 2nd phalange length (5PII) from E to F. For the 4th digit, the length of the metacarpal (4MC) was the measured from landmark G to H, length of the 1st phalange (4PI) from H to I, and length of the 2nd phalange (4PII) from I to J. For the 3rd digit, the length metacarpal (3MC) was measured from landmark K to L, length of the 1st phalange (3PI) from L to M, and length of the 2nd phalange (3PII) from M to N. Half wingspan (½B) is from the centre of the body tip of the wing (as indicated by the black line), and half wing area (½S) includes the wing (shaded in grey).

Phylogenetic Analysis of the Bat ZRS

Sequences corresponding to all 18 bat species were aligned to the mouse, human and horse ZRS using PRANKSTER (Löytynoja & Goldman 2005; Löytynoja & Goldman 2008) and DIALIGN-TX (Subramanian et al. 2005; Subramanian et al. 2008).

A Maximum Likelihood phylogenetic tree was constructed for the ZRS sequences using Phylogeny.fr (Dereeper et al. 2008), using approximate likelihood-ratio test (aLRT) (Anisimova & Gascuel 2006) to generate the most accurate tree.

Statistical Analysis

Statistica 10 (StatSoft, USA) was used for all statistical analyses. The morphological data from the 53 species were log-transformed and subsequently analysed using Principal Component Analysis (PCA).

The aspect ratio data for the ZRS bat species (Table 3.2) was not normally distributed since there were a small and unequal number of individuals per group. To increase the sample number, species from the PCA data set were grouped by similarity of wing shape and then categorized into one of the three ZRS clades (identified in the phylogenetic analysis), based on which ZRS bat species were included in those groups (Figure 3.3 A). The Shapiro-Wilk W test was used to test for normality of the data, and an Analysis of Variance (ANOVA) was used to compare the ZRS clades with respect to wing elements identified in the PCA. The Bonferroni post-hoc test was used to test significance ($p \leq 0.05$).

Results

The raw data set comprises forearm length, and lengths of the metacarpals, phalange 1 and phalange 2 of digits 3-5 for the 53 different bat species measured in this study, summarized in Table 3.1. This data set includes the imputed values (highlighted in blue)

PCA results

Principle Component Analysis of this dataset showed that the first three factors accounted for 82.6% of the variation in the data. The plot of Factor 1 (which explains 60.7% of the variation) against Factor 2 (13.4%; Figure 3.2) indicates that most separation of species occurs along Factor 1 (Figure 3.2 A) and that forearm length i.e. body size is largely responsible for this separation (Figure 3.2 B). Species (e.g. *Laephotis wintoni* and *Pipistrellus rusticus*) which load highest on Factor 1 (Figure 3.2 A) have shorter forearms (Table 3.1) than species (e.g. *Rousettus aegyptiacus* and *Epomorhous wavhlbergii*; Table 3.1) which load lower on Factor 1 (Figure 3.2 B). The distribution of the species along Factor 2 (Figure 3.2 A) is determined by aspect ratio (A), length of 2^{nd} phalanges of digits 3, 4 and 5 (3PII, 4PII and 5PII), with 4PI, 3MC and 3PI contributing to a lesser extent (Figure 3.2 B). Species with highest loading values on Factor 2, e.g. *Sauromys petrophilus* and *Mops midas* (Table 3.1), have shorter 2^{nd} phalanges, in all three digits, and higher A than species that load lower on Factor 2, e.g. *Rhinolophus hildebrandtii* and *Rhinolophus landeri* (Table 3.1).

Plots of Factor 2 against Factor 3 (which explains 8.4% of the variation) indicate differences in wing shape after the effects of differences in body size (Factor 1) have been removed (Figure 3.3). The separation of species along Factor 2 (Figure 3.3 A) is largely determined by 5PII and 4PII; with contribution from 3PII, 3MC and 4MC to lesser degree (Figure 3.3 B). Species with low loading values on Factor 2, e.g. *Rhinolophus swinnyi* and *Rhinolophus blasii* (Table 3.1), have long 5PII and 4PII, while species with higher loading values, e.g. *Sauromys petrophilus* and *Mops midas* (Table 3.1), have shorter 4PII and 5PII (Table 3.1). The species distribution along Factor 3 is mostly due to 3PI, 3PII, 4PI, 4PII, and A (Figure 3.3 B). Species that load the lowest, e.g. *Pipistrellus zuluensis* and *Nycteris thebaica* (Table 3.1), have long 3PI and 4PI, short 3PII and 4PII, and low A, while the highest loading species, e.g. *Phyllostomus discolor* and *M. natalensis* (Table 3.1), have short 3PI and 4PI, long 3PII and 4PII, and high A.

Table 3.1: The morphological data for 53 bat species. Variables measured (in mm) were Forearm length (FA), 1st digit (1st) the 5th digit's metacarpal length (5MC) the 5th digit's 1st phalange (5PI), the 5th digit's 2nd phalange (5PII), the 4th digit's metacarpal length (4MC) the 4th digit's 1st phalange (4PI), the 4th digit's 2nd phalange (4PII), the 3rd digits metacarpal (3MC), the 3rd digit's 1st phalange length (3PI), the 3rd digit's 2nd phalange length (3PII), aspect ratio (A) and aspect ratio classification (AC). Missing values which were imputed by K-nearest neighbour are highlighted in blue. The column labelled 'Code' list the abbreviations of the species used in Figure 3.2 and 3.3.

Family	Species	Code	FA	1st	3MC	3PI	3PII	4MC	4PI	4PII	5MC	5PI	5PII	A	AC	ZRS Clade
Emballonuridae	*Rhynconycteris naso*	Ryn	39.9	5.3	36.4	16.2	22.3	30.7	9.1	6.7	28.6	9.3	9.8	6.4	L	B
Emballonuridae	*Taphozous mauritianus*	Tm	35.4	3.3	32.6	12.9	13.6	32.0	7.5	6.3	29.6	7.5	9.9	7.2	M	C
Hipposideridae	*Cleoetis percivali*	Clp	34.1	2.1	25.7	16.2	22.3	25.4	9.1	6.0	21.6	11.8	6.9	4.8	L	A
Hipposideridae	*Hipposideros caffer*	Hc	46.4	6.1	34.1	17.7	24.7	33.9	10.0	8.3	29.4	12.5	10.5	5.5	L	A
Hipposideridae	*Hipposideros commersoni*	Hco	93.7	17.7	65.0	21.3	31.1	61.9	24.1	15.5	63.4	24.7	17.1	6.3	L	A
Miniopteridae	*Miniopterus natalensis*	Mn	46.7	6.1	40.8	10.2	36.5	39.8	9.1	18.9	37.9	9.7	10.0	7.0	M	C
Molossidae	*Chaerophon pumilus*	Chp	37.4	3.1	36.7	15.1	24.8	34.6	12.4	12.1	21.1	9.9	5.1	8.2	H	C
Molossidae	*Mops condylurus*	Moc	45.7	8.5	41.4	17.8	28.4	39.8	16.1	14.8	28.8	11.6	6.0	7.7	H	C
Molossidae	*Mops Midas*	Mom	61.0	8.7	57.6	24.4	33.9	55.3	19.6	15.0	34.1	15.4	9.8	7.9	H	C
Molossidae	*Mops niventus*	Mon	44.3	6.7	44.4	18.7	25.9	44.2	15.8	13.2	27.1	13.0	6.7	7.6	H	C
Molossidae	*Otomops martiensseni*	Om	66.0	6.6	59.1	22.9	28.4	54.4	15.3	9.3	29.9	19.8	9.3	6.5	M	C
Molossidae	*Sauromys petrophilus*	Sp	41.4	7.0	41.6	32.7	8.3	40.0	13.8	7.5	24.7	12.3	5.8	7.0	M	C
Molossidae	*Tadarida aegyptiaca*	Tda	62.2	8.6	61.3	23.6	26.5	48.3	13.7	8.2	37.0	13.3	10.8	7.1	M	C
Nycteridae	*Nycteris macrotis*	Nm	49.6	11.5	37.3	18.3	27.5	39.7	15.3	15.0	41.8	14.8	16.9	5.1	L	A
Nycteridae	*Nycteris thebaica*	Nt	49.4	9.6	37.1	25.8	28.4	37.7	14.6	12.3	37.8	13.8	12.4	4.7	L	A
Phyllostomidae	*Artibeus watsoni*	Aw	38.7	6.1	32.9	12.1	18.9	32.8	11.3	13.7	34.9	8.1	11.0	5.5	L	B
Phyllostomidae	*Carollia castanea*	Cc	36.2	8.9	34.0	14.7	20.6	31.5	11.0	13.6	32.9	11.2	11.0	5.9	L	B
Phyllostomidae	*Carollia perspicillata*	Cp	39.5	7.6	37.1	16.6	22.5	35.9	13.8	15.6	37.9	12.4	14.2	5.7	L	B
Phyllostomidae	*Phyllostomus discolour*	Pd	65.5	8.2	53.2	14.1	27.7	54.2	11.6	21.3	56.4	10.8	14.6	9.8	H	C
Pteropodidae	*Epomorhous wahlbergii*	Ew	77.3	8.6	50.9	36.2	49.4	49.4	27.8	29.8	51.1	25.7	25.8	7.1	M	B
Pteropodidae	*Rousettus aegyptiacus*	Roa	96.6	20.4	62.4	43.1	66.6	63.4	34.9	41.6	58.1	33.4	30.1	5.7	L	A
Rhinolophodae	*Rhinolophus blasii*	Rb	45.1	5.0	27.9	14.1	25.5	30.7	8.1	14.9	31.9	10.5	12.5	5.5	L	B
Rhinolophodae	*Rhinolophus capensis*	Rc	49.1	5.9	31.8	15.4	26.9	34.7	8.2	16.7	35.0	10.6	13.6	5.7	L	B
Rhinolophodae	*Rhinolophus clivosus*	Rcl	53.4	6.5	34.3	18.1	32.8	38.2	11.2	19.4	41.8	11.7	15.9	5.7	L	B
Rhinolophodae	*Rhinolophus darlingii*	Rd	48.3	5.8	31.7	14.3	27.2	35.6	8.8	12.8	34.8	9.8	11.1	5.9	L	B

Table 3.1 continued

Family	Species	Code	FA	1st	3MC	3PI	3PII	4MC	4PI	4PII	5MC	5PI	5PII	A	A - Code	ZRS Clade
Rhinolophodae	*Rhinolophus denti*	Rdt	41.3	4.5	29.0	14.1	24.2	31.3	7.1	14.6	30.6	8.7	12.3	6.3	L	B
Rhinolophodae	*Rhinolophus fumigatus*	Rf	50.8	6.4	33.8	15.5	31.9	36.6	9.5	18.8	37.5	10.6	14.7	5.7	L	B
Rhinolophodae	*Rhinolophus hildebrandtii*	Rh	64.3	8.5	44.7	20.7	38.4	45.9	12.7	23.5	47.9	15.7	21.5	5.5	L	B
Rhinolophodae	*Rhinolophus landeri*	Rl	42.4	6.8	31.0	14.6	25.0	34.1	7.2	15.4	33.0	9.0	16.2	4.8	L	B
Rhinolophodae	*Rhinolophus simulator*	Rsi	43.3	4.9	29.1	14.7	25.3	33.4	8.1	15.3	32.7	10.2	12.9	5.9	L	B
Rhinolophodae	*Rhinolophus swinnyi*	Rsw	44.2	5.8	29.0	15.0	27.3	33.0	8.6	16.3	34.2	10.7	12.8	5.3	L	B
Thyropteridae	*Thyroptera tricolor*	Tht	43.8	6.8	37.9	17.5	7.4	40.8	11.5	8.4	39.3	9.4	5.0	5.7	L	A
Vespertilionidae	*Chalinolobis variegatus*	Clv	43.1	5.6	39.4	15.2	28.4	38.4	11.7	13.1	36.3	9.2	8.3	6.0	L	B
Vespertilionidae	*Eptesicus hottentotus*	Eph	48.3	7.2	45.9	19.6	25.6	44.7	15.2	11.8	45.1	11.0	8.1	6.9	M	C
Vespertilionidae	*Laephotis wintoni*	Lw	28.0	3.7	25.7	15.9	21.7	25.7	8.4	8.4	25.7	7.3	5.4	5.1	L	A
Vespertilionidae	*Myotis bocagei*	Myb	36.3	4.7	33.7	16.9	21.5	32.5	10.7	11.0	33.8	9.4	9.3	5.5	L	B
Vespertilionidae	*Myotis tricolor*	Myt	48.2	6.6	45.8	18.4	23.9	45.2	13.1	12.8	43.4	12.6	12.2	5.5	L	B
Vespertilionidae	*Myotis welwitschii*	Myw	56.1	8.7	52.2	22.5	28.1	49.6	15.7	15.8	51.0	13.7	12.9	5.6	L	B
Vespertilionidae	*Neoromicia Capensis*	Nec	33.7	4.9	31.6	15.8	21.3	31.2	10.4	8.7	30.9	8.4	6.8	8.2	H	C
Vespertilionidae	*Neoromicia somalicus*	Nes	32.4	4.5	32.9	15.8	21.3	30.9	11.1	8.2	31.1	8.6	5.1	8.0	H	C
Vespertilionidae	*Nycticeinops schlieffeni*	Nys	34.6	6.8	31.0	15.8	21.3	32.0	10.7	8.2	31.9	8.1	6.2	5.7	L	B
Vespertilionidae	*Pipistrellus anchietai*	Pia	32.4	3.9	32.9	15.8	21.3	28.3	9.3	9.2	28.5	8.4	7.5	5.4	L	B
Vespertilionidae	*Pipistrellus hesperidus*	Pih	30.6	6.6	30.1	11.3	8.6	29.7	10.4	7.9	28.7	6.9	5.1	5.8	L	A
Vespertilionidae	*Pipistrellus kuhlii*	Pik	31.3	4.9	29.7	15.8	21.3	30.5	10.3	8.5	29.7	8.5	5.7	6.7	M	C
Vespertilionidae	*Pipistrellus nanus*	Pin	30.0	5.0	28.5	15.9	21.7	27.9	8.8	7.8	26.9	8.0	5.0	5.7	L	B
Vespertilionidae	*Pipistrellus rusticus*	Pir	28.2	4.3	26.0	15.9	21.7	26.0	9.1	7.0	25.8	6.8	3.9	7.2	M	C
Vespertilionidae	*Pipistrellus zuluensis*	Piz	29.1	4.8	27.6	19.2	8.3	28.0	9.9	8.4	27.9	7.9	6.0	5.5	L	A
Vespertilionidae	*Scotoecus albigula*	Sa	32.9	5.4	32.9	15.8	7.3	30.6	11.4	8.8	28.9	7.3	5.5	5.7	L	A
Vespertilionidae	*Scotoecus albofucus*	Saf	29.6	7.0	28.4	10.6	17.0	28.1	10.3	10.4	27.5	7.4	6.1	5.6	L	B
Vespertilionidae	*Scotophilus dinganii*	Spd	51.8	7.7	50.4	17.0	22.5	49.8	13.3	10.4	46.2	9.5	7.7	6.8	M	C
Vespertilionidae	*Scotophilus mishangani*	Spm	44.0	7.0	42.7	14.7	19.9	42.0	11.9	9.7	40.8	8.1	6.8	5.9	L	C
Vespertilionidae	*Scotophilus Nigrita*	Spn	79.1	9.0	70.6	21.0	30.3	71.0	19.5	14.5	68.4	10.8	8.6	5.8	L	C
Vespertilionidae	*Scotophilus viridis*	Spv	46.1	6.0	46.1	18.6	26.7	45.5	16.1	7.6	26.8	14.4	6.4	5.8	L	A

Aspect ratio (Figure 3.3 B) greatly influences the separation of species (Figure 3.3 A) along both axes (Figure 3.3 A). Species with lowest A are located at the bottom left corner of the graph, e.g. *Nycteris macrotis* and *Nycteris thebaica*, and species with the highest A are located at the top right corner of the graph, e.g. *Chaerophon pumilus* and *Neoromicia somalicus* (Figure 3.3 A, Table 3.1). The species with the highest A is *Phyllostomus discolour* (Table 3.1), but although it appears in the top right quadrant, it is very close to the top left quadrant (Figure 3.3 A). Similarly, *Sauromys petrophilus* has a relatively high A (Table 3.1), but it occurs in the bottom right quadrant (Figure 3.3 A). The distribution of the species in Figure 3.3 A is a result of an interaction between A and the other skeletal elements, e.g. in the case of 5PII; when comparing species *Rhinolophus denti* (L, 5PII – 12.3mm), *Taphozous mauritianus* (M, 5PII – 9.9mm), and *N. somalicus* (H, 5PII –5.1mm). Whereas various combination of 3PI, 3PII, 4PI and 4PII lengths give the same A, this is apparent when comparing species *C. perspicillata, N. thebaica* and *M. Natalensis,* which all have low A, but have different lengths of 3PI, 3PII, 4PI and 4PII (Table 3.1).

Forearm length (i.e. size) and aspect ratio contribute to most of the variation within the data. Within the handwing, it is the second phalange of all three digits, and the first phalange of digit 3 and 4 that are the most variable elements between species, and not the metacarpals (Figures 3.2 and 3.3). To ensure that no bias was introduced through use of imputed values in the data, the PCA analysis was repeated using only species for which there was a complete dataset (31 species), and yielded the same results (results not shown).

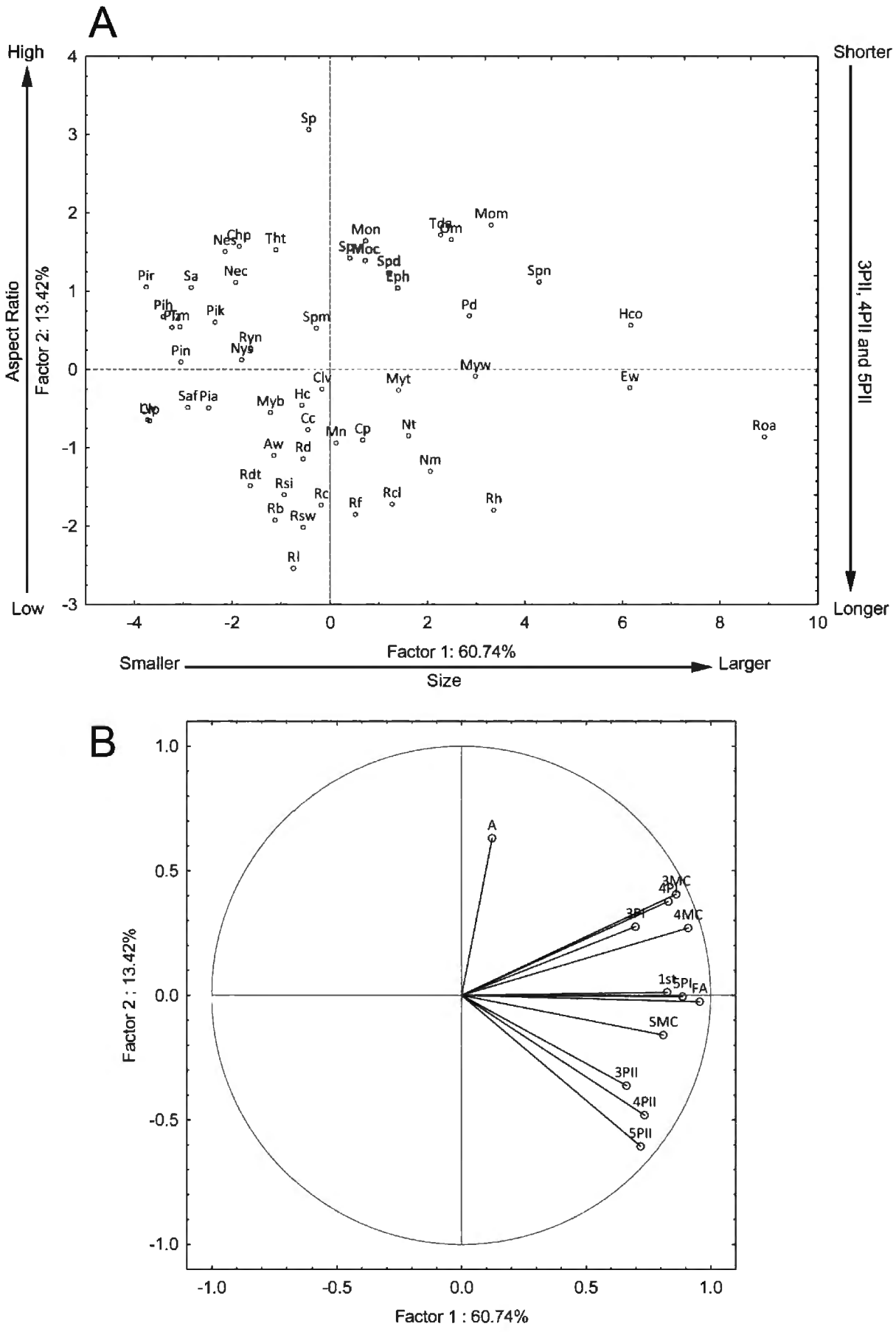

Figure 3.2: Plot of the first two factors yielded by PCA. A: Plot of factor weights for each of the species on the first two factors. B: Plot of factor weights for each of the wing parameters included in the PCA (see Table 3.1).

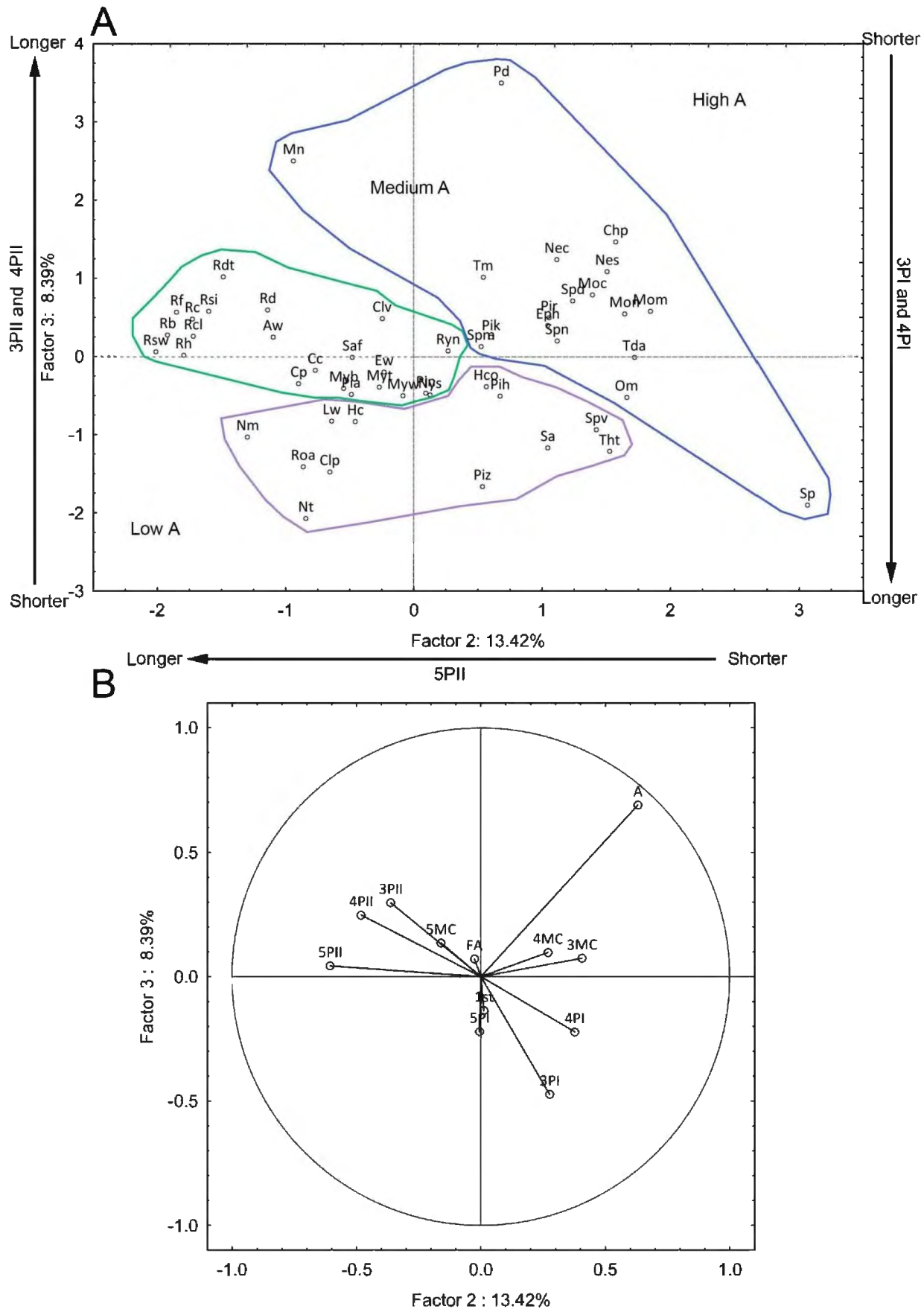

Figure 3.3: Plot of the factors two and three yielded by PCA. A: Plot of factor weights for each of the species on the factors two and three factors. Species encompassed by a purple line are part of ZRS clade A, species in the green line are part of ZRS clade B and species in the blue line are part of ZRS clade C. B: Plot of factor weights for each of the wing parameters included in the PCA (see Table 3.1).

Phylogenetic Analysis of the Bat ZRS and Wing Morphology

The 18 bat ZRSs were also aligned to the horse ZRS, the mouse ZRS and the human ZRS using either PRANKSTER or DnalignTX alignment tools (Figure A.6 and A.7 respectively). These alignments were then used to construct phylogenetic trees that indicate the evolutionary relationships between the ZRS of the various bat species. Both alignments yielded the same maximum likelihood tree (Figure 3.4). The aLTR scores of the branches are quite low - a result of polytomy - but there are three distinct clades: clade A (Purple), clade B (Green) and clade C (Blue).

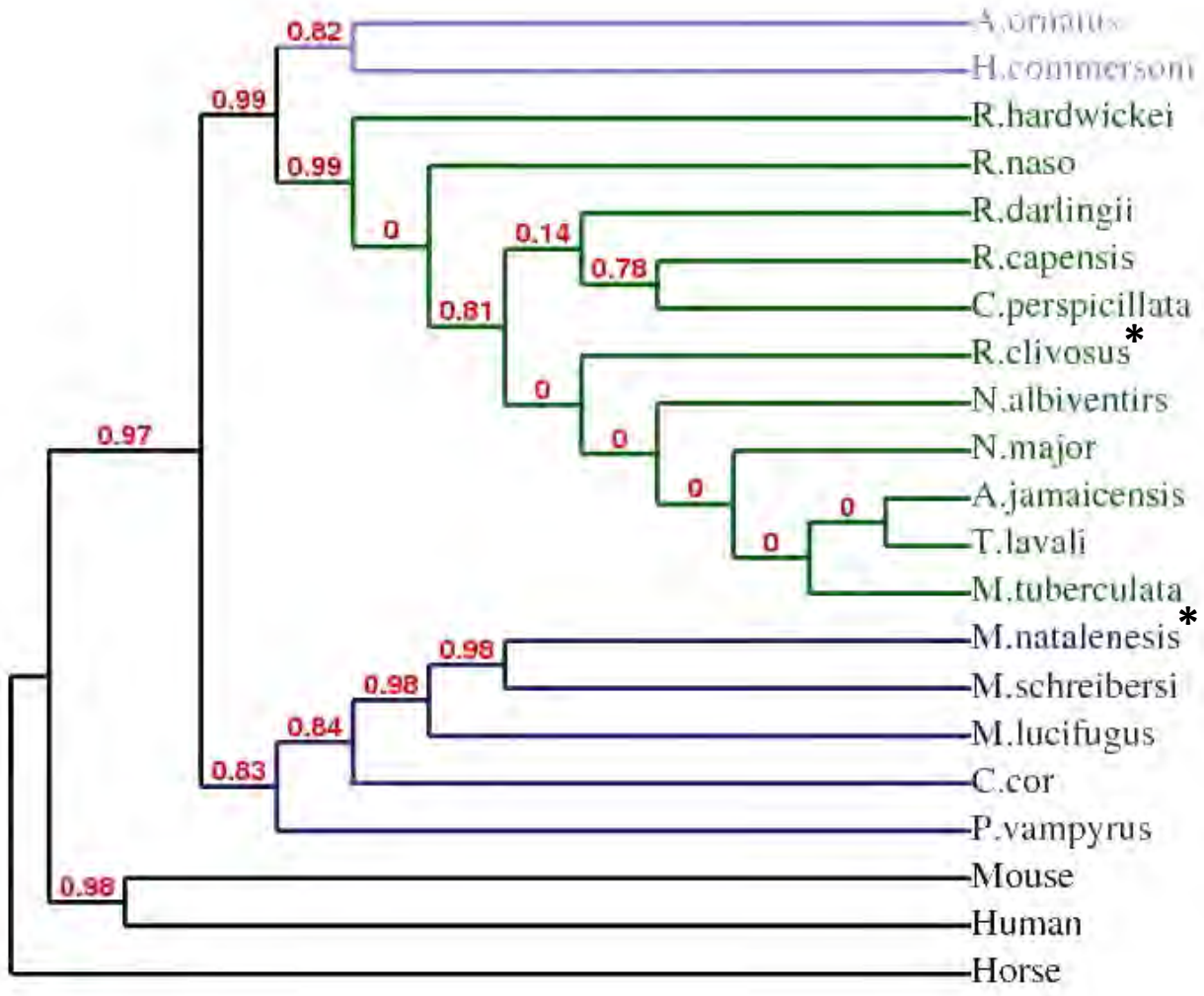

Figure 3.4: Phylogenetic tree of the bat ZRS sequences with horse, mouse and human ZRS sequence as out groups. The Maximum likelihood tree has three major clades: clade A (purple), clade B (green) and clade C (blue). In red are the aLTR values to show the support of each branch. Asterisks indicate the positions of *M. natalensis* and *R. clivosus*.

Although data on aspect ratio was available for 15 of the bat species used in the analysis of ZRS sequences, detailed morphological data were unfortunately only available for seven of the species in this dataset; namely *H. commersoni*, *C. perspicillata, R. capensis, R. clivosus, R. darlingii, R. naso,* and *M. natalensis* (Table 3.2). Therefore, to increase the sample number, the 53 bat species from the data set above were grouped by similarity of wing shape (Table 3.1) and later categorized into the one of the three ZRS clades (Figure 3.4) based on which ZRS bat species were included in those groups (Figure 3.3 A).

Table 3.2: The aspect ratio (A) of the 18 bat species used for the analysis of the ZRS. Values with a black dot (•) next them were taken from Norberg & Rayner (1987), and values with a double dagger (‡) were taken from O'Shea & Vaughan (1980). Species with morphological data (Table 3.1) are indicated by an asterisk (*).

Family	Species	Clade	A
Emballonuridae	Rhynconycteris naso*	B	6.40
Hipposideridae	Anthops ornatus	A	-
Hipposideridae	Hipposideros commersoni*	A	6.30
Megadermatidae	Carioderma cor	C	5.70‡
Miniopteridae	Miniopterus natalensis*	C	7.00
Miniopteridae	Miniopterus schreibersi	C	7.00•
Mystacinidae	Mystacina tuberculata	B	7.00•
Natalidae	Natalus major	B	-
Noctilionidae	Noctilio albiventris	B	7.80•
Phyllostomidae	Artibeus jamaicensis	B	6.40•
Phyllostomidae	Carollia perspicillata*	B	6.10•
Pteropodidae	Pteropus vampyrus	C	8.40•
Rhinolophidae	Rhinlophus capensis*	B	5.70
Rhinolophidae	Rhinlophus clivosus*	B	5.70
Rhinolophidae	Rhinolophus darlingii*	B	5.90
Rhinopomatidae	Rhinopoma hardwickii	B	6.90•
Thyropteridae	Thyroptera lavalii	B	-
Vespertilionidae	Myotis lucifugus	C	6.00•

I tested the hypothesis that variation in the ZRS sequence of different bat species correlated with changes in wing shape and the significant skeletal elements identified in the PCA results (3PI, 3PII, 4PI, 4PII and 5PII). Data was normally distributed (Table 3.3), and therefore, an ANOVA was used to test this hypothesis. The Bonferroni test was used to check whether there was a significant difference between the aspect ratios, 3PI, 3PII, 4PI, 4PII and 5PII of the bat species grouped in the ZRS clades.

Table 3.3: Shapiro-Wilk W test results of the significant wing variables. N - Sample size, W - Shapiro-Wilk W value.

Variable	N	Mean	W	p-value
A	53	6.21	0.89	0.00013
3PI	53	17.96	0.77	0.00000
3PII	53	24.89	0.85	0.00001
4PI	53	12.53	0.77	0.00000
4PII	53	12.99	0.80	0.00000
5PII	53	10.39	0.86	0.00002

The ANOVA results revealed that there was a difference in aspect ratio and 5PII length between species in the three ZRS clades (Table 3.4, Figure 3.5), but no differences in the length of 3PI, 3PII, 4PI and 4PII. The Bonferroni results showed that species in clade C have significantly higher aspect ratio than species in clades A and B (p=0.00), while there was no significant difference in A between species in clade A and B (p=0.78, Figure 3.5 A). For the 2nd phalange of digit 5 (Figure 3.5 B), the Bonferroni test indicated that species in clade B have significantly longer 5PII than species in clade C (p=0.02), but there was no significant difference in 5PII length between species of clades A and B (p=1.00) or between species of clades A and C (p=0.42). These results imply that the ZRS might play a role in determining wing shape through the regulation of *Shh*.

Table 3.4: Summary of the ANOVA results. Asterisks indicate significant p-values. SS – sum of squares, MS – mean square and F – F statistic.

Variable	Effect	SS	MS	F	p-value
A	ZRS clade	32.79	16.39	39.09	0.00*
	Error	20.97	0.42		
3PI	ZRS clade	91.60	45.80	1.34	0.27
	Error	1711.34	34.23		
3PII	ZRS clade	68.77	34.38	0.36	0.70
	Error	4779.20	95.58		
4PI	ZRS clade	114.10	57.05	2.28	0.11
	Error	1249.55	24.99		
4PII	ZRS clade	107.46	53.73	1.41	0.25
	Error	1911.03	38.22		
5PII	ZRS clade	202.75	101.37	4.08	0.02*
	Error	1243.61	24.87		

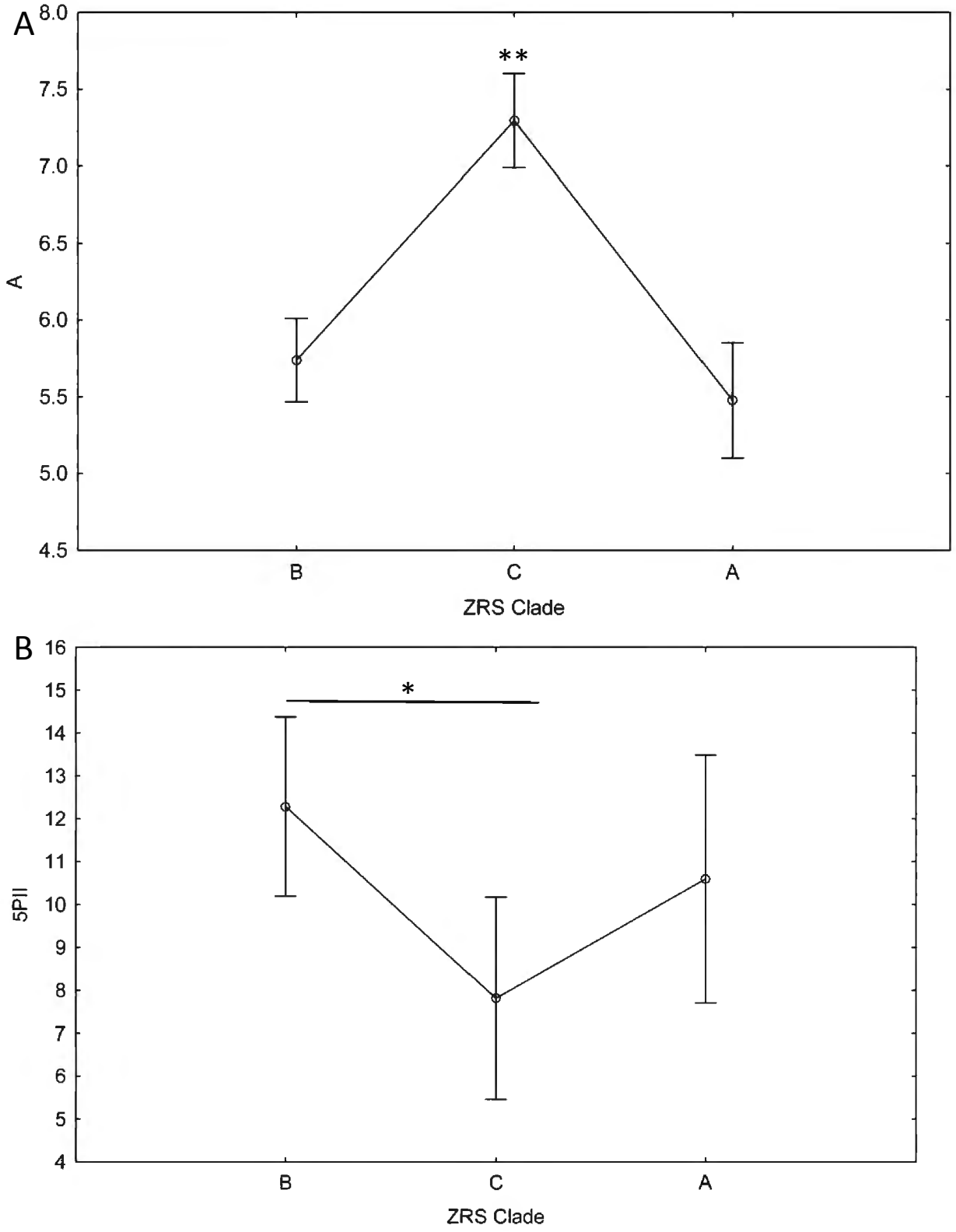

Figure 3.5: The ANOVA result of aspect ratio (A) and 2nd phalange of digit 5 (5PII). A: aspect ratio results: Species have significantly higher A than species in clades A and C, there was no significant difference in A between species in clade A and B. B: Second phalange of digit 5 results: Species in clade B have significantly longer 5PII than species in clade C, and there was no significant difference in 5PII length between species in clades A and B or between species in clades C and A. Vertical bars denote 0.95 confidence intervals, p≤0.05 (*), and p≤0.01 (**).

Discussion

The aim of this chapter was to identify those skeletal elements within the handwing (i.e. metacarpals and phalanges) responsible for the variation of wing shape across bat species, and to test whether there is a correlation with the variation in the ZRS sequence of different bat species.

Variation in Wing Shape

There appeared to be marked differences in wing skeletal elements between species even after the difference in body size was accounted for. Aspect ratio, the length of the second phalange of digits 3 to 5 and first phalange of digit 3 and 4 accounted for most of the variation in wing parameters between the species (Figure 3.2 and 3.3). Surprisingly, there was little variation in metacarpal lengths between bat species. Although these results are supported by those of previous studies (Swartz 1997; Swartz & Middleton 2008; Adams 2008; Lin et al. 2011), the variation in the lengths of the metacarpals of digits 3 to 5 has a insignificant contribution to overall wing shape variation across. In this study, results showed that, while the metacarpals do indeed contribute to some of the variation in across species, the variation is not significant and it seems to be correlated to the size of the bats, i.e. large bats have long metacarpals in the handwing. The reason for this is that this study focused specifically on the skeletal elements in the handwing (autopod) and only compared the variation between bat species and not with the skeletal element in the autopod of other mammals. The relatively low variation in the relative lengths of metacarpals might be because these elements provide stability to the wing during flight and are not free to vary (Norberg & Rayner 1987; Thewissen & Babcock 1992; Norberg 1998; Swartz et al. 2006). The results imply that wing shape, i.e. aspect ratio, is determined by variable combinations of the lengths of 3PII, 3PI, 4PI, 4PII, and 5PII. The variation of the 3PII, 3PI, 4PI, 4PII, and 5PII may be a result of compensation growth that occurs during the postnatal development of the wing as the bat learns to fly (Adams 2008; Lin et al. 2011). Alternatively, wing shapes evolved independently across the bat phylogeny, and as a result, there are different bat species with the same wing shape but with variations in the length of these five skeletal elements.

Phylogenetic Analysis of the Bat ZRS and Wing Shape

A phylogenetic analysis of the bat ZRS sequences showed that the 18 bat species could be sub-divided into 3 groups based on their ZRS sequence (Figure 3.4). The phylogenetic tree produced was different to that of the bat evolutionary tree reported by Eick et al. (2005) and Teeling et al. (2005). This suggests that the evolution of the ZRS is independent of the speciation during the evolution of the bat phylogeny. This is interesting when conserving the allometric relationship

between bat wing and body size (Swartz, 1997). To determine if variation in the ZRS sequences of the bat species played a role in variation in wing shape, the 53 species were subdivided into the three clades and tested for significant differences in aspect ratio, the lengths of the second phalange of digits 3-5 and first phalange of digit 3 and 4. Results showed that the bat species in clade C had significantly higher aspect ratio than bat species in clade A and B, and that there was a significant difference in the length of the second phalange of digits 5 between bat species in clades B and C. This result hints at the possibility of the ZRS playing a role in determination of wing shape through the regulation of *Shh* expression during embryonic development, and suggests that the same wing shape is made by different combinations of the length of 3PII, 3PI, 4PI, 4PII, and 5PII.

The great limitations of this study are that only one individual was used per species, and intraspecies variation was not taken into account, which may have skewed some of the results. To establish the relative roles of genetics and environment (i.e. compensation growth) in the development of the adult wing in each species, this experiment would have to be repeated with more individuals per species to obtain more conclusive findings. Another limitation is the sample size for both the bat ZRS sequences and the data for those species. The assumption that bats in the same ZRS clade will have similar wing shape (i.e. the grouping in Figure 3.4 A) may have introduced bias into the analysis - on wing shape similarities bias. That is, based on the above assumption, the significant differences in aspect ratio and the second phalange of digit 5 indicated above may be a result of dividing the 53 bat species into the three ZRS clades. I therefore suggest that more bat ZRS sequences for the 53 species should be acquired so as to avoid any bias and to resolve the evolution relationships the bat ZRS. To properly determine if the bat ZRS sequences are important in the wing shape variation across bat species, the measurements of the five skeletal elements identified above should be made for as many species as possible, possibly including other wing shape parameters such as the Tip Shape Index, which is independent of size (Norberg & Rayner 1987). If these experiments yield positive results, then the next step will be to determine the different bats ZRS genotypes corresponding to different *Shh* expression patterns in the forelimb during embryonic development (and consequently, to the adult wing phenotype), using transgenic mice or *in situ* hybridization experiments. If such experiments yield negative results, other development genes, such as the *Hox* genes, *Bmps, Fgfs* and *Prrx1* (which have been shown to be involved in bone formation, and have been identified as differently expressed in bats; (Sears, 2008), should be investigated.

Chapter 4: Conclusions and Future Experiments

Bats are unique mammals that have the ability of powered flight which is enabled by their highly specialized forelimb (Thewissen & Babcock 1992; Norberg 1998; Simmons 2005; Simmons et al. 2008). The bat wing has elongated digits (2 to 5) and interdigital webbing that provide the structural support needed to withstand the aerodynamic stresses involved in flight (Thewissen & Babcock 1992; Swartz 1997; Norberg 1998; Swartz & Middleton 2008). To understand how such a unique structure came to be, researchers have looked at the developmental genes involved in limb formation. Most of them took the candidate gene approach, focusing on characterizing gene expression in the bat developing limb and comparing it to the closest related model organism, the mouse. Genes that are differentially expressed during bat development are: *Hoxd13*, *Prrx1*, *Bmps, Fgfs* and *Shh* (Chen et al. 2005; Weatherbee et al. 2006; Cretekos et al. 2007; Cretekos et al. 2008; Ray & Capecchi 2008; Hockman et al. 2008). The focus of this thesis is how *Sonic hedgehog* (*Shh)* is regulated in the bat forelimb. *Sonic hedgehog* (*Shh*) expression in the limbs is regulated by a long distance *cis*-regulatory sequence located on 1Mb upstream of *Shh* in intron 5 of the *Lmbr1* gene (Heutink et al. 1994; Hing et al. 1995; Heus et al. 1999; Zguricas et al. 1999; Lettice et al. 2002). The ZPA-regulatory sequence (ZRS) is found to be conserved throughout the Vertebrate lineage, but is absent in limb-less newt and snakes (Sagai et al. 2004; Sagai et al. 2005). Mutation in the ZRS has been found to cause PPD in humans, mice and cats, and transgenic analysis confirmed that those mutations cause a disruption in *Shh* expression (Lettice et al. 2002; Lettice et al. 2003; Hill et al. 2003; Maas & Fallon 2005; Hill 2007; Gurnett et al. 2007; Lettice et al. 2008; Furniss et al. 2008). Based on this, I proposed that the pattern of expression of *Shh* in the limbs of developing bat embryos is a result of conserved mutations in the bat ZRS. The aims of this thesis was to identify conserved changes in the bat ZRS and characterise the effects of ZRS on the expression of β-gal in transgenic mice. Another focus of this research was to identify those skeletal elements important in defining wing shape in the adult bat wing.

Analysis of the ZRS from 18 bat species and 20 other vertebrates revealed that there are 5 conserved changes in the bat ZRS in regions of high conservation. To determine whether or not the bat ZRS was capable of altering the spatiotemporal expression pattern of *Shh,* the ZRS from *M. natalensis* (MnaZRS) and *R. clivosus* (RclZRS) were linked to the β-globin-*LacZ* reporter construct and used in transgenic mice experiments. The MnaZRS G_0 embryos and transgenic line embryos showed the same expression patterns. The transgenic mice containing the MnaZRS had ectopic β-

gal expression at the anterior end and along the distal edge of the autopod at stages E10.5-11.5. These embryos also showed expression at the posterior end of the autopod, similar to what was seen in mouse ZRS (MmuZRS) transgenic embryos. At E12.5-13.5, the MnaZRS had β-gal expression at the tips of digits 2-4, and from tips of digit 5 along the posterior end of the limb. The RclZRS transgenic mice had a very low level of β-gal expression that gave inconsistent results. In RclZRS G_0 embryos at stage E11.5, β-gal expression was similar to that seen in the control embryos, i.e., expression at the posterior end of the autopod. At E13.5, RclZRS G_0 embryos either had β-gal expression that was limited to the posterior domain of the limb extending from digit 4 to 5 along the length of the posterior edge of the limb, or showed β-gal expression that was restricted to the cells between digits 4 and 5. The RclZRS transgenic lines showed the same expression pattern as the MmuZRS transgenic lines. To test whether the five conserved bat mutations were responsible for the change of *Shh* expression in bats, they were inserted into the mouse ZRS (Mmu^{5M}-ZRS) and linked with the BGZ construct. The Mmu^{5M}-ZRS transgenic mice showed a similar pattern of expression to that of the control embryos, at E11.5 and E13.5. None of the bat transgenic mice showed similarity to the expression of *Shh* in developing bat embryos, nor was there evidence of a second wave of β-gal expression. There was also no overlap of expression aside from that observed in those areas of expression common to the control between the MnaZRS, RclZRS and Mmu^{5M}-ZRS. These results imply that not all bats have the expression patterns of *Shh* in the limb during development, and that there might be other elements (mutations) within the bat ZRS that cause changes in *Shh* expression not identified here.

In fact, a phylogenetic analysis of the bat ZRS sequences revealed that the 18 bat species were categorized into 3 distinct groups (clades: A, B and C). Since different mutations in the ZRS have been shown to correspond to differences in severity of PPD in humans, it is possible that the polymorphisms of the ZRS between bat species may correspond to differences in adult wing morphology.

To test whether this is true, I first had to identify what skeletal elements (i.e. the metacarpals and the phalanges) within the handwing were most variable, and how they related to wing shape by looking at aspect ratio. The PCA results of 53 bat species showed that the most variable wing parameters across species were aspect ratio, the second phalange of digits 3 to 5 and the first phalange of digits 3 and 4. To investigate any connection between wing shape and the ZRS, the 53 bat species were classified into the three ZRS clades. The comparison of aspect ratio between bat species in the three clades revealed that bat species in clade C had significantly higher aspect

ratios than the bat species in clades A and B. Comparison of the second phalange of digits 3 to 5 and the first phalange of digits 3 and 4 between the ZRS clades, showed no significant variation except for the second phalange of digit 5 which was significantly longer in bat species in clade B compared to bat species in clade C.

Conclusions

The bat ZRS does show potential to alter the expression of *Shh* during development but that alteration potential does not seem to be caused by the five conserved bat mutations identified in the analysis of the ZRS. The transgenic results suggest that not all bats have the same expression profile of *Shh,* and that the bat ZRS is not enough to induce a second round of expression at stage E12.5, as seen in bats. Therefore, it could be that the information to reactivate *Shh* at a later stage lies in the regulation of *Shh*, i.e. through the activators *Hoxd13* and *dHand*. Another reason for the lack of a second wave of β-gal could be that the BGZ transgenic assay did not mimic the mechanism by which *Shh* is regulated and therefore, could not induce a second wave. It was also clear even in the control experiments that the expression of β-gal was continuous once activated at stage E10.5. Thus, there is a possibility that a second wave of expression does occur but is not noticeable with this assay.

Analysis of the skeletal elements within the handwing revealed that the second phalange of digits 3 to 5, and the first phalange of digits 3 and 4 significantly vary across the 53 bat species, thereby suggesting that they contribute to variation in wing shape across species. Since only one individual per species was used, the variation seen here could be a result of compensation growth that occurs post-natal as juvenile bats learn to fly. On other hand, the variation could be genetically pre-determined so that the bats can have the proper wing shape required for survival in their respective habitats. Comparisons of aspect ratio between bat species in the ZRS clades imply that there is a relationship between differences in the ZRS sequences of bats and wings. Analysis of the variation of the lengths of the 3PII, 3PI, 4PI, 4PII, and 5PII between the ZRS clades suggest that the same wing shape is made by different combinations of the length of 3PII, 3PI, 4PI, 4PII, and 5PII.

Future experiments

In this study it was shown that the bat ZRS produces a different expression pattern to that of the mouse ZRS. To further validate that the bat ZRS is responsible for the change in *Shh* expression in the limbs of developing bats, transgenic knock-in experiments need to be done. In knock-in experiments, the endogenous mouse ZRS is replaced by the bat ZRS. The *Shh* gene in the

transgenic embryo is regulated by the natural mechanism, and therefore should mimic *Shh* expression in bat embryos. To determine whether *Shh* expression patterns do vary across species, *in situ* hybridization experiments should be done for characterisation of *Shh* expression in *R. clivosus* embryos.

Wing morphology is an important factor in the survival of bats. Hence the old debate on whether it is genetics or the environment that determines wing shape continues. Results from the analysis revealed that the most variable skeletal elements within the handwing are phalanges II of digits 3 to 5, and phalange I from digits 3 to 4. Because only one individual was used per species, the significance of this result should not be taken at face value. To further validate this finding, the experiment should be redone with more individuals per species - preferably a minimum of ten - to conclusively show that the existing variation is not a by-product of growth compensation, but true interspecies variation. Possibly, other measurements of wings shape, such as Tip Shape Index, can also be used in the analysis to see if a similar relationship exists. Future experiments should also include transgenic mice or *in situ* hybridization experiments to test whether the different bats ZRS polymorphisms correspond to different *Shh* expression patterns in the bat forelimb during embryonic development. If such experiments yield negative results, other development genes, such as the *Hox* genes, *Bmps, Fgfs* and *Prrx1* (which have been observed to be involved in bone formation, and have been identified as differently expressed in bats; Sears, 2008), should be investigated.

Limb development is a result of networks of genes working together to produce a proper limb. It is therefore not a surprise that the whole SHH-BMP-FGF feedback loop is reactivated at a later stage in the bat development. Thus, to further understand the origins of the bat wing, researchers should also look at the regulations of those genes that activate *Shh*, such as *dHand* and *Hoxd13*, and of genes that work in conjunction with *Shh,* such as *Fgf* and *Bmps*. They should also investigate interspecies variation of genes involved in bone formation - shown to be differently expressed in bats - such as the *Hox* genes, *Bmps and Prrx1***.**

References

Adams, Rick A. 2008. Morphogenesis in Bat Wings: Linking Development, Evolution and Ecology. *Cells Tissues Organs*, 187(1), pp.13-23.

Amano, Takanori, Tomoko Sagai, Hideyuki Tanabe, Yoichi Mizushina, Hiromi Nakazawa, and Toshihiko Shiroishi. 2009. Chromosomal dynamics at the Shh locus: limb bud-specific differential regulation of competence and active transcription. *Developmental cell*, 16(1), pp.47-57.

Anisimova, Maria, and Olivier Gascuel. 2006. Approximate likelihood-ratio test for branches: A fast, accurate, and powerful alternative. *Systematic biology*, 55(4), pp.539-52.

Bangs, Fiona, Monique Welten, Megan G Davey, Malcolm Fisher, Yili Yin, Helen Downie, Bob Paton, Richard Baldock, David W Burt, and Cheryll Tickle. 2010. Identification of genes downstream of the Shh signalling in the developing chick wing and syn-expressed with Hoxd13 using microarray and 3D computational analysis. *Mechanisms of development*, (August).

Berge, Derk, Antje Brouwer, Jeroen Korving, James F Martin, and Frits Meijlink. 1998. Prx1 and Prx2 in skeletogenesis: roles in the craniofacial region, inner ear and limbs. *Development (Cambridge, England)*, 125(19), pp.3831-42.

Bouldin, Cortney M, Amel Gritli-Linde, Sohyun Ahn, and Brian D Harfe. 2010. Shh pathway activation is present and required within the vertebrate limb bud apical ectodermal ridge for normal autopod patterning. *Proceedings of the National Academy of Sciences of the United States of America*, 107(12), pp.5489-94.

Camacho, Christiam, George Coulouris, Vahram Avagyan, Ning Ma, Jason Papadopoulos, Kevin Bealer, and Thomas L Madden. 2009. BLAST + : architecture and applications. *BMC Bioinformatics*, 9, pp.1-9.

Chen, Chih-Hsin, Chris J Cretekos, John J Rasweiler, and Richard R Behringer. 2005. Hoxd13 expression in the developing limbs of the short-tailed fruit bat, Carollia perspicillata. *Evolution & development*, 7(2), pp.130-41.

Cooper, Kimberly L, and Clifford J Tabin. 2008. Understanding of bat wing evolution takes flight. *Genes & development*, 22(2), pp.121-4.

Cretekos, Chris J, Jian-Min Deng, Eric D Green, John J Rasweiler, and Richard R Behringer. 2007. Isolation, genomic structure and developmental expression of Fgf8 in the short-tailed fruit bat, Carollia perspicillata. *The International journal of developmental biology*, 51(4), pp.333-8.

Cretekos, Chris J, Ying Wang, Eric D Green, James F Martin, John J Rasweiler, and Richard R Behringer. 2008. Regulatory divergence modifies limb length between mammals. *Genes & development*, 22(2), pp.141-51.

Dereeper, Alexis, V Guignon, Guillaume Blanc, Stephane Audic, S Buffet, F Chevenet, J Dufayard, et al. 2008. Phylogeny.fr: robust phylogenetic analysis for the non-specialist. *Nucleic Acids Research*, 36(Web Server issue), pp.W465-9.

Duboc, Veronique, and Malcolm PO Logan. 2009. Building limb morphology through integration of signalling modules. *Current opinion in genetics & development*, 19(5), pp.497-503.

Eick, Geeta N, David S Jacobs, and Conrad A Matthee. 2005. A Nuclear DNA Phylogenetic Perspective on the Evolution of Echolocation and Historical Biogeography of Extant Bats (Chiroptera). *Molecular biology and evolution*, 22(9), pp.1869-86.

Falgueras, Juan, Antonio J Lara, Noé Fernández-Pozo, Francisco R Cantón, Guillermo Pérez-Trabado, and M Gonzalo Claros. 2010. SeqTrim: a high-throughput pipeline for pre-processing any type of sequence read. *BMC bioinformatics*, 11, p.38.

Fernandez-Teran, M, M E Piedra, I S Kathiriya, D Srivastava, J C Rodriguez-Rey, and M A Ros. , 2000. Role of dHAND in the anterior-posterior polarization of the limb bud: implications for the Sonic hedgehog pathway. *Development (Cambridge, England)*, 127(10), pp.2133-42. Available at: http://www.ncbi.nlm.nih.gov/pubmed/10769237.

Flicek, Paul, Bronwen L Aken, Benoit Ballester, Kathryn Beal, Eugene Bragin, Simon Brent, Yuan Chen, et al. 2010. Ensembl's 10th year. *Nucleic acids research*, 38 (Database issue), pp.D557-62.

Furniss, Dominic, Laura A Lettice, Indira B Taylor, Paul S Critchley, Henk Giele, Robert E Hill, and Andrew O M Wilkie. 2008. A variant in the sonic hedgehog regulatory sequence (ZRS) is associated with triphalangeal thumb and deregulates expression in the developing limb. *Human molecular genetics*, 17(16), pp.2417-23.

Galli, Antonella, Dimitri Robay, Marco Osterwalder, Xiaozhong Bao, Jean-Denis Bénazet, Muhammad Tariq, Renato Paro, Susan Mackem, and Rolf Zeller. 2010. Distinct roles of Hand2 in initiating polarity and posterior Shh expression during the onset of mouse limb bud development. *PLoS genetics*, 6(4).

Gordon, J W, G A Scangos, D J Plotkin, J A Barbosa, and F H Ruddle. 1980. Genetic transformation of mouse embryos by microinjection of purified DNA. *Proceedings of the National Academy of Sciences of the United States of America*, 77(12), pp.7380-4.

Gurnett, Christina A, Anne M Bowcock, Frederick R Dietz, Jose A Morcuende, Jeffrey C Murray, and Matthew B Dobbs. 2007. Two novel point mutations in the long-range SHH enhancer in three families with triphalangeal thumb and preaxial polydactyly. *American Journal of Medical Genetics Part A*, 143A, pp.27 - 32.

Hall, Thomas A, 1999. BioEdit: a user friendly biological sequence alignment editor and analyses program for Windows 95/98/NT. *Nucleic Acids Symposium Series*, 41, pp.95-98.

Heus, Henk, Anne V Hing, Marijke J van Baren, Marijke Joosse, Guido J Breedveld, Jen C Wang, Andrea Burgess, et al. 1999. A physical and transcriptional map of the preaxial polydactyly locus on chromosome 7q36. *Genomics*, 57(3), pp.342-351.

Heutink, Peter, Julia Zguricas, L van Oosterhout, Guido J Breedveld, Leon Testers, Lodewijk A Sandkuijl, P J Snijders, Jean Weissenbach, Dick Lindhout, and Steven E R Hovius. 1994. The gene for triphalangeal thumb maps to the subtelomeric region of chromosome 7q. *Nature genetics*, 6(3), pp.287-292.

Hill, Robert E. 2007. How to make a zone of polarizing activity: insights into limb development via the abnormality preaxial polydactyly. *Development, growth & differentiation*, 49(6), pp.439-48.

Hill, Robert E, Simon J H Heaney, and Laura A Lettice. 2003. Sonic hedgehog: restricted expression and limb dysmorphologies. *Journal of anatomy*, 202(1), pp.13-20.

Hing, Anne V, Cynthia Helms, Rachel Slaugh, Andrea Burgess, Jen C Wang, Thomas Herman, S Bruce Dowton, and Helen Donis-Keller. 1995. Linkage of preaxial polydactyly type 2 to 7q36. *American journal of medical genetics*, 58(2), pp.128-135.

Hockman, Dorit, Chris J Cretekos, Mandy K Mason, Richard R Behringer, David S Jacobs, and Nicola Illing. 2008. A second wave of Sonic hedgehog expression during the development of the bat

limb. *Proceedings of the National Academy of Sciences of the United States of America*, 105(44), pp.16982-7.

Hockman, Dorit, Mandy K Mason, David S Jacobs, and Nicola Illing. 2009. The Role of Early Development in Mammalian Limb Diversification : A Descriptive Comparison of Early Limb Development Between the Natal Long-Fingered Bat (Miniopterus natalensis) and the Mouse (Mus musculus). *Cell*, (February), pp.965-979.

Lettice, Laura A, and Robert E Hill,, 2005. Preaxial polydactyly: a model for defective long-range regulation in congenital abnormalities. *Current opinion in genetics & development*, 15(3), pp.294-300.

Lettice, Laura A, Simon J H Heaney, Lorna A Purdie, Li Li, Philippe De Beer, Ben A Oostra, Debbie K Goode, Greg Elgar, Robert E Hill, and Esther De Graaff. 2003. A long-range Shh enhancer regulates expression in the developing limb and fin and is associated with preaxial polydactyly. *Human Molecular Genetics*, 12(14), pp.1725-1735.

Lettice, Laura A, Alison E Hill, Paul S Devenney, and Robert E Hill. 2008. Point mutations in a distant sonic hedgehog cis-regulator generate a variable regulatory output responsible for preaxial polydactyly. *Human molecular genetics*, 17(7), pp.978-85.

Lettice, Laura A, Taizo Horikoshi, Simon J H Heaney, Marijke J van Baren, Herma C van der Linde, Guido J Breedveld, Marijke Joosse, et al. 2002. Disruption of a long-range cis-acting regulator for Shh causes preaxial polydactyly. *Proceedings of the National Academy of Sciences of the United States of America*, 99(11), pp.7548-7553.

Li, Qiliang, Susanna Harju, and Kenneth R Peterson, 1999. Locus control regions: coming of age at a decade plus. *Trends in genetics : TIG*, 15(10), pp.403-8.

Lin, Ai-Qing, Long-Ru Jin, Li-Min Shi, Ke-Ping Sun, Sean W Berquist, Ying Liu, and Jiang Feng. 2011. Postnatal development in Andersen's leaf-nosed bat Hipposideros pomona: flight, wing shape, and wing bone lengths. *Zoology (Jena, Germany)*, 114(2), pp.69-77.

Löytynoja, Ari, and Nick Goldman. 2005. An algorithm for progressive multiple alignment of sequences with insertions. *Proceedings of the National Academy of Sciences of the United States of America*, 102(30), pp.10557-62.

Löytynoja, Ari, and Nick Goldman. 2008. Phylogeny-Aware Gap Placement Prevents Errors in Sequence Alignment and Evolutionary Analysis. *Science (New York, N.Y.)*, 320(5883), pp.1632-5.

Maas, Sarah a, and John F Fallon. 2005. Single base pair change in the long-range Sonic hedgehog limb-specific enhancer is a genetic basis for preaxial polydactyly. *Developmental dynamics : an official publication of the American Association of Anatomists*, 232(2), pp.345-8.

McGlinn, Edwina, and Clifford J Tabin. 2006. Mechanistic insight into how Shh patterns the vertebrate limb. *Current opinion in genetics & development*, 16(4), pp.426-32.

Merino, R, J. Rodriguez-Leon, D Macias, Y Gañan, A N Economides, and J M Hurle. 1999. The BMP antagonist Gremlin regulates outgrowth, chondrogenesis and programmed cell death in the developing limb. *Development (Cambridge, England)*, 126(23), pp.5515-22.

Neuweiler, Gerhard. 2000. *The biology of bats* E. Covey, ed. New York: Oxford University Press.

Niswander, Lee A. 2003. Pattern formation: old models out on a limb. *Nature reviews. Genetics*, 4(2), pp.133-43.

Norberg, Ulla M. 1998. Morphological Adaptations for Flight in Bats. In T. H. Kunz & P. A. Racey, eds. *Bat Biology and Conservation*. Washington, DC: Smithsonian Insistitution Press, pp. 93-108.

Norberg, Ulla M, and J. M. V. Rayner. 1987. Ecological Morphology and Flight in Bats (Mammalia; Chiroptera): Wing Adaptations, Flight Performance, Foraging Strategy and Echolocation. *Philosophical Transactions of the Royal Society B: Biological Sciences*, 316(1179), pp.335-427.

O'Shea, Thomas J. and Terry A. Vaughan. 1980. Ecological observations on an East African bat community. *Mammalia*, 44(4), pp.485-496.

Palstra, Robert-Jan, Wouter de Laat, and Frank Grosveld, 2008. Beta-globin regulation and long-range interactions. *Advances in genetics*, 61(07), pp.107-42.

Park, Kiyun, Joohyun Kang, Krishna Pd Subedi, Ji-Hong Ha, and Chankyu Park. 2008. Canine polydactyl mutations with heterogeneous origin in the conserved intronic sequence of LMBR1. *Genetics*, 179(4), pp.2163-72.

Ray, Russell, and Mario Capecchi. 2008. An examination of the Chiropteran HoxD locus from an evolutionary perspective. *Evolution & development*, 10(6), pp.657-70.

Sagai, Tomoko, Masaki Hosoya, Youichi Mizushina, Masaru Tamura, and Toshihiko Shiroishi. 2005. Elimination of a long-range cis-regulatory module causes complete loss of limb-specific Shh expression and truncation of the mouse limb. *Development (Cambridge, England)*, 132(4), pp.797-803.

Sagai, Tomoko, Hiroshi Masuya, Masaru Tamura, Kunihiko Shimizu, Yukari Yada, Shigeharu Wakana, Yoichi Gondo, Tetsuo Noda, and Toshihiko Shiroishi. 2004. Phylogenetic conservation of a limb-specific, cis-acting regulator of Sonic hedgehog (Shh). *Mammalian genome : official journal of the International Mammalian Genome Society*, 15(1), pp.23-34.

Schwabe, J W, C Rodriguez-Esteban, and J C Izpisúa Belmonte. 1998. Limbs are moving: where are they going? *Trends in genetics : TIG*, 14(6), pp.229-35.

Sears, Karen E. 2008. Molecular determinants of bat wing development. *Cells, tissues, organs*, 187(1), pp.6-12.

Sears, Karen E, Richard R Behringer, John J Rasweiler, and Lee A Niswander. 2006. Development of bat flight: morphologic and molecular evolution of bat wing digits. *Proceedings of the National Academy of Sciences of the United States of America*, 103(17), pp.6581-6.

Shapiro, Michael D, James Hanken, and Nadia Rosenthal. 2003. Developmental basis of evolutionary digit loss in the Australian lizard Hemiergis. *Journal of experimental zoology. Part B, Molecular and developmental evolution*, 297(1), pp.48-56.

Simmons, Nancy B, 2005. Evolution. An Eocene big bang for bats. *Science (New York, N.Y.)*, 307(5709), pp.527-8.

Simmons, Nancy B, Kevin L Seymour, Jörg Habersetzer, and Gregg F Gunnell. 2008. Primitive Early Eocene bat from Wyoming and the evolution of flight and echolocation. *Nature*, 451(7180), pp.818-21.

Speakman, John R. 2008. Evolutionary biology: a first for bats. *Nature*, 451(7180), pp.774-5.

Speakman, John R. 2001. The evolution of flight and echolocation in bats: another leap in the dark. *Mammal Review*, 31(2), pp.111-130.

Stockwell, Elizabeth F. 2001. Morphology and flight maneuverability in New World leaf-nosed bats (Chiroptera: Phyllostomidae). *Journal of Zoology*, 254(4), pp.505-514.

Subramanian, Amarendran R, Michael Kaufmann, and Burkhard Morgenstern. 2008. DIALIGN-TX: greedy and progressive approaches for segment-based multiple sequence alignment. *Algorithms for molecular biology : AMB*, 3, p.6.

Subramanian, Amarendran R, Jan Weyer-Menkhoff, Michael Kaufmann, and Burkhard Morgenstern. 2005. DIALIGN-T: an improved algorithm for segment-based multiple sequence alignment. *BMC bioinformatics*, 6, p.66.

Swartz, Sharon M. 1997. Allometric Patterning in the Limb Skeleton of Bats : Implications for the Mechanics and Energetics of Powered Flight. *Journal of Morphology*, 234(3), pp.277-294.

Swartz, Sharon M, and Kevin M Middleton. 2008. Biomechanics of the bat limb skeleton: scaling, material properties and mechanics. *Cells, tissues, organs*, 187(1), pp.59-84.

Swartz, Sharon M, Kristin Bishop, and Maryem-Fama Ismael Aguirre. 2006. Dynamic Complaxity of Wing Form in Bats: Implications for Flight Performance. In A. Zubaid, G. F. McCracken, & T. H. Kunz, eds. *Functional and Evolutionary Ecology of Bats*. Oxford: Oxford University Press, pp. 110-130.

Tanaka, Mikiko, Andrea Münsterberg, W Gary Anderson, Alan R Prescott, Neil Hazon, and Cheryll Tickle. 2002. Fin development in a cartilaginous fish and the origin of vertebrate limbs. *Nature*, 416(6880), pp.527-31.

Teeling, Emma C, Mark S Springer, Ole Madsen, Paul Bates, Stephen J O'brien, and William J Murphy.. 2005. A molecular phylogeny for bats illuminates biogeography and the fossil record. *Science (New York, N.Y.)*, 307(5709), pp.580-4.

Thewissen, J. G. M. and S. K. Babcock. 1992. The Origin of Flight in Bats. *BioScience*, 42(5), p.340.

Tickle, Cheryll. 2006. Making digit patterns in the vertebrate limb. *Nature reviews. Molecular cell biology*, 7(1), pp.45-53.

Tárraga, Joaquín, Ignacio Medina, José Carbonell, Jaime Huerta-Cepas, Pablo Minguez, Eva Alloza, Fátima Al-Shahrour, et al. 2008. GEPAS, a web-based tool for microarray data analysis and interpretation. *Nucleic acids research*, 36(Web Server issue), pp.W308-14.

Vaquerizas, Juan M, Lucía Conde, Patricio Yankilevich, Amaya Cabezón, Pablo Minguez, Ramón Díaz-Uriarte, Fátima Al-Shahrour, Javier Herrero, and Joaquín Dopazo, 2005. GEPAS, an

experiment-oriented pipeline for the analysis of microarray gene expression data. *Nucleic acids research*, 33(Web Server issue), pp.W616-20.

Weatherbee, Scott D, Richard R Behringer, John J Rasweiler, and Lee A Niswander. 2006. Interdigital webbing retention in bat wings illustrates genetic changes underlying amniote limb diversification. *Proceedings of the National Academy of Sciences of the United States of America*, 103(41), pp.15103-7.

Zeller, Rolf. 2010. The temporal dynamics of vertebrate limb development, teratogenesis and evolution. *Current opinion in genetics & development*, 20(4), pp.384-90.

Zeller, Rolf, and Aimée Zuniga. 2007. Shh and Gremlin1 chromosomal landscapes in development and disease. *Current opinion in genetics & development*, 17(5), pp.428-34.

Zeller, Rolf, Javier López-Ríos, and Aimée Zuniga 2009. Vertebrate limb bud development: moving towards integrative analysis of organogenesis. *Nature reviews. Genetics*, 10(12), pp.845-58.

Zguricas, Julia, Henk Heus, Estela Morales-Peralta, Guido J Breedveld, Bertus Kuyt, Ethem F Mumcu, Wendela Bakker, et al. 1999. Clinical and genetic studies on 12 preaxial polydactyly families and refinement of the localisation of the gene responsible to a 1.9 cM region on chromosome 7q36. *Journal of Medical Genetics*, 36(1), pp.33-40.

Appendix

Table A.1: Spectrometric result of the gDNA extraction from selected bat species: *A. ornatus, C. cor, C. jabensis, H. commersoni, M. gigas, M. lyra, M. natalensis, M. tuberculata, N. major, N. micropus, N. albirentras, P. parentelli, R. clivosus, R. darlingii, R. swinnyi, R. hardwickii and R. microphyllum*

Sub-order	Family	Species	Concentration (ng/µl)	260/280	260/230
Pteropodiformes	Hipposideridae	*Anthops ornatus*	97	1.28	0.51
Pteropodiformes	Hipposideridae	*Hipposderos commersoni*	132.5	2.09	1.96
Pteropodiformes	Megadermatidae	*Cardioderma cor*	4.7	2.98	2.9
Pteropodiformes	Megadermatidae	*Macroderma gigas*	109.6	1.34	0.26
Pteropodiformes	Megadermatidae	*Megaderma lyra*	41.6	1.57	0.58
Pteropodiformes	Rhinolophodae	*Rhinolophus clivosus*	142.8	1.91	2.48
Pteropodiformes	Rhinolophodae	*Rhinolophus darlingii*	28.8	1.63	0.75
Pteropodiformes	Rhinolophodae	*Rhinolophus swinnyi*	215.8	1.12	0.34
Pteropodiformes	Rhinopomatidae	*Rhinopoma hardwickii*	189.4	1.9	1.38
Pteropodiformes	Rhinopomatidae	*Rhinopoma microphyllum*	59.1	1.4	0.49
Vespertilioniformses	Miniopteridae	*Miniopterus natalensis*	115.6	1.87	2.4
Vespertilioniformses	Molossidae	*Chaerophan jabensis*	13.8	1.6	1.2
Vespertilioniformses	Mormoopidae	*Pteronotus parentelli*	207.7	1.57	0.77
Vespertilioniformses	Mystacinidae	*Mystacinca tuberculata*	307.1	1.74	1.05
Vespertilioniformses	Natalidae	*Natalus major*	25.8	1.37	0.35
Vespertilioniformses	Natalidae	*Natalus micropus*	353.7	1.76	0.93
Vespertilioniformses	Noctilionidae	*Nocitilio albirentras*	32.3	1.75	1.63

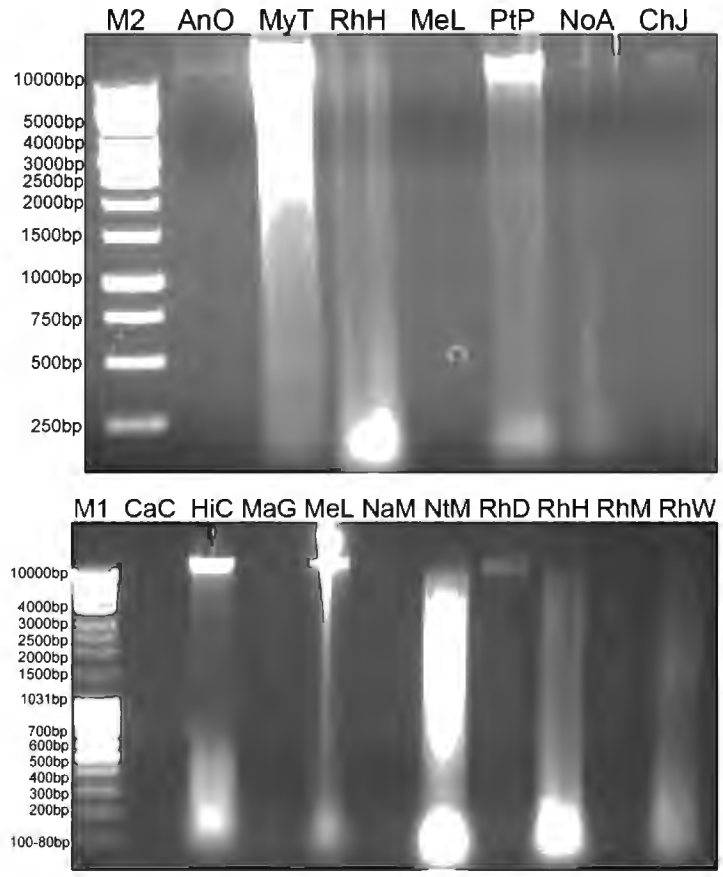

Figure A.1: Genomic DNA from *Anthops ornatus* (AnO), *Cardioderma cor* (CaC), *Chaerophan jabensis* (ChJ), *Hipposderos commersoni* (HiC), *Macroderma gigas* (MaG), *Megaderma lyra* (MeL), *Mystacinca tuberculata* (MyT), *Natalus major* (NtM), *Natalus micropus* (NaM), *Nocitilio albirentras* (NoA), *Pteronotus parentelli* (PtP), *Rhinolophus darlingii* (RhD), *Rhinolophus swinnyi* (RhW), *Rhinopoma hardwickii* (RhH) and *Rhinopoma microphyllum* (RhM)

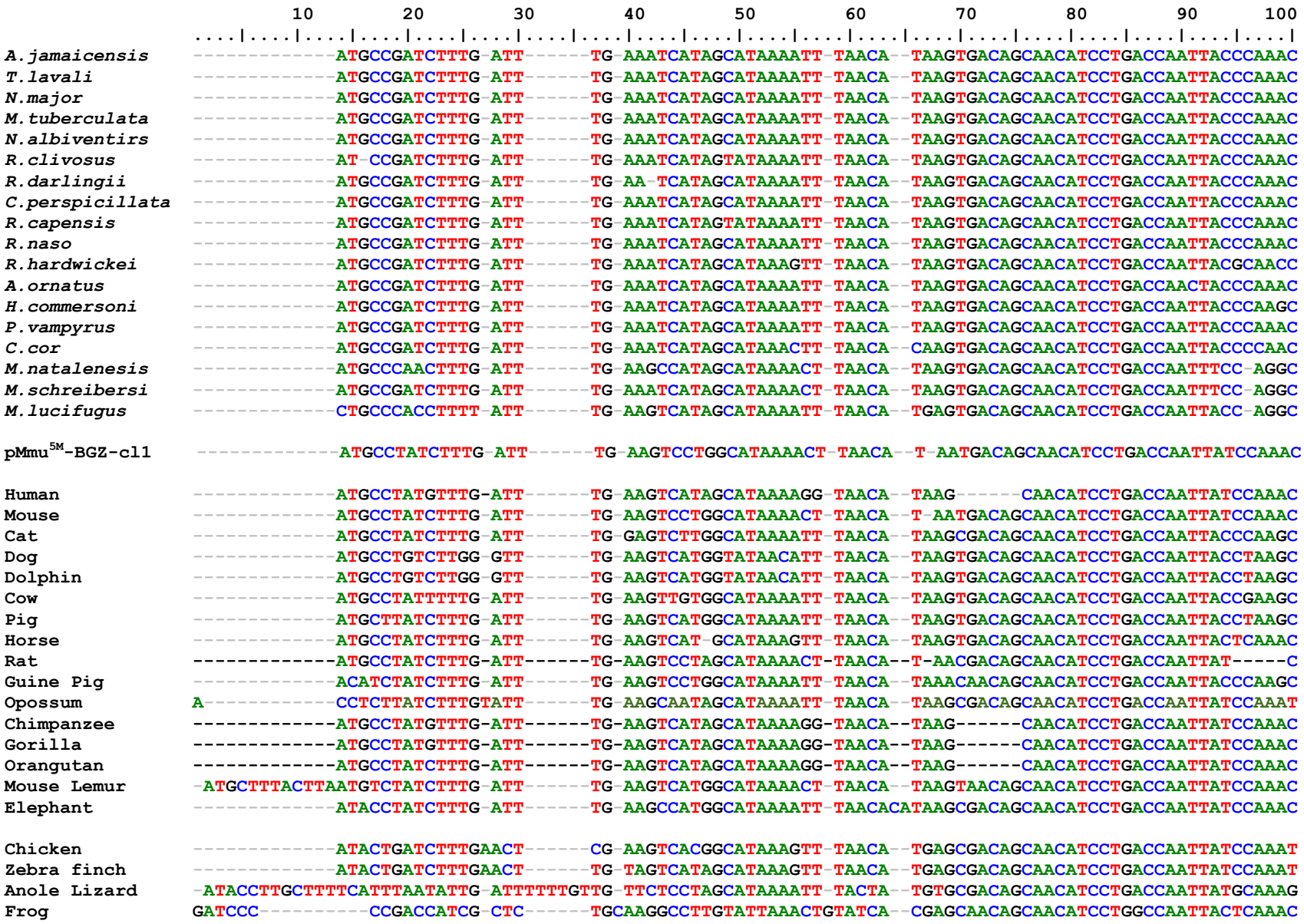
10 20 30 40 50 60 70 80 90 100
A.jamaicensis
T.lavali
N.major
M.tuberculata
N.albiventirs
R.clivosus
R.darlingii
C.perspicillata
R.capensis
R.naso
R.hardwickei
A.ornatus
H.commersoni
P.vampyrus
C.cor
M.natalenesis
M.schreibersi
M.lucifugus
pMmu5M-BGZ-cl1
Human
Mouse
Cat
Dog
Dolphin
Cow
Pig
Horse
Rat
Guine Pig
Opossum
Chimpanzee
Gorilla
Orangutan
Mouse Lemur
Elephant
Chicken
Zebra finch
Anole Lizard
Frog

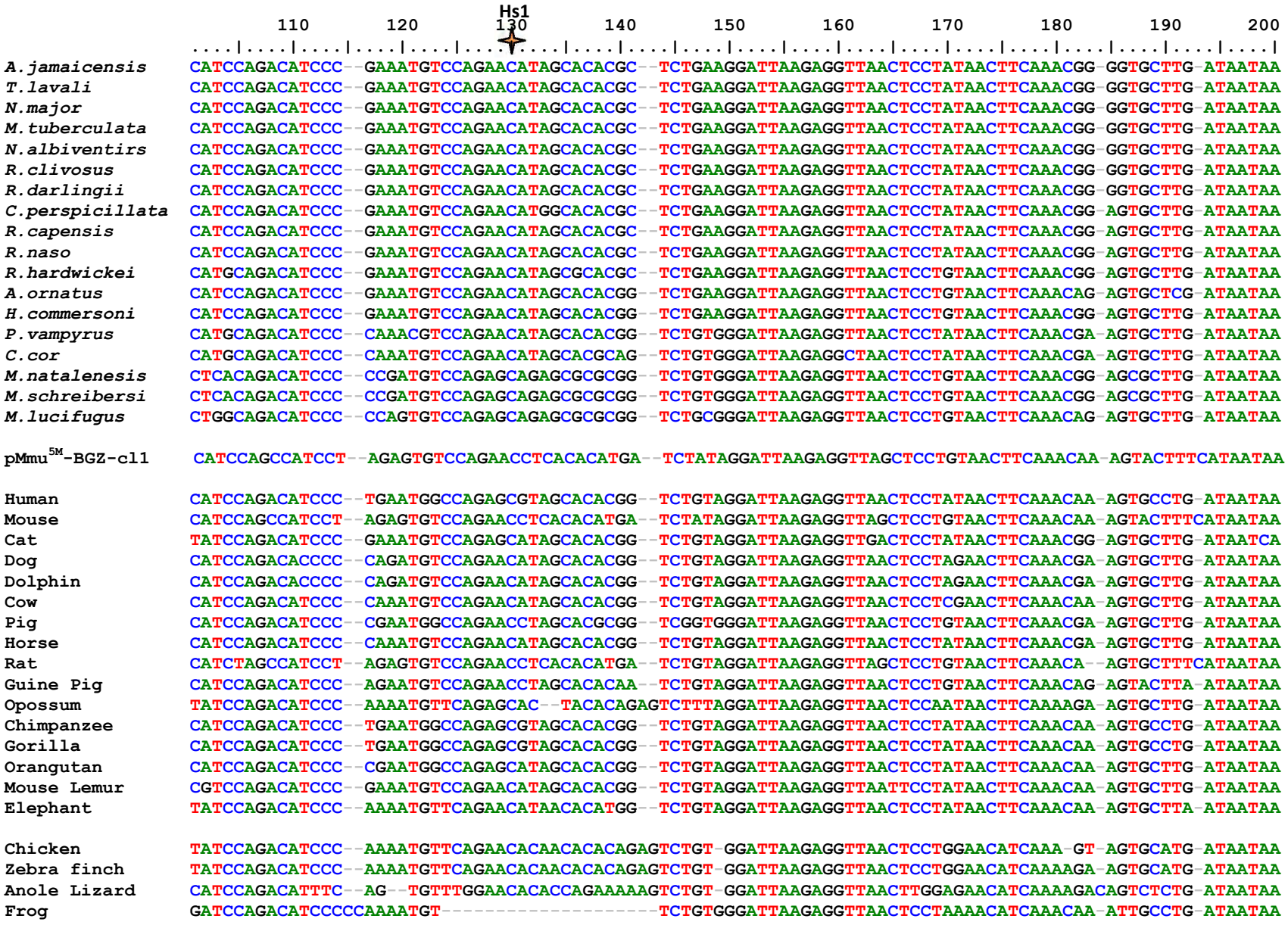
Hs1
110
120
130
140
150
160
170
180
190
200
A.jamaicensis CATCCAGACATCCC--GAAATGTCCAGAACATAGCACACGC--TCTGAAGGATTAAGAGGTTAACTCCTATAACTTCAAACGG-GGTGCTTG-ATAATAA
T.lavali CATCCAGACATCCC--GAAATGTCCAGAACATAGCACACGC--TCTGAAGGATTAAGAGGTTAACTCCTATAACTTCAAACGG-GGTGCTTG-ATAATAA
N.major CATCCAGACATCCC--GAAATGTCCAGAACATAGCACACGC--TCTGAAGGATTAAGAGGTTAACTCCTATAACTTCAAACGG-GGTGCTTG-ATAATAA
M.tuberculata CATCCAGACATCCC--GAAATGTCCAGAACATAGCACACGC--TCTGAAGGATTAAGAGGTTAACTCCTATAACTTCAAACGG-GGTGCTTG-ATAATAA
N.albiventirs CATCCAGACATCCC--GAAATGTCCAGAACATAGCACACGC--TCTGAAGGATTAAGAGGTTAACTCCTATAACTTCAAACGG-GGTGCTTG-ATAATAA
R.clivosus CATCCAGACATCCC--GAAATGTCCAGAACATAGCACACGC--TCTGAAGGATTAAGAGGTTAACTCCTATAACTTCAAACGG-GGTGCTTG-ATAATAA
R.darlingii CATCCAGACATCCC--GAAATGTCCAGAACATAGCACACGC--TCTGAAGGATTAAGAGGTTAACTCCTATAACTTCAAACGG-GGTGCTTG-ATAATAA
C.perspicillata CATCCAGACATCCC--GAAATGTCCAGAACATGGCACACGC--TCTGAAGGATTAAGAGGTTAACTCCTATAACTTCAAACGG-AGTGCTTG-ATAATAA
R.capensis CATCCAGACATCCC--GAAATGTCCAGAACATAGCACACGC--TCTGAAGGATTAAGAGGTTAACTCCTATAACTTCAAACGG-AGTGCTTG-ATAATAA
R.naso CATCCAGACATCCC--GAAATGTCCAGAACATAGCACACGC--TCTGAAGGATTAAGAGGTTAACTCCTATAACTTCAAACGG-AGTGCTTG-ATAATAA
R.hardwickei CATGCAGACATCCC--GAAATGTCCAGAACATAGCGCACGC--TCTGAAGGATTAAGAGGTTAACTCCTGTAACTTCAAACGG-AGTGCTTG-ATAATAA
A.ornatus CATCCAGACATCCC--GAAATGTCCAGAACATAGCACACGG--TCTGAAGGATTAAGAGGTTAACTCCTGTAACTTCAAACAG-AGTGCTCG-ATAATAA
H.commersoni CATCCAGACATCCC--GAAATGTCCAGAACATAGCACACGG--TCTGAAGGATTAAGAGGTTAACTCCTGTAACTTCAAACGG-AGTGCTTG-ATAATAA
P.vampyrus CATGCAGACATCCC--CAAACGTCCAGAACATAGCACACGG--TCTGTGGGATTAAGAGGTTAACTCCTATAACTTCAAACGA-AGTGCTTG-ATAATAA
C.cor CATGCAGACATCCC--CAAATGTCCAGAACATAGCACGCAG--TCTGTGGGATTAAGAGGCTAACTCCTATAACTTCAAACGA-AGTGCTTG-ATAATAA
M.natalenesis CTCACAGACATCCC--CCGATGTCCAGAGCAGAGCGCGCGG--TCTGTGGGATTAAGAGGTTAACTCCTGTAACTTCAAACGG-AGCGCTTG-ATAATAA
M.schreibersi CTCACAGACATCCC--CCGATGTCCAGAGCAGAGCGCGCGG--TCTGTGGGATTAAGAGGTTAACTCCTGTAACTTCAAACGG-AGCGCTTG-ATAATAA
M.lucifugus CTGGCAGACATCCC--CCAGTGTCCAGAGCAGAGCGCGCGG--TCTGCGGGATTAAGAGGTTAACTCCTGTAACTTCAAACAG-AGTGCTTG-ATAATAA
pMmu5M-BGZ-cl1 CATCCAGCCATCCT--AGAGTGTCCAGAACCTCACACATGA--TCTATAGGATTAAGAGGTTAGCTCCTGTAACTTCAAACAA-AGTACTTTCATAATAA
Human CATCCAGACATCCC--TGAATGGCCAGAGCGTAGCACACGG--TCTGTAGGATTAAGAGGTTAACTCCTATAACTTCAAACAA-AGTGCCTG-ATAATAA
Mouse CATCCAGCCATCCT--AGAGTGTCCAGAACCTCACACATGA--TCTATAGGATTAAGAGGTTAGCTCCTGTAACTTCAAACAA-AGTACTTTCATAATAA
Cat TATCCAGACATCCC--GAAATGTCCAGAGCATAGCACACGG--TCTGTAGGATTAAGAGGTTGACTCCTATAACTTCAAACGG-AGTGCTTG-ATAATCA
Dog CATCCAGACACCCC--CAGATGTCCAGAACATAGCACACGG--TCTGTAGGATTAAGAGGTTAACTCCTAGAACTTCAAACGA-AGTGCTTG-ATAATAA
Dolphin CATCCAGACACCCC--CAGATGTCCAGAACATAGCACACGG--TCTGTAGGATTAAGAGGTTAACTCCTAGAACTTCAAACGA-AGTGCTTG-ATAATAA
Cow CATCCAGACATCCC--CAAATGTCCAGAACATAGCACACGG--TCTGTAGGATTAAGAGGTTAACTCCTCGAACTTCAAACAA-AGTGCTTG-ATAATAA
Pig CATCCAGACATCCC--CGAATGGCCAGAACCTAGCACGCGG--TCGGTGGGATTAAGAGGTTAACTCCTGTAACTTCAAACGA-AGTGCTTG-ATAATAA
Horse CATCCAGACATCCC--CAAATGTCCAGAACATAGCACACGG--TCTGTAGGATTAAGAGGTTAACTCCTATAACTTCAAACGA-AGTGCTTG-ATAATAA
Rat CATCTAGCCATCCT--AGAGTGTCCAGAACCTCACACATGA--TCTGTAGGATTAAGAGGTTAGCTCCTGTAACTTCAAACA--AGTGCTTTCATAATAA
Guine Pig CATCCAGACATCCC--AGAATGTCCAGAACCTAGCACACAA--TCTGTAGGATTAAGAGGTTAACTCCTGTAACTTCAAACAG-AGTACTTA-ATAATAA
Opossum TATCCAGACATCCC--AAAATGTTCAGAGCAC--TACACAGAGTCTTTAGGATTAAGAGGTTAACTCCAATAACTTCAAAAGA-AGTGCTTG-ATAATAA
Chimpanzee CATCCAGACATCCC--TGAATGGCCAGAGCGTAGCACACGG--TCTGTAGGATTAAGAGGTTAACTCCTATAACTTCAAACAA-AGTGCCTG-ATAATAA
Gorilla CATCCAGACATCCC--TGAATGGCCAGAGCGTAGCACACGG--TCTGTAGGATTAAGAGGTTAACTCCTATAACTTCAAACAA-AGTGCCTG-ATAATAA
Orangutan CATCCAGACATCCC--CGAATGGCCAGAGCATAGCACACGG--TCTGTAGGATTAAGAGGTTAACTCCTATAACTTCAAACAA-AGTGCTTG-ATAATAA
Mouse Lemur CGTCCAGACATCCC--GAAATGTCCAGAACATAGCACACGG--TCTGTAGGATTAAGAGGTTAATTCCTATAACTTCAAACAA-AGTGCTTG-ATAATAA
Elephant TATCCAGACATCCC--AAAATGTTCAGAACATAACACATGG--TCTGTAGGATTAAGAGGTTAACTCCTATAACTTCAAACAA-AGTGCTTA-ATAATAA
Chicken TATCCAGACATCCC--AAAATGTTCAGAACACAACACACAGAGTCTGT-GGATTAAGAGGTTAACTCCTGGAACATCAAA-GT-AGTGCATG-ATAATAA
Zebra finch TATCCAGACATCCC--AAAATGTTCAGAACACAACACACAGAGTCTGT-GGATTAAGAGGTTAACTCCTGGAACATCAAAAGA-AGTGCATG-ATAATAA
Anole Lizard CATCCAGACATTTC--AG--TGTTTGGAACACACCAGAAAAAGTCTGT-GGATTAAGAGGTTAACTTGGAGAACATCAAAAGACAGTCTCTG-ATAATAA
Frog GATCCAGACATCCCCCAAAATGT----------TCTGTGGGATTAAGAGGTTAACTCCTAAAACATCAAACAA-ATTGCCTG-ATAATAA

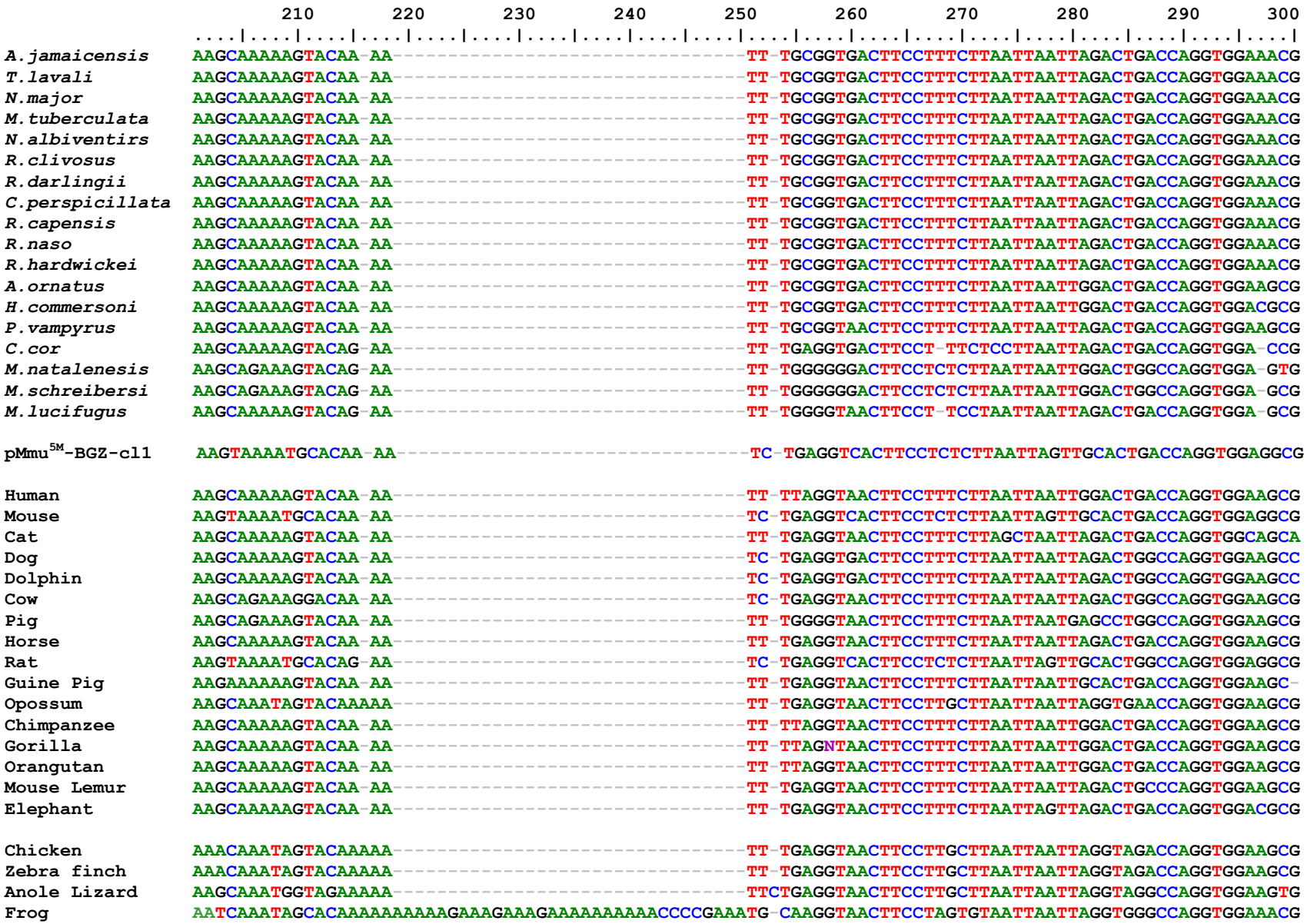
210 220 230 240 250 260 270 280 290 300
A.jamaicensis AAGCAAAAAGTACAA-AA----------TT-TGCGGTGACTTCCTTTCTTAATTAATTAGACTGACCAGGTGGAAACG
T.lavali AAGCAAAAAGTACAA-AA----------TT-TGCGGTGACTTCCTTTCTTAATTAATTAGACTGACCAGGTGGAAACG
N.major AAGCAAAAAGTACAA-AA----------TT-TGCGGTGACTTCCTTTCTTAATTAATTAGACTGACCAGGTGGAAACG
M.tuberculata AAGCAAAAAGTACAA-AA----------TT-TGCGGTGACTTCCTTTCTTAATTAATTAGACTGACCAGGTGGAAACG
N.albiventirs AAGCAAAAAGTACAA-AA----------TT-TGCGGTGACTTCCTTTCTTAATTAATTAGACTGACCAGGTGGAAACG
R.clivosus AAGCAAAAAGTACAA-AA----------TT-TGCGGTGACTTCCTTTCTTAATTAATTAGACTGACCAGGTGGAAACG
R.darlingii AAGCAAAAAGTACAA-AA----------TT-TGCGGTGACTTCCTTTCTTAATTAATTAGACTGACCAGGTGGAAACG
C.perspicillata AAGCAAAAAGTACAA-AA----------TT-TGCGGTGACTTCCTTTCTTAATTAATTAGACTGACCAGGTGGAAACG
R.capensis AAGCAAAAAGTACAA-AA----------TT-TGCGGTGACTTCCTTTCTTAATTAATTAGACTGACCAGGTGGAAACG
R.naso AAGCAAAAAGTACAA-AA----------TT-TGCGGTGACTTCCTTTCTTAATTAATTAGACTGACCAGGTGGAAACG
R.hardwickei AAGCAAAAAGTACAA-AA----------TT-TGCGGTGACTTCCTTTCTTAATTAATTAGACTGACCAGGTGGAAACG
A.ornatus AAGCAAAAAGTACAA-AA----------TT-TGCGGTGACTTCCTTTCTTAATTAATTGGACTGACCAGGTGGAAGCG
H.commersoni AAGCAAAAAGTACAA-AA----------TT-TGCGGTGACTTCCTTTCTTAATTAATTGGACTGACCAGGTGGACGCG
P.vampyrus AAGCAAAAAGTACAA-AA----------TT-TGCGGTAACTTCCTTTCTTAATTAATTAGACTGACCAGGTGGAAGCG
C.cor AAGCAAAAAGTACAG-AA----------TT-TGAGGTGACTTCCT-TTCTCCTTAATTAGACTGACCAGGTGGA-CCG
M.natalenesis AAGCAGAAAGTACAG-AA----------TT-TGGGGGGACTTCCTCTCTTAATTAATTGGACTGGCCAGGTGGA-GTG
M.schreibersi AAGCAGAAAGTACAG-AA----------TT-TGGGGGGACTTCCTCTCTTAATTAATTGGACTGGCCAGGTGGA-GCG
M.lucifugus AAGCAAAAAGTACAG-AA----------TT-TGGGGTAACTTCCT-TCCTAATTAATTAGACTGACCAGGTGGA-GCG
pMmu5M-BGZ-cl1 AAGTAAAATGCACAA-AA----------TC-TGAGGTCACTTCCTCTCTTAATTAGTTGCACTGACCAGGTGGAGGCG
Human AAGCAAAAAGTACAA-AA----------TT-TTAGGTAACTTCCTTTCTTAATTAATTGGACTGACCAGGTGGAAGCG
Mouse AAGTAAAATGCACAA-AA----------TC-TGAGGTCACTTCCTCTCTTAATTAGTTGCACTGACCAGGTGGAGGCG
Cat AAGCAAAAAGTACAA-AA----------TT-TGAGGTAACTTCCTTTCTTAGCTAATTAGACTGACCAGGTGGCAGCA
Dog AAGCAAAAAGTACAA-AA----------TC-TGAGGTGACTTCCTTTCTTAATTAATTAGACTGGCCAGGTGGAAGCC
Dolphin AAGCAAAAAGTACAA-AA----------TC-TGAGGTGACTTCCTTTCTTAATTAATTAGACTGGCCAGGTGGAAGCC
Cow AAGCAGAAAGGACAA-AA----------TC-TGAGGTAACTTCCTTTCTTAATTAATTAGACTGGCCAGGTGGAAGCG
Pig AAGCAGAAAGTACAA-AA----------TT-TGGGGTAACTTCCTTTCTTAATTAATGAGCCTGGCCAGGTGGAAGCG
Horse AAGCAAAAAGTACAA-AA----------TT-TGAGGTAACTTCCTTTCTTAATTAATTAGACTGACCAGGTGGAAGCG
Rat AAGTAAAATGCACAG-AA----------TC-TGAGGTCACTTCCTCTCTTAATTAGTTGCACTGGCCAGGTGGAGGCG
Guine Pig AAGAAAAAAGTACAA-AA----------TT-TGAGGTAACTTCCTTTCTTAATTAATTGCACTGACCAGGTGGAAGC-
Opossum AAGCAAATAGTACAAAAA----------TT-TGAGGTAACTTCCTTGCTTAATTAATTAGGTGAACCAGGTGGAAGCG
Chimpanzee AAGCAAAAAGTACAA-AA----------TT-TTAGGTAACTTCCTTTCTTAATTAATTGGACTGACCAGGTGGAAGCG
Gorilla AAGCAAAAAGTACAA-AA----------TT-TTAGNTAACTTCCTTTCTTAATTAATTGGACTGACCAGGTGGAAGCG
Orangutan AAGCAAAAAGTACAA-AA----------TT-TTAGGTAACTTCCTTTCTTAATTAATTGGACTGACCAGGTGGAAGCG
Mouse Lemur AAGCAAAAAGTACAA-AA----------TT-TGAGGTAACTTCCTTTCTTAATTAATTAGACTGCCCAGGTGGAAGCG
Elephant AAGCAAAAAGTACAA-AA----------TT-TGAGGTAACTTCCTTTCTTAATTAGTTAGACTGACCAGGTGGACGCG
Chicken AAACAAATAGTACAAAAA----------TT-TGAGGTAACTTCCTTGCTTAATTAATTAGGTAGACCAGGTGGAAGCG
Zebra finch AAACAAATAGTACAAAAA----------TT-TGAGGTAACTTCCTTGCTTAATTAATTAGGTAGACCAGGTGGAAGCG
Anole Lizard AAGCAAATGGTAGAAAAA----------TTCTGAGGTAACTTCCTTGCTTAATTAATTAGGTAGGCCAGGTGGAAGTG
Frog AATCAAATAGCACAAAAAAAAAAGAAAGAAAGAAAAAAAAAACCCCGAAATG-CAAGGTAACTTCCTAGTGTAATTAATTAGGTGGGCCAGGTGGAAACG

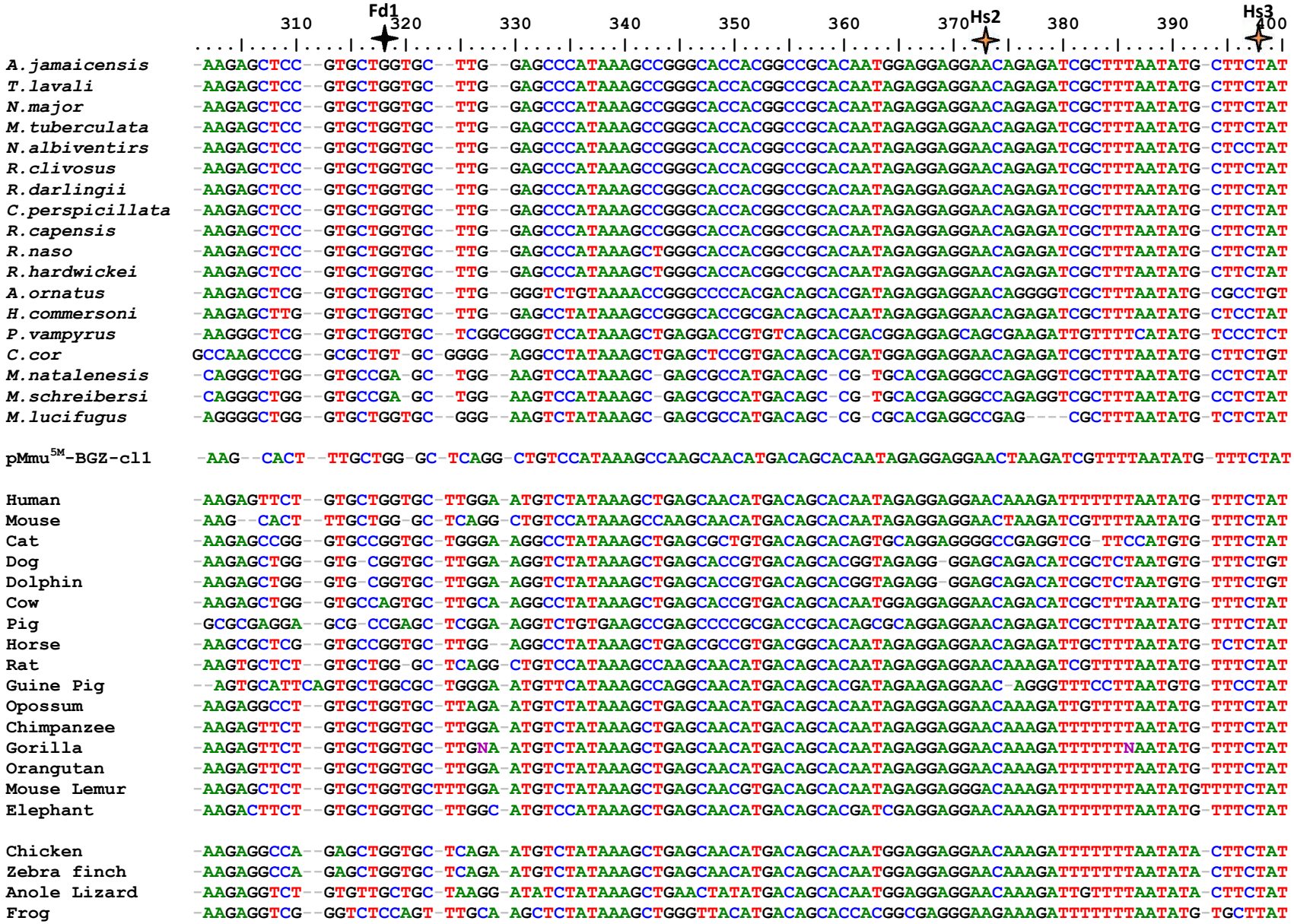
Fd1
Hs2
Hs3
310
320
330
340
350
360
370
380
390
400
A.jamaicensis
T.lavali
N.major
M.tuberculata
N.albiventirs
R.clivosus
R.darlingii
C.perspicillata
R.capensis
R.naso
R.hardwickei
A.ornatus
H.commersoni
P.vampyrus
C.cor
M.natalenesis
M.schreibersi
M.lucifugus
pMmu5M-BGZ-cl1
Human
Mouse
Cat
Dog
Dolphin
Cow
Pig
Horse
Rat
Guine Pig
Opossum
Chimpanzee
Gorilla
Orangutan
Mouse Lemur
Elephant
Chicken
Zebra finch
Anole Lizard
Frog

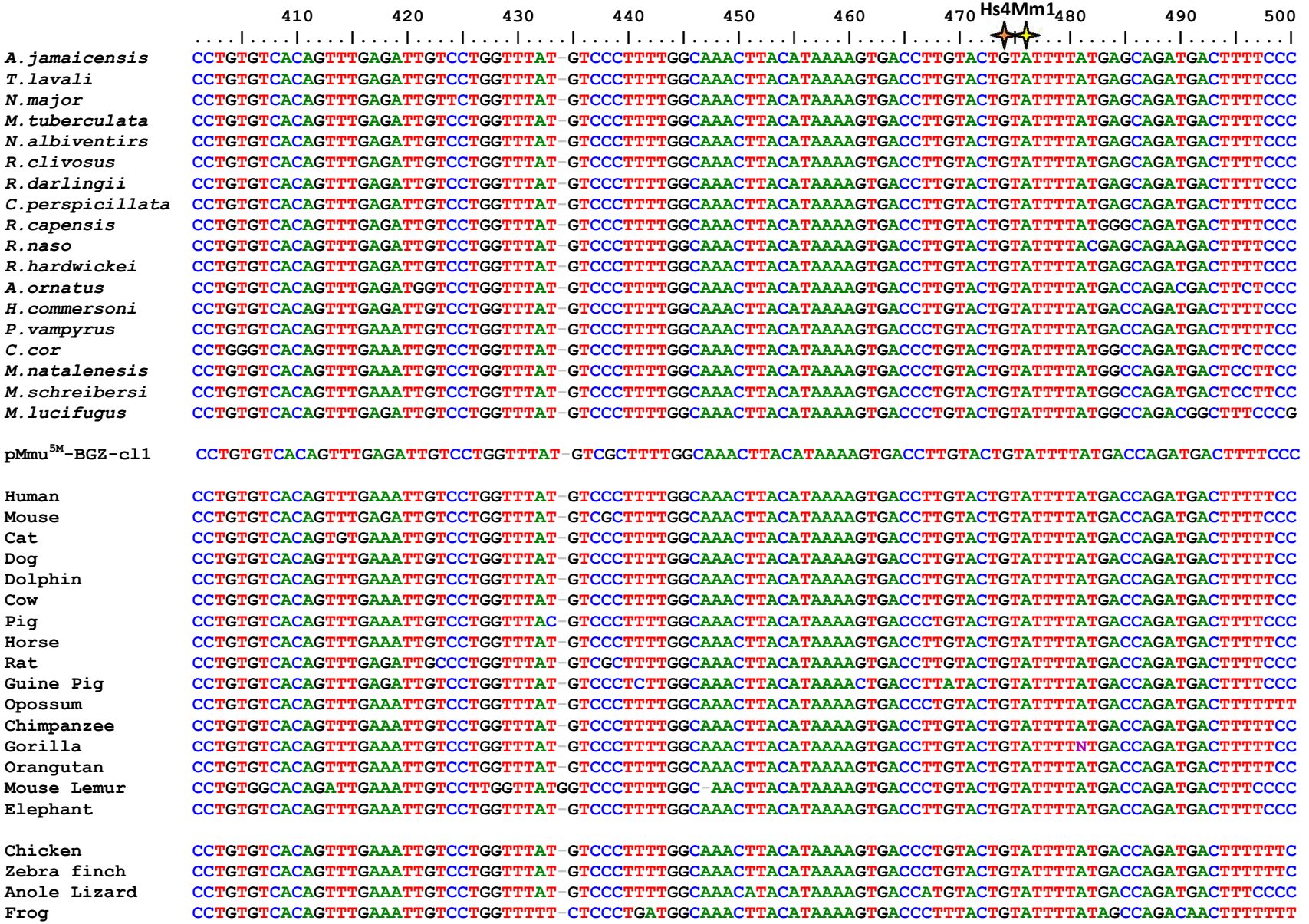
410
420
430
440
450
460
470
Hs4Mm1
480
490
500
A.jamaicensis CCTGTGTCACAGTTTGAGATTGTCCTGGTTTAT-GTCCCTTTTGGCAAACTTACATAAAAGTGACCTTGTACTGTATTTTATGAGCAGATGACTTTTCCC
T.lavali CCTGTGTCACAGTTTGAGATTGTCCTGGTTTAT-GTCCCTTTTGGCAAACTTACATAAAAGTGACCTTGTACTGTATTTTATGAGCAGATGACTTTTCCC
N.major CCTGTGTCACAGTTTGAGATTGTTCTGGTTTAT-GTCCCTTTTGGCAAACTTACATAAAAGTGACCTTGTACTGTATTTTATGAGCAGATGACTTTTCCC
M.tuberculata CCTGTGTCACAGTTTGAGATTGTCCTGGTTTAT-GTCCCTTTTGGCAAACTTACATAAAAGTGACCTTGTACTGTATTTTATGAGCAGATGACTTTTCCC
N.albiventirs CCTGTGTCACAGTTTGAGATTGTCCTGGTTTAT-GTCCCTTTTGGCAAACTTACATAAAAGTGACCTTGTACTGTATTTTATGAGCAGATGACTTTTCCC
R.clivosus CCTGTGTCACAGTTTGAGATTGTCCTGGTTTAT-GTCCCTTTTGGCAAACTTACATAAAAGTGACCTTGTACTGTATTTTATGAGCAGATGACTTTTCCC
R.darlingii CCTGTGTCACAGTTTGAGATTGTCCTGGTTTAT-GTCCCTTTTGGCAAACTTACATAAAAGTGACCTTGTACTGTATTTTATGAGCAGATGACTTTTCCC
C.perspicillata CCTGTGTCACAGTTTGAGATTGTCCTGGTTTAT-GTCCCTTTTGGCAAACTTACATAAAAGTGACCTTGTACTGTATTTTATGAGCAGATGACTTTTCCC
R.capensis CCTGTGTCACAGTTTGAGATTGTCCTGGTTTAT-GTCCCTTTTGGCAAACTTACATAAAAGTGACCTTGTACTGTATTTTATGGGCAGATGACTTTTCCC
R.naso CCTGTGTCACAGTTTGAGATTGTCCTGGTTTAT-GTCCCTTTTGGCAAACTTACATAAAAGTGACCTTGTACTGTATTTTACGAGCAGAAGACTTTTCCC
R.hardwickei CCTGTGTCACAGTTTGAGATTGTCCTGGTTTAT-GTCCCTTTTGGCAAACTTACATAAAAGTGACCTTGTACTGTATTTTATGAGCAGATGACTTTTCCC
A.ornatus CCTGTGTCACAGTTTGAGATGGTCCTGGTTTAT-GTCCCTTTTGGCAAACTTACATAAAAGTGACCTTGTACTGTATTTTATGACCAGACGACTTCTCCC
H.commersoni CCTGTGTCACAGTTTGAGATTGTCCTGGTTTAT-GTCCCTTTTGGCAAACTTACATAAAAGTGACCTTGTACTGTATTTTATGACCAGATGACTTTTCCC
P.vampyrus CCTGTGTCACAGTTTGAAATTGTCCTGGTTTAT-GTCCCTTTTGGCAAACTTACATAAAAGTGACCCTGTACTGTATTTTATGACCAGATGACTTTTTCC
C.cor CCTGGGTCACAGTTTGAAATTGTCCTGGTTTAT-GTCCCTTTTGGCAAACTTACATAAAAGTGACCCTGTACTGTATTTTATGGCCAGATGACTTCTCCC
M.natalenesis CCTGTGTCACAGTTTGAAATTGTCCTGGTTTAT-GTCCCTTTTGGCAAACTTACATAAAAGTGACCCTGTACTGTATTTTATGGCCAGATGACTCCTTCC
M.schreibersi CCTGTGTCACAGTTTGAAATTGTCCTGGTTTAT-GTCCCTTTTGGCAAACTTACATAAAAGTGACCCTGTACTGTATTTTATGGCCAGATGACTCCTTCC
M.lucifugus CCTGTGTCACAGTTTGAGATTGTCCTGGTTTAT-GTCCCTTTTGGCAAACTTACATAAAAGTGACCCTGTACTGTATTTTATGGCCAGACGGCTTTCCCG
pMmu5M-BGZ-cl1 CCTGTGTCACAGTTTGAGATTGTCCTGGTTTAT-GTCGCTTTTGGCAAACTTACATAAAAGTGACCTTGTACTGTATTTTATGACCAGATGACTTTTCCC
Human CCTGTGTCACAGTTTGAAATTGTCCTGGTTTAT-GTCCCTTTTGGCAAACTTACATAAAAGTGACCTTGTACTGTATTTTATGACCAGATGACTTTTTCC
Mouse CCTGTGTCACAGTTTGAGATTGTCCTGGTTTAT-GTCGCTTTTGGCAAACTTACATAAAAGTGACCTTGTACTGTATTTTATGACCAGATGACTTTTCCC
Cat CCTGTGTCACAGTGTGAAATTGTCCTGGTTTAT-GTCCCTTTTGGCAAACTTACATAAAAGTGACCTTGTACTGTATTTTATGACCAGATGACTTTTTCC
Dog CCTGTGTCACAGTTTGAAATTGTCCTGGTTTAT-GTCCCTTTTGGCAAACTTACATAAAAGTGACCTTGTACTGTATTTTATGACCAGATGACTTTTTCC
Dolphin CCTGTGTCACAGTTTGAAATTGTCCTGGTTTAT-GTCCCTTTTGGCAAACTTACATAAAAGTGACCTTGTACTGTATTTTATGACCAGATGACTTTTTCC
Cow CCTGTGTCACAGTTTGAAATTGTCCTGGTTTAT-GTCCCTTTTGGCAAACTTACATAAAAGTGACCTTGTACTGTATTTTATGACCAGATGACTTTTTCC
Pig CCTGTGTCACAGTTTGAAATTGTCCTGGTTTAC-GTCCCTTTTGGCAAACTTACATAAAAGTGACCCTGTACTGTATTTTATGACCAGATGACTTTTCCC
Horse CCTGTGTCACAGTTTGAAATTGTCCTGGTTTAT-GTCCCTTTTGGCAAACTTACATAAAAGTGACCTTGTACTGTATTTTATGACCAGATGACTTTTTCC
Rat CCTGTGTCACAGTTTGAGATTGCCCTGGTTTAT-GTCGCTTTTGGCAAACTTACATAAAAGTGACCTTGTACTGTATTTTATGACCAGATGACTTTTCCC
Guine Pig CCTGTGTCACAGTTTGAGATTGTCCTGGTTTAT-GTCCCTCTTGGCAAACTTACATAAAACTGACCTTATACTGTATTTTATGACCAGATGACTTTTCCC
Opossum CCTGTGTCACAGTTTGAAATTGTCCTGGTTTAT-GTCCCTTTTGGCAAACTTACATAAAAGTGACCCTGTACTGTATTTTATGACCAGATGACTTTTTTT
Chimpanzee CCTGTGTCACAGTTTGAAATTGTCCTGGTTTAT-GTCCCTTTTGGCAAACTTACATAAAAGTGACCTTGTACTGTATTTTATGACCAGATGACTTTTTCC
Gorilla CCTGTGTCACAGTTTGAAATTGTCCTGGTTTAT-GTCCCTTTTGGCAAACTTACATAAAAGTGACCTTGTACTGTATTTTNTGACCAGATGACTTTTTCC
Orangutan CCTGTGTCACAGTTTGAAATTGTCCTGGTTTAT-GTCCCTTTTGGCAAACTTACATAAAAGTGACCTTGTACTGTATTTTATGACCAGATGACTTTTTCC
Mouse Lemur CCTGTGGCACAGATTGAAATTGTCCTTGGTTATGGTCCCTTTTGGC-AACTTACATAAAAGTGACCCTGTACTGTATTTTATGACCAGATGACTTTCCCC
Elephant CCTGTGTCACAGTTTGAAATTGTCCTGGTTTAT-GTCCCTTTTGGCAAACTTACATAAAAGTGACCTTGTACTGTATTTTATGACCAGATGACTTTTCCC
Chicken CCTGTGTCACAGTTTGAAATTGTCCTGGTTTAT-GTCCCTTTTGGCAAACTTACATAAAAGTGACCCTGTACTGTATTTTATGACCAGATGACTTTTTTC
Zebra finch CCTGTGTCACAGTTTGAAATTGTCCTGGTTTAT-GTCCCTTTTGGCAAACTTACATAAAAGTGACCCTGTACTGTATTTTATGACCAGATGACTTTTTTC
Anole Lizard CCTGTGTCACAGTTTGAAATTGTCCTGGTTTAT-GTCCCTTTTGGCAAACATACATAAAAGTGACCATGTACTGTATTTTATGACCAGATGACTTTCCCC
Frog CCTGTGTCACAGTTTGAAATTGTCCTGGTTTTT-CTCCCTGATGGCAAACTTACATAAAAGTGACCCTTTACTGTATTTTATAGCCAGACAACTTTTTTT

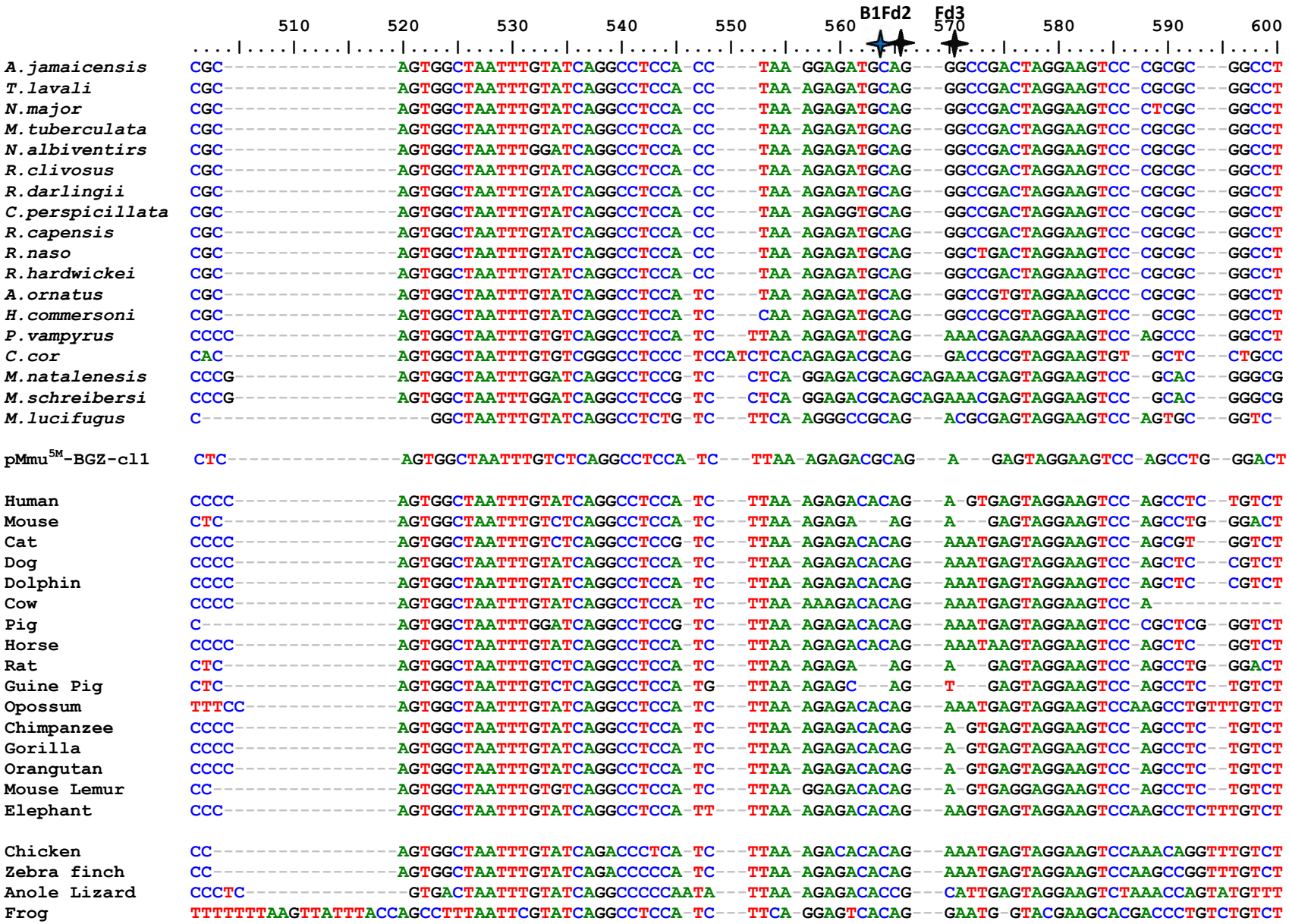
B1Fd2
Fd3
510
520
530
540
550
560
570
580
590
600
A.jamaicensis
T.lavali
N.major
M.tuberculata
N.albiventirs
R.clivosus
R.darlingii
C.perspicillata
R.capensis
R.naso
R.hardwickei
A.ornatus
H.commersoni
P.vampyrus
C.cor
M.natalenesis
M.schreibersi
M.lucifugus
pMmu5M-BGZ-cl1
Human
Mouse
Cat
Dog
Dolphin
Cow
Pig
Horse
Rat
Guine Pig
Opossum
Chimpanzee
Gorilla
Orangutan
Mouse Lemur
Elephant
Chicken
Zebra finch
Anole Lizard
Frog

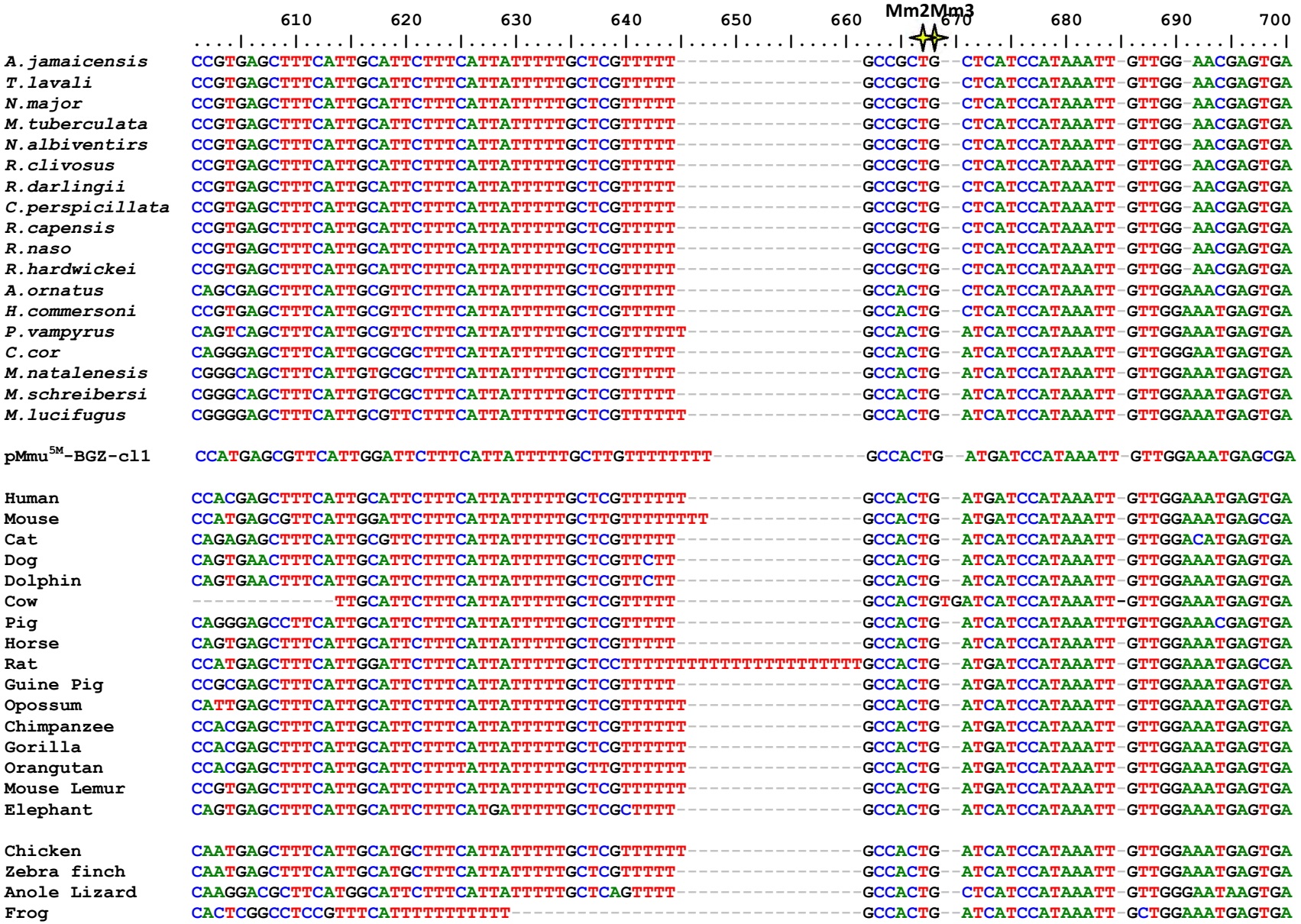
Mm2Mm3
610
620
630
640
650
660
670
680
690
700
A.jamaicensis
T.lavali
N.major
M.tuberculata
N.albiventirs
R.clivosus
R.darlingii
C.perspicillata
R.capensis
R.naso
R.hardwickei
A.ornatus
H.commersoni
P.vampyrus
C.cor
M.natalenesis
M.schreibersi
M.lucifugus
pMmu5M-BGZ-cl1
Human
Mouse
Cat
Dog
Dolphin
Cow
Pig
Horse
Rat
Guine Pig
Opossum
Chimpanzee
Gorilla
Orangutan
Mouse Lemur
Elephant
Chicken
Zebra finch
Anole Lizard
Frog

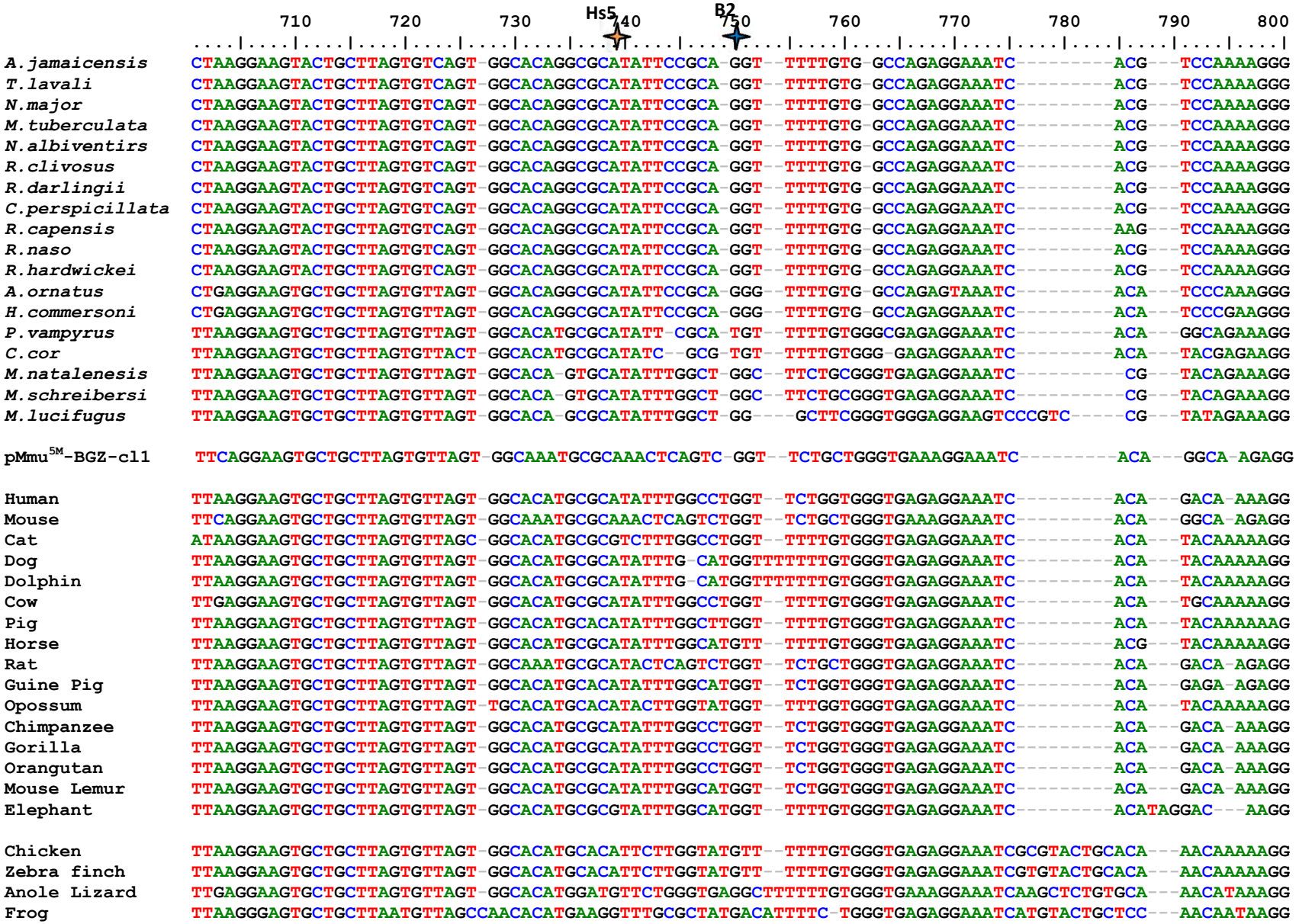
Hs5
B2
710
720
730
740
750
760
770
780
790
800
A.jamaicensis
T.lavali
N.major
M.tuberculata
N.albiventirs
R.clivosus
R.darlingii
C.perspicillata
R.capensis
R.naso
R.hardwickei
A.ornatus
H.commersoni
P.vampyrus
C.cor
M.natalenesis
M.schreibersi
M.lucifugus
pMmu5M-BGZ-cl1
Human
Mouse
Cat
Dog
Dolphin
Cow
Pig
Horse
Rat
Guine Pig
Opossum
Chimpanzee
Gorilla
Orangutan
Mouse Lemur
Elephant
Chicken
Zebra finch
Anole Lizard
Frog

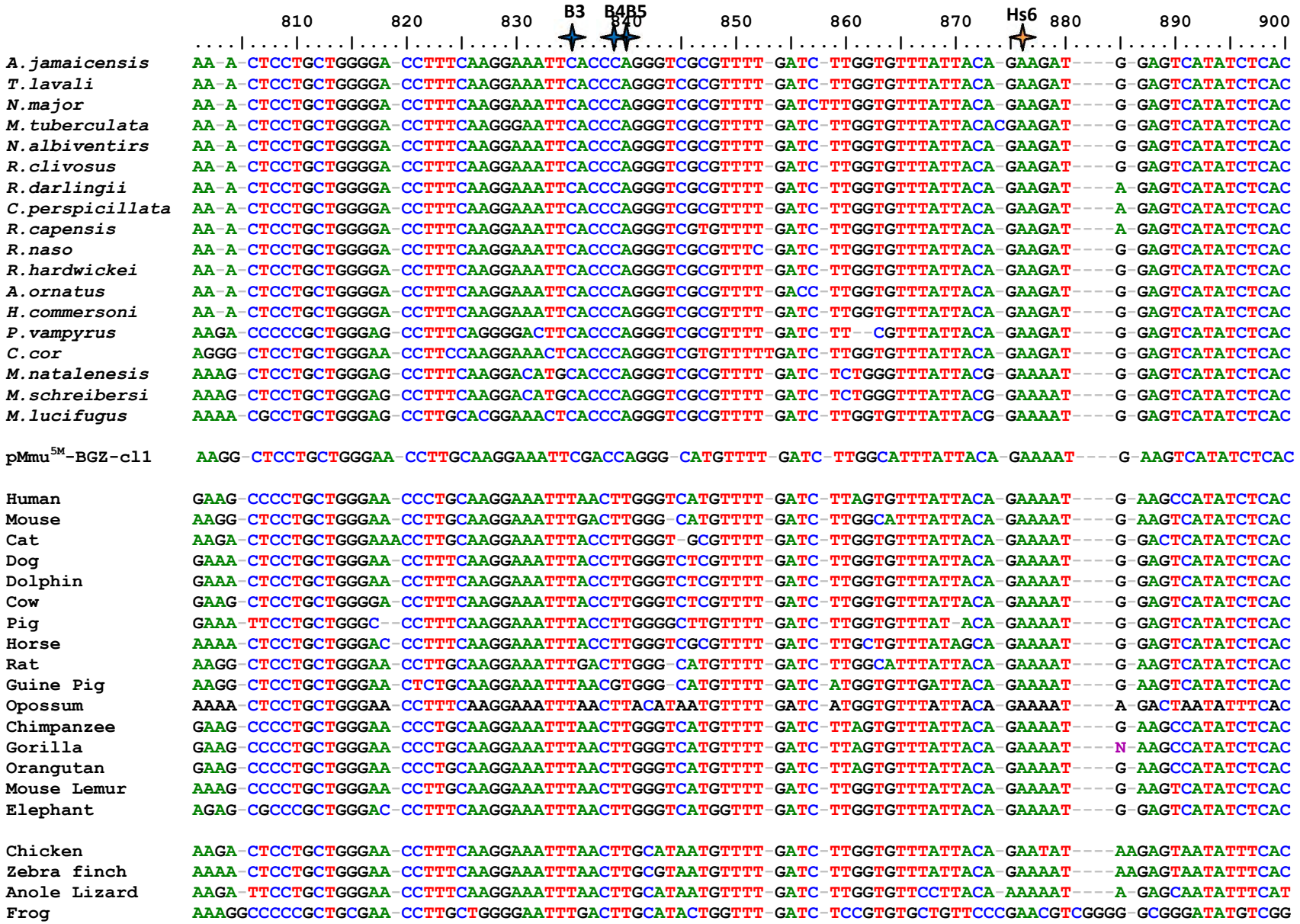
B3
B4B5
Hs6
810
820
830
840
850
860
870
880
890
900
A.jamaicensis
T.lavali
N.major
M.tuberculata
N.albiventirs
R.clivosus
R.darlingii
C.perspicillata
R.capensis
R.naso
R.hardwickei
A.ornatus
H.commersoni
P.vampyrus
C.cor
M.natalenesis
M.schreibersi
M.lucifugus
pMmu5M-BGZ-cl1
Human
Mouse
Cat
Dog
Dolphin
Cow
Pig
Horse
Rat
Guine Pig
Opossum
Chimpanzee
Gorilla
Orangutan
Mouse Lemur
Elephant
Chicken
Zebra finch
Anole Lizard
Frog

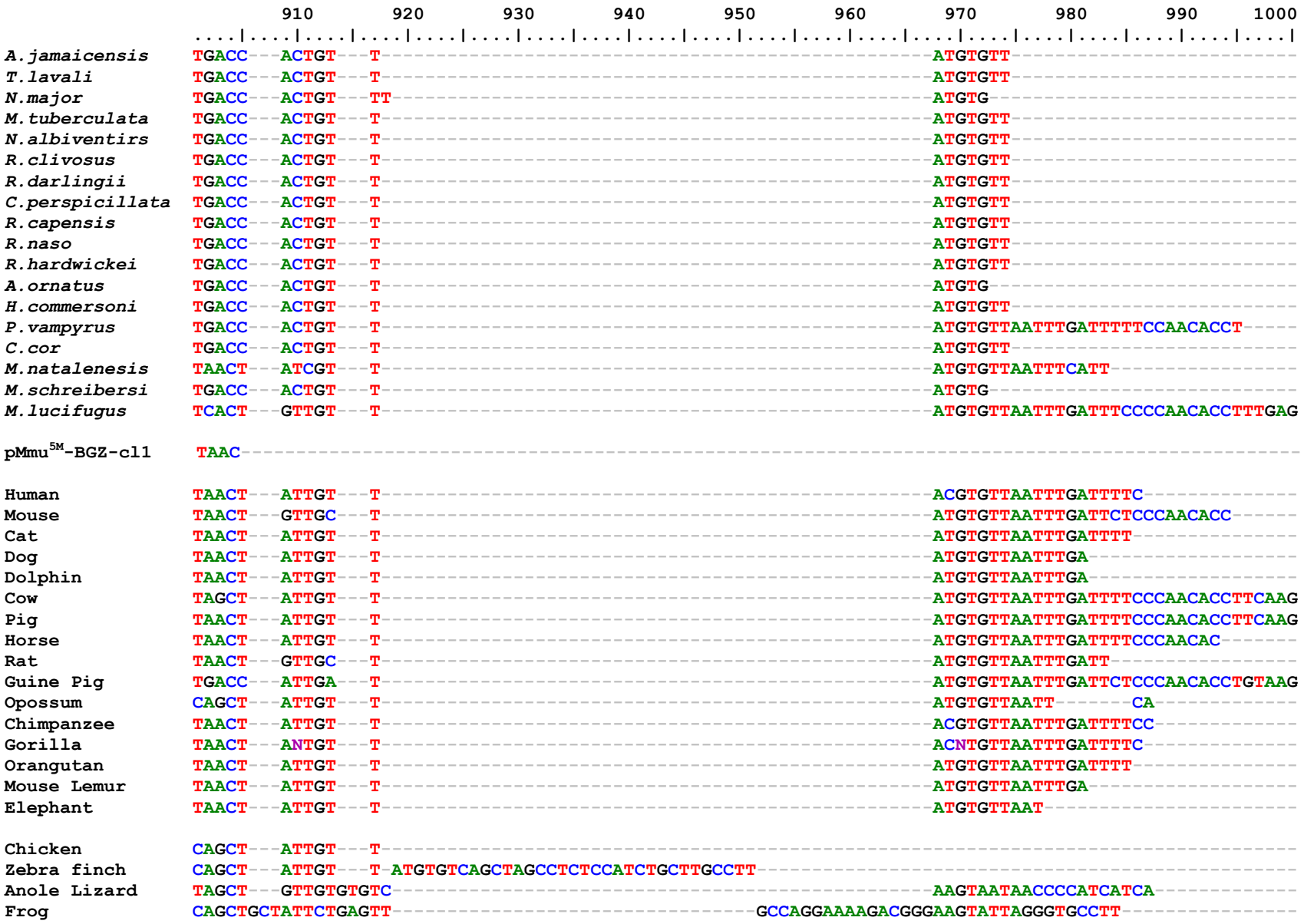
910
920
930
940
950
960
970
980
990
1000
A.jamaicensis TGACC ACTGT T ATGTGTT
T.lavali TGACC ACTGT T ATGTGTT
N.major TGACC ACTGT TT ATGTG
M.tuberculata TGACC ACTGT T ATGTGTT
N.albiventirs TGACC ACTGT T ATGTGTT
R.clivosus TGACC ACTGT T ATGTGTT
R.darlingii TGACC ACTGT T ATGTGTT
C.perspicillata TGACC ACTGT T ATGTGTT
R.capensis TGACC ACTGT T ATGTGTT
R.naso TGACC ACTGT T ATGTGTT
R.hardwickei TGACC ACTGT T ATGTGTT
A.ornatus TGACC ACTGT T ATGTG
H.commersoni TGACC ACTGT T ATGTGTT
P.vampyrus TGACC ACTGT T ATGTGTTAATTTGATTTTTCCAACACCT
C.cor TGACC ACTGT T ATGTGTT
M.natalenesis TAACT ATCGT T ATGTGTTAATTTCATT
M.schreibersi TGACC ACTGT T ATGTG
M.lucifugus TCACT GTTGT T ATGTGTTAATTTGATTTCCCCAACACCTTTGAG
pMmu5M-BGZ-cl1 TAAC
Human TAACT ATTGT T ACGTGTTAATTTGATTTTC
Mouse TAACT GTTGC T ATGTGTTAATTTGATTCTCCCAACACC
Cat TAACT ATTGT T ATGTGTTAATTTGATTTT
Dog TAACT ATTGT T ATGTGTTAATTTGA
Dolphin TAACT ATTGT T ATGTGTTAATTTGA
Cow TAGCT ATTGT T ATGTGTTAATTTGATTTTCCCAACACCTTCAAG
Pig TAACT ATTGT T ATGTGTTAATTTGATTTTCCCAACACCTTCAAG
Horse TAACT ATTGT T ATGTGTTAATTTGATTTTCCCAACAC
Rat TAACT GTTGC T ATGTGTTAATTTGATT
Guine Pig TGACC ATTGA T ATGTGTTAATTTGATTCTCCCAACACCTGTAAG
Opossum CAGCT ATTGT T ATGTGTTAATT CA
Chimpanzee TAACT ATTGT T ACGTGTTAATTTGATTTTCC
Gorilla TAACT ANTGT T ACNTGTTAATTTGATTTTC
Orangutan TAACT ATTGT T ATGTGTTAATTTGATTTT
Mouse Lemur TAACT ATTGT T ATGTGTTAATTTGA
Elephant TAACT ATTGT T ATGTGTTAAT
Chicken CAGCT ATTGT T
Zebra finch CAGCT ATTGT T ATGTGTCAGCTAGCCTCTCCATCTGCTTGCCTT
Anole Lizard TAGCT GTTGTGTGTC AAGTAATAACCCCATCATCA
Frog CAGCTGCTATTCTGAGTT GCCAGGAAAAGACGGGAAGTATTAGGGTGCCTT

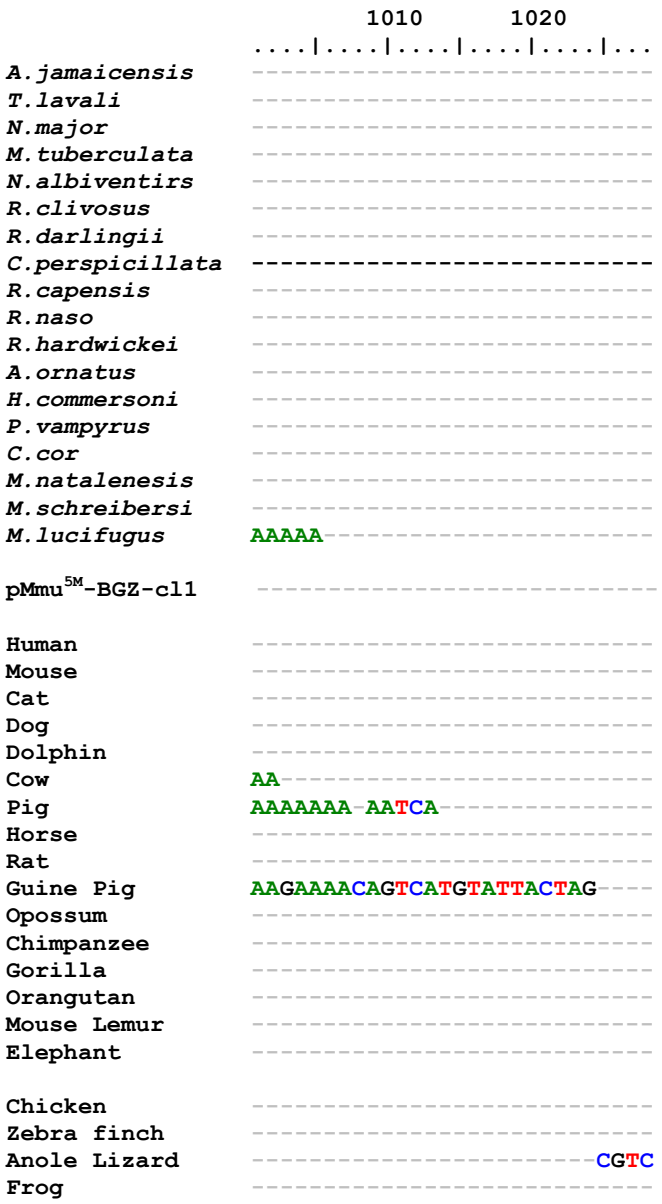

Figure A.2: The full alignment of the ZRS of 18 bat species and 20 other vertebrates using PRANKSTER. The five point mutations that are conserved in all bats are shown by blue stars: Mutation 1(B1) is a transition from an adenine to a guanine at alignment position 563 (G466A). Mutation 2 (B2) is a deletion of a thymine at position 749 (Δ625T), Mutation 3 and 4 (B3 and B4, respectively) are another transition from thymine to cytosine at positions 835 (C694T) and 839 (C698T) respectively. Mutation 5 (B5) is a transversion from a thymine to an adenine at position 840 (A699T). Previously identified mouse mutations in ZRS are shown by yellow stars: M100081 (Mm1, A to G), HxNeb (Mm2, T to C), and Hx (Mm, G to A) (Lettice et al. 2003; Lettice et al. 2008). Previously identified human mutations in ZRS are shown by orange stars: Dutch (Hs1, C to G), Belgian1 (Hs2, A to T), Belgian2 (Hs3, T to C), Cuban (Hs4, G to A), European 1 (Hs5, C to G) and European 2 (Hs6, A to G) (Lettice et al. 2003; Lettice et al. 2008; Gurnett et al. 2007). Previously identified cat mutations in ZRS are shown by purple stars: UK1 (Fd1, G to T), Hw (Fd2, A to G) and UK2 (Fd3, A to T) (Lettice et al. 2008).

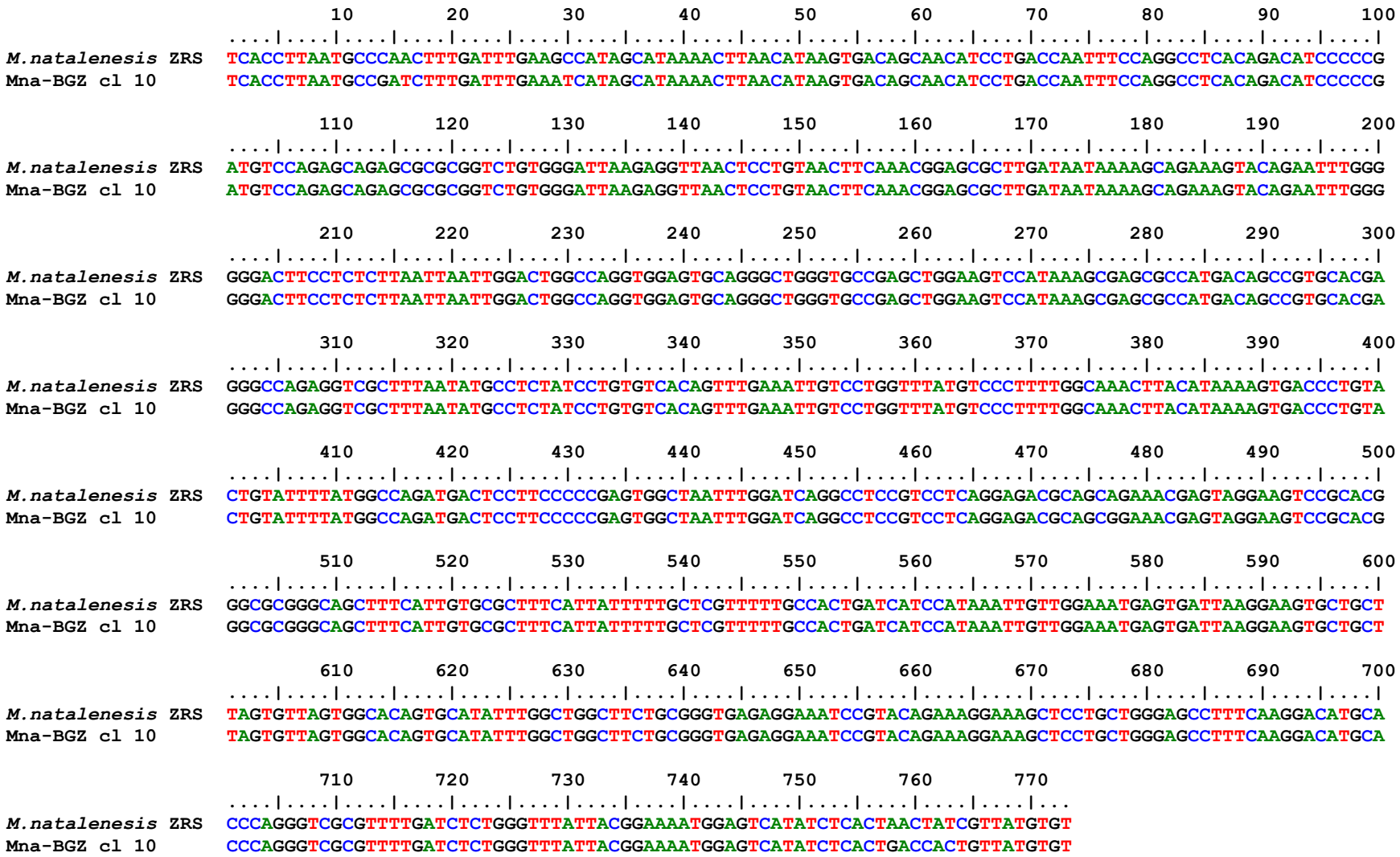

Figure A.3: A comparison of the *M. natalenesis* ZRS subcloned in pBGZ40 reporter plasmid to the original sequence. There were no significant mutations identified in the pGZ40 clones.

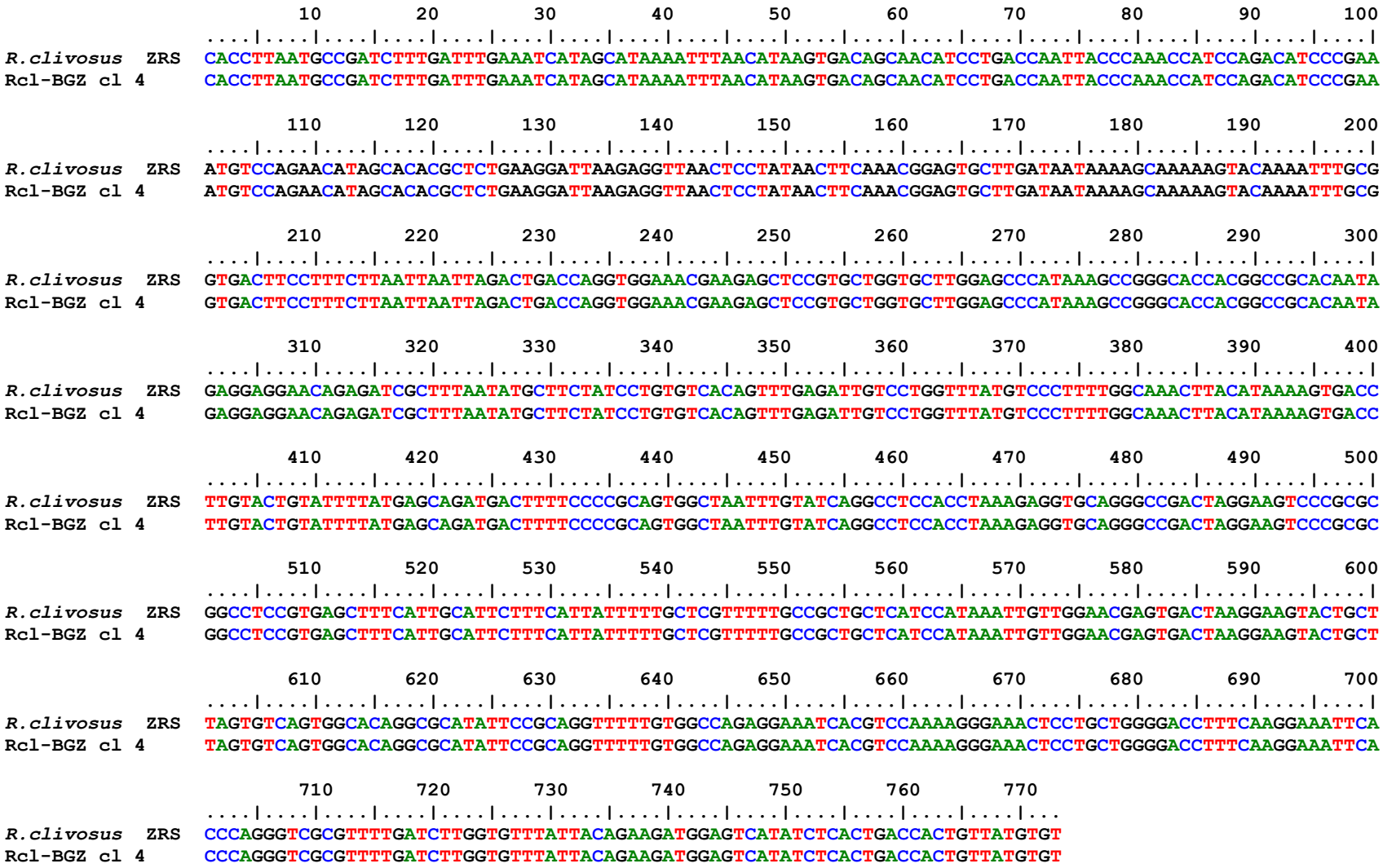

Figure A.4: A comparison of the R. clivosus ZRS subcloned in pBGZ40 reporter plasmid to the original sequence. There were no significant mutations identified in the pGZ40 clones.

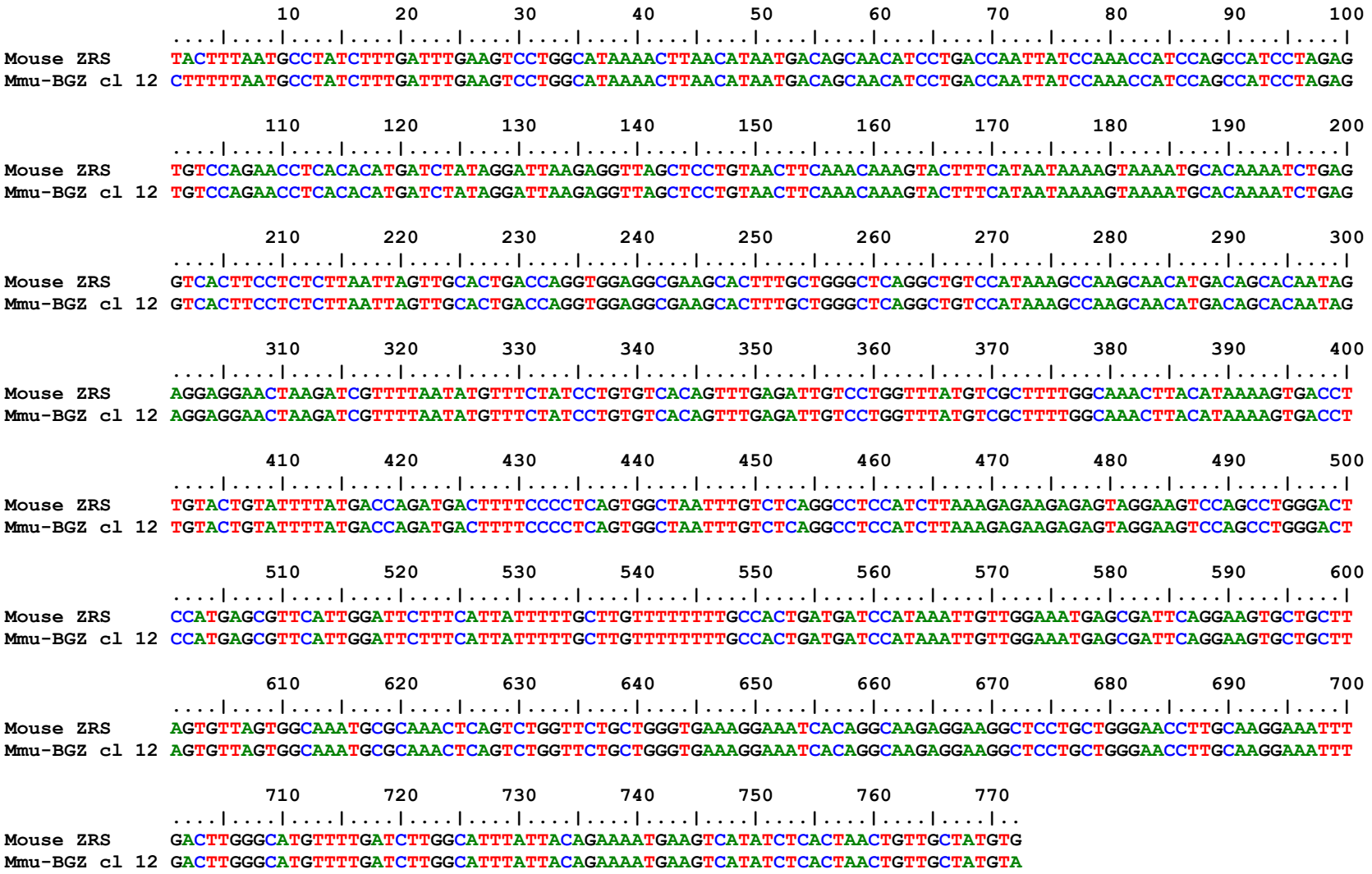

Figure A.5: A comparison of the Mouse ZRS subcloned in pBGZ40 reporter plasmid to the original sequence. There were no significant mutations identified in the pGZ40 clones.

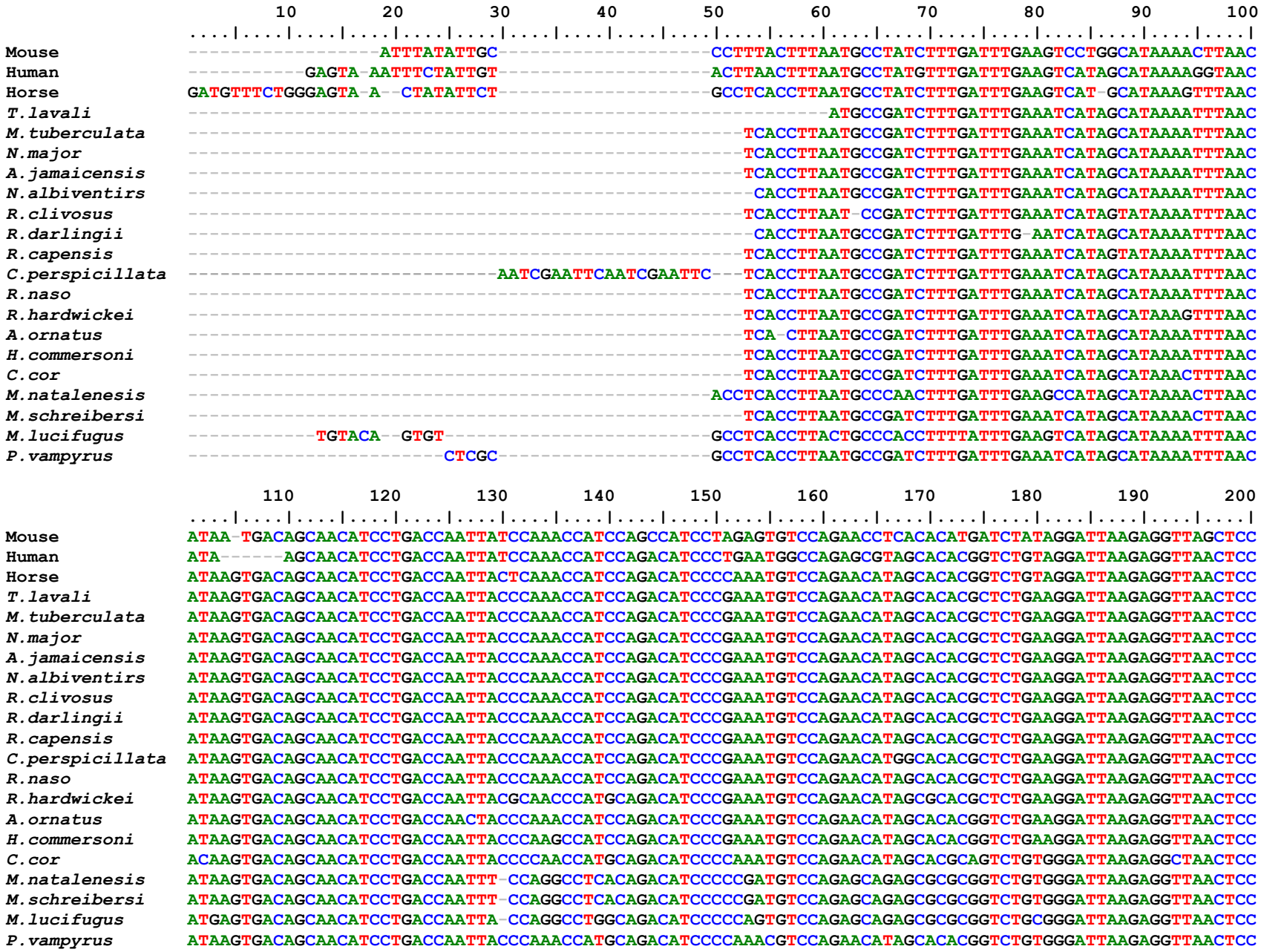
10 20 30 40 50 60 70 80 90 100
Mouse ATTTATATTGC CCTTTACTTTAATGCCTATCTTTGATTTGAAGTCCTGGCATAAAACTTAAC
Human GAGTA AATTTCTATTGT ACTTAACTTTAATGCCTATGTTTGATTTGAAGTCATAGCATAAAAGGTAAC
Horse GATGTTTCTGGGAGTA A CTATATTCT GCCTCACCTTAATGCCTATCTTTGATTTGAAGTCAT GCATAAAGTTTAAC
T.lavali ATGCCGATCTTTGATTTGAAATCATAGCATAAAATTTAAC
M.tuberculata TCACCTTAATGCCGATCTTTGATTTGAAATCATAGCATAAAATTTAAC
N.major TCACCTTAATGCCGATCTTTGATTTGAAATCATAGCATAAAATTTAAC
A.jamaicensis TCACCTTAATGCCGATCTTTGATTTGAAATCATAGCATAAAATTTAAC
N.albiventirs CACCTTAATGCCGATCTTTGATTTGAAATCATAGCATAAAATTTAAC
R.clivosus TCACCTTAAT CCGATCTTTGATTTGAAATCATAGTATAAAATTTAAC
R.darlingii CACCTTAATGCCGATCTTTGATTTG AATCATAGCATAAAATTTAAC
R.capensis TCACCTTAATGCCGATCTTTGATTTGAAATCATAGTATAAAATTTAAC
C.perspicillata AATCGAATTCAATCGAATTC TCACCTTAATGCCGATCTTTGATTTGAAATCATAGCATAAAATTTAAC
R.naso TCACCTTAATGCCGATCTTTGATTTGAAATCATAGCATAAAATTTAAC
R.hardwickei TCACCTTAATGCCGATCTTTGATTTGAAATCATAGCATAAAGTTTAAC
A.ornatus TCA CTTAATGCCGATCTTTGATTTGAAATCATAGCATAAAATTTAAC
H.commersoni TCACCTTAATGCCGATCTTTGATTTGAAATCATAGCATAAAATTTAAC
C.cor TCACCTTAATGCCGATCTTTGATTTGAAATCATAGCATAAACTTTAAC
M.natalenesis ACCTCACCTTAATGCCCAACTTTGATTTGAAGCCATAGCATAAAACTTAAC
M.schreibersi TCACCTTAATGCCGATCTTTGATTTGAAATCATAGCATAAAACTTAAC
M.lucifugus TGTACA GTGT GCCTCACCTTACTGCCCACCTTTTATTTGAAGTCATAGCATAAAATTTAAC
P.vampyrus CTCGC GCCTCACCTTAATGCCGATCTTTGATTTGAAATCATAGCATAAAATTTAAC
110 120 130 140 150 160 170 180 190 200
Mouse ATAA TGACAGCAACATCCTGACCAATTATCCAAACCATCCAGCCATCCTAGAGTGTCCAGAACCTCACACATGATCTATAGGATTAAGAGGTTAGCTCC
Human ATA AGCAACATCCTGACCAATTATCCAAACCATCCAGACATCCCTGAATGGCCAGAGCGTAGCACACGGTCTGTAGGATTAAGAGGTTAACTCC
Horse ATAAGTGACAGCAACATCCTGACCAATTACTCAAACCATCCAGACATCCCCAAATGTCCAGAACATAGCACACGGTCTGTAGGATTAAGAGGTTAACTCC
T.lavali ATAAGTGACAGCAACATCCTGACCAATTACCCAAACCATCCAGACATCCCGAAATGTCCAGAACATAGCACACGCTCTGAAGGATTAAGAGGTTAACTCC
M.tuberculata ATAAGTGACAGCAACATCCTGACCAATTACCCAAACCATCCAGACATCCCGAAATGTCCAGAACATAGCACACGCTCTGAAGGATTAAGAGGTTAACTCC
N.major ATAAGTGACAGCAACATCCTGACCAATTACCCAAACCATCCAGACATCCCGAAATGTCCAGAACATAGCACACGCTCTGAAGGATTAAGAGGTTAACTCC
A.jamaicensis ATAAGTGACAGCAACATCCTGACCAATTACCCAAACCATCCAGACATCCCGAAATGTCCAGAACATAGCACACGCTCTGAAGGATTAAGAGGTTAACTCC
N.albiventirs ATAAGTGACAGCAACATCCTGACCAATTACCCAAACCATCCAGACATCCCGAAATGTCCAGAACATAGCACACGCTCTGAAGGATTAAGAGGTTAACTCC
R.clivosus ATAAGTGACAGCAACATCCTGACCAATTACCCAAACCATCCAGACATCCCGAAATGTCCAGAACATAGCACACGCTCTGAAGGATTAAGAGGTTAACTCC
R.darlingii ATAAGTGACAGCAACATCCTGACCAATTACCCAAACCATCCAGACATCCCGAAATGTCCAGAACATAGCACACGCTCTGAAGGATTAAGAGGTTAACTCC
R.capensis ATAAGTGACAGCAACATCCTGACCAATTACCCAAACCATCCAGACATCCCGAAATGTCCAGAACATAGCACACGCTCTGAAGGATTAAGAGGTTAACTCC
C.perspicillata ATAAGTGACAGCAACATCCTGACCAATTACCCAAACCATCCAGACATCCCGAAATGTCCAGAACATGGCACACGCTCTGAAGGATTAAGAGGTTAACTCC
R.naso ATAAGTGACAGCAACATCCTGACCAATTACCCAAACCATCCAGACATCCCGAAATGTCCAGAACATAGCACACGCTCTGAAGGATTAAGAGGTTAACTCC
R.hardwickei ATAAGTGACAGCAACATCCTGACCAATTACGCAACCCATGCAGACATCCCGAAATGTCCAGAACATAGCGCACGCTCTGAAGGATTAAGAGGTTAACTCC
A.ornatus ATAAGTGACAGCAACATCCTGACCAACTACCCAAACCATCCAGACATCCCGAAATGTCCAGAACATAGCACACGGTCTGAAGGATTAAGAGGTTAACTCC
H.commersoni ATAAGTGACAGCAACATCCTGACCAATTACCCAAGCCATCCAGACATCCCGAAATGTCCAGAACATAGCACACGGTCTGAAGGATTAAGAGGTTAACTCC
C.cor ACAAGTGACAGCAACATCCTGACCAATTACCCCAACCATGCAGACATCCCCAAATGTCCAGAACATAGCACGCAGTCTGTGGGATTAAGAGGCTAACTCC
M.natalenesis ATAAGTGACAGCAACATCCTGACCAATTT CCAGGCCTCACAGACATCCCCCGATGTCCAGAGCAGAGCGCGCGGTCTGTGGGATTAAGAGGTTAACTCC
M.schreibersi ATAAGTGACAGCAACATCCTGACCAATTT CCAGGCCTCACAGACATCCCCCGATGTCCAGAGCAGAGCGCGCGGTCTGTGGGATTAAGAGGTTAACTCC
M.lucifugus ATGAGTGACAGCAACATCCTGACCAATTA CCAGGCCTGGCAGACATCCCCCAGTGTCCAGAGCAGAGCGCGCGGTCTGCGGGATTAAGAGGTTAACTCC
P.vampyrus ATAAGTGACAGCAACATCCTGACCAATTACCCAAACCATGCAGACATCCCCAAACGTCCAGAACATAGCACACGGTCTGTGGGATTAAGAGGTTAACTCC

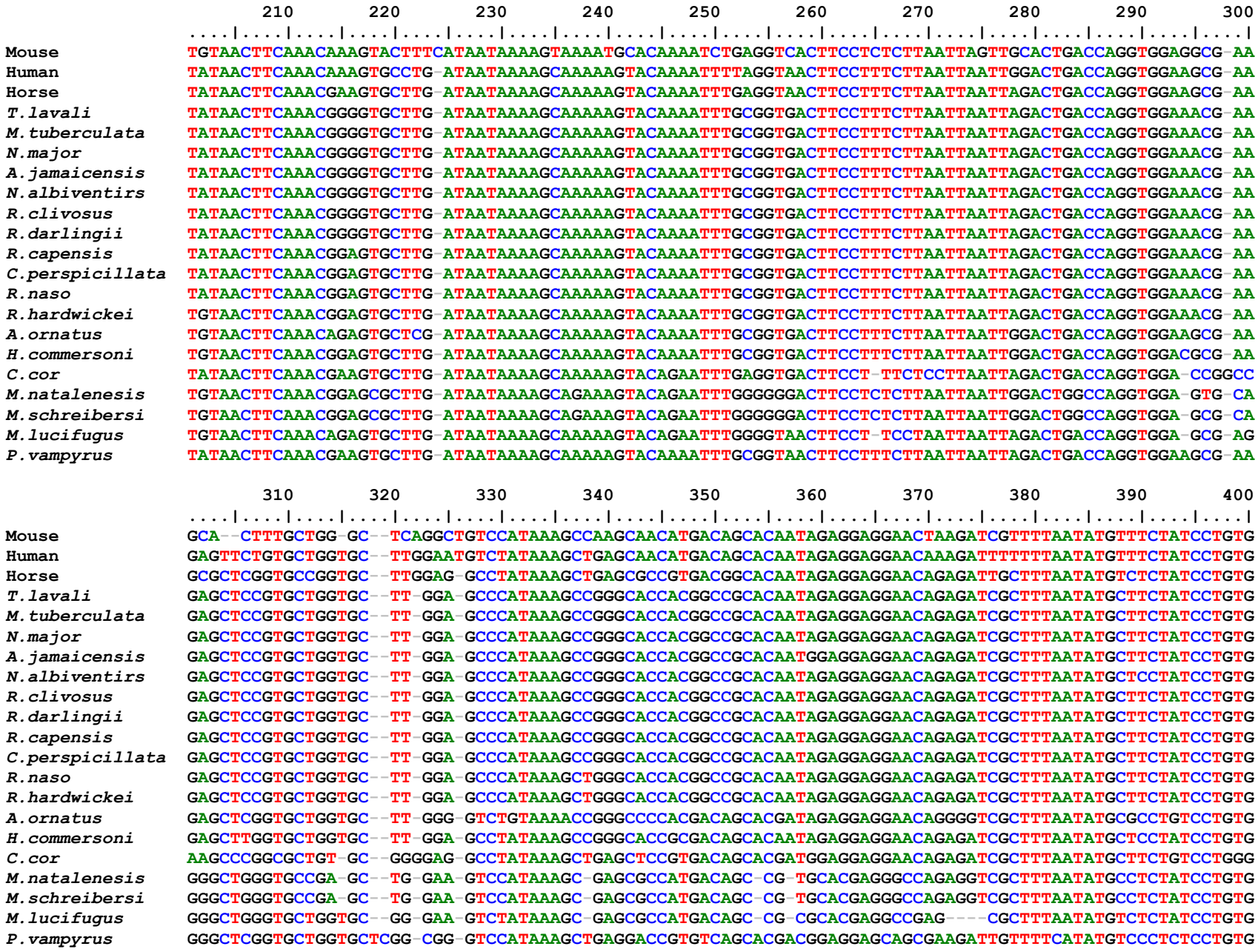
210 220 230 240 250 260 270 280 290 300
Mouse TGTAACTTCAAACAAAGTACTTTCATAATAAAAGTAAAATGCACAAAATCTGAGGTCACTTCCTCTCTTAATTAGTTGCACTGACCAGGTGGAGGCG-AA
Human TATAACTTCAAACAAAGTGCCTG-ATAATAAAAGCAAAAAGTACAAAATTTTAGGTAACTTCCTTTCTTAATTAATTGGACTGACCAGGTGGAAGCG-AA
Horse TATAACTTCAAACGAAGTGCTTG-ATAATAAAAGCAAAAAGTACAAAATTTGAGGTAACTTCCTTTCTTAATTAATTAGACTGACCAGGTGGAAGCG-AA
T.lavali TATAACTTCAAACGGGGTGCTTG-ATAATAAAAGCAAAAAGTACAAAATTTGCGGTGACTTCCTTTCTTAATTAATTAGACTGACCAGGTGGAAACG-AA
M.tuberculata TATAACTTCAAACGGGGTGCTTG-ATAATAAAAGCAAAAAGTACAAAATTTGCGGTGACTTCCTTTCTTAATTAATTAGACTGACCAGGTGGAAACG-AA
N.major TATAACTTCAAACGGGGTGCTTG-ATAATAAAAGCAAAAAGTACAAAATTTGCGGTGACTTCCTTTCTTAATTAATTAGACTGACCAGGTGGAAACG-AA
A.jamaicensis TATAACTTCAAACGGGGTGCTTG-ATAATAAAAGCAAAAAGTACAAAATTTGCGGTGACTTCCTTTCTTAATTAATTAGACTGACCAGGTGGAAACG-AA
N.albiventirs TATAACTTCAAACGGGGTGCTTG-ATAATAAAAGCAAAAAGTACAAAATTTGCGGTGACTTCCTTTCTTAATTAATTAGACTGACCAGGTGGAAACG-AA
R.clivosus TATAACTTCAAACGGGGTGCTTG-ATAATAAAAGCAAAAAGTACAAAATTTGCGGTGACTTCCTTTCTTAATTAATTAGACTGACCAGGTGGAAACG-AA
R.darlingii TATAACTTCAAACGGGGTGCTTG-ATAATAAAAGCAAAAAGTACAAAATTTGCGGTGACTTCCTTTCTTAATTAATTAGACTGACCAGGTGGAAACG-AA
R.capensis TATAACTTCAAACGGAGTGCTTG-ATAATAAAAGCAAAAAGTACAAAATTTGCGGTGACTTCCTTTCTTAATTAATTAGACTGACCAGGTGGAAACG-AA
C.perspicillata TATAACTTCAAACGGAGTGCTTG-ATAATAAAAGCAAAAAGTACAAAATTTGCGGTGACTTCCTTTCTTAATTAATTAGACTGACCAGGTGGAAACG-AA
R.naso TATAACTTCAAACGGAGTGCTTG-ATAATAAAAGCAAAAAGTACAAAATTTGCGGTGACTTCCTTTCTTAATTAATTAGACTGACCAGGTGGAAACG-AA
R.hardwickei TGTAACTTCAAACGGAGTGCTTG-ATAATAAAAGCAAAAAGTACAAAATTTGCGGTGACTTCCTTTCTTAATTAATTAGACTGACCAGGTGGAAACG-AA
A.ornatus TGTAACTTCAAACAGAGTGCTCG-ATAATAAAAGCAAAAAGTACAAAATTTGCGGTGACTTCCTTTCTTAATTAATTGGACTGACCAGGTGGAAGCG-AA
H.commersoni TGTAACTTCAAACGGAGTGCTTG-ATAATAAAAGCAAAAAGTACAAAATTTGCGGTGACTTCCTTTCTTAATTAATTGGACTGACCAGGTGGACGCG-AA
C.cor TATAACTTCAAACGAAGTGCTTG-ATAATAAAAGCAAAAAGTACAGAATTTGAGGTGACTTCCT-TTCTCCTTAATTAGACTGACCAGGTGGA-CCGGCC
M.natalenesis TGTAACTTCAAACGGAGCGCTTG-ATAATAAAAGCAGAAAGTACAGAATTTGGGGGGACTTCCTCTCTTAATTAATTGGACTGGCCAGGTGGA-GTG-CA
M.schreibersi TGTAACTTCAAACGGAGCGCTTG-ATAATAAAAGCAGAAAGTACAGAATTTGGGGGGACTTCCTCTCTTAATTAATTGGACTGGCCAGGTGGA-GCG-CA
M.lucifugus TGTAACTTCAAACAGAGTGCTTG-ATAATAAAAGCAAAAAGTACAGAATTTGGGGTAACTTCCT-TCCTAATTAATTAGACTGACCAGGTGGA-GCG-AG
P.vampyrus TATAACTTCAAACGAAGTGCTTG-ATAATAAAAGCAAAAAGTACAAAATTTGCGGTAACTTCCTTTCTTAATTAATTAGACTGACCAGGTGGAAGCG-AA
310 320 330 340 350 360 370 380 390 400
Mouse GCA--CTTTGCTGG-GC--TCAGGCTGTCCATAAAGCCAAGCAACATGACAGCACAATAGAGGAGGAACTAAGATCGTTTTAATATGTTTCTATCCTGTG
Human GAGTTCTGTGCTGGTGC--TTGGAATGTCTATAAAGCTGAGCAACATGACAGCACAATAGAGGAGGAACAAAGATTTTTTTAATATGTTTCTATCCTGTG
Horse GCGCTCGGTGCCGGTGC--TTGGAG-GCCTATAAAGCTGAGCGCCGTGACGGCACAATAGAGGAGGAACAGAGATTGCTTTAATATGTCTCTATCCTGTG
T.lavali GAGCTCCGTGCTGGTGC--TT-GGA-GCCCATAAAGCCGGGCACCACGGCCGCACAATAGAGGAGGAACAGAGATCGCTTTAATATGCTTCTATCCTGTG
M.tuberculata GAGCTCCGTGCTGGTGC--TT-GGA-GCCCATAAAGCCGGGCACCACGGCCGCACAATAGAGGAGGAACAGAGATCGCTTTAATATGCTTCTATCCTGTG
N.major GAGCTCCGTGCTGGTGC--TT-GGA-GCCCATAAAGCCGGGCACCACGGCCGCACAATAGAGGAGGAACAGAGATCGCTTTAATATGCTTCTATCCTGTG
A.jamaicensis GAGCTCCGTGCTGGTGC--TT-GGA-GCCCATAAAGCCGGGCACCACGGCCGCACAATGGAGGAGGAACAGAGATCGCTTTAATATGCTTCTATCCTGTG
N.albiventirs GAGCTCCGTGCTGGTGC--TT-GGA-GCCCATAAAGCCGGGCACCACGGCCGCACAATAGAGGAGGAACAGAGATCGCTTTAATATGCTCCTATCCTGTG
R.clivosus GAGCTCCGTGCTGGTGC--TT-GGA-GCCCATAAAGCCGGGCACCACGGCCGCACAATAGAGGAGGAACAGAGATCGCTTTAATATGCTTCTATCCTGTG
R.darlingii GAGCTCCGTGCTGGTGC--TT-GGA-GCCCATAAAGCCGGGCACCACGGCCGCACAATAGAGGAGGAACAGAGATCGCTTTAATATGCTTCTATCCTGTG
R.capensis GAGCTCCGTGCTGGTGC--TT-GGA-GCCCATAAAGCCGGGCACCACGGCCGCACAATAGAGGAGGAACAGAGATCGCTTTAATATGCTTCTATCCTGTG
C.perspicillata GAGCTCCGTGCTGGTGC--TT-GGA-GCCCATAAAGCCGGGCACCACGGCCGCACAATAGAGGAGGAACAGAGATCGCTTTAATATGCTTCTATCCTGTG
R.naso GAGCTCCGTGCTGGTGC--TT-GGA-GCCCATAAAGCTGGGCACCACGGCCGCACAATAGAGGAGGAACAGAGATCGCTTTAATATGCTTCTATCCTGTG
R.hardwickei GAGCTCCGTGCTGGTGC--TT-GGA-GCCCATAAAGCTGGGCACCACGGCCGCACAATAGAGGAGGAACAGAGATCGCTTTAATATGCTTCTATCCTGTG
A.ornatus GAGCTCGGTGCTGGTGC--TT-GGG-GTCTGTAAAACCGGGCCCCACGACAGCACGATAGAGGAGGAACAGGGGTCGCTTTAATATGCGCCTGTCCTGTG
H.commersoni GAGCTTGGTGCTGGTGC--TT-GGA-GCCTATAAAGCCGGGCACCGCGACAGCACAATAGAGGAGGAACAGAGATCGCTTTAATATGCTCCTATCCTGTG
C.cor AAGCCCGGCGCTGT-GC--GGGGAG-GCCTATAAAGCTGAGCTCCGTGACAGCACGATGGAGGAGGAACAGAGATCGCTTTAATATGCTTCTGTCCTGGG
M.natalenesis GGGCTGGGTGCCGA-GC--TG-GAA-GTCCATAAAGC-GAGCGCCATGACAGC-CG-TGCACGAGGGCCAGAGGTCGCTTTAATATGCCTCTATCCTGTG
M.schreibersi GGGCTGGGTGCCGA-GC--TG-GAA-GTCCATAAAGC-GAGCGCCATGACAGC-CG-TGCACGAGGGCCAGAGGTCGCTTTAATATGCCTCTATCCTGTG
M.lucifugus GGGCTGGGTGCTGGTGC--GG-GAA-GTCTATAAAGC-GAGCGCCATGACAGC-CG-CGCACGAGGCCGAG----CGCTTTAATATGTCTCTATCCTGTG
P.vampyrus GGGCTCGGTGCTGGTGCTCGG-CGG-GTCCATAAAGCTGAGGACCGTGTCAGCACGACGGAGGAGCAGCGAAGATTGTTTTCATATGTCCCTCTCCTGTG

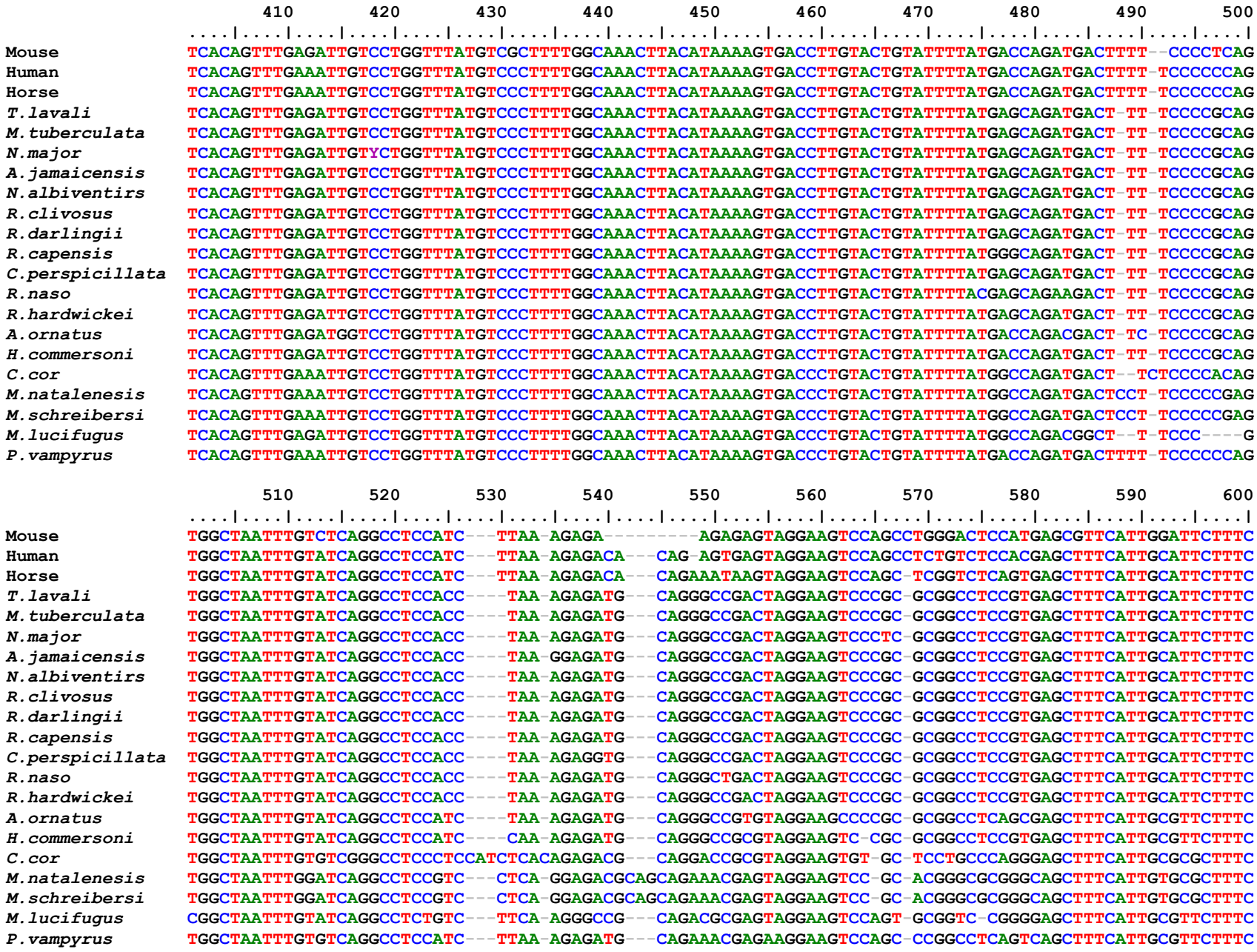
410 420 430 440 450 460 470 480 490 500
Mouse TCACAGTTTGAGATTGTCCTGGTTTATGTCGCTTTTGGCAAACTTACATAAAAGTGACCTTGTACTGTATTTTATGACCAGATGACTTTT--CCCCTCAG
Human TCACAGTTTGAAATTGTCCTGGTTTATGTCCCTTTTGGCAAACTTACATAAAAGTGACCTTGTACTGTATTTTATGACCAGATGACTTTT-TCCCCCCAG
Horse TCACAGTTTGAAATTGTCCTGGTTTATGTCCCTTTTGGCAAACTTACATAAAAGTGACCTTGTACTGTATTTTATGACCAGATGACTTTT-TCCCCCCAG
T.lavali TCACAGTTTGAGATTGTCCTGGTTTATGTCCCTTTTGGCAAACTTACATAAAAGTGACCTTGTACTGTATTTTATGAGCAGATGACT-TT-TCCCCGCAG
M.tuberculata TCACAGTTTGAGATTGTCCTGGTTTATGTCCCTTTTGGCAAACTTACATAAAAGTGACCTTGTACTGTATTTTATGAGCAGATGACT-TT-TCCCCGCAG
N.major TCACAGTTTGAGATTGTYCTGGTTTATGTCCCTTTTGGCAAACTTACATAAAAGTGACCTTGTACTGTATTTTATGAGCAGATGACT-TT-TCCCCGCAG
A.jamaicensis TCACAGTTTGAGATTGTCCTGGTTTATGTCCCTTTTGGCAAACTTACATAAAAGTGACCTTGTACTGTATTTTATGAGCAGATGACT-TT-TCCCCGCAG
N.albiventirs TCACAGTTTGAGATTGTCCTGGTTTATGTCCCTTTTGGCAAACTTACATAAAAGTGACCTTGTACTGTATTTTATGAGCAGATGACT-TT-TCCCCGCAG
R.clivosus TCACAGTTTGAGATTGTCCTGGTTTATGTCCCTTTTGGCAAACTTACATAAAAGTGACCTTGTACTGTATTTTATGAGCAGATGACT-TT-TCCCCGCAG
R.darlingii TCACAGTTTGAGATTGTCCTGGTTTATGTCCCTTTTGGCAAACTTACATAAAAGTGACCTTGTACTGTATTTTATGAGCAGATGACT-TT-TCCCCGCAG
R.capensis TCACAGTTTGAGATTGTCCTGGTTTATGTCCCTTTTGGCAAACTTACATAAAAGTGACCTTGTACTGTATTTTATGGGCAGATGACT-TT-TCCCCGCAG
C.perspicillata TCACAGTTTGAGATTGTCCTGGTTTATGTCCCTTTTGGCAAACTTACATAAAAGTGACCTTGTACTGTATTTTATGAGCAGATGACT-TT-TCCCCGCAG
R.naso TCACAGTTTGAGATTGTCCTGGTTTATGTCCCTTTTGGCAAACTTACATAAAAGTGACCTTGTACTGTATTTTACGAGCAGAAGACT-TT-TCCCCGCAG
R.hardwickei TCACAGTTTGAGATTGTCCTGGTTTATGTCCCTTTTGGCAAACTTACATAAAAGTGACCTTGTACTGTATTTTATGAGCAGATGACT-TT-TCCCCGCAG
A.ornatus TCACAGTTTGAGATGGTCCTGGTTTATGTCCCTTTTGGCAAACTTACATAAAAGTGACCTTGTACTGTATTTTATGACCAGACGACT-TC-TCCCCGCAG
H.commersoni TCACAGTTTGAGATTGTCCTGGTTTATGTCCCTTTTGGCAAACTTACATAAAAGTGACCTTGTACTGTATTTTATGACCAGATGACT-TT-TCCCCGCAG
C.cor TCACAGTTTGAAATTGTCCTGGTTTATGTCCCTTTTGGCAAACTTACATAAAAGTGACCCTGTACTGTATTTTATGGCCAGATGACT--TCTCCCCACAG
M.natalenesis TCACAGTTTGAAATTGTCCTGGTTTATGTCCCTTTTGGCAAACTTACATAAAAGTGACCCTGTACTGTATTTTATGGCCAGATGACTCCT-TCCCCCGAG
M.schreibersi TCACAGTTTGAAATTGTCCTGGTTTATGTCCCTTTTGGCAAACTTACATAAAAGTGACCCTGTACTGTATTTTATGGCCAGATGACTCCT-TCCCCCGAG
M.lucifugus TCACAGTTTGAGATTGTCCTGGTTTATGTCCCTTTTGGCAAACTTACATAAAAGTGACCCTGTACTGTATTTTATGGCCAGACGGCT--T-TCCC----G
P.vampyrus TCACAGTTTGAAATTGTCCTGGTTTATGTCCCTTTTGGCAAACTTACATAAAAGTGACCCTGTACTGTATTTTATGACCAGATGACTTTT-TCCCCCCAG
510 520 530 540 550 560 570 580 590 600
Mouse TGGCTAATTTGTCTCAGGCCTCCATC---TTAA-AGAGA---------AGAGAGTAGGAAGTCCAGCCTGGGACTCCATGAGCGTTCATTGGATTCTTTC
Human TGGCTAATTTGTATCAGGCCTCCATC---TTAA-AGAGACA---CAG-AGTGAGTAGGAAGTCCAGCCTCTGTCTCCACGAGCTTTCATTGCATTCTTTC
Horse TGGCTAATTTGTATCAGGCCTCCATC---TTAA-AGAGACA---CAGAAATAAGTAGGAAGTCCAGC-TCGGTCTCAGTGAGCTTTCATTGCATTCTTTC
T.lavali TGGCTAATTTGTATCAGGCCTCCACC----TAA-AGAGATG---CAGGGCCGACTAGGAAGTCCCGC-GCGGCCTCCGTGAGCTTTCATTGCATTCTTTC
M.tuberculata TGGCTAATTTGTATCAGGCCTCCACC----TAA-AGAGATG---CAGGGCCGACTAGGAAGTCCCGC-GCGGCCTCCGTGAGCTTTCATTGCATTCTTTC
N.major TGGCTAATTTGTATCAGGCCTCCACC----TAA-AGAGATG---CAGGGCCGACTAGGAAGTCCCTC-GCGGCCTCCGTGAGCTTTCATTGCATTCTTTC
A.jamaicensis TGGCTAATTTGTATCAGGCCTCCACC----TAA-GGAGATG---CAGGGCCGACTAGGAAGTCCCGC-GCGGCCTCCGTGAGCTTTCATTGCATTCTTTC
N.albiventirs TGGCTAATTTGTATCAGGCCTCCACC----TAA-AGAGATG---CAGGGCCGACTAGGAAGTCCCGC-GCGGCCTCCGTGAGCTTTCATTGCATTCTTTC
R.clivosus TGGCTAATTTGTATCAGGCCTCCACC----TAA-AGAGATG---CAGGGCCGACTAGGAAGTCCCGC-GCGGCCTCCGTGAGCTTTCATTGCATTCTTTC
R.darlingii TGGCTAATTTGTATCAGGCCTCCACC----TAA-AGAGATG---CAGGGCCGACTAGGAAGTCCCGC-GCGGCCTCCGTGAGCTTTCATTGCATTCTTTC
R.capensis TGGCTAATTTGTATCAGGCCTCCACC----TAA-AGAGATG---CAGGGCCGACTAGGAAGTCCCGC-GCGGCCTCCGTGAGCTTTCATTGCATTCTTTC
C.perspicillata TGGCTAATTTGTATCAGGCCTCCACC----TAA-AGAGGTG---CAGGGCCGACTAGGAAGTCCCGC-GCGGCCTCCGTGAGCTTTCATTGCATTCTTTC
R.naso TGGCTAATTTGTATCAGGCCTCCACC----TAA-AGAGATG---CAGGGCTGACTAGGAAGTCCCGC-GCGGCCTCCGTGAGCTTTCATTGCATTCTTTC
R.hardwickei TGGCTAATTTGTATCAGGCCTCCACC----TAA-AGAGATG---CAGGGCCGACTAGGAAGTCCCGC-GCGGCCTCCGTGAGCTTTCATTGCATTCTTTC
A.ornatus TGGCTAATTTGTATCAGGCCTCCATC----TAA-AGAGATG---CAGGGCCGTGTAGGAAGCCCCGC-GCGGCCTCAGCGAGCTTTCATTGCGTTCTTTC
H.commersoni TGGCTAATTTGTATCAGGCCTCCATC----CAA-AGAGATG---CAGGGCCGCGTAGGAAGTC-CGC-GCGGCCTCCGTGAGCTTTCATTGCGTTCTTTC
C.cor TGGCTAATTTGTGTCGGGCCTCCCTCCATCTCACAGAGACG---CAGGACCGCGTAGGAAGTGT-GC-TCCTGCCCAGGGAGCTTTCATTGCGCGCTTTC
M.natalenesis TGGCTAATTTGGATCAGGCCTCCGTC---CTCA-GGAGACGCAGCAGAAACGAGTAGGAAGTCC-GC-ACGGGCGCGGGCAGCTTTCATTGTGCGCTTTC
M.schreibersi TGGCTAATTTGGATCAGGCCTCCGTC---CTCA-GGAGACGCAGCAGAAACGAGTAGGAAGTCC-GC-ACGGGCGCGGGCAGCTTTCATTGTGCGCTTTC
M.lucifugus CGGCTAATTTGTATCAGGCCTCTGTC---TTCA-AGGGCCG---CAGACGCGAGTAGGAAGTCCAGT-GCGGTC-CGGGGAGCTTTCATTGCGTTCTTTC
P.vampyrus TGGCTAATTTGTGTCAGGCCTCCATC---TTAA-AGAGATG---CAGAAACGAGAAGGAAGTCCAGC-CCGGCCTCAGTCAGCTTTCATTGCGTTCTTTC

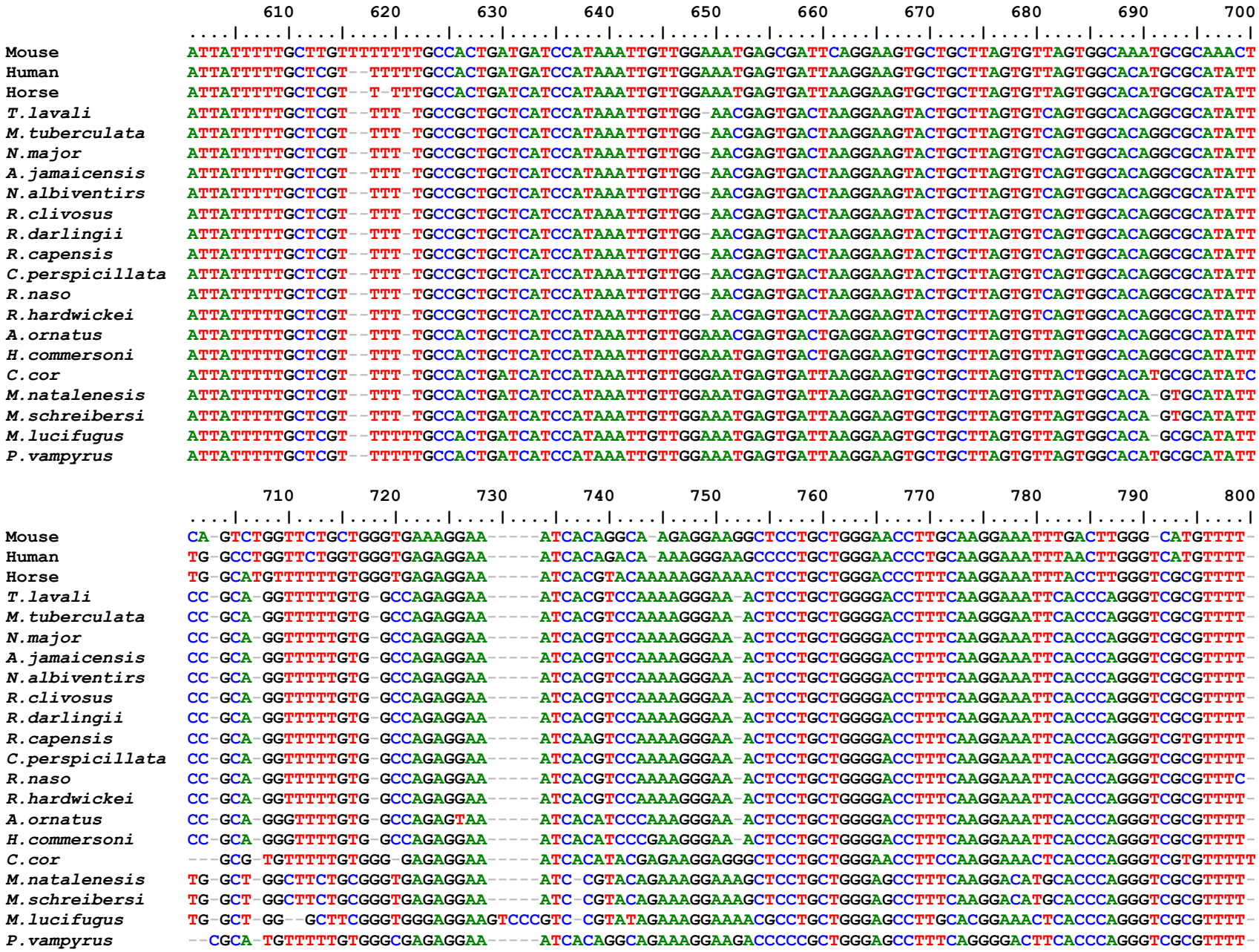
610 620 630 640 650 660 670 680 690 700
Mouse ATTATTTTTGCTTGTTTTTTTTGCCACTGATGATCCATAAATTGTTGGAAATGAGCGATTCAGGAAGTGCTGCTTAGTGTTAGTGGCAAATGCGCAAACT
Human ATTATTTTTGCTCGT--TTTTTGCCACTGATGATCCATAAATTGTTGGAAATGAGTGATTAAGGAAGTGCTGCTTAGTGTTAGTGGCACATGCGCATATT
Horse ATTATTTTTGCTCGT--T-TTTGCCACTGATCATCCATAAATTGTTGGAAATGAGTGATTAAGGAAGTGCTGCTTAGTGTTAGTGGCACATGCGCATATT
T.lavali ATTATTTTTGCTCGT--TTT-TGCCGCTGCTCATCCATAAATTGTTGG-AACGAGTGACTAAGGAAGTACTGCTTAGTGTCAGTGGCACAGGCGCATATT
M.tuberculata ATTATTTTTGCTCGT--TTT-TGCCGCTGCTCATCCATAAATTGTTGG-AACGAGTGACTAAGGAAGTACTGCTTAGTGTCAGTGGCACAGGCGCATATT
N.major ATTATTTTTGCTCGT--TTT-TGCCGCTGCTCATCCATAAATTGTTGG-AACGAGTGACTAAGGAAGTACTGCTTAGTGTCAGTGGCACAGGCGCATATT
A.jamaicensis ATTATTTTTGCTCGT--TTT-TGCCGCTGCTCATCCATAAATTGTTGG-AACGAGTGACTAAGGAAGTACTGCTTAGTGTCAGTGGCACAGGCGCATATT
N.albiventirs ATTATTTTTGCTCGT--TTT-TGCCGCTGCTCATCCATAAATTGTTGG-AACGAGTGACTAAGGAAGTACTGCTTAGTGTCAGTGGCACAGGCGCATATT
R.clivosus ATTATTTTTGCTCGT--TTT-TGCCGCTGCTCATCCATAAATTGTTGG-AACGAGTGACTAAGGAAGTACTGCTTAGTGTCAGTGGCACAGGCGCATATT
R.darlingii ATTATTTTTGCTCGT--TTT-TGCCGCTGCTCATCCATAAATTGTTGG-AACGAGTGACTAAGGAAGTACTGCTTAGTGTCAGTGGCACAGGCGCATATT
R.capensis ATTATTTTTGCTCGT--TTT-TGCCGCTGCTCATCCATAAATTGTTGG-AACGAGTGACTAAGGAAGTACTGCTTAGTGTCAGTGGCACAGGCGCATATT
C.perspicillata ATTATTTTTGCTCGT--TTT-TGCCGCTGCTCATCCATAAATTGTTGG-AACGAGTGACTAAGGAAGTACTGCTTAGTGTCAGTGGCACAGGCGCATATT
R.naso ATTATTTTTGCTCGT--TTT-TGCCGCTGCTCATCCATAAATTGTTGG-AACGAGTGACTAAGGAAGTACTGCTTAGTGTCAGTGGCACAGGCGCATATT
R.hardwickei ATTATTTTTGCTCGT--TTT-TGCCGCTGCTCATCCATAAATTGTTGG-AACGAGTGACTAAGGAAGTACTGCTTAGTGTCAGTGGCACAGGCGCATATT
A.ornatus ATTATTTTTGCTCGT--TTT-TGCCACTGCTCATCCATAAATTGTTGGAAACGAGTGACTGAGGAAGTGCTGCTTAGTGTTAGTGGCACAGGCGCATATT
H.commersoni ATTATTTTTGCTCGT--TTT-TGCCACTGCTCATCCATAAATTGTTGGAAATGAGTGACTGAGGAAGTGCTGCTTAGTGTTAGTGGCACAGGCGCATATT
C.cor ATTATTTTTGCTCGT--TTT-TGCCACTGATCATCCATAAATTGTTGGGAATGAGTGATTAAGGAAGTGCTGCTTAGTGTTACTGGCACATGCGCATATC
M.natalenesis ATTATTTTTGCTCGT--TTT-TGCCACTGATCATCCATAAATTGTTGGAAATGAGTGATTAAGGAAGTGCTGCTTAGTGTTAGTGGCACA-GTGCATATT
M.schreibersi ATTATTTTTGCTCGT--TTT-TGCCACTGATCATCCATAAATTGTTGGAAATGAGTGATTAAGGAAGTGCTGCTTAGTGTTAGTGGCACA-GTGCATATT
M.lucifugus ATTATTTTTGCTCGT--TTTTTGCCACTGATCATCCATAAATTGTTGGAAATGAGTGATTAAGGAAGTGCTGCTTAGTGTTAGTGGCACA-GCGCATATT
P.vampyrus ATTATTTTTGCTCGT--TTTTTGCCACTGATCATCCATAAATTGTTGGAAATGAGTGATTAAGGAAGTGCTGCTTAGTGTTAGTGGCACATGCGCATATT
710 720 730 740 750 760 770 780 790 800
Mouse CA-GTCTGGTTCTGCTGGGTGAAAGGAA-----ATCACAGGCA-AGAGGAAGGCTCCTGCTGGGAACCTTGCAAGGAAATTTGACTTGGG-CATGTTTT-
Human TG-GCCTGGTTCTGGTGGGTGAGAGGAA-----ATCACAGACA-AAAGGGAAGCCCCTGCTGGGAACCCTGCAAGGAAATTTAACTTGGGTCATGTTTT-
Horse TG-GCATGTTTTTTGTGGGTGAGAGGAA-----ATCACGTACAAAAAGGAAAACTCCTGCTGGGACCCTTTCAAGGAAATTTACCTTGGGTCGCGTTTT-
T.lavali CC-GCA-GGTTTTTGTG-GCCAGAGGAA-----ATCACGTCCAAAAGGGAA-ACTCCTGCTGGGGACCTTTCAAGGAAATTCACCCAGGGTCGCGTTTT-
M.tuberculata CC-GCA-GGTTTTTGTG-GCCAGAGGAA-----ATCACGTCCAAAAGGGAA-ACTCCTGCTGGGGACCTTTCAAGGGAATTCACCCAGGGTCGCGTTTT-
N.major CC-GCA-GGTTTTTGTG-GCCAGAGGAA-----ATCACGTCCAAAAGGGAA-ACTCCTGCTGGGGACCTTTCAAGGAAATTCACCCAGGGTCGCGTTTT-
A.jamaicensis CC-GCA-GGTTTTTGTG-GCCAGAGGAA-----ATCACGTCCAAAAGGGAA-ACTCCTGCTGGGGACCTTTCAAGGAAATTCACCCAGGGTCGCGTTTT-
N.albiventirs CC-GCA-GGTTTTTGTG-GCCAGAGGAA-----ATCACGTCCAAAAGGGAA-ACTCCTGCTGGGGACCTTTCAAGGAAATTCACCCAGGGTCGCGTTTT-
R.clivosus CC-GCA-GGTTTTTGTG-GCCAGAGGAA-----ATCACGTCCAAAAGGGAA-ACTCCTGCTGGGGACCTTTCAAGGAAATTCACCCAGGGTCGCGTTTT-
R.darlingii CC-GCA-GGTTTTTGTG-GCCAGAGGAA-----ATCACGTCCAAAAGGGAA-ACTCCTGCTGGGGACCTTTCAAGGAAATTCACCCAGGGTCGCGTTTT-
R.capensis CC-GCA-GGTTTTTGTG-GCCAGAGGAA-----ATCAAGTCCAAAAGGGAA-ACTCCTGCTGGGGACCTTTCAAGGAAATTCACCCAGGGTCGTGTTTT-
C.perspicillata CC-GCA-GGTTTTTGTG-GCCAGAGGAA-----ATCACGTCCAAAAGGGAA-ACTCCTGCTGGGGACCTTTCAAGGAAATTCACCCAGGGTCGCGTTTT-
R.naso CC-GCA-GGTTTTTGTG-GCCAGAGGAA-----ATCACGTCCAAAAGGGAA-ACTCCTGCTGGGGACCTTTCAAGGAAATTCACCCAGGGTCGCGTTTC-
R.hardwickei CC-GCA-GGTTTTTGTG-GCCAGAGGAA-----ATCACGTCCAAAAGGGAA-ACTCCTGCTGGGGACCTTTCAAGGAAATTCACCCAGGGTCGCGTTTT-
A.ornatus CC-GCA-GGGTTTTGTG-GCCAGAGTAA-----ATCACATCCCAAAGGGAA-ACTCCTGCTGGGGACCTTTCAAGGAAATTCACCCAGGGTCGCGTTTT-
H.commersoni CC-GCA-GGGTTTTGTG-GCCAGAGGAA-----ATCACATCCCGAAGGGAA-ACTCCTGCTGGGGACCTTTCAAGGAAATTCACCCAGGGTCGCGTTTT-
C.cor ---GCG-TGTTTTTGTGGG-GAGAGGAA-----ATCACATACGAGAAGGAGGGCTCCTGCTGGGAACCTTCCAAGGAAACTCACCCAGGGTCGTGTTTTT
M.natalenesis TG-GCT-GGCTTCTGCGGGTGAGAGGAA-----ATC-CGTACAGAAAGGAAAGCTCCTGCTGGGAGCCTTTCAAGGACATGCACCCAGGGTCGCGTTTT-
M.schreibersi TG-GCT-GGCTTCTGCGGGTGAGAGGAA-----ATC-CGTACAGAAAGGAAAGCTCCTGCTGGGAGCCTTTCAAGGACATGCACCCAGGGTCGCGTTTT-
M.lucifugus TG-GCT-GG--GCTTCGGGTGGGAGGAAGTCCCGTC-CGTATAGAAAGGAAAACGCCTGCTGGGAGCCTTGCACGGAAACTCACCCAGGGTCGCGTTTT-
P.vampyrus --CGCA-TGTTTTTGTGGGCGAGAGGAA-----ATCACAGGCAGAAAGGAAGACCCCCGCTGGGAGCCTTTCAGGGGACTTCACCCAGGGTCGCGTTTT-

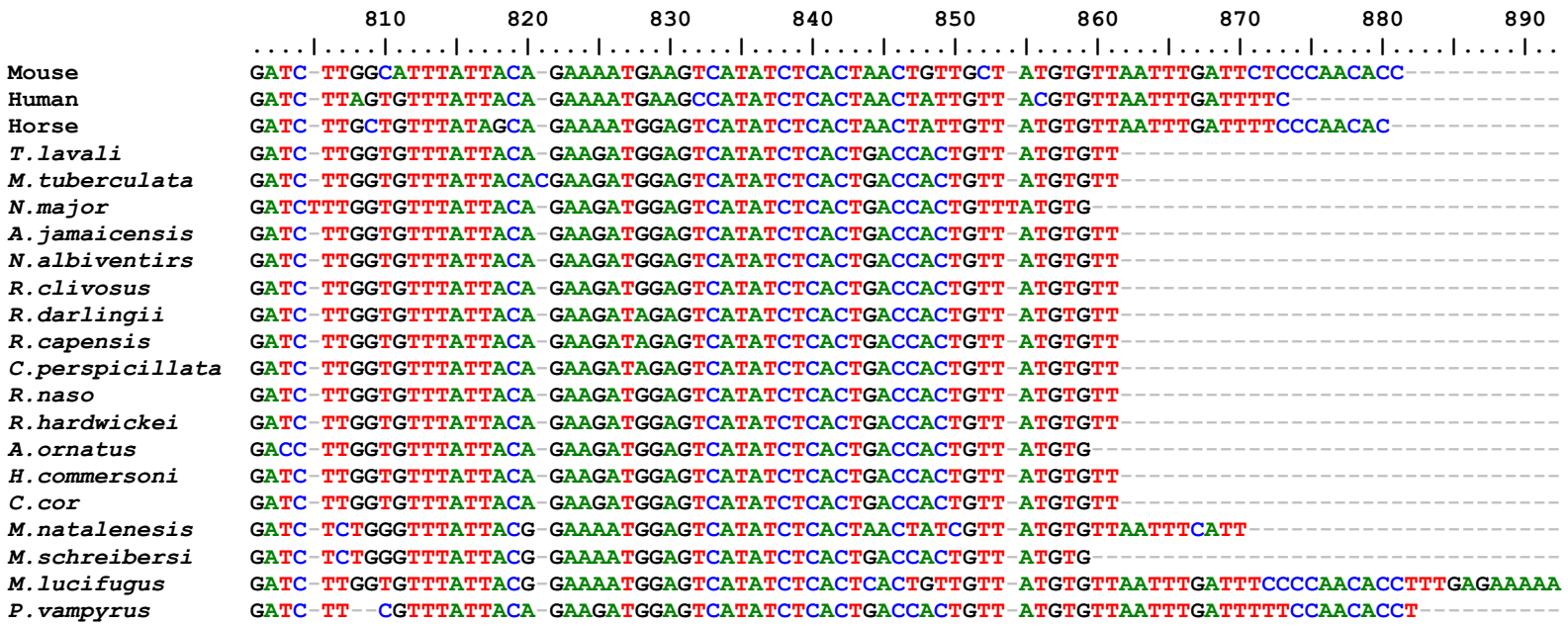

Figure A.6: PRANK alignment of the 18 Bat ZRS, the horse ZRS, the mouse ZRS and the human ZRS.

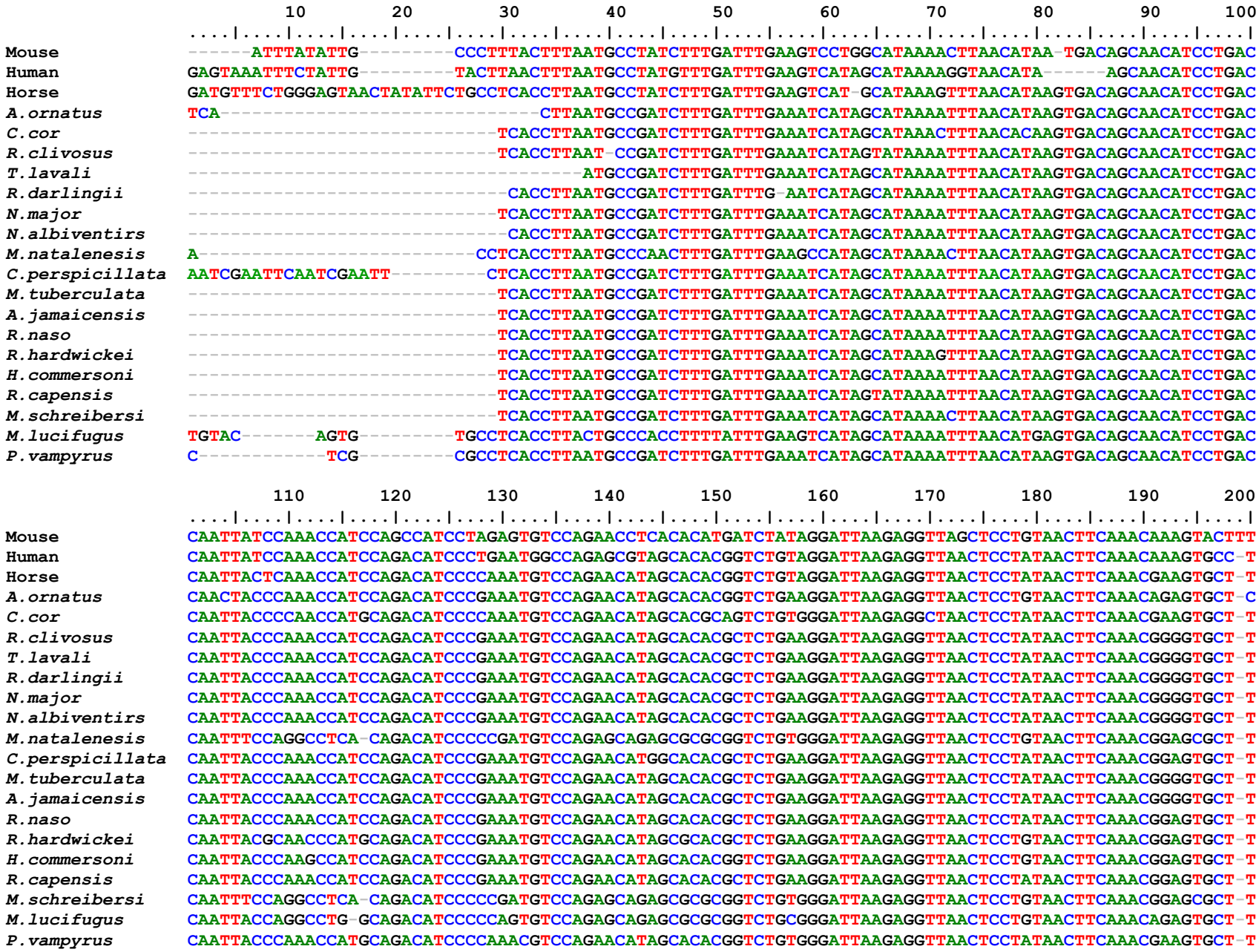
10 20 30 40 50 60 70 80 90 100
Mouse ------ATTTATATTG---------CCCTTTACTTTAATGCCTATCTTTGATTTGAAGTCCTGGCATAAAACTTAACATAA-TGACAGCAACATCCTGAC
Human GAGTAAATTTCTATTG---------TACTTAACTTTAATGCCTATGTTTGATTTGAAGTCATAGCATAAAAGGTAACATA------AGCAACATCCTGAC
Horse GATGTTTCTGGGAGTAACTATATTCTGCCTCACCTTAATGCCTATCTTTGATTTGAAGTCAT-GCATAAAGTTTAACATAAGTGACAGCAACATCCTGAC
A.ornatus TCA----------CTTAATGCCGATCTTTGATTTGAAATCATAGCATAAAATTTAACATAAGTGACAGCAACATCCTGAC
C.cor ----------TCACCTTAATGCCGATCTTTGATTTGAAATCATAGCATAAACTTTAACACAAGTGACAGCAACATCCTGAC
R.clivosus ----------TCACCTTAAT-CCGATCTTTGATTTGAAATCATAGTATAAAATTTAACATAAGTGACAGCAACATCCTGAC
T.lavali ----------ATGCCGATCTTTGATTTGAAATCATAGCATAAAATTTAACATAAGTGACAGCAACATCCTGAC
R.darlingii ----------CACCTTAATGCCGATCTTTGATTTG-AATCATAGCATAAAATTTAACATAAGTGACAGCAACATCCTGAC
N.major ----------TCACCTTAATGCCGATCTTTGATTTGAAATCATAGCATAAAATTTAACATAAGTGACAGCAACATCCTGAC
N.albiventirs ----------CACCTTAATGCCGATCTTTGATTTGAAATCATAGCATAAAATTTAACATAAGTGACAGCAACATCCTGAC
M.natalenesis A----------CCTCACCTTAATGCCCAACTTTGATTTGAAGCCATAGCATAAAACTTAACATAAGTGACAGCAACATCCTGAC
C.perspicillata AATCGAATTCAATCGAATT---------CTCACCTTAATGCCGATCTTTGATTTGAAATCATAGCATAAAATTTAACATAAGTGACAGCAACATCCTGAC
M.tuberculata ----------TCACCTTAATGCCGATCTTTGATTTGAAATCATAGCATAAAATTTAACATAAGTGACAGCAACATCCTGAC
A.jamaicensis ----------TCACCTTAATGCCGATCTTTGATTTGAAATCATAGCATAAAATTTAACATAAGTGACAGCAACATCCTGAC
R.naso ----------TCACCTTAATGCCGATCTTTGATTTGAAATCATAGCATAAAATTTAACATAAGTGACAGCAACATCCTGAC
R.hardwickei ----------TCACCTTAATGCCGATCTTTGATTTGAAATCATAGCATAAAGTTTAACATAAGTGACAGCAACATCCTGAC
H.commersoni ----------TCACCTTAATGCCGATCTTTGATTTGAAATCATAGCATAAAATTTAACATAAGTGACAGCAACATCCTGAC
R.capensis ----------TCACCTTAATGCCGATCTTTGATTTGAAATCATAGTATAAAATTTAACATAAGTGACAGCAACATCCTGAC
M.schreibersi ----------TCACCTTAATGCCGATCTTTGATTTGAAATCATAGCATAAAACTTAACATAAGTGACAGCAACATCCTGAC
M.lucifugus TGTAC-------AGTG---------TGCCTCACCTTACTGCCCACCTTTTATTTGAAGTCATAGCATAAAATTTAACATGAGTGACAGCAACATCCTGAC
P.vampyrus C----------TCG---------CGCCTCACCTTAATGCCGATCTTTGATTTGAAATCATAGCATAAAATTTAACATAAGTGACAGCAACATCCTGAC
110 120 130 140 150 160 170 180 190 200
Mouse CAATTATCCAAACCATCCAGCCATCCTAGAGTGTCCAGAACCTCACACATGATCTATAGGATTAAGAGGTTAGCTCCTGTAACTTCAAACAAAGTACTTT
Human CAATTATCCAAACCATCCAGACATCCCTGAATGGCCAGAGCGTAGCACACGGTCTGTAGGATTAAGAGGTTAACTCCTATAACTTCAAACAAAGTGCC-T
Horse CAATTACTCAAACCATCCAGACATCCCCAAATGTCCAGAACATAGCACACGGTCTGTAGGATTAAGAGGTTAACTCCTATAACTTCAAACGAAGTGCT-T
A.ornatus CAACTACCCAAACCATCCAGACATCCCGAAATGTCCAGAACATAGCACACGGTCTGAAGGATTAAGAGGTTAACTCCTGTAACTTCAAACAGAGTGCT-C
C.cor CAATTACCCCAACCATGCAGACATCCCCAAATGTCCAGAACATAGCACGCAGTCTGTGGGATTAAGAGGCTAACTCCTATAACTTCAAACGAAGTGCT-T
R.clivosus CAATTACCCAAACCATCCAGACATCCCGAAATGTCCAGAACATAGCACACGCTCTGAAGGATTAAGAGGTTAACTCCTATAACTTCAAACGGGGTGCT-T
T.lavali CAATTACCCAAACCATCCAGACATCCCGAAATGTCCAGAACATAGCACACGCTCTGAAGGATTAAGAGGTTAACTCCTATAACTTCAAACGGGGTGCT-T
R.darlingii CAATTACCCAAACCATCCAGACATCCCGAAATGTCCAGAACATAGCACACGCTCTGAAGGATTAAGAGGTTAACTCCTATAACTTCAAACGGGGTGCT-T
N.major CAATTACCCAAACCATCCAGACATCCCGAAATGTCCAGAACATAGCACACGCTCTGAAGGATTAAGAGGTTAACTCCTATAACTTCAAACGGGGTGCT-T
N.albiventirs CAATTACCCAAACCATCCAGACATCCCGAAATGTCCAGAACATAGCACACGCTCTGAAGGATTAAGAGGTTAACTCCTATAACTTCAAACGGGGTGCT-T
M.natalenesis CAATTTCCAGGCCTCA-CAGACATCCCCCGATGTCCAGAGCAGAGCGCGCGGTCTGTGGGATTAAGAGGTTAACTCCTGTAACTTCAAACGGAGCGCT-T
C.perspicillata CAATTACCCAAACCATCCAGACATCCCGAAATGTCCAGAACATGGCACACGCTCTGAAGGATTAAGAGGTTAACTCCTATAACTTCAAACGGAGTGCT-T
M.tuberculata CAATTACCCAAACCATCCAGACATCCCGAAATGTCCAGAACATAGCACACGCTCTGAAGGATTAAGAGGTTAACTCCTATAACTTCAAACGGGGTGCT-T
A.jamaicensis CAATTACCCAAACCATCCAGACATCCCGAAATGTCCAGAACATAGCACACGCTCTGAAGGATTAAGAGGTTAACTCCTATAACTTCAAACGGGGTGCT-T
R.naso CAATTACCCAAACCATCCAGACATCCCGAAATGTCCAGAACATAGCACACGCTCTGAAGGATTAAGAGGTTAACTCCTATAACTTCAAACGGAGTGCT-T
R.hardwickei CAATTACGCAACCCATGCAGACATCCCGAAATGTCCAGAACATAGCGCACGCTCTGAAGGATTAAGAGGTTAACTCCTGTAACTTCAAACGGAGTGCT-T
H.commersoni CAATTACCCAAGCCATCCAGACATCCCGAAATGTCCAGAACATAGCACACGGTCTGAAGGATTAAGAGGTTAACTCCTGTAACTTCAAACGGAGTGCT-T
R.capensis CAATTACCCAAACCATCCAGACATCCCGAAATGTCCAGAACATAGCACACGCTCTGAAGGATTAAGAGGTTAACTCCTATAACTTCAAACGGAGTGCT-T
M.schreibersi CAATTTCCAGGCCTCA-CAGACATCCCCCGATGTCCAGAGCAGAGCGCGCGGTCTGTGGGATTAAGAGGTTAACTCCTGTAACTTCAAACGGAGCGCT-T
M.lucifugus CAATTACCAGGCCTG-GCAGACATCCCCCAGTGTCCAGAGCAGAGCGCGCGGTCTGCGGGATTAAGAGGTTAACTCCTGTAACTTCAAACAGAGTGCT-T
P.vampyrus CAATTACCCAAACCATGCAGACATCCCCAAACGTCCAGAACATAGCACACGGTCTGTGGGATTAAGAGGTTAACTCCTATAACTTCAAACGAAGTGCT-T

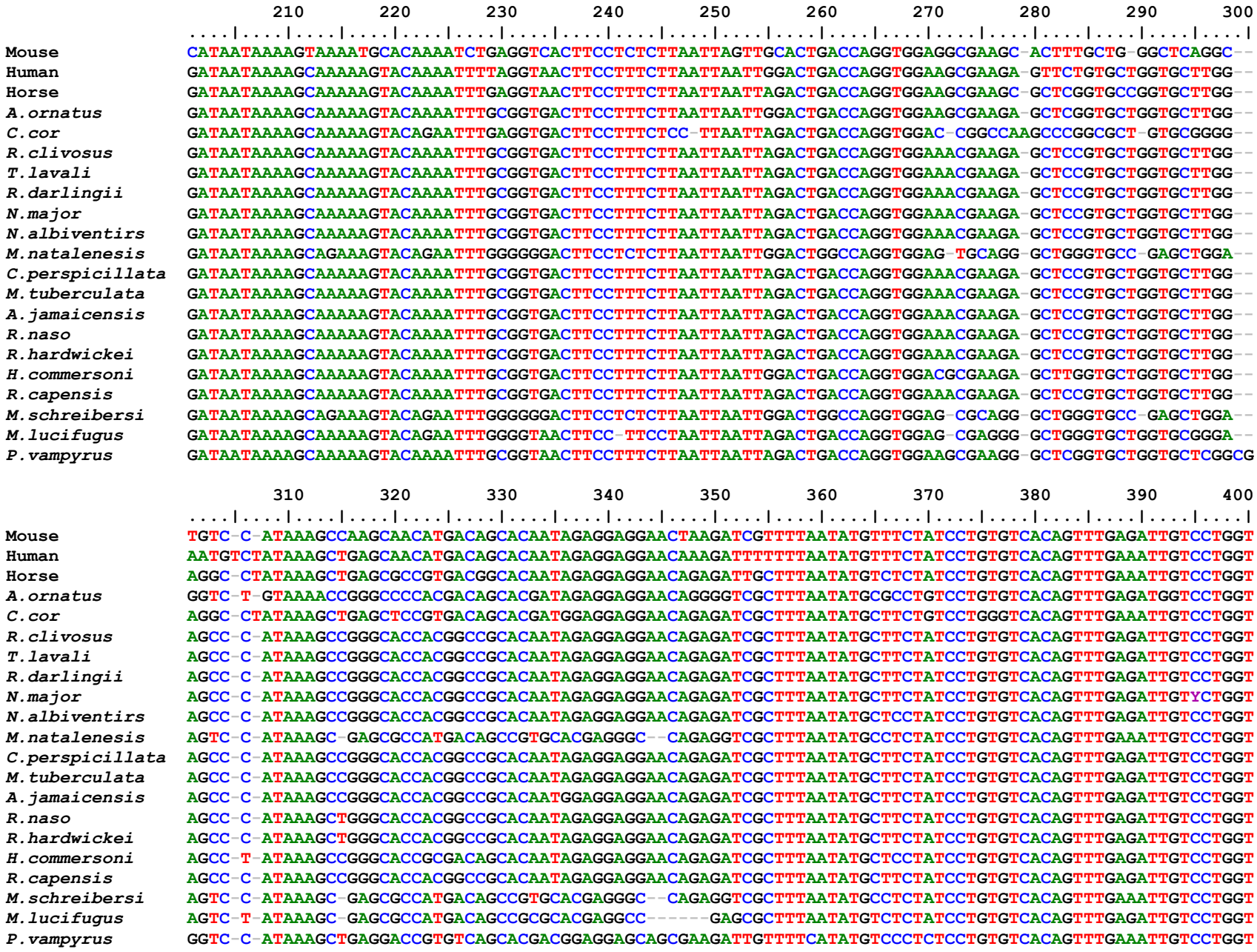
210 220 230 240 250 260 270 280 290 300
Mouse CATAATAAAAGTAAAATGCACAAAATCTGAGGTCACTTCCTCTCTTAATTAGTTGCACTGACCAGGTGGAGGCGAAGC-ACTTTGCTG-GGCTCAGGC--
Human GATAATAAAAGCAAAAAGTACAAAATTTTAGGTAACTTCCTTTCTTAATTAATTGGACTGACCAGGTGGAAGCGAAGA-GTTCTGTGCTGGTGCTTGG--
Horse GATAATAAAAGCAAAAAGTACAAAATTTGAGGTAACTTCCTTTCTTAATTAATTAGACTGACCAGGTGGAAGCGAAGC-GCTCGGTGCCGGTGCTTGG--
A.ornatus GATAATAAAAGCAAAAAGTACAAAATTTGCGGTGACTTCCTTTCTTAATTAATTGGACTGACCAGGTGGAAGCGAAGA-GCTCGGTGCTGGTGCTTGG--
C.cor GATAATAAAAGCAAAAAGTACAGAATTTGAGGTGACTTCCTTTCTCC-TTAATTAGACTGACCAGGTGGAC-CGGCCAAGCCCGGCGCT-GTGCGGGG--
R.clivosus GATAATAAAAGCAAAAAGTACAAAATTTGCGGTGACTTCCTTTCTTAATTAATTAGACTGACCAGGTGGAAACGAAGA-GCTCCGTGCTGGTGCTTGG--
T.lavali GATAATAAAAGCAAAAAGTACAAAATTTGCGGTGACTTCCTTTCTTAATTAATTAGACTGACCAGGTGGAAACGAAGA-GCTCCGTGCTGGTGCTTGG--
R.darlingii GATAATAAAAGCAAAAAGTACAAAATTTGCGGTGACTTCCTTTCTTAATTAATTAGACTGACCAGGTGGAAACGAAGA-GCTCCGTGCTGGTGCTTGG--
N.major GATAATAAAAGCAAAAAGTACAAAATTTGCGGTGACTTCCTTTCTTAATTAATTAGACTGACCAGGTGGAAACGAAGA-GCTCCGTGCTGGTGCTTGG--
N.albiventirs GATAATAAAAGCAAAAAGTACAAAATTTGCGGTGACTTCCTTTCTTAATTAATTAGACTGACCAGGTGGAAACGAAGA-GCTCCGTGCTGGTGCTTGG--
M.natalenesis GATAATAAAAGCAGAAAGTACAGAATTTGGGGGGACTTCCTCTCTTAATTAATTGGACTGGCCAGGTGGAG-TGCAGG-GCTGGGTGCC-GAGCTGGA--
C.perspicillata GATAATAAAAGCAAAAAGTACAAAATTTGCGGTGACTTCCTTTCTTAATTAATTAGACTGACCAGGTGGAAACGAAGA-GCTCCGTGCTGGTGCTTGG--
M.tuberculata GATAATAAAAGCAAAAAGTACAAAATTTGCGGTGACTTCCTTTCTTAATTAATTAGACTGACCAGGTGGAAACGAAGA-GCTCCGTGCTGGTGCTTGG--
A.jamaicensis GATAATAAAAGCAAAAAGTACAAAATTTGCGGTGACTTCCTTTCTTAATTAATTAGACTGACCAGGTGGAAACGAAGA-GCTCCGTGCTGGTGCTTGG--
R.naso GATAATAAAAGCAAAAAGTACAAAATTTGCGGTGACTTCCTTTCTTAATTAATTAGACTGACCAGGTGGAAACGAAGA-GCTCCGTGCTGGTGCTTGG--
R.hardwickei GATAATAAAAGCAAAAAGTACAAAATTTGCGGTGACTTCCTTTCTTAATTAATTAGACTGACCAGGTGGAAACGAAGA-GCTCCGTGCTGGTGCTTGG--
H.commersoni GATAATAAAAGCAAAAAGTACAAAATTTGCGGTGACTTCCTTTCTTAATTAATTGGACTGACCAGGTGGACGCGAAGA-GCTTGGTGCTGGTGCTTGG--
R.capensis GATAATAAAAGCAAAAAGTACAAAATTTGCGGTGACTTCCTTTCTTAATTAATTAGACTGACCAGGTGGAAACGAAGA-GCTCCGTGCTGGTGCTTGG--
M.schreibersi GATAATAAAAGCAGAAAGTACAGAATTTGGGGGGACTTCCTCTCTTAATTAATTGGACTGGCCAGGTGGAG-CGCAGG-GCTGGGTGCC-GAGCTGGA--
M.lucifugus GATAATAAAAGCAAAAAGTACAGAATTTGGGGTAACTTCC-TTCCTAATTAATTAGACTGACCAGGTGGAG-CGAGGG-GCTGGGTGCTGGTGCGGGA--
P.vampyrus GATAATAAAAGCAAAAAGTACAAAATTTGCGGTAACTTCCTTTCTTAATTAATTAGACTGACCAGGTGGAAGCGAAGG-GCTCGGTGCTGGTGCTCGGCG
310 320 330 340 350 360 370 380 390 400
Mouse TGTC-C-ATAAAGCCAAGCAACATGACAGCACAATAGAGGAGGAACTAAGATCGTTTTAATATGTTTCTATCCTGTGTCACAGTTTGAGATTGTCCTGGT
Human AATGTCTATAAAGCTGAGCAACATGACAGCACAATAGAGGAGGAACAAAGATTTTTTTAATATGTTTCTATCCTGTGTCACAGTTTGAAATTGTCCTGGT
Horse AGGC-CTATAAAGCTGAGCGCCGTGACGGCACAATAGAGGAGGAACAGAGATTGCTTTAATATGTCTCTATCCTGTGTCACAGTTTGAAATTGTCCTGGT
A.ornatus GGTC-T-GTAAAACCGGGCCCCACGACAGCACGATAGAGGAGGAACAGGGGTCGCTTTAATATGCGCCTGTCCTGTGTCACAGTTTGAGATGGTCCTGGT
C.cor AGGC-CTATAAAGCTGAGCTCCGTGACAGCACGATGGAGGAGGAACAGAGATCGCTTTAATATGCTTCTGTCCTGGGTCACAGTTTGAAATTGTCCTGGT
R.clivosus AGCC-C-ATAAAGCCGGGCACCACGGCCGCACAATAGAGGAGGAACAGAGATCGCTTTAATATGCTTCTATCCTGTGTCACAGTTTGAGATTGTCCTGGT
T.lavali AGCC-C-ATAAAGCCGGGCACCACGGCCGCACAATAGAGGAGGAACAGAGATCGCTTTAATATGCTTCTATCCTGTGTCACAGTTTGAGATTGTCCTGGT
R.darlingii AGCC-C-ATAAAGCCGGGCACCACGGCCGCACAATAGAGGAGGAACAGAGATCGCTTTAATATGCTTCTATCCTGTGTCACAGTTTGAGATTGTCCTGGT
N.major AGCC-C-ATAAAGCCGGGCACCACGGCCGCACAATAGAGGAGGAACAGAGATCGCTTTAATATGCTTCTATCCTGTGTCACAGTTTGAGATTGTYCTGGT
N.albiventirs AGCC-C-ATAAAGCCGGGCACCACGGCCGCACAATAGAGGAGGAACAGAGATCGCTTTAATATGCTCCTATCCTGTGTCACAGTTTGAGATTGTCCTGGT
M.natalenesis AGTC-C-ATAAAGC-GAGCGCCATGACAGCCGTGCACGAGGGC--CAGAGGTCGCTTTAATATGCCTCTATCCTGTGTCACAGTTTGAAATTGTCCTGGT
C.perspicillata AGCC-C-ATAAAGCCGGGCACCACGGCCGCACAATAGAGGAGGAACAGAGATCGCTTTAATATGCTTCTATCCTGTGTCACAGTTTGAGATTGTCCTGGT
M.tuberculata AGCC-C-ATAAAGCCGGGCACCACGGCCGCACAATAGAGGAGGAACAGAGATCGCTTTAATATGCTTCTATCCTGTGTCACAGTTTGAGATTGTCCTGGT
A.jamaicensis AGCC-C-ATAAAGCCGGGCACCACGGCCGCACAATGGAGGAGGAACAGAGATCGCTTTAATATGCTTCTATCCTGTGTCACAGTTTGAGATTGTCCTGGT
R.naso AGCC-C-ATAAAGCTGGGCACCACGGCCGCACAATAGAGGAGGAACAGAGATCGCTTTAATATGCTTCTATCCTGTGTCACAGTTTGAGATTGTCCTGGT
R.hardwickei AGCC-C-ATAAAGCTGGGCACCACGGCCGCACAATAGAGGAGGAACAGAGATCGCTTTAATATGCTTCTATCCTGTGTCACAGTTTGAGATTGTCCTGGT
H.commersoni AGCC-T-ATAAAGCCGGGCACCGCGACAGCACAATAGAGGAGGAACAGAGATCGCTTTAATATGCTCCTATCCTGTGTCACAGTTTGAGATTGTCCTGGT
R.capensis AGCC-C-ATAAAGCCGGGCACCACGGCCGCACAATAGAGGAGGAACAGAGATCGCTTTAATATGCTTCTATCCTGTGTCACAGTTTGAGATTGTCCTGGT
M.schreibersi AGTC-C-ATAAAGC-GAGCGCCATGACAGCCGTGCACGAGGGC--CAGAGGTCGCTTTAATATGCCTCTATCCTGTGTCACAGTTTGAAATTGTCCTGGT
M.lucifugus AGTC-T-ATAAAGC-GAGCGCCATGACAGCCGCGCACGAGGCC------GAGCGCTTTAATATGTCTCTATCCTGTGTCACAGTTTGAGATTGTCCTGGT
P.vampyrus GGTC-C-ATAAAGCTGAGGACCGTGTCAGCACGACGGAGGAGCAGCGAAGATTGTTTTCATATGTCCCTCTCCTGTGTCACAGTTTGAAATTGTCCTGGT

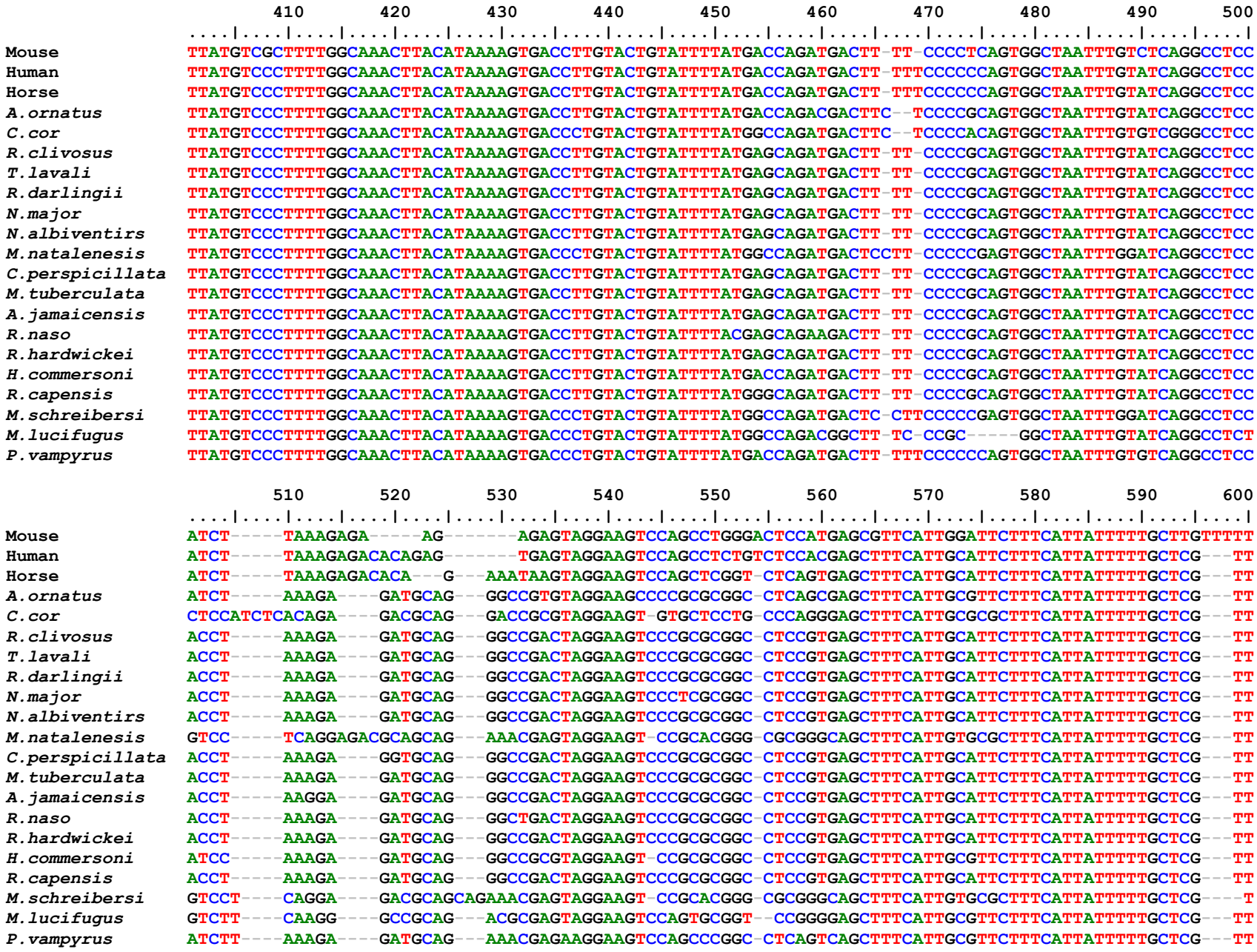
410 420 430 440 450 460 470 480 490 500
Mouse TTATGTCGCTTTTGGCAAACTTACATAAAAGTGACCTTGTACTGTATTTTATGACCAGATGACTT-TT-CCCCTCAGTGGCTAATTTGTCTCAGGCCTCC
Human TTATGTCCCTTTTGGCAAACTTACATAAAAGTGACCTTGTACTGTATTTTATGACCAGATGACTT-TTTCCCCCCAGTGGCTAATTTGTATCAGGCCTCC
Horse TTATGTCCCTTTTGGCAAACTTACATAAAAGTGACCTTGTACTGTATTTTATGACCAGATGACTT-TTTCCCCCCAGTGGCTAATTTGTATCAGGCCTCC
A.ornatus TTATGTCCCTTTTGGCAAACTTACATAAAAGTGACCTTGTACTGTATTTTATGACCAGACGACTTC--TCCCCGCAGTGGCTAATTTGTATCAGGCCTCC
C.cor TTATGTCCCTTTTGGCAAACTTACATAAAAGTGACCCTGTACTGTATTTTATGGCCAGATGACTTC--TCCCCACAGTGGCTAATTTGTGTCGGGCCTCC
R.clivosus TTATGTCCCTTTTGGCAAACTTACATAAAAGTGACCTTGTACTGTATTTTATGAGCAGATGACTT-TT-CCCCGCAGTGGCTAATTTGTATCAGGCCTCC
T.lavali TTATGTCCCTTTTGGCAAACTTACATAAAAGTGACCTTGTACTGTATTTTATGAGCAGATGACTT-TT-CCCCGCAGTGGCTAATTTGTATCAGGCCTCC
R.darlingii TTATGTCCCTTTTGGCAAACTTACATAAAAGTGACCTTGTACTGTATTTTATGAGCAGATGACTT-TT-CCCCGCAGTGGCTAATTTGTATCAGGCCTCC
N.major TTATGTCCCTTTTGGCAAACTTACATAAAAGTGACCTTGTACTGTATTTTATGAGCAGATGACTT-TT-CCCCGCAGTGGCTAATTTGTATCAGGCCTCC
N.albiventirs TTATGTCCCTTTTGGCAAACTTACATAAAAGTGACCTTGTACTGTATTTTATGAGCAGATGACTT-TT-CCCCGCAGTGGCTAATTTGTATCAGGCCTCC
M.natalenesis TTATGTCCCTTTTGGCAAACTTACATAAAAGTGACCCTGTACTGTATTTTATGGCCAGATGACTCCTT-CCCCCGAGTGGCTAATTTGGATCAGGCCTCC
C.perspicillata TTATGTCCCTTTTGGCAAACTTACATAAAAGTGACCTTGTACTGTATTTTATGAGCAGATGACTT-TT-CCCCGCAGTGGCTAATTTGTATCAGGCCTCC
M.tuberculata TTATGTCCCTTTTGGCAAACTTACATAAAAGTGACCTTGTACTGTATTTTATGAGCAGATGACTT-TT-CCCCGCAGTGGCTAATTTGTATCAGGCCTCC
A.jamaicensis TTATGTCCCTTTTGGCAAACTTACATAAAAGTGACCTTGTACTGTATTTTATGAGCAGATGACTT-TT-CCCCGCAGTGGCTAATTTGTATCAGGCCTCC
R.naso TTATGTCCCTTTTGGCAAACTTACATAAAAGTGACCTTGTACTGTATTTTACGAGCAGAAGACTT-TT-CCCCGCAGTGGCTAATTTGTATCAGGCCTCC
R.hardwickei TTATGTCCCTTTTGGCAAACTTACATAAAAGTGACCTTGTACTGTATTTTATGAGCAGATGACTT-TT-CCCCGCAGTGGCTAATTTGTATCAGGCCTCC
H.commersoni TTATGTCCCTTTTGGCAAACTTACATAAAAGTGACCTTGTACTGTATTTTATGACCAGATGACTT-TT-CCCCGCAGTGGCTAATTTGTATCAGGCCTCC
R.capensis TTATGTCCCTTTTGGCAAACTTACATAAAAGTGACCTTGTACTGTATTTTATGGGCAGATGACTT-TT-CCCCGCAGTGGCTAATTTGTATCAGGCCTCC
M.schreibersi TTATGTCCCTTTTGGCAAACTTACATAAAAGTGACCCTGTACTGTATTTTATGGCCAGATGACTC-CTTCCCCCGAGTGGCTAATTTGGATCAGGCCTCC
M.lucifugus TTATGTCCCTTTTGGCAAACTTACATAAAAGTGACCCTGTACTGTATTTTATGGCCAGACGGCTT-TC-CCGC-----GGCTAATTTGTATCAGGCCTCT
P.vampyrus TTATGTCCCTTTTGGCAAACTTACATAAAAGTGACCCTGTACTGTATTTTATGACCAGATGACTT-TTTCCCCCCAGTGGCTAATTTGTGTCAGGCCTCC
510 520 530 540 550 560 570 580 590 600
Mouse ATCT-----TAAAGAGA-----AG-------AGAGTAGGAAGTCCAGCCTGGGACTCCATGAGCGTTCATTGGATTCTTTCATTATTTTTGCTTGTTTTT
Human ATCT-----TAAAGAGACACAGAG-------TGAGTAGGAAGTCCAGCCTCTGTCTCCACGAGCTTTCATTGCATTCTTTCATTATTTTTGCTCG---TT
Horse ATCT-----TAAAGAGACACA---G---AAATAAGTAGGAAGTCCAGCTCGGT-CTCAGTGAGCTTTCATTGCATTCTTTCATTATTTTTGCTCG---TT
A.ornatus ATCT-----AAAGA----GATGCAG---GGCCGTGTAGGAAGCCCCGCGCGGC-CTCAGCGAGCTTTCATTGCGTTCTTTCATTATTTTTGCTCG---TT
C.cor CTCCATCTCACAGA----GACGCAG---GACCGCGTAGGAAGT-GTGCTCCTG-CCCAGGGAGCTTTCATTGCGCGCTTTCATTATTTTTGCTCG---TT
R.clivosus ACCT-----AAAGA----GATGCAG---GGCCGACTAGGAAGTCCCGCGCGGC-CTCCGTGAGCTTTCATTGCATTCTTTCATTATTTTTGCTCG---TT
T.lavali ACCT-----AAAGA----GATGCAG---GGCCGACTAGGAAGTCCCGCGCGGC-CTCCGTGAGCTTTCATTGCATTCTTTCATTATTTTTGCTCG---TT
R.darlingii ACCT-----AAAGA----GATGCAG---GGCCGACTAGGAAGTCCCGCGCGGC-CTCCGTGAGCTTTCATTGCATTCTTTCATTATTTTTGCTCG---TT
N.major ACCT-----AAAGA----GATGCAG---GGCCGACTAGGAAGTCCCTCGCGGC-CTCCGTGAGCTTTCATTGCATTCTTTCATTATTTTTGCTCG---TT
N.albiventirs ACCT-----AAAGA----GATGCAG---GGCCGACTAGGAAGTCCCGCGCGGC-CTCCGTGAGCTTTCATTGCATTCTTTCATTATTTTTGCTCG---TT
M.natalenesis GTCC-----TCAGGAGACGCAGCAG---AAACGAGTAGGAAGT-CCGCACGGG-CGCGGGCAGCTTTCATTGTGCGCTTTCATTATTTTTGCTCG---TT
C.perspicillata ACCT-----AAAGA----GGTGCAG---GGCCGACTAGGAAGTCCCGCGCGGC-CTCCGTGAGCTTTCATTGCATTCTTTCATTATTTTTGCTCG---TT
M.tuberculata ACCT-----AAAGA----GATGCAG---GGCCGACTAGGAAGTCCCGCGCGGC-CTCCGTGAGCTTTCATTGCATTCTTTCATTATTTTTGCTCG---TT
A.jamaicensis ACCT-----AAGGA----GATGCAG---GGCCGACTAGGAAGTCCCGCGCGGC-CTCCGTGAGCTTTCATTGCATTCTTTCATTATTTTTGCTCG---TT
R.naso ACCT-----AAAGA----GATGCAG---GGCTGACTAGGAAGTCCCGCGCGGC-CTCCGTGAGCTTTCATTGCATTCTTTCATTATTTTTGCTCG---TT
R.hardwickei ACCT-----AAAGA----GATGCAG---GGCCGACTAGGAAGTCCCGCGCGGC-CTCCGTGAGCTTTCATTGCATTCTTTCATTATTTTTGCTCG---TT
H.commersoni ATCC-----AAAGA----GATGCAG---GGCCGCGTAGGAAGT-CCGCGCGGC-CTCCGTGAGCTTTCATTGCGTTCTTTCATTATTTTTGCTCG---TT
R.capensis ACCT-----AAAGA----GATGCAG---GGCCGACTAGGAAGTCCCGCGCGGC-CTCCGTGAGCTTTCATTGCATTCTTTCATTATTTTTGCTCG---TT
M.schreibersi GTCCT----CAGGA----GACGCAGCAGAAACGAGTAGGAAGT-CCGCACGGG-CGCGGGCAGCTTTCATTGTGCGCTTTCATTATTTTTGCTCG----T
M.lucifugus GTCTT----CAAGG----GCCGCAG---ACGCGAGTAGGAAGTCCAGTGCGGT--CCGGGGAGCTTTCATTGCGTTCTTTCATTATTTTTGCTCG---TT
P.vampyrus ATCTT----AAAGA----GATGCAG---AAACGAGAAGGAAGTCCAGCCCGGC-CTCAGTCAGCTTTCATTGCGTTCTTTCATTATTTTTGCTCG---TT

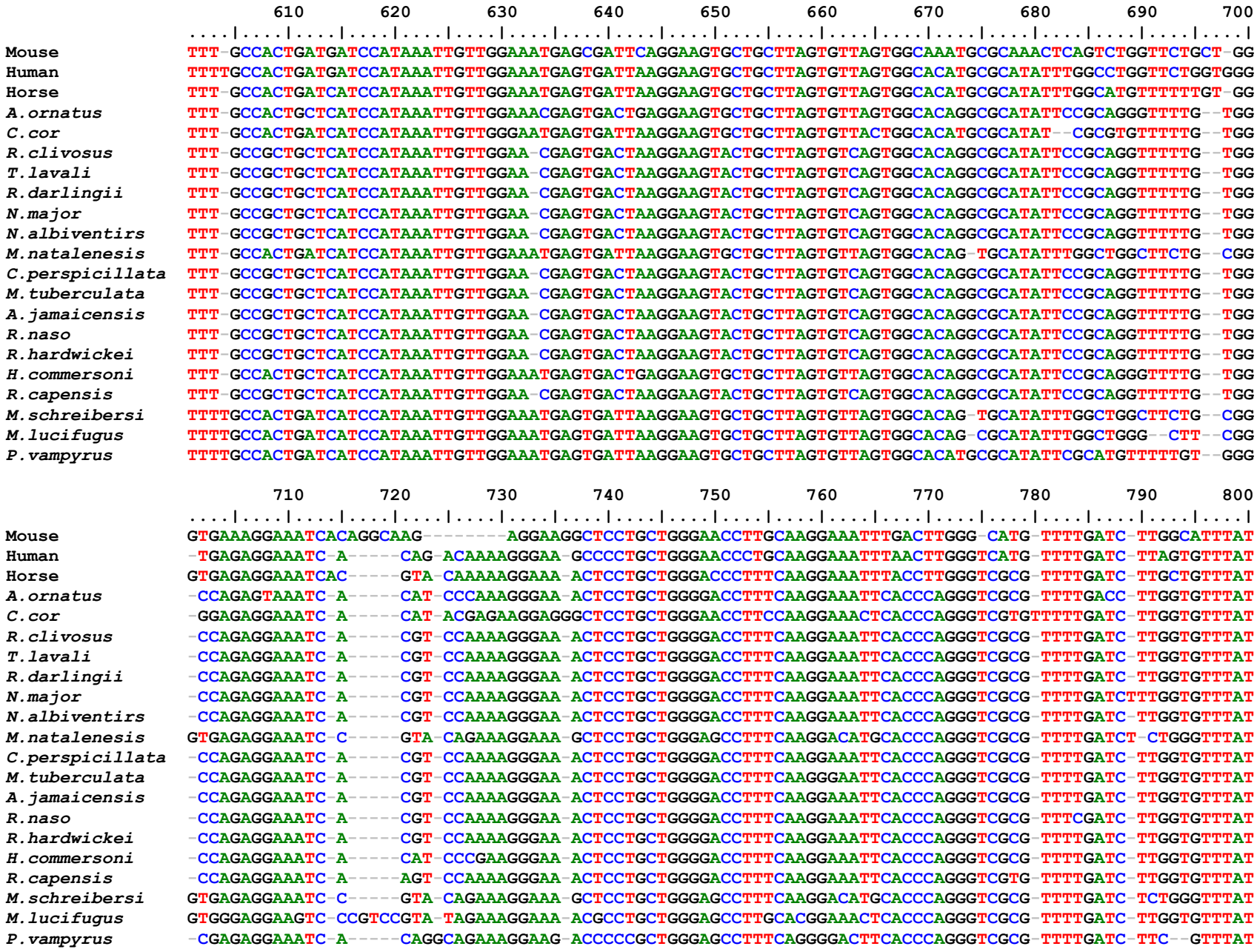
610 620 630 640 650 660 670 680 690 700
Mouse TTT-GCCACTGATGATCCATAAATTGTTGGAAATGAGCGATTCAGGAAGTGCTGCTTAGTGTTAGTGGCAAATGCGCAAACTCAGTCTGGTTCTGCT-GG
Human TTTTGCCACTGATGATCCATAAATTGTTGGAAATGAGTGATTAAGGAAGTGCTGCTTAGTGTTAGTGGCACATGCGCATATTTGGCCTGGTTCTGGTGGG
Horse TTT-GCCACTGATCATCCATAAATTGTTGGAAATGAGTGATTAAGGAAGTGCTGCTTAGTGTTAGTGGCACATGCGCATATTTGGCATGTTTTTTGT-GG
A.ornatus TTT-GCCACTGCTCATCCATAAATTGTTGGAAACGAGTGACTGAGGAAGTGCTGCTTAGTGTTAGTGGCACAGGCGCATATTCCGCAGGGTTTTG--TGG
C.cor TTT-GCCACTGATCATCCATAAATTGTTGGGAATGAGTGATTAAGGAAGTGCTGCTTAGTGTTACTGGCACATGCGCATAT--CGCGTGTTTTTG--TGG
R.clivosus TTT-GCCGCTGCTCATCCATAAATTGTTGGAA-CGAGTGACTAAGGAAGTACTGCTTAGTGTCAGTGGCACAGGCGCATATTCCGCAGGTTTTTG--TGG
T.lavali TTT-GCCGCTGCTCATCCATAAATTGTTGGAA-CGAGTGACTAAGGAAGTACTGCTTAGTGTCAGTGGCACAGGCGCATATTCCGCAGGTTTTTG--TGG
R.darlingii TTT-GCCGCTGCTCATCCATAAATTGTTGGAA-CGAGTGACTAAGGAAGTACTGCTTAGTGTCAGTGGCACAGGCGCATATTCCGCAGGTTTTTG--TGG
N.major TTT-GCCGCTGCTCATCCATAAATTGTTGGAA-CGAGTGACTAAGGAAGTACTGCTTAGTGTCAGTGGCACAGGCGCATATTCCGCAGGTTTTTG--TGG
N.albiventirs TTT-GCCGCTGCTCATCCATAAATTGTTGGAA-CGAGTGACTAAGGAAGTACTGCTTAGTGTCAGTGGCACAGGCGCATATTCCGCAGGTTTTTG--TGG
M.natalenesis TTT-GCCACTGATCATCCATAAATTGTTGGAAATGAGTGATTAAGGAAGTGCTGCTTAGTGTTAGTGGCACAG-TGCATATTTGGCTGGCTTCTG--CGG
C.perspicillata TTT-GCCGCTGCTCATCCATAAATTGTTGGAA-CGAGTGACTAAGGAAGTACTGCTTAGTGTCAGTGGCACAGGCGCATATTCCGCAGGTTTTTG--TGG
M.tuberculata TTT-GCCGCTGCTCATCCATAAATTGTTGGAA-CGAGTGACTAAGGAAGTACTGCTTAGTGTCAGTGGCACAGGCGCATATTCCGCAGGTTTTTG--TGG
A.jamaicensis TTT-GCCGCTGCTCATCCATAAATTGTTGGAA-CGAGTGACTAAGGAAGTACTGCTTAGTGTCAGTGGCACAGGCGCATATTCCGCAGGTTTTTG--TGG
R.naso TTT-GCCGCTGCTCATCCATAAATTGTTGGAA-CGAGTGACTAAGGAAGTACTGCTTAGTGTCAGTGGCACAGGCGCATATTCCGCAGGTTTTTG--TGG
R.hardwickei TTT-GCCGCTGCTCATCCATAAATTGTTGGAA-CGAGTGACTAAGGAAGTACTGCTTAGTGTCAGTGGCACAGGCGCATATTCCGCAGGTTTTTG--TGG
H.commersoni TTT-GCCACTGCTCATCCATAAATTGTTGGAAATGAGTGACTGAGGAAGTGCTGCTTAGTGTTAGTGGCACAGGCGCATATTCCGCAGGGTTTTG--TGG
R.capensis TTT-GCCGCTGCTCATCCATAAATTGTTGGAA-CGAGTGACTAAGGAAGTACTGCTTAGTGTCAGTGGCACAGGCGCATATTCCGCAGGTTTTTG--TGG
M.schreibersi TTTTGCCACTGATCATCCATAAATTGTTGGAAATGAGTGATTAAGGAAGTGCTGCTTAGTGTTAGTGGCACAG-TGCATATTTGGCTGGCTTCTG--CGG
M.lucifugus TTTTGCCACTGATCATCCATAAATTGTTGGAAATGAGTGATTAAGGAAGTGCTGCTTAGTGTTAGTGGCACAG-CGCATATTTGGCTGGG--CTT--CGG
P.vampyrus TTTTGCCACTGATCATCCATAAATTGTTGGAAATGAGTGATTAAGGAAGTGCTGCTTAGTGTTAGTGGCACATGCGCATATTCGCATGTTTTTGT--GGG
710 720 730 740 750 760 770 780 790 800
Mouse GTGAAAGGAAATCACAGGCAAG--------AGGAAGGCTCCTGCTGGGAACCTTGCAAGGAAATTTGACTTGGG-CATG-TTTTGATC-TTGGCATTTAT
Human -TGAGAGGAAATC-A-----CAG-ACAAAAGGGAA-GCCCCTGCTGGGAACCCTGCAAGGAAATTTAACTTGGGTCATG-TTTTGATC-TTAGTGTTTAT
Horse GTGAGAGGAAATCAC-----GTA-CAAAAAGGAAA-ACTCCTGCTGGGACCCTTTCAAGGAAATTTACCTTGGGTCGCG-TTTTGATC-TTGCTGTTTAT
A.ornatus -CCAGAGTAAATC-A-----CAT-CCCAAAGGGAA-ACTCCTGCTGGGGACCTTTCAAGGAAATTCACCCAGGGTCGCG-TTTTGACC-TTGGTGTTTAT
C.cor -GGAGAGGAAATC-A-----CAT-ACGAGAAGGAGGGCTCCTGCTGGGAACCTTCCAAGGAAACTCACCCAGGGTCGTGTTTTTGATC-TTGGTGTTTAT
R.clivosus -CCAGAGGAAATC-A-----CGT-CCAAAAGGGAA-ACTCCTGCTGGGGACCTTTCAAGGAAATTCACCCAGGGTCGCG-TTTTGATC-TTGGTGTTTAT
T.lavali -CCAGAGGAAATC-A-----CGT-CCAAAAGGGAA-ACTCCTGCTGGGGACCTTTCAAGGAAATTCACCCAGGGTCGCG-TTTTGATC-TTGGTGTTTAT
R.darlingii -CCAGAGGAAATC-A-----CGT-CCAAAAGGGAA-ACTCCTGCTGGGGACCTTTCAAGGAAATTCACCCAGGGTCGCG-TTTTGATC-TTGGTGTTTAT
N.major -CCAGAGGAAATC-A-----CGT-CCAAAAGGGAA-ACTCCTGCTGGGGACCTTTCAAGGAAATTCACCCAGGGTCGCG-TTTTGATCTTTGGTGTTTAT
N.albiventirs -CCAGAGGAAATC-A-----CGT-CCAAAAGGGAA-ACTCCTGCTGGGGACCTTTCAAGGAAATTCACCCAGGGTCGCG-TTTTGATC-TTGGTGTTTAT
M.natalenesis GTGAGAGGAAATC-C-----GTA-CAGAAAGGAAA-GCTCCTGCTGGGAGCCTTTCAAGGACATGCACCCAGGGTCGCG-TTTTGATCT-CTGGGTTTAT
C.perspicillata -CCAGAGGAAATC-A-----CGT-CCAAAAGGGAA-ACTCCTGCTGGGGACCTTTCAAGGAAATTCACCCAGGGTCGCG-TTTTGATC-TTGGTGTTTAT
M.tuberculata -CCAGAGGAAATC-A-----CGT-CCAAAAGGGAA-ACTCCTGCTGGGGACCTTTCAAGGGAATTCACCCAGGGTCGCG-TTTTGATC-TTGGTGTTTAT
A.jamaicensis -CCAGAGGAAATC-A-----CGT-CCAAAAGGGAA-ACTCCTGCTGGGGACCTTTCAAGGAAATTCACCCAGGGTCGCG-TTTTGATC-TTGGTGTTTAT
R.naso -CCAGAGGAAATC-A-----CGT-CCAAAAGGGAA-ACTCCTGCTGGGGACCTTTCAAGGAAATTCACCCAGGGTCGCG-TTTCGATC-TTGGTGTTTAT
R.hardwickei -CCAGAGGAAATC-A-----CGT-CCAAAAGGGAA-ACTCCTGCTGGGGACCTTTCAAGGAAATTCACCCAGGGTCGCG-TTTTGATC-TTGGTGTTTAT
H.commersoni -CCAGAGGAAATC-A-----CAT-CCCGAAGGGAA-ACTCCTGCTGGGGACCTTTCAAGGAAATTCACCCAGGGTCGCG-TTTTGATC-TTGGTGTTTAT
R.capensis -CCAGAGGAAATC-A-----AGT-CCAAAAGGGAA-ACTCCTGCTGGGGACCTTTCAAGGAAATTCACCCAGGGTCGTG-TTTTGATC-TTGGTGTTTAT
M.schreibersi GTGAGAGGAAATC-C-----GTA-CAGAAAGGAAA-GCTCCTGCTGGGAGCCTTTCAAGGACATGCACCCAGGGTCGCG-TTTTGATC-TCTGGGTTTAT
M.lucifugus GTGGGAGGAAGTC-CCGTCCGTA-TAGAAAGGAAA-ACGCCTGCTGGGAGCCTTGCACGGAAACTCACCCAGGGTCGCG-TTTTGATC-TTGGTGTTTAT
P.vampyrus -CGAGAGGAAATC-A-----CAGGCAGAAAGGAAG-ACCCCCGCTGGGAGCCTTTCAGGGGACTTCACCCAGGGTCGCG-TTTTGATC-TTC--GTTTAT

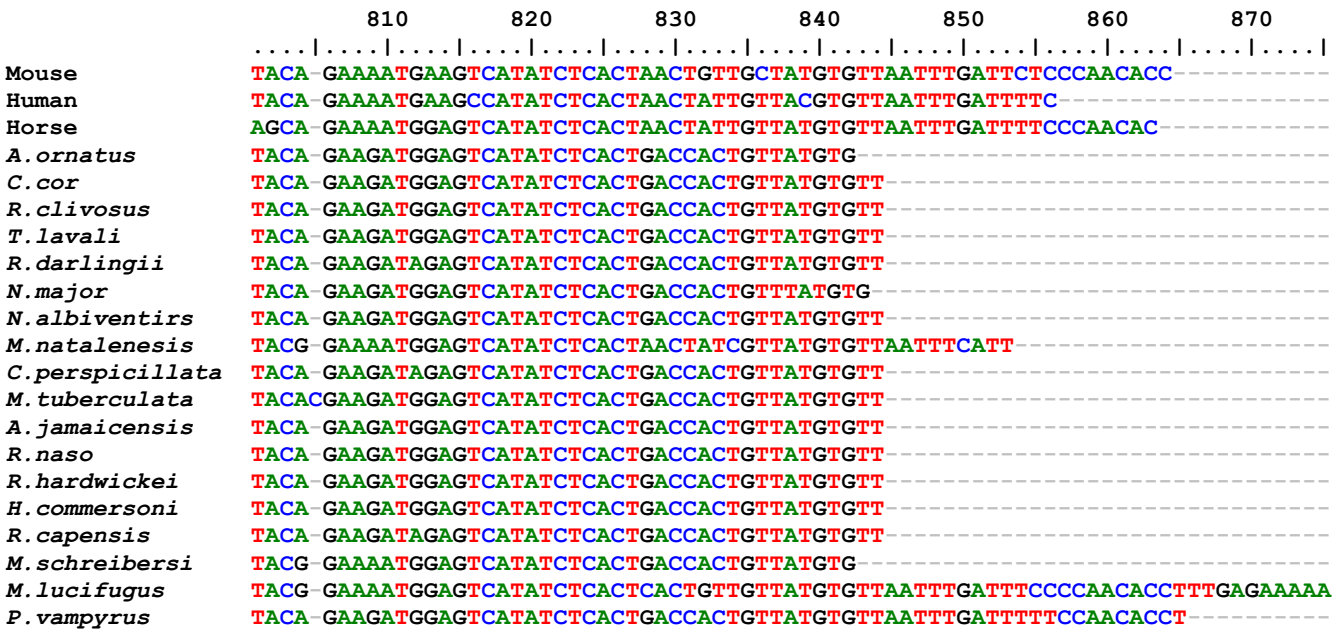

Figure A.7: DNalign alignment of the 18 Bat ZRS, the horse ZRS, the mouse ZRS and the human ZRS.